UNIVERSITY OF READING

The role of isoquercetin, zafirlukast and its novel analogues for thiol isomerase inhibition in relation to thrombosis, cancer and other complications

A thesis submitted for the degree of Doctor of Philosophy

By

Justine Keovilay

Institute for Cardiovascular and Metabolic Research School of Biological Sciences

July 2025

Declaration

I can confirm that this is my own work and the use of all material from other sources has been properly and fully acknowledged.

Signed: Justine Keovilay

Date: 8th July 2025

Abstract

Background: Thiol isomerases including PDI, ERp57, ERp72 and ERp5 play essential and distinct roles in thrombosis, cancer progression, cancer cell signalling and metastasis. Thiol isomerase inhibitors constitute a class of agents to combat these complications where they generally have been studied to combat either thrombosis or cancer but not both. Recently, our lab has identified the FDA approved leukotriene receptor antagonist, zafirlukast, as a broad-spectrum thiol isomerase inhibitor able to inhibit platelet aggregation and thrombus formation.

Aims: The aims of this thesis begin with the goal to improve the efficacy of zafirlukast for thrombotic inhibition via the exploration of zafirlukast analogues. It continues by exploring how zafirlukast fairs against and ovarian cancer model, and whether its effects can be improved by combining it with a standard chemotherapy regimen or with another thiol isomerase inhibitor, isoquercetin. It concludes by exploring the mechanistic effects of thiol isomerase inhibition, and pathways affected through zafirlukast and isoquercetin treatment.

Results: One of 35 zafirlukast analogues, termed compound **21**, demonstrated greater potency than zafirlukast and was able to better inhibit platelet aggregation, P-selectin exposure and thrombus formation. Both zafirlukast and compound **21** demonstrated reversibility of thiol isomerase inhibition and demonstrated no cytotoxicity towards cultured lung liver and kidney cells. Although compound **21** was a better inhibitor overall, it only held a 2.5-fold increase in potency, so to explore the effects of zafirlukast on cancer inhibition I remained with the parent compound, which demonstrated inhibition of cancer growth in an ovarian xenograft model. With this data we performed a pilot clinical trial of zafirlukast's anticancer effects in ovarian cancer patients. These results however were inconclusive; therefore, I tried improving the efficacy of zafirlukast by combining it with isoquercetin or cisplatin/gemcitabine. When combined with isoquercetin in low doses the

effects were similar to that of a high dose of zafirlukast on its own. Then when zafirlukast was combined with cisplatin/gemcitabine a greater inhibition was seen than just the chemotherapy on its own. Finally, in addition to inhibiting thiol isomerases zafirlukast and isoquercetin were able to inhibit factors involved in cancer induced thrombosis, angiogenesis and inflammation including tissue factor, VEGF, TMEM176B and PD-L1.

Conclusions: One conclusion drawn from this thesis is that thiol isomerase inhibitors, such as zafirlukast, are able to act as both anti-thrombotic and anti-cancer agents, making zafirlukast an interesting drug to continue exploring in combination with chemotherapeutic drugs to potentially combat cancer induced thrombosis. Another conclusion is that it is possible to alter zafirlukast to perform better as an inhibitor, where it can continue to be explored for even better analogue development. Additionally, zafirlukast in combination with another thiol isomerase inhibitor, such as isoquercetin can also improve efficacy and target other pathways beyond thiol isomerases.

Acknowledgements

Dan, thank you for being a wonderful advisor and mentor. I appreciate all of the guidance and support you have provided throughout my time at WNE. Thank you for allowing me to start as your research assistant, and progress into the opportunity of a PhD student, guiding me through until the end.

Jon, thank you for advising me through the world of platelet biology and allowing me the opportunity to be a part of the University of Reading. I appreciate the knowledge you have shared with me and guidance you have provided. Also, thank you for your kind hospitality during my trips to Reading.

Alex, thank you for all of your knowledge, help and support during the mouse studies, I couldn't have done them without you.

Sabeeya, thank you for being a kind friend throughout this journey and all your help in the lab during my trips to Reading.

Thank you to my family, especially my husband John, for all of the support throughout my PhD journey and believing that I could finish through to the end.

To Doug, Emily and Kate, thank you for keeping me sane throughout and being the most supportive best friends.

Publications

Manuscripts submitted

- **Keovilay JK,** Hoskins JW, Lines TC, Kennedy DR. *Isoquercetin and zafirlukast cooperatively suppress tumour growth and thromboinflammatory signalling in a xenograft model of ovarian cancer*. Submitted to FASEB Journal. **Data from this manuscript is shown in Chapter 4.**

Published

- **Keovilay JK,** Howard KC, Taylor KA, Khan S, Wurl SE, Szahaj MK, Sage T, Thamban Chandrika N, Hou C, Tsodikov OV, Gibbins JM, Garneau-Tsodikova S, Kennedy, DR (2025). *Development of zafirlukast analogues for improved antithrombotic activity through thiol isomerase inhibition*. Arteriosclerosis, Thrombosis and Vascular Biology (ATVB) 20 February 2025. Volume 45, Number 4, e136-e149. doi.org/10.1161/ATVBAHA.124.321579. **Data from this manuscript is shown in Chapter 2.**
- **Keovilay JK,** Szahaj MK, Bekendam RH, Wurl SE, Pantos MM, Verbetsky CA, Dufresne A, Shea M, Howard KC, Tsodikov OV, Garneau-Tsodikova S, Zwicker JI, Kennedy DR (2023). *Targeting thiol isomerase activity with zafirlukast to treat ovarian cancer from the bench to clinic.* FASEB J May 2023. 37(5): e22914. doi: 10.1096/fj.202201952R. **Data from this manuscript is shown in Chapter 3.**
- Holbrook LM, Keeton SJ, Sasikumar P, Nock S, **Gelzinis J**, Brunt E, Ryan S, Pantos MM, Verbetsky CA, Gibbins JM, Kennedy DR (2021). *Zafirlukast is a broad-spectrum thiol isomerase inhibitor that inhibits thrombosis without altering bleeding*

times. British Journal of Pharmacology February 2021. 178(3): 550-563. doi: 10.1111/bph.15291

- Krajewski D, Polukort SH, **Gelzinis J**, Rovatti J, Kaczenski E, Galinski C, Pantos M, Shah NN, Schneider SS, Kennedy DR, Mathias CB (2020). *Protein disulfide isomerases regulate IgE-mediated mast cell responses and their inhibition confers protective effects during food allergy.* Frontiers in Immunology December 2020. 11: 606837. doi: 10.3389/fimmu.2020.606837

Presentations and Awards

Presentations

POSTER: Vrabel CT, **Keovilay JA**, Szahaj MK, and Kennedy DR. *Investigating pranlukast's role in thiol isomerase inhibition and application in cancer induced thrombosis*. In: AACP annual meeting, 2024, Boston, MA – United States.

POSTER: Gelzinis JA and Kennedy, DR. *The role of zafirlukast and isoquercetin in thiol isomerase inhibition in relation to cancer and its complications*. In: AACR annual meeting, 2023, Orlando, FL – United States.

POSTER: Wurl S, Howard K, **Gelzinis JA**, Gibbins JM, Garneau-Tsodikova S, and Kennedy DR. *Optimizing the potential of zafirlukast as an antithrombotic agent through the creation of second-generation analogues*. In: American Society of Health System Pharmacists midyear clinical meeting, 2022, Las Vegas, NV – United States.

Awards

- **Best poster by a student pharmacist –** AACP annual meeting 2024.

Table of Contents

List of Figures

List of Tables

Chapter 1

General Introduction

In **Chapter 1** I will discuss the overall topics and concepts related to this thesis. I will begin by introducing the background of thiol isomerases including protein disulphide isomerase (PDI) and endoplasmic reticulum resident proteins (ERp) 57, 72 and 5, which will be explored throughout this thesis. I will discuss their general overall function and then move on to how they play into cancer and haemostasis and thrombosis. Additionally, I will introduce different hallmarks of cancer such as angiogenesis, metastasis and inflammation, which will be investigated further within this thesis. Furthermore, I will review different thiol isomerase inhibitors, two of which are a major part of this thesis, zafirlukast and isoquercetin. Finally, I will present the overall study aims, and outline of this thesis.

All figures in this Chapter are original and were made using BioRender.

Please note that the Introduction section of each experimental Chapter (**Chapters 2, 3 and 4**) will further address specific topics related to each Chapter.

Chapter 1. Introduction

1.1 Thiol Isomerase structure and function

1.1.1 Thiol isomerases and their normal function in cells

Thiol isomerases are a family of enzymes mainly localized in the endoplasmic reticulum. There are a total of 21 members in this thioredoxin superfamily (Sharda & Furie, 2018), where the main and most abundant isoform is protein disulphide isomerase (PDI) (Flaumenhaft & Furie, 2016). They are responsible for multiple important cellular activities, especially the oxidation, reduction and isomerization of disulphide bonds in nascent proteins. Through these mechanisms, they ensure proper protein folding in the endoplasmic reticulum but can also act as chaperones by assisting in protein folding without catalytic activity. Normally, localization to the endoplasmic reticulum is obtained through a KDEL retention sequence (Lys-Asp-Glu-Leu), or similar, on the C-terminus, which is recognized by a KDEL-receptor in the Golgi, allowing for the recovery of the protein back to the endoplasmic reticulum (Furie & Flaumenhaft, 2014; Munro & Pelham, 1987). Even with this retention mechanism, they are also able to present themselves on the cell surface of platelets (Chen et al., 1995; Holbrook et al., 2010) and some cancer cells, (Beckmann et al., 2021; Goplen et al., 2006) where they play roles in activities such as haemostasis, thrombus formation, and metastasis (Cho et al., 2012; Stojak et al., 2020; Wu & Essex, 2020). Interestingly, the KDEL sequence is necessary for the presentation of PDI at the cell surface, which occurs through transportation via KDEL receptor 1 (Bartels et al., 2019), and once at the cell surface PDI continues to retain this KDEL sequence (Yoshimori et al., 1990).

Each member of the thiol isomerase protein family has a unique structure and differing functions, but all maintain a common element. They all hold a thioredoxin-like domain which can either reside in a catalytic domain (denoted a, a' or a^0), a substrate binding domain (b or b'), or most commonly, both (Powell & Foster, 2021).

The Cys-X-X-Cys (X is any amino acid) motif in the catalytic domain of thiol isomerases is responsible for oxidoreductase activity (Shili Xu et al., 2014). A thiol isomerase with oxidase activity can interact and form disulphide bonds within a thiol containing substrate that has a lower redox potential (Figure 1.1). As reductases they cleave disulphide bonds of a substrate (Figure 1.1). Finally, as an isomerase they can alter disulphide bond formation and structure with no change in the amount of free thiols effectively causing the rearrangement of disulphide bonds within the substrate protein (Figure 1.1) (Flaumenhaft & Furie, 2016). Meanwhile, the substrate binding domain lacks the CXXC motif and is instead involved with protein-protein interactions (Powell & Foster, 2021).

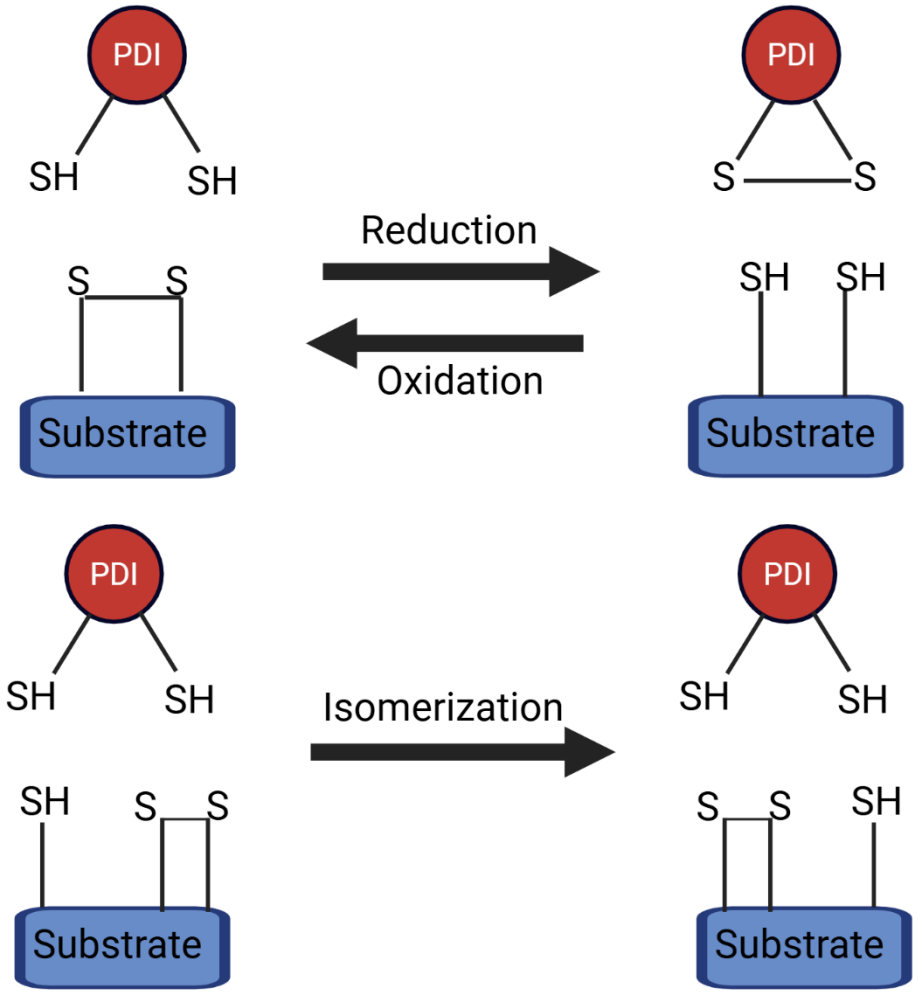

Figure 1.1 The above schematic demonstrates how PDI is involved in the reduction, oxidation and isomerization of disulphide bonds, which ensures proper protein folding in the endoplasmic reticulum.

Thiol isomerases have been found to be present on the surface of platelets and endothelial cells where they carry out multiple processes such as thrombus formation, platelet aggregation and fibrin formation (Cho et al., 2012; Flaumenhaft & Furie, 2016; Holbrook et al., 2010; Jack D. Stopa & Jeffrey I. Zwicker, 2018). Over-expression of these proteins in cancer cells is associated with cell proliferation, metastasis and thrombosis (Kuo et al., 2017; Stojak et al., 2020; Jack D. Stopa & Jeffrey I. Zwicker, 2018). Important thiol isomerases involved with platelets and cancer function include PDI, ERp57, ERp72 and ERp5 (Chen et al., 1995; Goplen et al., 2006; Holbrook et al., 2010; Kranz et al., 2020).

1.1.2 PDI

PDI (gene name PDIA1) was discovered in 1963, through a reaction that reactivated reduced ribonuclease A from chicken pancreas or microsomal preparations of rat liver and given its name in 1972 (Ali Khan & Mutus, 2014; Goldberger et al., 1963; Shergalis & Neamati, 2017; Venetianer & Straub, 1963). It is composed of 508 amino acids and is a 55 kDa "U" shaped protein. The a and a' catalytic domains of PDI reside at the end of its "U" shape and contain the distinctive CGHC motif responsible for oxidoreductase activity. The domains are connected in the following manner: a-b-b'-x link-a'. The a and a' domains are connected through the bottom of the "U" by b and b', the latter which connects to a' via an x-linker (19 amino acids). The b' domain contains a hydrophobic pocket which allows for substrate binding, while the C-terminal holds the KDEL sequence and negatively charged amino acids associated with its chaperone function (Figure 1.2) (Darby et al., 1996; Edman et al., 1985; Hatahet & Ruddock, 2009; Chenghui Liang et al., 2022).

The chaperone activity of PDI is essential to its role in protein folding, where it can differentiate between unfolded, partially folded and fully folded proteins (Irvine et al., 2014). This chaperone activity is regulated through the redox state of PDI, where the oxidized state

has a more open conformation and the reduced state has a closed conformation, allowing in or deterring chaperone substrates respectively (C. Wang et al., 2013).

Under nitrosative or oxidative stress, PDI can undergo post translational modifications from the accumulation of reactive nitrogen species, hydrogen peroxide and reactive oxygen species. One post translational modification of PDI, S-nitrosylation, has been linked to neurogenerative diseases such as Parkinsons's disease, Alzheimer's disease and amyotrophic lateral sclerosis (Nakamura & Lipton, 2011; Uehara et al., 2006a). Another post translational modification of PDI, S-glutathionylation, has been associated with cancer (Townsend et al., 2009). These post translational modifications result in inhibition of the isomerase activity of PDI, leading to misfolded proteins and the unfolded protein response (Townsend et al., 2009; Uehara et al., 2006a), where the cell then attempts to reduce the number of unfolded proteins, but if unsuccessful can result in cell death (Read & Schroder, 2021).

1.1.3 ERp57

Endoplasmic reticulum resident protein 57 (ERp57), encoded by gene PDIA3, was first sequenced in 1988, and mistakenly named phospholipase C alpha (Bennett et al., 1988; Chichiarelli et al., 2022). It is a 57 kDa protein made up of 505 amino acids and goes by multiple names including P58, ER60, ERp60, ERp61, GRP57, GRP58, PI-PLC, HST17083, HEL-S-269, HEL-S-93n and 1,25D3-MARRS. It has a 33% sequence homology to PDI demonstrating a similar "U" structure, domains that are connected in the same fashion and the catalytic site motif remains CGHC (Figure 1.2). However, unlike PDI, ERp57 contains a positively charged pocket on the b' domain. This positive charge is important for interaction with negatively charged substrates (Chichiarelli et al., 2022; Chenghui Liang et al., 2022). Another difference from PDI is that ERp57s retention motif on the C-terminus is QEDL

(Gln-Glu-Asp-Leu) rather than the KDEL (Figure 1.2). This motif is specific to ERp57, as replacing the KDEL with QDEL on PDI demonstrated no ER retention (Urade et al., 1997).

In 1997 it was shown that ERp57 plays a major role in the endoplasmic reticulum interacting in a carbohydrate-dependent manner with newly synthesized secretory and integral membrane glycoproteins and either calnexin or calreticulin (Elliott et al., 1997; Oliver et al., 1997). Later it was determined ERp57 is necessary for the proper folding of these glycoproteins, and some, but not all, require calnexin or calreticulin for correct folding (Jessop et al., 2007). Other processes ERp57 is involved with include proper assembly of the major histocompatibility complex class I peptide loading complex (Hughes & Cresswell, 1998), glucose depletion (Lee, 1981) and vitamin D_3 activity (Nemere et al., 1994; Nemere et al., 2004), the last two of which it was termed GRP58 and 1,25D3-MARRS respectively (Chichiarelli et al., 2022).

1.1.4 ERp72

Endoplasmic reticulum resident protein 72 (ERp72), encoded by PDIA4, is a 72 kDa protein composed of 645 amino acids. ERp72 is the only thiol isomerase that contains 5 thioredoxin-like domains, and it also differs from PDI and ERp57 with its lack of a x-linker and a more crescent like shape. The domains are connected in a: a^0-a-b-b'-a' manner. Catalytic sites reside in a^0 and a', while substrate binding occurs in a' and a. ERp72's b' domain has a negatively charged area making is a poor site for binding (Figure 1.2). However, there are hydrophobic areas next to the catalytic sites that allow for substrate binding (Chenghui Liang et al., 2022). The ER retrieval motif for ERp72 is different from that of both PDI and ERp57, where instead at the C-terminus is a KEEL motif (Lys-Glu-Glu-Leu) needed for ER retention (Figure 1.2) (Mazzarella et al., 1990), where deletion of this motif in COS-7 cells results in ERp72 secretion (Wang et al., 2020). It is thought that ERp72 responds to endoplasmic reticulum stress as CHO cells stimulated with thapsigargin or

tunicamycin (known to cause endoplasmic reticulum stress) results in an increase in ERp72 secretion (Dorner et al., 1990). Additionally, ERp72 is involved in the folding of certain proteins such as being part of the complex of endoplasmic reticulum chaperones that properly folds interferon-γ (Vandenbroeck et al., 2006). Additionally, ERp72 has the ability to retain misfolded proteins, such as cholera toxin, in the endoplasmic reticulum and properly refold them (Forster et al., 2006). Other than the endoplasmic reticulum, ERp72 has also been found to be important in the signal transduction pathway for priming human neutrophils (Weisbart, 1992). Where recently it was discovered endothelial ERp72 plays a role in in the inflammatory response following skeletal muscle injury through the regulation of neutrophil adhesion (Khalaf et al., 2021).

1.1.5 ERp5

Endoplasmic reticulum resident protein 5 (ERp5), encoded by its gene PDIA6, is a 440 amino acid 48 kDa protein with two thioredoxin domains (Jordan et al., 2005). The domains are arranged in an a-a'-b formation, with active sites residing on a and a' (Figure 1.2) (Kikuchi et al., 2002; Sharda & Furie, 2018). These active domains have a 47% sequence identity with those of PDI. Like PDI, it's ER retrieval motif on the C-terminus is the KDEL sequence (Furie & Flaumenhaft, 2014). ERp5 is linked to MHC class I chain-related protein A (MICA) shedding (Jinushi et al., 2008) through an interaction of ERp5 with a six amino acid motif in the α3 domain of MICA (Wang et al., 2009).

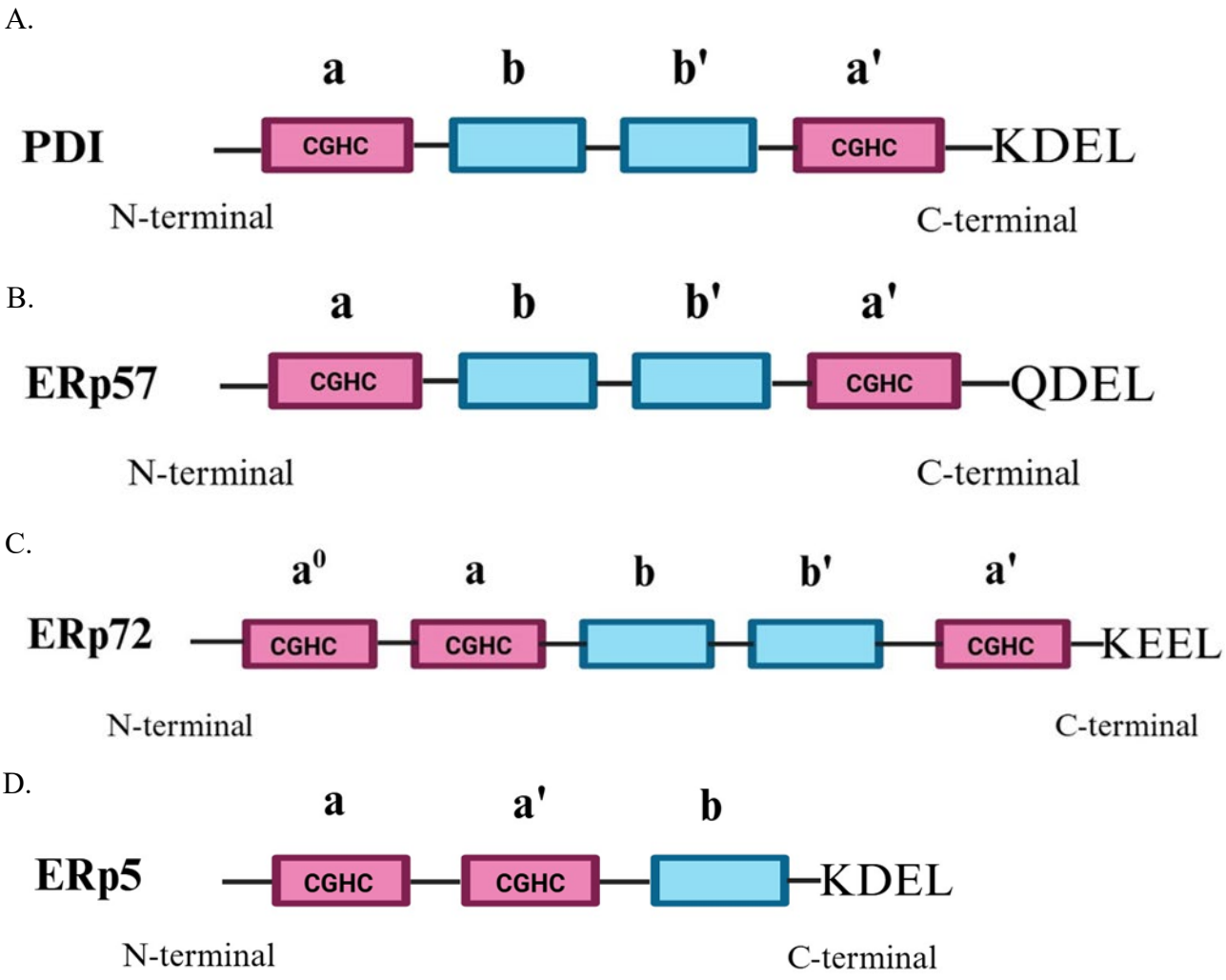

Figure 1.2 A representative schematic of PDI, ERp57, ERp72 and ERp5. (A) For PDI, the a and a' domains contain the CGHC catalytic motif responsible for oxidoreductase activity, while the b' domain contains a hydrophobic pocket necessary for substrate binding. The KDEL retention sequence resides at the C-terminal. (B) For ERp57, the a and a' domains contain the CGHC catalytic motif responsible for oxidoreductase activity, where the b' domain contains a positively charged pocket important for interaction with negatively charged substrates. The QDEL retention sequence resides at the C-terminal. (C) ERp72 consists of 5 thioredoxin-like domains, where a^0 and a' contain the catalytic sites and a and a' substrate binding sites. The b' domain is negatively charged, and the KEEL retention sequence resides at the C-terminal. (D) ERp5 consists of only 3 thioredoxin-like domains, where a and a' contain the active sites. The KDEL retention sequence resides at the C-terminal.

1.2 Thiol isomerases and their role in cancer

1.2.3 Cancer cell biology and thiol isomerases

The second leading cause of death in the United States and globally is cancer (CDC, 2023; Mortality & Causes of Death, 2016; Nagai & Kim, 2017). Alteration of proteins, signalling pathways and other factors play a role in the transition of a healthy, normal cell into one that is malignant (Gupta et al., 2010). Malignant cells acquire the abilities to abnormally proliferate, avoid apoptosis, sustain angiogenesis, invade other tissues and metastasise (Hanahan & Weinberg, 2000). The extracellular activity of PDI, ERp57, ERp72 and ERp5 play important roles in cancer progression, and their expression is upregulated in a variety of cancer types such as brain, lymphoma, kidney, ovarian, prostate and lung (Shili Xu et al., 2014). High expression of these proteins can affect proliferation, adhesion and metastasis of malignant cells and increase the risk of thromboembolism (Kuo et al., 2017; Stojak et al., 2020; Jeffrey I. Zwicker et al., 2019). Elevated levels of PDI have been reported in colorectal and ovarian tumours (Samanta et al., 2017), which correlates to tumour states and poor survival within patients. Elevated levels of ERp57 have also been reported in colorectal cancer cells, and knock down of ERp57 leads to a decrease in proliferation, an increase in apoptosis, and morphological changes of the cell (Yang et al., 2018). In chemotherapy resistant He-La cells, PDI was shown to be upregulated, and when treated with the thiol isomerase inhibitor bacitracin, allowed for the chemotherapy drug (Aplidin) to overcome its resistance and demonstrate some inhibition (González-Santiago et al., 2007). However, bacitracin is nephrotoxic (Michie et al., 1949) and would not be a good candidate to use with a chemotherapy regimen *in vivo*. Nevertheless, this study suggests investigating a chemotherapy and thiol isomerase inhibitor combination could prove to be a useful therapeutic regimen.

1.2.4 Thiol isomerases interact with other associated cancer proteins

Thiol isomerases have also been shown to affect other cancer associated proteins such as epidermal growth factor receptor (EGFR), a cell surface receptor that is often overexpressed and improperly activated in many cancers such as lung, breast and glioblastoma leading to tumorigenesis (Sigismund et al., 2018). Silencing of ERp57 in breast cancer cells (MDA-MB-468) reduced the phosphorylation of EGFR and its downstream target, STAT-3 after EGF stimulation (Elisa Gaucci et al., 2013) (Figure 1.3). In addition, EGFR is also related to another thiol isomerase, thioredoxin, which is required in order for EGFR to be presented at the surface of the cell (Dong et al., 2015). Downstream of EGFR is GRB2-associated binder 1 (GAB1), where elevated levels of the protein in multiple cancer types leads to a generally worse prognosis (Perez-Baena et al., 2023).

Depletion of PDI also induces endoplasmic reticulum stress triggering multiple pathways such as the PERK and p53 pathways (Kranz et al., 2020; Ozcelik & Pezacki, 2019). A major tumour suppressor gene, p53 is involved in activating cell cycle checkpoints in response to DNA damage, halting cell division (Shiloh, 2003). Inhibition of PDI activity with the drug origamicin was able to activate p53 and downstream targets involved in cancer regulation (Ozcelik & Pezacki, 2019) (Figure 1.3). Another protein associated with PDI is PERK, which is a transmembrane protein kinase which regulates endoplasmic reticulum chaperones by reducing new protein synthesis and has been associated with facilitating tumour growth (Bobrovnikova-Marjon et al., 2010). Recently it has been shown that PDI is necessary for PERK signalling, and knockdown of PDI induced endoplasmic reticulum stress in human pancreatic, lung and colon cancer cells reducing the expression of proteins in the PERK signalling pathway including PERK, elF2α, ATF4, CHOP and BiP (Kranz et al., 2020) (Figure 1.3).

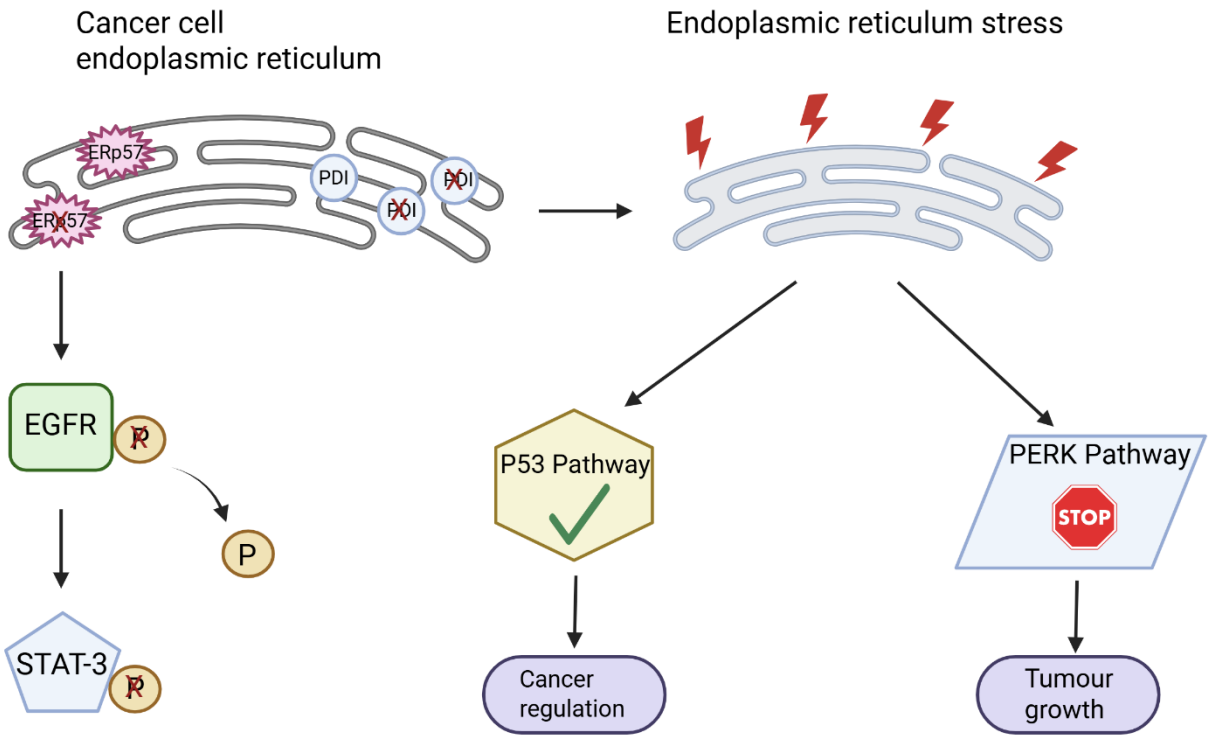

Figure 1.3 Thiol isomerases regulate cancer cell signalling. Silencing of ERp57 in breast cancer cells leads to reduced phosphorylation of EGFR and downstream target STAT-3, while depletion of PDI in cancer cells leads to endoplasmic reticulum stress. This stress can turn on the P53 pathway leading to cancer regulation, while reducing expression of proteins in the PERK pathway leading to suppression of tumour growth.

1.3 Hallmarks of cancer

1.3.1 Angiogenesis and its related factors

Angiogenesis is the formation and growth of new blood vessels, essential for healthy embryonic development, wound healing and normal distribution of proteins and nutrients throughout the body (Carmeliet, 2005; Song et al., 2024). Although this process is a normal function, it can also prove to be dangerous under the wrong conditions. In order for cancer cells to grow and metastasise, angiogenesis is necessary to expand the vascular network (Nishida et al., 2006).

1.3.1.1 Vascular endothelial growth factor

Vascular endothelial growth factors (VEGFs) are the major players in mediating angiogenesis in cancer and are found to be upregulated by oncogene expression and multiple growth factors (Carmeliet, 2005). Therefore, the inhibition of VEGFs is a favourable target in cancer therapy.

There are multiple VEGFs and multiple receptor tyrosine kinase VEGF receptors (VEGFRs), where the most notable combination is the VEGFA/VEGFR-2 signalling pathway (Abhinand et al., 2016). When bound, this complex activates other downstream pathways including mitogen activated protein kinases (MAPK), PI3K, Akt, PLC-γ, and small GTPases leading to endothelial proliferation, filopodial extension, degradation of the extracellular matrix (ECM) and angiogenesis (Figure 1.4) (Abhinand et al., 2016).

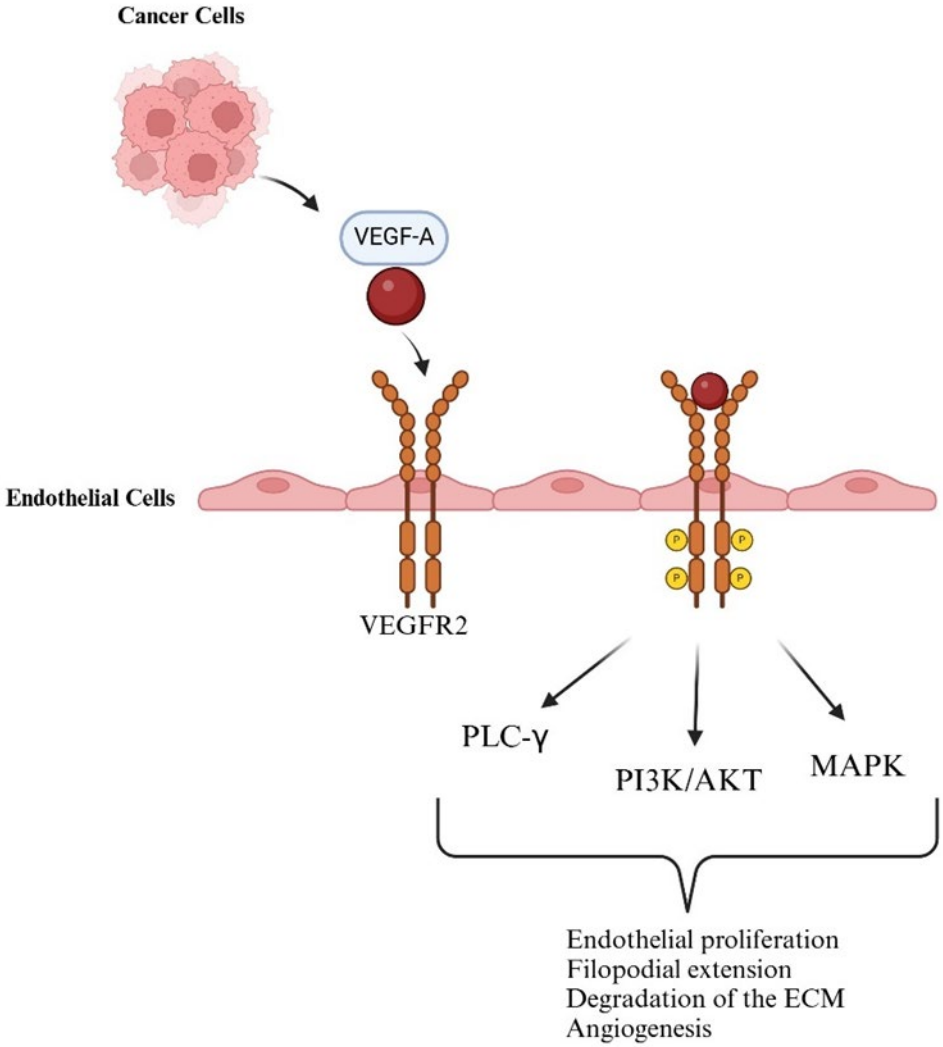

Figure 1.4 A representative schematic of the VEGFA/VEGFR2 signalling pathway. VEGFA is secreted from cells such as cancer cells and binds to the VEGFR2 receptor. Upon binding, the receptor becomes phosphorylated, in turn activating pathways such as PLC-γ, PI3K/AKT and MAPK leading to processes such as endothelial proliferation, filopodial extension, degradation of the ECM and angiogenesis.

Recently, PDI has been shown to be associated with VEGF-induced H_2O_2 signalling and VEGFR2. Here it was determined PDI acts as a redox sensor leading to angiogenesis (Nagarkoti et al., 2023). Although this study aimed to use PDI as a therapeutic to promote reparative neovascularization in response to tissue ischemia, it would be interesting to study the relationship between PDI and VEGF in a cancer model, as both have been shown to be overexpressed.

1.3.1.2 Degradation of the extracellular matrix

Associated with VEGF is the urokinase-type plasminogen activator receptor (uPAR). Binding of VEGF to VEGFR2 triggers uPAR to bind to urokinase-plasminogen activator in turn leading to cleavage of plasminogen to activated plasmin. Activated plasmin then initiates the degradation of the extracellular matrix allowing endothelial cells to migrate (Breuss & Uhrin, 2012; Uhrin & Breuss, 2013).

In order for the extracellular matrix to degrade, the activated plasmin triggers pro-metalloproteinases into active metalloproteinases (Breuss & Uhrin, 2012). Some notable metalloproteinases are matrix metalloproteinase 1 (MMP-1) and matrix metalloproteinase 9 (MMP-9). MMP-1 degrades collagen types I, II and III in the extracellular matrix and has also been shown to upregulate VEGFR2 when used to stimulate endothelial cells leading to increased VEGFA signalling (Mazor et al., 2013). In addition, MMP-1 is associated with multiple cancer types including colorectal, gastric, oesophageal, pancreatic, and breast cancer (Inoue et al., 1999; Ito et al., 1999; Murray et al., 1998; Murray et al., 1996; Nakopoulou et al., 1999; Poola et al., 2005). MMP-9 rearranges the extracellular matrix through the alteration of aggrecan, collagens, elastin, fibronectin, laminins glycosaminoglycans and latent signalling proteins (Quintero-Fabian et al., 2019). It was demonstrated that MMP-9 acts as an angiogenic switch in pancreatic carcinogenic model by increasing the availability of VEGF (Bergers et al., 2000).

1.3.1.3 Tissue inhibitors of metalloproteinases

In order for MMPs to function properly they are regulated by tissue inhibitors of metalloproteinases (TIMPs). TIMP-2 is a direct inhibitor of angiogenesis and endothelial cell proliferation. It can inhibit MMP's, in turn stopping the rearrangement of the extracellular matrix leading to the inhibition of angiogenesis (Figure 1.5) (Stetler-Stevenson & Seo, 2005). Additionally, TIMP-2 inhibits phosphorylation of VEGFR-2 on endothelial cells stimulated with VEGFA independently of MMP inhibition (Figure 1.5) (Lee et al., 2010).

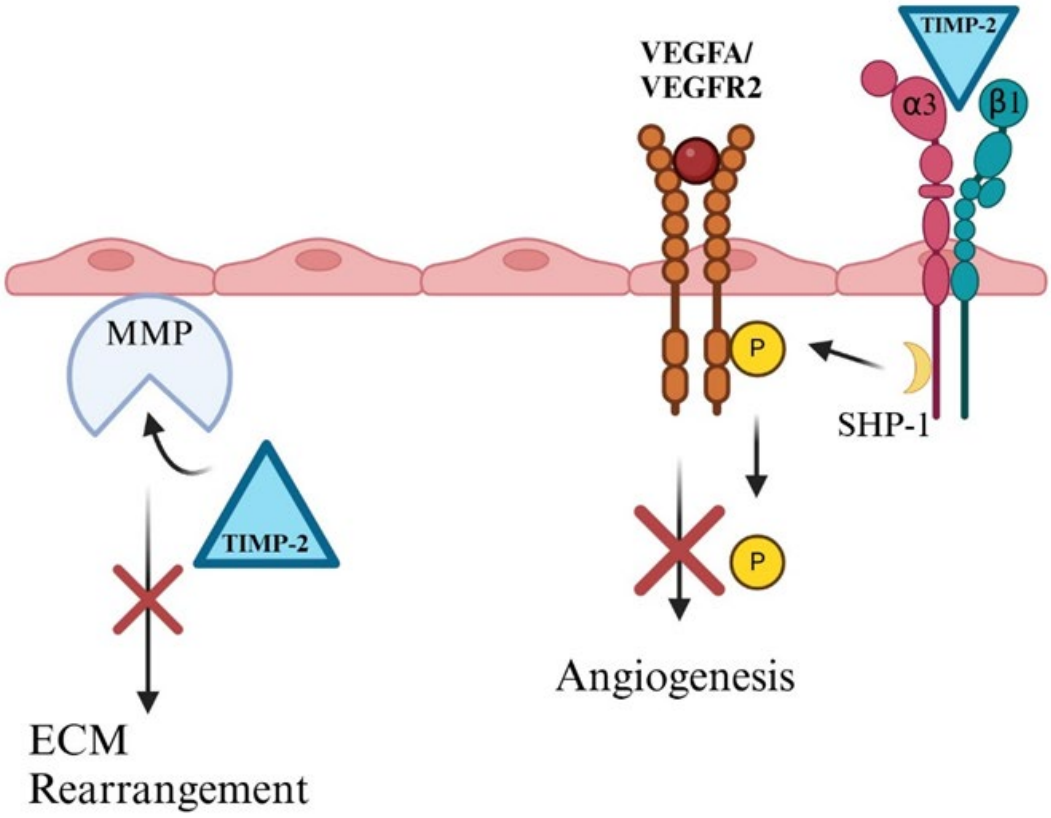

Figure 1.5 TIMP-2 regulates MMPs and inhibits angiogenesis. TIMP-2 can inhibit angiogenesis by directly binding and inhibiting MMPs therefore stopping the MMPs from ECM rearrangement. Alternatively, TIMP-2 can bind to α3β1, allowing SHP-1 to dephosphorylate the VEGFA/VEGFR2 complex leading to inhibition of angiogenesis.

1.3.2 Metastasis

Metastasis, the migration of cells from a primary tumour to other organs of the body, uses the new blood vessels developed through angiogenic processes to leave the primary tumour and enter circulation. It is the primary cause of mortality in cancer patients (Suhail et al., 2019). In order for cells from a primary tumour to invade distant tissues they must be able to attach to the vascular endothelium via selectins and integrins (Bendas & Borsig, 2012). Integrins are glycoprotein receptors that can attach cancer cells to extracellular matrix proteins such as fibronectin, fibrinogen, vitronectin, laminins, collagens, plasminogen, osteopontin and von Willebrand factor (VWF) (Hamidi & Ivaska, 2018). Receptors associated with metastasis include integrins $\alpha_v\beta_3$, $\alpha_v\beta_5$, $\alpha_5\beta_1$, $\alpha_2\beta_1$ and $\alpha_6\beta_4$ (Hamidi & Ivaska, 2018; Popielarski et al., 2019). The vascular adhesion molecules known as selectins play a role in metastasis by recruiting myeloid derived cells and promoting tumour cell adhesion (Borsig, 2018).

Thiol isomerases can also contribute to metastasis. On the surface of Mn^{2+} activated endothelial cells, PDI forms a complex with $\alpha_v\beta_3$ converting the integrin to a high affinity state for ligand binding, such as vitronectin, likely mediating cell adhesion and migration (Swiatkowska et al., 2008). Inhibition of PDI was able to suppress the adhesion of breast cancer cells to the endothelium, fibronectin and collagen as well as decrease their trans endothelial migration (Stojak et al., 2020). In specimens taken from patients with uveal melanoma that is likely to metastasize, ERp57 demonstrated increased expression (Linge et al., 2012). Additionally, cell surface ERp5 is necessary for associated tumour ligand shedding required for metastasis (Kaiser et al., 2007). With multiple thiol isomerases being involved in metastasis investigating a broad-spectrum inhibitor could prove useful for inhibiting migration.

1.3.3 Inflammation and its related markers

Inflammation is the body's response to repair tissue injury, fight off infection or combat toxic compounds and irradiation (Chen et al., 2018). An inflammatory response, no matter the stimuli, will follow a common mechanism including recognition of the stimuli, which activates inflammatory pathways, then the release of inflammatory markers and finally recruitment of inflammatory cells (Chen et al., 2018). Acute inflammation is a response to a stimulus that lasts for only a short period of time, where chronic inflammation lasts for a prolonged period of time, and when left untreated leads to a poor prognosis (Pahwa et al., 2025). Chronic inflammation also promotes tumour progression and treatment resistance and is a prime characteristic of cancer (Zhao et al., 2021). It is known that thiol isomerases play a role in vascular inflammation (Essex & Wang, 2024), and they likely play a role in cancer related inflammation. Targeting inflammation markers can be a useful strategy in slowing tumour growth and progression.

1.3.3.1 Transmembrane protein 176B

Transmembrane protein 176B (TMEM176B) an immunoregulatory cation channel, is expressed in cells involved in inflammation including monocytes, macrophages and $CD11b^+$ dendritic cells and acts as a negative regulator of inflammasome activation (Segovia et al., 2019). Interfering with TMEM176B, such as with TMEM176B inhibitor BayK8644, results in inflammasome activation and allows for the inhibition of thymic lymphoma, lung and colon tumour growth through $CD8^+$ T cell-mediation (Segovia et al., 2019) TMEM176B has also been demonstrated to contribute to breast (Kang et al., 2021), gastric (Li et al., 2024) and melanoma cancer (Jiang et al., 2022), yielding it to be an interesting inflammatory marker for exploration in regard to tumour growth and progression.

1.3.3.2 Programmed cell death ligand 1

Another marker involved in inflammation which is highly expressed on tumour cells is programmed cell death ligand 1 (PD-L1). PD-L1 expressed on tumour cells will bind to programmed cell death protein 1 (PD-1) on T-cells and through inhibition of T-cell function allows tumour cells to escape from T-cell mediated cell death (Figure 1.6) (Lu et al., 2019). PD-L1 has been associated with breast, lung, colorectal, gastric, bladder, pancreatic and prostate cancer where high levels of expression are associated with malignancy and poor prognosis (Han et al., 2020). Inhibition of PD-1 or PD-L1 can block their interaction and signalling resulting in restored T-cell activity leading to tumour cell death (Lin et al., 2024). PD-1/PD-L1 receptor antagonists including nivolumab, pembrolizumab, JQ1, atezolizumab, avelumab, and cemiplimab can block the effects of the PD-1/PD-L1 complex playing a critical role in cancer treatment (Han et al., 2020).

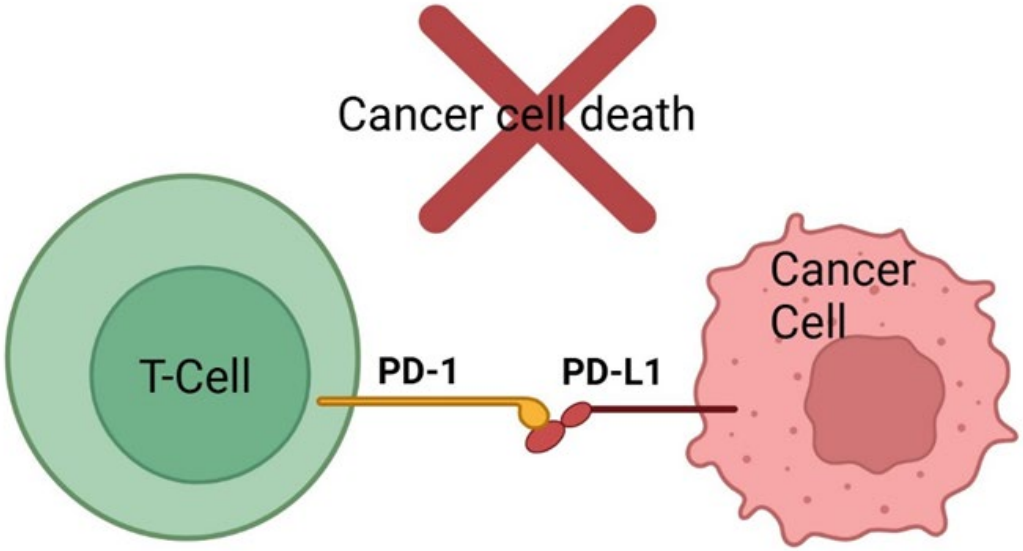

Figure 1.6 PD-L1 from cancer cells binds to PD-1 on T-Cells blocking the T-Cells from attacking the cancer cells and preventing cancer cell death. Inhibition of PD-L1 on cancer cells allows for T-Cells to properly attack the cancer cells leading to cancer cell death.

1.3.3.3 Interleukins

Interleukins play a major role in inflammation, having both pro and anti-inflammatory properties. Although mainly produced by leukocytes, interleukins have been found to be expressed by many cell types including cancer cells (Justiz Vaillant & Qurie, 2025; Kobold et al., 2013; Kumari et al., 2016; Ning et al., 2011). Two interleukins that play a major role in cancer progression include interleukin 6 (IL-6) and interleukin 8 (IL-8). IL-6 has been found to be expressed highly in the tumour and serum of colorectal (Waldner et al., 2012), breast (Dethlefsen et al., 2013), prostate (Culig & Puhr, 2012), ovarian (Maccio & Madeddu, 2013), pancreatic (Miura et al., 2015), lung (Chang et al., 2013), renal (Altundag et al., 2005), and cervical cancers (Wei et al., 2003), where it is involved in proliferation and differentiation (Kumari et al., 2016). High levels of circulating IL-6 have been associated with poor prognosis and shorter survival in patients, where lower levels are related to a greater therapy response (Kumari et al., 2016). IL-8 has been shown to be associated with melanoma, prostate, colon, pancreatic, breast and lung cancers (Fousek et al., 2021). It has the ability to influence tumour cells into a proliferative and migratory state, to alter the immune microenvironment and to increase angiogenesis (Fousek et al., 2021).

1.3.3.4 Soluble tumour necrosis factor receptor 1

Another protein involved in inflammation and related to cancer survival is soluble tumour necrosis factor receptor 1 (sTNFR1). sTNFR1 results from enzymatic cleavage of tumour necrosis factor receptor 1 in the plasma (Befekadu et al., 2022) where it binds to circulating tumour necrosis factor (TNF) to reduce TNF-mediated inflammation (Salai et al., 2023). sTNFR1 is associated with both cardiovascular and cancer mortality (Carlsson et al., 2014), and is found to be elevated in the plasma of cancer patients (Hassan et al., 2024). In patients with non-small-cell lung cancer a higher level of sTNFR1 is associated with a higher risk of mortality (Hassan et al., 2024).

1.3.3.5 Platelet derived growth factor-BB

Platelet derived growth factor (PDGF) – BB is a disulphide bonded homodimer and one of the isoforms of the PDGF family (Li et al., 2021). It is an inflammation marker also associated with increased tumour growth and poor prognosis. PDGF-BB has been found to be upregulated in lung adenocarcinoma patients where it is associated with poor survival. Additionally, knockdown of PDGF-BB in A549 lung cancer cells xenografted into mice, reduced tumour growth along with PI3k/AKT and Ras/MAPK signalling (Xiu-Ying et al., 2024).

1.4 Thiol isomerases and their role in haemostasis and thrombosis

1.4.1 Arterial thrombosis and platelet activation

Arterial thrombosis is the blocking of an artery due to platelet activation and formation of a thrombi under high shear stress (Mackman, 2012). It is a leading cause of mortality, and the major sequalae of arterial thromboses include myocardial infarction and ischemic stroke. Myocardial infarction is the obstruction of the flow of blood caused from a buildup of atherosclerotic plaques or when a thrombi forms over a ruptured plaque in an artery (atherothrombosis) (Ojha & Dhamoon, 2025). Ischemic stroke is similar, except with obstruction in circulation to or within the brain (Wendelboe & Raskob, 2016). Treatment for arterial thrombosis include anti-platelet drugs that target platelet activation and aggregation (Koupenova et al., 2017; Mackman, 2012).

In the traditional sense, after vessel wall injury, platelets in circulation bind via surface receptors and become activated by collagen and VWF (Golebiewska & Poole, 2015; Stalker et al., 2012), and aggregate. Thrombin, ADP and thromboxane A_2 activate surface receptors (PAR1 and PAR4; $P2Y_1$ and $P2Y_{12}$; TP respectively) on platelets in the vicinity causing a change in shape allowing them to attach to the original monolayer and begin forming a thrombus (Golebiewska & Poole, 2015; Stalker et al., 2012). In addition, integrin $\alpha_{IIb}\beta_3$ increases its affinity for fibrinogen and VWF via "inside-out signalling." Subsequent receptor clustering leads to "outside-in signalling" driving processes necessary for haemostasis such as thrombus formation and platelet spreading (Durrant et al., 2017).

1.4.1.1 Inside-out signalling

Inside-out signalling to integrin $\alpha_{IIb}\beta_3$ begins with the binding of soluble agonists such as ADP, thromboxane A_2, thrombin or epinephrine to G Protein-coupled seven transmembrane domain receptors or via immobilized agonists, such as VWF or collagen, through GPIb-IX-V or GPVI (Huang et al., 2019). The process of inside-out signalling

involves the binding of intracellular activators to $\alpha_{IIb}\beta_3$ tails followed by the separation of the α and β transmembrane domain and cytoplasmic tail (Huang et al., 2019), where then the $\alpha_{IIb}\beta_3$ extracellular domain undergoes a conformational change and ends with a strengthened ligand binding affinity and avidity (Huang et al., 2019). Thioredoxin related transmembrane protein 1 (TMX1) is an inhibitor of $\alpha_{IIb}\beta_3$ activation by keeping cystine residues of $\alpha_{IIb}\beta_3$ as disulphide bonds. When platelet activation occurs, a threshold is reached where inside-out signalling surpasses the inhibitory effect of TMX1 has on $\alpha_{IIb}\beta_3$. It is then that thiol isomerases including PDI, ERp46 and possibly ERp57 and ERp72 will contribute to changes in $\alpha_{IIb}\beta_3$ leaving the integrin in a high-affinity form (Figure 1.7) (Essex & Wang, 2024).

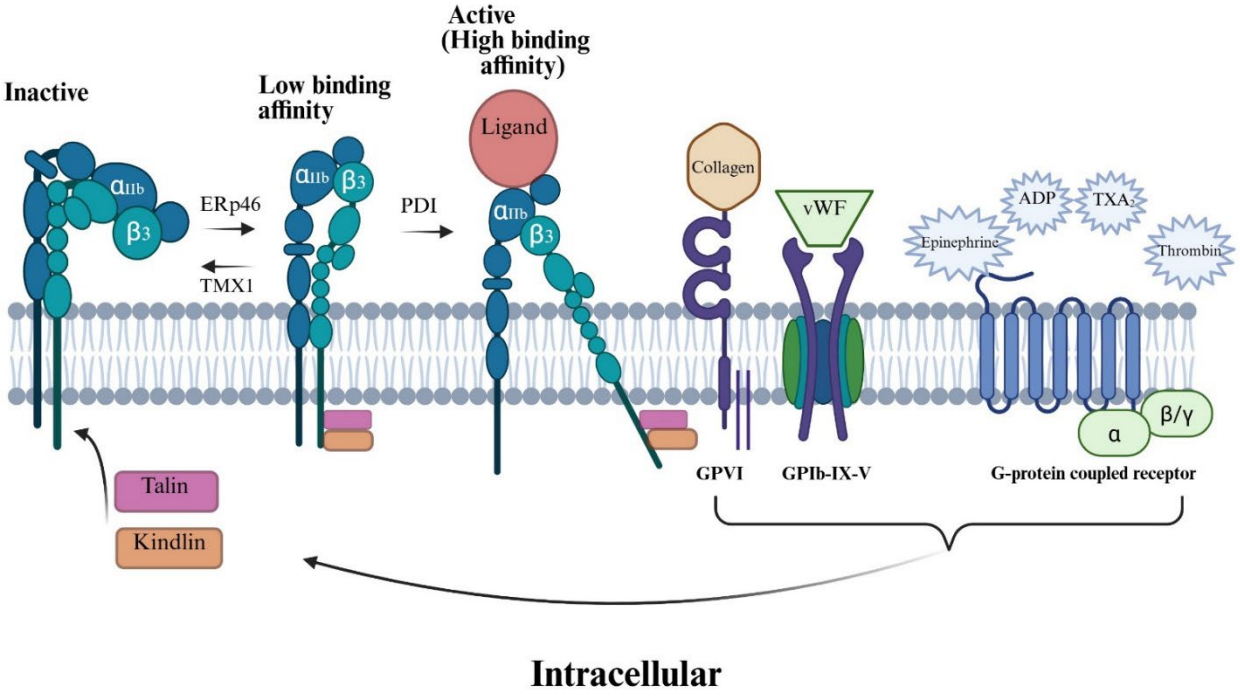

Figure 1.7 A schematic of inside-out signalling. Inside-out signalling begins with the binding of collagen to GPVI, VWF to GPIb-IX-V or, ADP, TXA_2 thrombin or epinephrine to a G-protein coupled seven-transmembrane domain receptor. This binding then allows intracellular activators such as talin and kindlin to bind to the $\alpha_{IIb}\beta_3$ tails. This binding along with thiol isomerases allows for the separation of the α and β transmembrane domain and cytoplasmic tail leading to a conformational change putting integrin in an active high binding affinity state.

1.4.1.2 Integrin outside-in signalling

The process of "inside-out" signalling then leads to "outside-in" signalling following ligand binding to integrins and αIIbβ3 clustering. Outside-in signalling begins by activating the tyrosine kinase c-Src, which then commences intracellular signalling with pathways including FAK, Syk, RhoGAP, RhoGEFs, PI3K and Rac-GEFs, leading to processes necessary for homeostasis such as platelet spreading and clot retraction (Figure 1.8) (Fong et al., 2016; Huang et al., 2019). These processes of clot retraction and platelet spreading on fibrinogen are mediated through the thiol isomerase ERp46 (Essex & Wang, 2024). In addition to ERp46, ERp57 has also been shown to modulate outside-in signalling (Holbrook et al., 2012b).

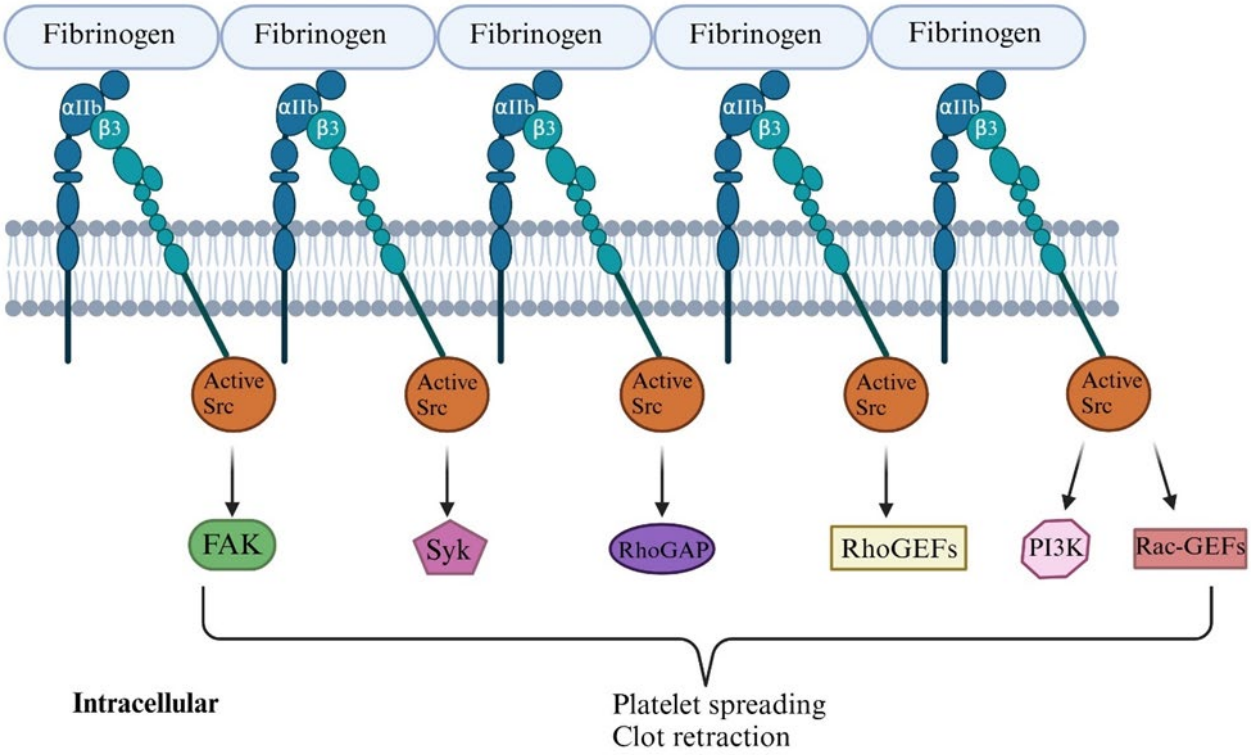

Figure 1.8 A schematic of outside-in signalling. Inside-out signalling leads to outside-in signalling, where the binding of fibrinogen to $\alpha_{IIb}\beta_3$ activates the tyrosine kinase c-Src, which can then activate multiple different pathways including FAK, Syk, RhoGAP, RhoGEFs, PI3K and Rac-GEFs. Activation of these pathways leads to processes necessary for homeostasis such as platelet spreading and clot retraction.

1.4.1.3 Thiol isomerases in arterial thrombosis

Interestingly, multiple thiol isomerases secreted by platelets and endothelial cells are involved in arterial thrombosis (Cho et al., 2008; Jasuja et al., 2010; L. Wang et al., 2013; Zhou et al., 2017). PDI is released from endothelial cells and platelets before tissue factor and platelet accumulation, almost immediately after injury, and interact with tissue factor and proteins on the platelet surface (Cho et al., 2008; Jasuja et al., 2010; Sharda & Furie, 2018) (Figure 1.9). In an arterial laser induced injury model, PDI accumulated quickly and prior to the accumulation of platelets at the site of vessel injury. When a PDI-inhibitory antibody was introduced, thrombus formation and fibrin generation were blocked (Cho et al., 2008). Then in 2010, Jasuja et al., showed through the same model that PDI secreted from platelets adds to the total thrombus formation, but it is actually PDI secreted from the injured endothelial cells that is essential for fibrin generation and thrombus formation. PDI binds to endothelial integrin $\alpha_v\beta_3$ and platelet integrin $\alpha_{IIb}\beta_3$, where β3 null mice have demonstrated this interaction is necessary for the fibrin and thrombus formation at the site of injury (Cho et al., 2012; Swiatkowska et al., 2008). Furthermore, it was shown with an ERp57 specific inhibitory antibody that inhibiting ERp57 also blocks platelet accumulation (Holbrook et al., 2012b) and fibrin formation (Zhou et al., 2014a) in an arterial laser induced injury model, where specifically it is the second active site of ERp57 that mediates these functions (Zhou et al., 2014a). In addition, in the same laser induced arterial thrombosis model, inhibiting ERp72 reduces platelet accumulation and thrombus size (Holbrook et al., 2018a), and a mouse knockout model for ERp72 in platelets demonstrated lower platelet accumulation without affecting fibrin formation (Zhou et al., 2017). However, when endothelial ERp72 was eliminated, both platelet accumulation and fibrin formation was decreased (Zhou et al., 2017). ERp5 has also been established to be involved in arterial thrombosis, where it was

first shown that anti-ERp5 antibodies inhibit platelet aggregation and fibrinogen binding (Jordan et al., 2005), and then later inhibit *in vivo* arterial thrombus formation and fibrin accumulation (Passam et al., 2015). Additionally, ERp46 is also involved in the formation of arterial thrombi. In both a ferric chloride and laser induced arterial injury model, ERp46 deficient mice demonstrated diminished platelet accumulation compared to control mice (Zhou et al., 2022). Finally, when endoplasmic reticulum oxidoreductase 1α (Ero1α), which regulates PDI activity to modulate platelet function, is inhibited, it demonstrates a decrease in arterial thrombus formation and infarct volume in an ischemic stroke model (Jha et al., 2023).

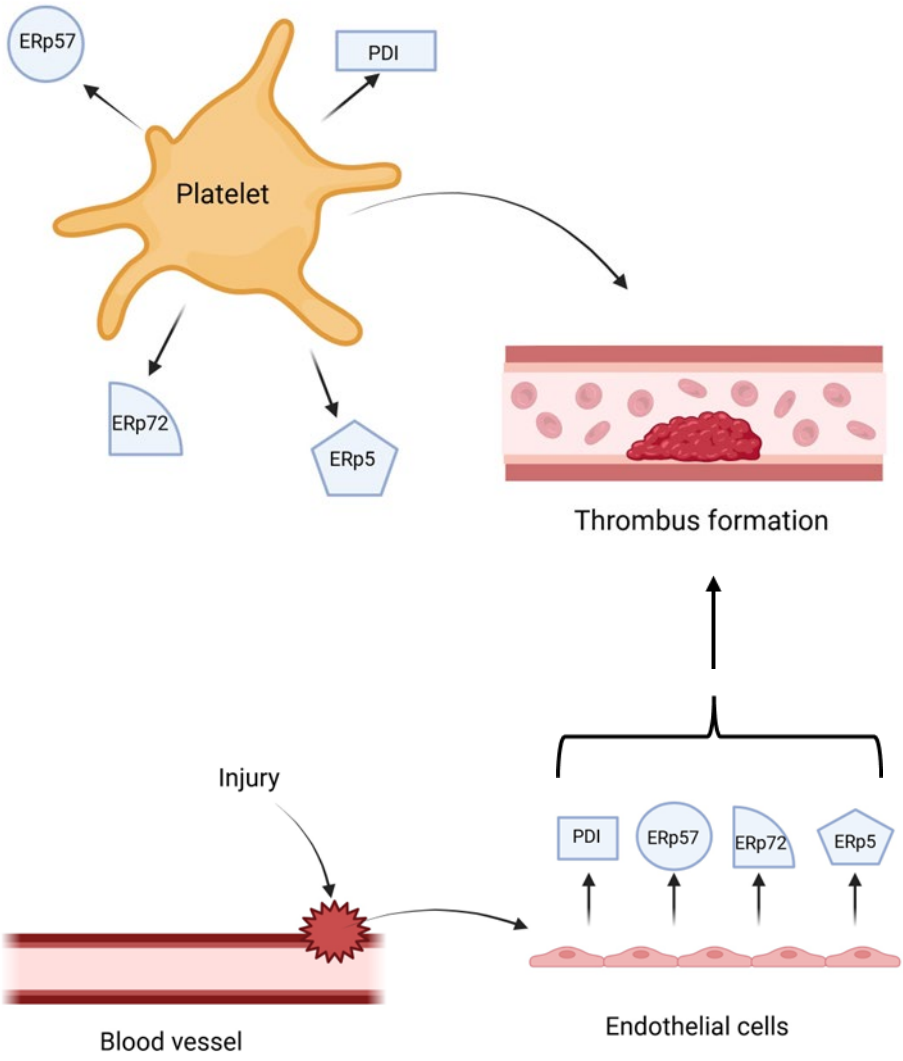

Figure 1.9 Thiol isomerases are involved in arterial thrombosis. Upon vessel injury, thiol isomerases are released from platelets and endothelial cells to interact with tissue factor and other proteins on the platelet surface leading to the formation of a thrombus.

1.4.2 Venous thrombosis and the coagulation cascade

Venous thrombosis is the formation of thrombi in the veins under low shear stress on the surface of an often intact endothelium and includes deep vein thrombosis and pulmonary embolism (Mackman, 2012). Venous thrombi are composed of activated platelets, fibrin and red blood cells and are treated with anti-coagulant drugs that are targeted towards coagulation proteins (Koupenova et al., 2017; Mackman, 2012). Venous thrombosis is related to hospitalizations where surgeries and acute illness account for approximately 50-60% of these venous thrombotic events, and cancer accounts for approximately 20% of these venous thrombotic events (Wendelboe & Raskob, 2016).

The coagulation cascade can be divided into three parts: the intrinsic pathway, the extrinsic pathway, and the common pathway. The intrinsic pathway is triggered through the activation of factor XII. This activation can be attributed to endothelial collagen, extracellular RNA and polyphosphates (Chaudhry et al., 2022; Mackman, 2012). After the activation of factor XII to factor XIIa, the cascade begins to then activate factor XI to factor XIa, which then activates factor IX to factor IXa which then allows for the activation of factor X to factor Xa (Chaudhry et al., 2022). The extrinsic pathway is triggered through tissue factor either released from endothelial cells, circulating leukocytes or microvesicles (Mackman, 2012). Tissue factor activates factor VII to factor VIIa, which then proceeds to activate factor X to Xa. The activation of factor X to Xa from either the intrinsic or extrinsic pathway leads into the common pathway. From here, with the help of factor V, factor Xa cleaves prothrombin (factor II) into thrombin (factor IIa). Thrombin then activates fibrinogen into fibrin to help stabilize the platelet plug (Figure 1.10) (Chaudhry et al., 2022). A proposed mechanism for the initiation of venous thrombosis begins with activation of the endothelium where it expresses P-selectin, E-selectin and VWF, which can then take on leukocytes, tissue factor expressing microvesicles and platelets. The expressed tissue factor

can then trigger the extrinsic pathway, followed by the common pathway leading to a fibrin clot.

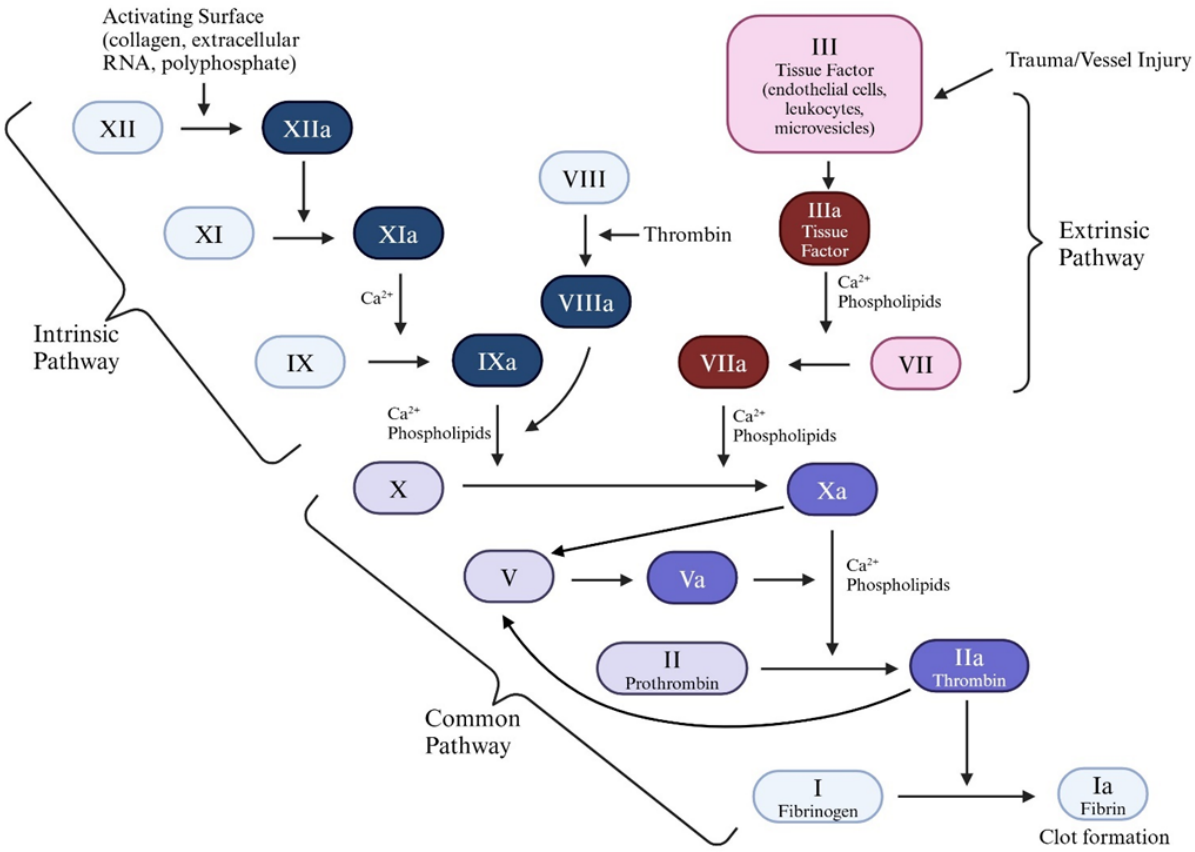

Figure 1.10 The coagulation cascade comprised of the extrinsic pathway, intrinsic pathway, and common pathway. The extrinsic pathway is triggered via trauma or vessel injury leading to the activation of tissue factor (III(a)), which in turn leads to the activation of factor VII (VII(a)), which then leads into the common pathway. The intrinsic pathway is stimulated via an activating surface leading to the activation of factor XII (XII(a)), then factor XI (XI(a)) and then factor IX (IX(a)) then falling into the common pathway. The common pathway begins by the activation of factor X (X(a)) then with the help of activated factor V (V(a)) converts prothrombin (II) into thrombin (IIa), which converts fibrinogen (I) into fibrin (Ia) resulting in a clot formation.

1.4.2.1 Tissue factor

Tissue factor is responsible for initiation of blood coagulation and can reside in its active form, of which it binds to factor VIIa and cleaves factor X, or its non-active or "cryptic" form that does not cleave factor X (Chen et al., 2006). One hypothesis is that PDI is responsible for de-encryption of non-active tissue factor (Chen et al., 2006). The mechanism upon which this occurs is the oxidation of the Cys186-Cys209 free sulphydryls into a disulphide bond, which is necessary for procoagulant activity (Ahamed et al., 2006; Chen et al., 2006). The Cys209 on tissue factor is linked with glutathione that maintains it in the "cryptic" form, where PDI then converts it to a disulphide state. Furthermore, reduced PDI is more efficient at activating tissue factor compared to oxidized PDI (Reinhardt et al., 2008). It has been demonstrated that PDI released from platelets plays a part in activation of tissue factor on microparticles, where the use of bacitracin or an anti-PDI antibody decreased activation (Reinhardt et al., 2008). Additionally, inhibiting PDI in various *in vivo* murine models of thrombus formation lowered tissue factor induced fibrin formation (Reinhardt et al., 2008). However, this mechanism still remains controversial, as it has also been shown PDI inhibition and silencing enhance coagulation and tissue factor procoagulant function (Popescu et al., 2010b). In an endothelial cell model, inhibition of cell surface PDI increased tissue factor procoagulant activity, and addition of exogenous PDI stopped tissue factor activation (Popescu et al., 2010a). This particular study identified PDI as a regulator of phosphatidylserine, where inhibition of PDI increased phosphatidylserine exposure, which is known to enhance coagulation (Popescu et al., 2010a).

1.4.2.2 Thiol isomerases in venous thrombosis

Thiol isomerase involvement in venous thrombosis has not been as extensively studied as its involvement in arterial thrombosis; however, a recent study sheds light on ERp18 in venous thrombosis. In an inferior vena cava stenosis model, ERp18 knockout mice

demonstrated thrombi smaller in both weight and length compared to controls. Interestingly, PDI, ERp57 and ERp5 knockouts demonstrated no significant differences (He et al., 2024). However, multiple studies have shown that inhibiting PDI, ERp57 or ERp5 blocks fibrin generation (Jasuja et al., 2012b; Passam et al., 2015; Zhou et al., 2014a), indicative of venous thrombosis. Therefore, it is possible that thiol isomerases involved in venous thrombosis inhibition is model dependent.

1.4.3 Thiol isomerases in cancer induced thrombosis

After metastasis, cancer induced thrombosis is the second leading cause of mortality in cancer patients (Abdol Razak et al., 2018). Cancer patients can have a 4-7 fold increase of risk of a venous thromboembolism (Falanga et al., 2017), however some studies report up to a 12-fold higher risk than the general population and a 23-fold higher risk in cancer patients receiving chemotherapy (Mulder et al., 2021). Deep vein thrombosis and pulmonary embolism can be caused by tumours compressing veins and reducing blood flow (Abdol Razak et al., 2018). As for arterial thrombosis, one study showed the incidence at 6 months after cancer diagnosis was 4.7% compared to the control cohort at 2.2% (Tuzovic et al., 2018). Many chemotherapy regimens are also associated with arterial thrombosis, such as cisplatin and ponatinib which have 8.3% and 20% rates of arterial thrombotic events respectively (Tuzovic et al., 2018). In hospitalized cancer patients 5.4-7.2% of patients developed a venous thromboembolism while 1.5-5.2% developed an arterial thromboembolism (Khorana et al., 2008; Khorana et al., 2006) Patient factors that have the potential to contribute to thrombosis include tumour type, therapeutics such as chemotherapy and lifestyle factors such as obesity (Khorana et al., 2013). Mechanistic factors that can induce thrombosis include proteins expressed by tumours such as tissue factor, inflammatory cytokines, microparticles, and signal proteins such as VEGF that induces angiogenesis (Falanga et al., 2017). Recently, it was established that cancer patients with high levels of

circulating PDI released from endothelial cells associate with a 7-fold higher risk of thromboembolic events compared to patients with low circulating PDI levels (Sharda et al., 2021).

Thiol isomerases are especially of interest for cancer induced thrombosis because platelets and endothelial cells secrete PDI, ERp57, ERp72 and ERp5 upon injury to the vessel wall where each has a distinct role in thrombosis and haemostasis (Chenghui Liang et al., 2022) as described earlier. Myeloproliferative neoplasms are a category of blood cancers that lead to an increase of red blood cells, white blood cells and platelets, where the most common complication are thromboembolic events. In a study of 92 patients, 65 with myeloproliferative neoplasms and 27 controls, 55 patients in the myeloproliferative neoplasm cohort showed elevated PDI levels (Sharda et al., 2021). Interestingly, in these patients 8 developed a thromboembolic event, 4 of which were arterial and 4 of which were venous. Patients with lower PDI levels had a cumulative incidence of 5.5%, while those with elevated PDI levels had a cumulative incidence of 26.6% (Sharda et al., 2021). PDI expression is also elevated in a variety of cancer types including brain, lymphoma, kidney, ovarian, prostate and lung cancers (Shili Xu et al., 2014) and found elevated in the blood of breast cancer patients (Yang et al., 2022) likely helping contribute to thrombotic events. Currently, there are no anti-thrombotic agents that target both venous and arterial thromboembolism. However targeting thiol isomerases and their individually distinct mechanisms could contribute to a new way to target both, which will be explored further on in this thesis.

1.5 Inhibitors of thiol isomerases

Considering the involvement of PDI, ERp57, ERp72 and ERp5 in both cancer and thrombosis, inhibitors of the enzymes would have strong therapeutic potential. Known thiol isomerase inhibitors include bacitracin (Dickerhof et al., 2011), PACMA 31 (Xu et al., 2012a), CCF642 (Vatolin et al., 2016), bepristats (Bekendam et al., 2016), zafirlukast (Holbrook et al., 2021), as well as the flavonoids rutin and isoquercetin (Jasuja et al., 2012b).

1.5.1 Bacitracin

Bacitracin is an antibiotic that works as a broad-spectrum thiol isomerase inhibitor with an IC_{50} of 90 μM, targeting PDI, ERp57, ERp72, ERp5 and possibly others by forming disulphide bonds with cysteine residues within the substrate binding domain (Dickerhof et al., 2011; Mandel et al., 1993; Shili Xu et al., 2014). In melanoma cells, it did not induce apoptosis or decrease cell viability, rather it enhanced cytotoxic effects of other drugs (Lovat et al., 2008). However, due to its severe nephrotoxicity, it can only be used topically and would not be suitable as a systemic therapy (Michie et al., 1949; Shili Xu et al., 2014).

1.5.2 PACMA31

PACMA31 is a membrane permeable, irreversible PDI selective inhibitor with a reported IC_{50} of 10 μM in ovarian cancer cells (Xu et al., 2012a; Shili Xu et al., 2014). The molecule binds to the active site of PDI through covalent bonds with cysteine residues (Xu et al., 2012a). It was shown to have cytotoxic effects on OVCAR8 cells *in vitro*, and *in vivo* in mice was well tolerated, orally available and suppressed ovarian tumour growth with no major side effects (Xu et al., 2012a).

1.5.3 CCF642

CCF642 can inhibit multiple thiol isomerases including PDI, ERp57 and ERp72, where it has been shown in PDI to covalently bind to lysine in the active site (Vatolin et al., 2016). In three multiple myeloma cell lines, the molecule exhibited an IC_{50} of less than 1

μM and showed a greater reduction in PDI activity at 3 μM compared to 100 μM of PACMA31 (Vatolin et al., 2016). An *in vivo* multiple myeloma mouse model demonstrated a significantly improved life span of mice treated with CCF642 compared to the vehicle control and was deemed well tolerated (Vatolin et al., 2016). Recently, a new analogue, CCF642-34, has been developed with improved solubility, selectivity, potency and which specifically inhibits PDI (Hasipek et al., 2021).

1.5.4 Bepristats

Bepristats are a family of reversible PDI inhibitors that target the b' substrate-binding pocket resulting in the displacement of the x-linker which in turn enhances catalytic activity of a and a' domains (Bekendam et al., 2016). Bepristat 1b and bepristat 2a were able to inhibit platelet aggregation but did not alter P-selectin exposure suggesting they inhibit aggregation through downstream intervention (Bekendam et al., 2016). Additionally, infusion of bepristat 1a and bepristat 2a into mice subjected to arterial laser injury demonstrated significant inhibition of platelet accumulation compared to controls (Bekendam et al., 2016).

1.5.5 Zafirlukast, Montelukast and Pranlukast

Recently, our lab has reported the leukotriene receptor (LTR) antagonist zafirlukast, an FDA approved drug originally developed for the treatment of asthma, to be a broad-spectrum thiol isomerase inhibitor (Holbrook et al., 2021). The structure of zafirlukast includes a cyclopentyl carbamate attached to an N-methylindole and an arylsulfonamide scaffold linked by a decorated benzoyl ring (Thamban Chandrika et al., 2019) (Figure 1.11).

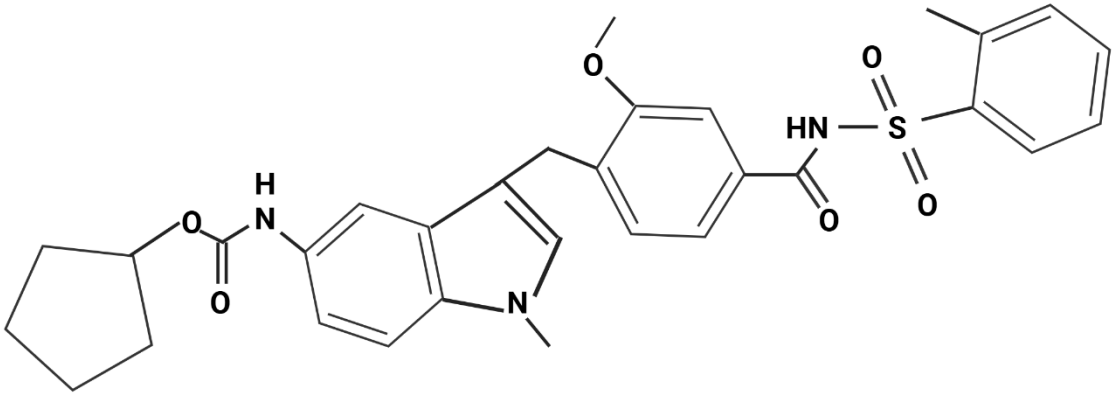

Figure 1.11 The chemical structure of zafirlukast.

It can be well tolerated in humans at a dose of up to 40 mg twice daily, and is most effective on an empty stomach as taken with food can result in up to a 40% loss of bioavailability (Dekhuijzen & Koopmans, 2002).

In the same LTR antagonist family as zafirlukast are the FDA approved compounds pranlukast and montelukast, where montelukast is more potent at inhibiting the LTR1 than zafirlukast (Aharony, 1998). A normal dose of montelukast for patients over 15 years of age is 10 mg once a day (Wermuth et al., 2025), and for pranlukast 225 mg twice daily (Keam et al., 2003). Unlike, zafirlukast, montelukast and pranlukast have no loss in bioavailability before or after a meal (Keam et al., 2003; Wermuth et al., 2025).

We have shown zafirlukast inhibits multiple thiol isomerases (PDI, ERp57, ERp72, ERp5) resulting in a reduction of platelet aggregation, fibrinogen binding and thrombus formation *in vivo*. We additionally deemed montelukast as a pan-thiol isomerase inhibitor, however its ability to inhibit is much weaker compared to zafirlukast (Holbrook et al., 2021). The effects of pranlukast's abilities to inhibit thiol isomerases are explored in **Appendix I** of this work.

Discovery of a pan-thiol isomerase inhibitor such as zafirlukast is an important step, as multiple thiol isomerases play a role in cancer (Powell & Foster, 2021) and thrombosis (Holbrook et al., 2010) and most other known thiol isomerase inhibitors are PDI selective. Recently, one study demonstrated zafirlukast as an inhibitor for lung adenocarcinoma tumour growth in mice (Shi et al., 2022) warranting further research into zafirlukast's effects on other cancer models. Furthermore, modifications to zafirlukast could prove useful, such as removal of the cyclopentyl moiety, which is predicted to reduce the potency of zafirlukast to the LTR1 by more than 100-fold (Bernstein, 1998a). With lower LTR binding affinity, zafirlukast could be more potent at targeting thiol isomerases. Zafirlukast has been shown to have anti-bacterial activity against *P. gingivalis*, and analogues developed from zafirlukast

demonstrated better antibacterial activity along with an increased safety profile (Howard & Garneau-Tsodikova, 2022; Howard et al., 2020a). Analogues of zafirlukast could show promise in areas related to thiol isomerase inhibition.

1.5.6 Flavonoids - Isoquercetin and Rutin

Glycosylated flavonoids, including isoquercetin and quercetin-3-rutinoside (rutin) are also selective PDI inhibitors. Flavonoids are diphenylpropanes containing a C_6-C_3-C_6 base structure (Hertog et al., 1992) and modifications on this base give rise to over 4000 distinct compounds (Cornard, 1998). There are six major groups of flavonoids including isoflavonoids, flavanones, flavanols, flavonols, flavones and anthocyanidins. The basic flavonol structure consists of an unsaturated C ring at the C2-C3 position and then oxidized at C4 and hydroxylated at C3. Positions of additional hydroxyl groups direct the flavonoids' biological activities, such as those in quercetin that reside at C3' and C4' (Abotaleb et al., 2018; Kopustinskiene et al., 2020) (Figure 1.12 A). Flavonoids are a natural part of a normal diet with compounds found in plant foods such as fruits, vegetables (Hertog et al., 1992), wine, black and green tea (Hertog et al., 1993), and cocoa products (Kofink et al., 2007). These compounds have been reported to exert antioxidant, anti-inflammatory, anti-bacterial, anti-viral, anti-allergy, and anti-carcinogenic effects (Abotaleb et al., 2018; Kopustinskiene et al., 2020; Y. Li et al., 2016). Some flavonoids also have an impact on platelet signalling and function. For example, quercetin when ingested can inhibit platelet aggregation and collagen-stimulated tyrosine phosphorylation of platelet proteins (Hubbard et al., 2004).

When quercetin is instead glycosylated at C3 it becomes isoquercetin (Figure 1.12 B). A change to a sugar group can also mean a change in function due to changes in solubility and absorption (Y. Li et al., 2016). Investigating flavonoids as potential treatments for disease is beneficial as they are naturally found in many foods and have the potential to be tolerated well such as isoquercetin at a 1000 mg daily dose (Jeffrey I. Zwicker et al., 2019).

A

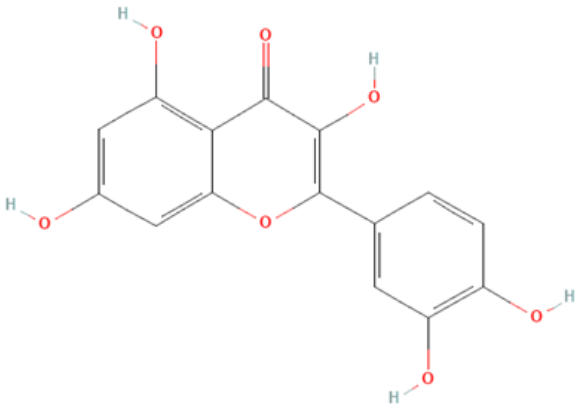

B

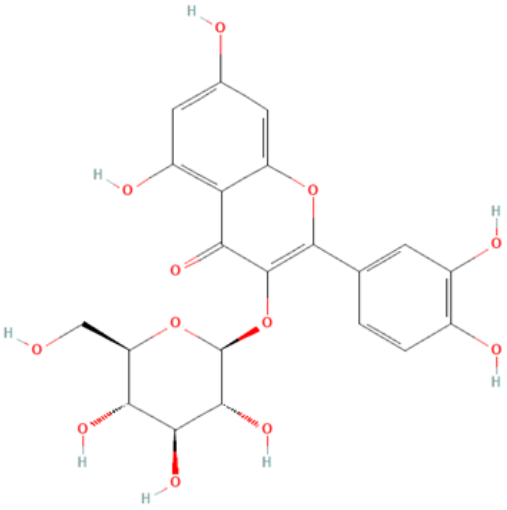

C

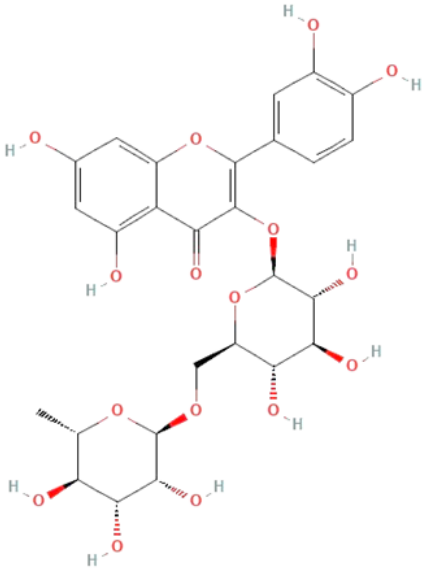

Figure 1.12 The chemical structures of the flavonoids quercetin (A), isoquercetin (B) and rutin (C).

Rutin is a well-known selective PDI inhibitor with poor membrane permeability (Jasuja et al., 2012b). Its inhibition is fully reversible and therefore does not covalently bind to the active site (a and a' domains, CGHC motifs), and instead binds to the b' domain (Jasuja et al., 2012b; Lin et al., 2015). The histidine 256 residue in PDI is essential for the binding of rutin, and when altered demonstrated no inhibition of PDI activity (Liao et al., 2022). Rutin was shown to inhibit platelet aggregation and fibrin formation after both laser induced arterial injury and $FeCl_3$ thrombus formation (Jasuja et al., 2012b).

Isoquercetin has a glucose attached at the 3-O position (Figure 1.12 B) and is similar to rutin which has a disaccharide at the 3-O position (Singh et al., 2021) (Figure 1.12 C). Both act as a PDI selective inhibitors along with other 3-O-glycosylated compounds (Jasuja et al., 2012b). Isoquercetin has been investigated *in vivo,* and was determined to correlate with PDI inhibition in healthy adults as only one 1000 mg dose reduced PDI activity along with thrombin generation (Stopa et al., 2017). When tested in cancer patients, similar results were obtained including a reduction in PDI activity, thrombin generation, circulating P-selectin and D-dimer plasma concentration, which when elevated is associated with higher risk of thrombosis (Jeffrey I. Zwicker et al., 2019). These results demonstrate flavonoids have the potential to be used as a therapy towards thrombotic complications related to cancer. It is also worth noting, isoquercetin obtained directly from plant sources showed effects in blood from oral dosing. An extract mixture from *Schisandra chinensis* (Magnolia berry) and *Morus alba* (Mulberry) containing an isoquercetin concentration of 13.6 mg/kg was found to block collagen-induced phosphorylation of ERK, JNK and Akt *ex vivo* in platelets obtained from rats (Kim et al., 2017). These proteins are part of the MAPK and PI3K/Akt pathways which are not only involved in platelet activation (Adam et al., 2008), but also play critical roles in cancer progression (Dhillon et al., 2007; Yang et al., 2019).

Isoquercetin shows little *in vitro* cytotoxicity to cancer cells, as concentrations as high as 400 μM were required to reach significant inhibition (Huang et al., 2014). Interestingly though, isoquercetin has been reported to inhibit tumour growth in a colon cancer xenograft via absorption through the digestive tract (Da Silva et al., 2022), which may indicate that metabolism plays a factor for this compound to exert anti-tumour activity. It is known that at the brush border membrane in the small intestine, isoquercetin is metabolised by lactase phlorizin hydrolase into quercetin where it can then be absorbed by the cell (Nakamura et al., 2018). Although quercetin is not a thiol isomerase inhibitor (Jasuja et al., 2012b) many reports have been made that demonstrate quercetin induces cytotoxicity and apoptosis *in vitro* in a dose dependent manner using cancer cell lines such prostate, leukaemia, multiple myeloma, breast cancer, pancreatic and liver while also inducing apoptosis (Angst et al., 2013; He et al., 2016; Jeon et al., 2019; Lee et al., 2015; Lu et al., 2020; Ranganathan et al., 2015; Seo et al., 2016). Interestingly, both isoquercetin and quercetin bioavailability can be increased by administering it in tandem with a high fat diet, alcohol or nondigestible oligosaccharides (Valentova et al., 2014).

Since isoquercetin is one of the best studied PDI inhibitors clinically for thrombosis (Stopa et al., 2017) and cancer induced thrombosis (Jeffrey I. Zwicker et al., 2019), more research is warranted on this drug for its effects on cancer alone and other underlying mechanisms. Additionally, it is a PDI selective inhibitor (Jasuja et al., 2012b) leading to the question of how it would fair in combination with other thiol isomerase inhibitors that can target more than just PDI.

1.6 Study Aims and Outline

Considering the involvement of thiol isomerases, which include PDI, ERp57, ERp72 and ERp5 in both cancer and thrombosis, inhibitors of these enzymes could have strong therapeutic potential. This leads to an overall hypothesis that thiol isomerase inhibitors maybe used to target cancer, thrombosis and cancer induced thrombosis either individually or in combination therapy. At the end of each introduction in the experimental chapters, specific hypotheses regarding the corresponding chapter are provided.

In thrombosis, current antithrombotic agents are associated with bleeding risks and are unable to target both arterial and venous thrombosis. Additionally, thiol isomerases, which are associated with thrombosis, are non-redundant, each with their own distinct role, resulting in a need for an overall inhibition. In order to expand upon our previous findings (Holbrook et al., 2021), this thesis begins by investigating the potential to develop analogues of zafirlukast for more potent thiol isomerase and thrombosis inhibition in **Chapter 2**. **Chapter 2** investigated 35 zafirlukast analogues for thiol isomerase and thrombosis inhibition. This study investigated the 35 analogues for thiol isomerase inhibition against ERp57, to determine activity against the parent compound. The analogue with the highest potency (lowest IC_{50}) was then confirmed to retain pan-thiol isomerase inhibition, compared against zafirlukast for surface thiol expression on platelets along with platelet aggregation, P-selectin exposure and *in vivo* thrombus formation.

To expand the study of zafirlukast into cancer and cancer induced thrombosis, we explored the effects of zafirlukast and its ability to modulate ovarian cancer cell proliferation and survival *in vitro*, in xenograft mouse models and in a pilot clinical trial in **Chapter 3**. **Chapter 3** investigates zafirlukast in an ovarian cancer model to determine the effects it has on thiol isomerase activity, cellular signalling and factor Xa generation. Additionally, a xenograft model was used to determine *in vivo* effects of zafirlukast on ovarian cancer when

injected intraperitoneally in addition to how it fairs when combined with a standard chemotherapy regimen. Finally, based on the results of the xenograft model, a small pilot clinical trial was performed to investigate zafirlukast's antineoplastic activity in women with tumour marker only (CA-125) relapsed ovarian cancer.

The zafirlukast analogues showed only modest improvement in efficacy, so in **Chapter 4** we decided to attempt to improve this by combining zafirlukast with a second thiol isomerase inhibitor, isoquercetin. **Chapter 4** investigates zafirlukast and isoquercetin in an ovarian cancer model to determine the effects they have on thiol isomerase activity, and factors associated with thrombosis, angiogenesis and inflammation. Here I explored zafirlukast and isoquercetin administered via the oral route to mice xenografted with ovarian cancer cells. Additionally, oral administration of a zafirlukast/isoquercetin combination is explored in this model.

Finally, **Chapter 5** provides a discussion to bring together the experimental chapters and the overall contributions of this thesis. Additionally, the limitations of this work and future ideas and prospects will be considered for upcoming work in this field.

Additionally, appendices highlight work done for this thesis that was not included in the published work.

Appendix I discusses the effects of pranlukast, another LTR antagonist in the same family as zafirlukast. Pranlukast was compared to zafirlukast first as a thiol isomerase inhibitor and for its reversibility. It was then compared to zafirlukast for factors related to cancer and cancer induced thrombosis including ovarian cancer cell cytotoxicity, factor Xa generation, and P-selectin exposure.

Appendix II explores zafirlukast, isoquercetin or a combination of both in a colon cancer xenograft model. The drugs were observed for their effects on tumour growth immediately after xenografting takes place.

Finally, **Appendices III, IV** and **V** include miscellaneous data that did not make it into **Chapters 2, 3** and **4** including thromboxane production, zafirlukast's effects on PERK, a pathway associated with PDI and cancer survival, and zafirlukast's effects on thiol isomerase activity and soluble P-selectin in mouse blood and D-Dimer levels.

1.7 References

Abdol Razak, N. B., Jones, G., Bhandari, M., Berndt, M. C., & Metharom, P. (2018). Cancer-Associated Thrombosis: An Overview of Mechanisms, Risk Factors, and Treatment. *Cancers (Basel)*, *10*(10). https://doi.org/10.3390/cancers10100380

Abhinand, C. S., Raju, R., Soumya, S. J., Arya, P. S., & Sudhakaran, P. R. (2016). VEGF-A/VEGFR2 signaling network in endothelial cells relevant to angiogenesis. *J Cell Commun Signal*, *10*(4), 347-354. https://doi.org/10.1007/s12079-016-0352-8

Abotaleb, M., Samuel, S. M., Varghese, E., Varghese, S., Kubatka, P., Liskova, A., & Busselberg, D. (2018). Flavonoids in Cancer and Apoptosis. *Cancers (Basel)*, *11*(1). https://doi.org/10.3390/cancers11010028

Adam, F., Kauskot, A., Rosa, J. P., & Bryckaert, M. (2008). Mitogen-activated protein kinases in hemostasis and thrombosis. *J Thromb Haemost*, *6*(12), 2007-2016. https://doi.org/10.1111/j.1538-7836.2008.03169.x

Ahamed, J., Versteeg, H. H., Kerver, M., Chen, V. M., Mueller, B. M., Hogg, P. J., & Ruf, W. (2006). Disulfide isomerization switches tissue factor from coagulation to cell signaling. *Proc Natl Acad Sci U S A*, *103*(38), 13932-13937. https://doi.org/10.1073/pnas.0606411103

Aharony, D. (1998). Pharmacology of leukotriene receptor antagonists. *Am J Respir Crit Care Med*, *157*(6 Pt 2), S214-218; discussion S218-219, S247-218. https://www.ncbi.nlm.nih.gov/pubmed/9647602

Ali Khan, H., & Mutus, B. (2014). Protein disulfide isomerase a multifunctional protein with multiple physiological roles. *Front Chem*, *2*, 70. https://doi.org/10.3389/fchem.2014.00070

Altundag, O., Altundag, K., & Gunduz, E. (2005). Interleukin-6 and C-reactive protein in metastatic renal cell carcinoma. *J Clin Oncol*, *23*(5), 1044; author reply 1044-1045. https://doi.org/10.1200/JCO.2005.05.155

Angst, E., Park, J. L., Moro, A., Lu, Q. Y., Lu, X., Li, G., King, J., Chen, M., Reber, H. A., Go, V. L., Eibl, G., & Hines, O. J. (2013). The flavonoid quercetin inhibits pancreatic cancer growth in vitro and in vivo. *Pancreas*, *42*(2), 223-229. https://doi.org/10.1097/MPA.0b013e318264ccae

Bartels, A. K., Gottert, S., Desel, C., Schafer, M., Krossa, S., Scheidig, A. J., Grotzinger, J., & Lorenzen, I. (2019). KDEL Receptor 1 Contributes to Cell Surface Association of Protein Disulfide Isomerases. *Cell Physiol Biochem*, *52*(4), 850-868. https://doi.org/10.33594/000000059

Beckmann, L., Rolling, C. C., Voigtlander, M., Mader, J., Klingler, F., Schulenkorf, A., Lehr, C., Bokemeyer, C., Ruf, W., & Langer, F. (2021). Bacitracin and Rutin Regulate Tissue Factor Production in Inflammatory Monocytes and Acute Myeloid Leukemia Blasts. *Cancers (Basel)*, *13*(16). https://doi.org/10.3390/cancers13163941

Befekadu, R., Grenegard, M., Larsson, A., Christensen, K., & Ramstrom, S. (2022). Levels of soluble tumor necrosis factor receptor 1 and 2 are associated with survival after ST segment elevation myocardial infarction. *Sci Rep*, *12*(1), 14762. https://doi.org/10.1038/s41598-022-18972-5

Bekendam, R. H., Bendapudi, P. K., Lin, L., Nag, P. P., Pu, J., Kennedy, D. R., Feldenzer, A., Chiu, J., Cook, K. M., Furie, B., Huang, M., Hogg, P. J., & Flaumenhaft, R. (2016). A substrate-driven allosteric switch that enhances PDI catalytic activity. *Nat Commun*, *7*, 12579. https://doi.org/10.1038/ncomms12579

Bendas, G., & Borsig, L. (2012). Cancer Cell Adhesion and Metastasis: Selectins, Integrins, and the Inhibitory Potential of Heparins. *International Journal of Cell Biology*, *2012*, 1-10. https://doi.org/10.1155/2012/676731

Bennett, C. F., Balcarek, J. M., Varrichio, A., & Crooke, S. T. (1988). Molecular cloning and complete amino-acid sequence of form-I phosphoinositide-specific phospholipase C. *Nature*, *334*(6179), 268-270. https://doi.org/10.1038/334268a0

Bergers, G., Brekken, R., McMahon, G., Vu, T. H., Itoh, T., Tamaki, K., Tanzawa, K., Thorpe, P., Itohara, S., Werb, Z., & Hanahan, D. (2000). Matrix metalloproteinase-9 triggers the angiogenic switch during carcinogenesis. *Nat Cell Biol*, *2*(10), 737-744. https://doi.org/10.1038/35036374

Bernstein, P. R. (1998). Chemistry and structure--activity relationships of leukotriene receptor antagonists. *Am J Respir Crit Care Med*, *157*(6 Pt 2), S220-225; discussion S225-226, S247-228. https://www.ncbi.nlm.nih.gov/pubmed/9647603

Bobrovnikova-Marjon, E., Grigoriadou, C., Pytel, D., Zhang, F., Ye, J., Koumenis, C., Cavener, D., & Diehl, J. A. (2010). PERK promotes cancer cell proliferation and tumor growth by limiting oxidative DNA damage. *Oncogene*, *29*(27), 3881-3895. https://doi.org/10.1038/onc.2010.153

Borsig, L. (2018). Selectins in cancer immunity. *Glycobiology*, *28*(9), 648-655. https://doi.org/10.1093/glycob/cwx105

Breuss, J. M., & Uhrin, P. (2012). VEGF-initiated angiogenesis and the uPA/uPAR system. *Cell Adh Migr*, *6*(6), 535-615. https://doi.org/10.4161/cam.22243

Carlsson, A. C., Juhlin, C. C., Larsson, T. E., Larsson, A., Ingelsson, E., Sundstrom, J., Lind, L., & Arnlov, J. (2014). Soluble tumor necrosis factor receptor 1 (sTNFR1) is associated with increased total mortality due to cancer and cardiovascular causes - findings from two community based cohorts of elderly. *Atherosclerosis*, *237*(1), 236-242. https://doi.org/10.1016/j.atherosclerosis.2014.09.005

Carmeliet, P. (2005). VEGF as a key mediator of angiogenesis in cancer. *Oncology*, *69 Suppl 3*, 4-10. https://doi.org/10.1159/000088478

CDC. (2023). *Data Brief 492 Mortality in the United States*.

Chang, C. H., Hsiao, C. F., Yeh, Y. M., Chang, G. C., Tsai, Y. H., Chen, Y. M., Huang, M. S., Chen, H. L., Li, Y. J., Yang, P. C., Chen, C. J., Hsiung, C. A., & Su, W. C. (2013). Circulating interleukin-6 level is a prognostic marker for survival in advanced nonsmall cell lung cancer patients treated with chemotherapy. *Int J Cancer*, *132*(9), 1977-1985. https://doi.org/10.1002/ijc.27892

Chaudhry, R., Usama, S. M., & Babiker, H. M. (2022). Physiology, Coagulation Pathways. In *StatPearls*. https://www.ncbi.nlm.nih.gov/pubmed/29489185

Chen, K., Detwiler, T. C., & Essex, D. W. (1995). Characterization of protein disulphide isomerase released from activated platelets. *Br J Haematol*, *90*(2), 425-431. https://doi.org/10.1111/j.1365-2141.1995.tb05169.x

Chen, L., Deng, H., Cui, H., Fang, J., Zuo, Z., Deng, J., Li, Y., Wang, X., & Zhao, L. (2018). Inflammatory responses and inflammation-associated diseases in organs. *Oncotarget*, *9*(6), 7204-7218. https://doi.org/10.18632/oncotarget.23208

Chen, V. M., Ahamed, J., Versteeg, H. H., Berndt, M. C., Ruf, W., & Hogg, P. J. (2006). Evidence for activation of tissue factor by an allosteric disulfide bond. *Biochemistry*, *45*(39), 12020-12028. https://doi.org/10.1021/bi061271a

Chichiarelli, S., Altieri, F., Paglia, G., Rubini, E., Minacori, M., & Eufemi, M. (2022). ERp57/PDIA3: new insight. *Cellular & Molecular Biology Letters*, *27*(1). https://doi.org/10.1186/s11658-022-00315-x

Cho, J., Furie, B. C., Coughlin, S. R., & Furie, B. (2008). A critical role for extracellular protein disulfide isomerase during thrombus formation in mice. *J Clin Invest*, *118*(3), 1123-1131. https://doi.org/10.1172/JCI34134

Cho, J., Kennedy, D. R., Lin, L., Huang, M., Merrill-Skoloff, G., Furie, B. C., & Furie, B. (2012). Protein disulfide isomerase capture during thrombus formation in vivo depends on the presence of β3 integrins. *Blood*, *120*(3), 647-655. https://doi.org/10.1182/blood-2011-08-372532

Cornard, J. P. B., A.C; Merlin, J.C. (1998). Theoretical investigation of the molecular structure of the isoquercitrin molecule. *Journal of Molecular Structure*, *508*(1999), 37-49.

Culig, Z., & Puhr, M. (2012). Interleukin-6: a multifunctional targetable cytokine in human prostate cancer. *Mol Cell Endocrinol*, *360*(1-2), 52-58. https://doi.org/10.1016/j.mce.2011.05.033

Da Silva, D. D. C., Orfali, G. D. C., Santana, M. G., Palma, J. K. Y., Assunção, I. R. D. O., Marchesi, I. M., Grizotto, A. Y. K., Martinez, N. P., Felliti, S., Pereira, J. A., & Priolli, D. G. (2022). Antitumor effect of isoquercetin on tissue vasohibin expression and colon cancer vasculature. *Oncotarget*, *13*(1), 307-318. https://doi.org/10.18632/oncotarget.28181

Darby, N. J., Kemmink, J., & Creighton, T. E. (1996). Identifying and characterizing a structural domain of protein disulfide isomerase. *Biochemistry*, *35*(32), 10517-10528. https://doi.org/10.1021/bi960763s

Dekhuijzen, P. N., & Koopmans, P. P. (2002). Pharmacokinetic profile of zafirlukast. *Clin Pharmacokinet*, *41*(2), 105-114. https://doi.org/10.2165/00003088-200241020-00003

Dethlefsen, C., Hojfeldt, G., & Hojman, P. (2013). The role of intratumoral and systemic IL-6 in breast cancer. *Breast Cancer Res Treat*, *138*(3), 657-664. https://doi.org/10.1007/s10549-013-2488-z

Dhillon, A. S., Hagan, S., Rath, O., & Kolch, W. (2007). MAP kinase signalling pathways in cancer. *Oncogene*, *26*(22), 3279-3290. https://doi.org/10.1038/sj.onc.1210421

Dickerhof, N., Kleffmann, T., Jack, R., & McCormick, S. (2011). Bacitracin inhibits the reductive activity of protein disulfide isomerase by disulfide bond formation with free cysteines in the substrate-binding domain. *FEBS J*, *278*(12), 2034-2043. https://doi.org/10.1111/j.1742-4658.2011.08119.x

Dong, A., Wodziak, D., & Lowe, A. W. (2015). Epidermal Growth Factor Receptor (EGFR) Signaling Requires a Specific Endoplasmic Reticulum Thioredoxin for the Post-translational Control of Receptor Presentation to the Cell Surface. *Journal of Biological Chemistry*, *290*(13), 8016-8027. https://doi.org/10.1074/jbc.m114.623207

Dorner, A. J., Wasley, L. C., Raney, P., Haugejorden, S., Green, M., & Kaufman, R. J. (1990). The stress response in Chinese hamster ovary cells. Regulation of ERp72 and protein disulfide isomerase expression and secretion. *J Biol Chem*, *265*(35), 22029-22034. https://www.ncbi.nlm.nih.gov/pubmed/2254345

Durrant, T. N., Van Den Bosch, M. T., & Hers, I. (2017). Integrin αIIbβ3 outside-in signaling. *Blood*, *130*(14), 1607-1619. https://doi.org/10.1182/blood-2017-03-773614

Edman, J. C., Ellis, L., Blacher, R. W., Roth, R. A., & Rutter, W. J. (1985). Sequence of protein disulphide isomerase and implications of its relationship to thioredoxin. *Nature*, *317*(6034), 267-270. https://doi.org/10.1038/317267a0

Elliott, J. G., Oliver, J. D., & High, S. (1997). The thiol-dependent reductase ERp57 interacts specifically with N-glycosylated integral membrane proteins. *J Biol Chem*, *272*(21), 13849-13855. https://doi.org/10.1074/jbc.272.21.13849

Essex, D. W., & Wang, L. (2024). Recent advances in vascular thiol isomerases and redox systems in platelet function and thrombosis. *J Thromb Haemost*, *22*(7), 1806-1818. https://doi.org/10.1016/j.jtha.2024.03.008

Falanga, A., Russo, L., Milesi, V., & Vignoli, A. (2017). Mechanisms and risk factors of thrombosis in cancer. *Crit Rev Oncol Hematol*, *118*, 79-83. https://doi.org/10.1016/j.critrevonc.2017.08.003

Flaumenhaft, R., & Furie, B. (2016). Vascular thiol isomerases. *Blood*, *128*(7), 893-901. https://doi.org/10.1182/blood-2016-04-636456

Fong, K. P., Zhu, H., Span, L. M., Moore, D. T., Yoon, K., Tamura, R., Yin, H., DeGrado, W. F., & Bennett, J. S. (2016). Directly Activating the Integrin alphaIIbbeta3 Initiates Outside-In Signaling by Causing alphaIIbbeta3 Clustering. *J Biol Chem*, *291*(22), 11706-11716. https://doi.org/10.1074/jbc.M116.716613

Forster, M. L., Sivick, K., Park, Y. N., Arvan, P., Lencer, W. I., & Tsai, B. (2006). Protein disulfide isomerase-like proteins play opposing roles during retrotranslocation. *J Cell Biol*, *173*(6), 853-859. https://doi.org/10.1083/jcb.200602046

Fousek, K., Horn, L. A., & Palena, C. (2021). Interleukin-8: A chemokine at the intersection of cancer plasticity, angiogenesis, and immune suppression. *Pharmacol Ther*, *219*, 107692. https://doi.org/10.1016/j.pharmthera.2020.107692

Furie, B., & Flaumenhaft, R. (2014). Thiol isomerases in thrombus formation. *Circ Res*, *114*(7), 1162-1173. https://doi.org/10.1161/CIRCRESAHA.114.301808

Gaucci, E., Altieri, F., Turano, C., & Chichiarelli, S. (2013). The protein ERp57 contributes to EGF receptor signaling and internalization in MDA-MB-468 breast cancer cells. *Journal of Cellular Biochemistry*, *114*(11), 2461-2470. https://doi.org/10.1002/jcb.24590

Goldberger, R. F., Epstein, C. J., & Anfinsen, C. B. (1963). Acceleration of reactivation of reduced bovine pancreatic ribonuclease by a microsomal system from rat liver. *J Biol Chem*, *238*, 628-635. https://www.ncbi.nlm.nih.gov/pubmed/13948694

Golebiewska, E. M., & Poole, A. W. (2015). Platelet secretion: From haemostasis to wound healing and beyond. *Blood Rev*, *29*(3), 153-162. https://doi.org/10.1016/j.blre.2014.10.003

González-Santiago, L., Alfonso, P., Suárez, Y., Núñez, A., García-Fernández, L. F., Alvarez, E., Muñoz, A., & Casal, J. I. (2007). Proteomic Analysis of the Resistance to Aplidin in Human Cancer Cells. *Journal of Proteome Research*, *6*(4), 1286-1294. https://doi.org/10.1021/pr060430+

Goplen, D., Wang, J., Enger, P. Ø., Tysnes, B. B., Terzis, A. J. A., Laerum, O. D., & Bjerkvig, R. (2006). Protein Disulfide Isomerase Expression Is Related to the Invasive Properties of Malignant Glioma. *Cancer Research*, *66*(20), 9895-9902. https://doi.org/10.1158/0008-5472.can-05-4589

Gupta, S. C., Kim, J. H., Prasad, S., & Aggarwal, B. B. (2010). Regulation of survival, proliferation, invasion, angiogenesis, and metastasis of tumor cells through modulation of inflammatory pathways by nutraceuticals. *Cancer Metastasis Rev*, *29*(3), 405-434. https://doi.org/10.1007/s10555-010-9235-2

Hamidi, H., & Ivaska, J. (2018). Every step of the way: integrins in cancer progression and metastasis. *Nat Rev Cancer*, *18*(9), 533-548. https://doi.org/10.1038/s41568-018-0038-z

Han, Y., Liu, D., & Li, L. (2020). PD-1/PD-L1 pathway: current researches in cancer. *Am J Cancer Res*, *10*(3), 727-742. https://www.ncbi.nlm.nih.gov/pubmed/32266087

Hanahan, D., & Weinberg, R. A. (2000). The hallmarks of cancer. *Cell*, *100*(1), 57-70. https://doi.org/10.1016/s0092-8674(00)81683-9

Hasipek, M., Grabowski, D., Guan, Y., Alugubelli, R. R., Tiwari, A. D., Gu, X., DeAvila, G. A., Silva, A. S., Meads, M. B., Parker, Y., Lindner, D. J., Saunthararajah, Y., Shain, K. H., Maciejewski, J. P., Reu, F. J., Phillips, J. G., & Jha, B. K. (2021). Therapeutic Targeting of Protein Disulfide Isomerase PDIA1 in Multiple Myeloma. *Cancers (Basel)*, *13*(11). https://doi.org/10.3390/cancers13112649

Hassan, L., Bedir, A., Kraus, F. B., Ostheimer, C., Vordermark, D., Mikolajczyk, R., Seliger, B., & Medenwald, D. (2024). Correlation of Increased Soluble Tumor Necrosis Factor Receptor 1 with Mortality and Dependence on Treatment in Non-Small-Cell Lung Cancer Patients: A Longitudinal Cohort Study. *Cancers (Basel)*, *16*(3). https://doi.org/10.3390/cancers16030525

Hatahet, F., & Ruddock, L. W. (2009). Protein disulfide isomerase: a critical evaluation of its function in disulfide bond formation. *Antioxid Redox Signal*, *11*(11), 2807-2850. https://doi.org/10.1089/ARS.2009.2466

He, C., Yang, A., Zhang, Y., Zhao, Z., Lu, Y., Zhang, J., & Wu, Y. (2024). A novel role for protein disulfide isomerase ERp18 in venous thrombosis. *Thromb J*, *22*(1), 110. https://doi.org/10.1186/s12959-024-00678-5

He, D., Guo, X., Zhang, E., Zi, F., Chen, J., Chen, Q., Lin, X., Yang, L., Li, Y., Wu, W., Yang, Y., He, J., & Cai, Z. (2016). Quercetin induces cell apoptosis of myeloma and displays a synergistic effect with dexamethasone in vitro and in vivo xenograft models. *Oncotarget*, *7*(29), 45489-45499. https://doi.org/10.18632/oncotarget.9993

Hertog, M. G. L., Hollman, P. C. H., & Katan, M. B. (1992). Content of potentially anticarcinogenic flavonoids of 28 vegetables and 9 fruits commonly consumed in the Netherlands. *Journal of Agricultural and Food Chemistry*, *40*(12), 2379-2383. https://doi.org/10.1021/jf00024a011

Hertog, M. G. L., Hollman, P. C. H., & van de Putte, B. (1993). Content of Potentially Anticarcinogenic Flavonoids of Tea Infusions, Wines, and Fruit Juices. *J. Agric. Food Chem.*, *41*, 1242-1246. https://doi.org/https://doi.org/10.1021/jf00032a015

Holbrook, L.-M., Watkins, N. A., Simmonds, A. D., Jones, C. I., Ouwehand, W. H., & Gibbins, J. M. (2010). Platelets release novel thiol isomerase enzymes which are recruited to the cell surface following activation. *British Journal of Haematology*, *148*(4), 627-637. https://doi.org/10.1111/j.1365-2141.2009.07994.x

Holbrook, L. M., Keeton, S. J., Sasikumar, P., Nock, S., Gelzinis, J., Brunt, E., Ryan, S., Pantos, M. M., Verbetsky, C. A., Gibbins, J. M., & Kennedy, D. R. (2021). Zafirlukast is a broad-spectrum thiol isomerase inhibitor that inhibits thrombosis without altering bleeding times. *Br J Pharmacol*, *178*(3), 550-563. https://doi.org/10.1111/bph.15291

Holbrook, L. M., Sandhar, G. K., Sasikumar, P., Schenk, M. P., Stainer, A. R., Sahli, K. A., Flora, G. D., Bicknell, A. B., & Gibbins, J. M. (2018). A humanized monoclonal antibody that inhibits platelet-surface ERp72 reveals a role for ERp72 in thrombosis. *J Thromb Haemost*, *16*(2), 367-377. https://doi.org/10.1111/jth.13878

Holbrook, L. M., Sasikumar, P., Stanley, R. G., Simmonds, A. D., Bicknell, A. B., & Gibbins, J. M. (2012). The platelet-surface thiol isomerase enzyme ERp57 modulates platelet function. *J Thromb Haemost*, *10*(2), 278-288. https://doi.org/10.1111/j.1538-7836.2011.04593.x

Howard, K. C., & Garneau-Tsodikova, S. (2022). Selective Inhibition of the Periodontal Pathogen Porphyromonas gingivalis by Third-Generation Zafirlukast Derivatives. *J Med Chem*, *65*(21), 14938-14956. https://doi.org/10.1021/acs.jmedchem.2c01471

Howard, K. C., Gonzalez, O. A., & Garneau-Tsodikova, S. (2020). Second Generation of Zafirlukast Derivatives with Improved Activity against the Oral Pathogen Porphyromonas gingivalis. *ACS Med Chem Lett*, *11*(10), 1905-1912. https://doi.org/10.1021/acsmedchemlett.9b00614

Huang, G., Tang, B., Tang, K., Dong, X., Deng, J., Liao, L., Liao, Z., Yang, H., & He, S. (2014). Isoquercitrin inhibits the progression of liver cancer in vivo and in vitro via the MAPK signalling pathway. *Oncol Rep*, *31*(5), 2377-2384. https://doi.org/10.3892/or.2014.3099

Huang, J., Li, X., Shi, X., Zhu, M., Wang, J., Huang, S., Huang, X., Wang, H., Li, L., Deng, H., Zhou, Y., Mao, J., Long, Z., Ma, Z., Ye, W., Pan, J., Xi, X., & Jin, J. (2019). Platelet integrin alphaIIbbeta3: signal transduction, regulation, and its therapeutic targeting. *J Hematol Oncol*, *12*(1), 26. https://doi.org/10.1186/s13045-019-0709-6

Hubbard, G. P., Wolffram, S., Lovegrove, J. A., & Gibbins, J. M. (2004). Ingestion of quercetin inhibits platelet aggregation and essential components of the collagen-stimulated platelet activation pathway in humans. *J Thromb Haemost*, *2*(12), 2138-2145. https://doi.org/10.1111/j.1538-7836.2004.01067.x

Hughes, E. A., & Cresswell, P. (1998). The thiol oxidoreductase ERp57 is a component of the MHC class I peptide-loading complex. *Curr Biol*, *8*(12), 709-712. https://doi.org/10.1016/s0960-9822(98)70278-7

Inoue, T., Yashiro, M., Nishimura, S., Maeda, K., Sawada, T., Ogawa, Y., Sowa, M., & Chung, K. H. (1999). Matrix metalloproteinase-1 expression is a prognostic factor for patients with advanced gastric cancer. *Int J Mol Med*, *4*(1), 73-77. https://doi.org/10.3892/ijmm.4.1.73

Irvine, A. G., Wallis, A. K., Sanghera, N., Rowe, M. L., Ruddock, L. W., Howard, M. J., Williamson, R. A., Blindauer, C. A., & Freedman, R. B. (2014). Protein disulfide-isomerase interacts with a substrate protein at all stages along its folding pathway. *PLoS One*, *9*(1), e82511. https://doi.org/10.1371/journal.pone.0082511

Ito, T., Ito, M., Shiozawa, J., Naito, S., Kanematsu, T., & Sekine, I. (1999). Expression of the MMP-1 in human pancreatic carcinoma: relationship with prognostic factor. *Mod Pathol*, *12*(7), 669-674. https://www.ncbi.nlm.nih.gov/pubmed/10430270

Jasuja, R., Furie, B., & Furie, B. C. (2010). Endothelium-derived but not platelet-derived protein disulfide isomerase is required for thrombus formation in vivo. *Blood*, *116*(22), 4665-4674. https://doi.org/10.1182/blood-2010-04-278184

Jasuja, R., Passam, F. H., Kennedy, D. R., Kim, S. H., van Hessem, L., Lin, L., Bowley, S. R., Joshi, S. S., Dilks, J. R., Furie, B., Furie, B. C., & Flaumenhaft, R. (2012). Protein disulfide isomerase inhibitors constitute a new class of antithrombotic agents. *J Clin Invest*, *122*(6), 2104-2113. https://doi.org/10.1172/JCI61228

Jeon, J.-S., Kwon, S., Ban, K., Kwon Hong, Y., Ahn, C., Sung, J.-S., & Choi, I. (2019). Regulation of the Intracellular ROS Level Is Critical for the Antiproliferative Effect of Quercetin in the Hepatocellular Carcinoma Cell Line HepG2. *Nutrition and Cancer*, *71*(5), 861-869. https://doi.org/10.1080/01635581.2018.1559929

Jessop, C. E., Chakravarthi, S., Garbi, N., Hammerling, G. J., Lovell, S., & Bulleid, N. J. (2007). ERp57 is essential for efficient folding of glycoproteins sharing common structural domains. *EMBO J*, *26*(1), 28-40. https://doi.org/10.1038/sj.emboj.7601505

Jha, V., Xiong, B., Kumari, T., Brown, G., Wang, J., Kim, K., Lee, J., Asquith, N., Gallagher, J., Asherman, L., Lambert, T., Bai, Y., Du, X., Min, J. K., Sah, R., Javaheri, A., Razani, B., Lee, J. M., Italiano, J. E., & Cho, J. (2023). A Critical Role for ERO1alpha in Arterial Thrombosis and Ischemic Stroke. *Circ Res*, *132*(11), e206-e222. https://doi.org/10.1161/CIRCRESAHA.122.322473

Jiang, L., Yang, Y., Liu, F., Ma, M., Gao, J., Sun, L., Chen, Y., Shen, Z., & Wu, D. (2022). A Potential Diagnostic and Prognostic Biomarker TMEM176B and Its Relationship With

Immune Infiltration in Skin Cutaneous Melanoma. *Front Cell Dev Biol*, *10*, 859958. https://doi.org/10.3389/fcell.2022.859958

Jinushi, M., Vanneman, M., Munshi, N. C., Tai, Y. T., Prabhala, R. H., Ritz, J., Neuberg, D., Anderson, K. C., Carrasco, D. R., & Dranoff, G. (2008). MHC class I chain-related protein A antibodies and
shedding are associated with the progression of multiple myeloma. *Proc Natl Acad Sci U S A*, *105*(4), 1285-1290. https://doi.org/10.1073/pnas.0711293105

Jordan, P. A., Stevens, J. M., Hubbard, G. P., Barrett, N. E., Sage, T., Authi, K. S., & Gibbins, J. M. (2005). A role for the thiol isomerase protein ERP5 in platelet function. *Blood*, *105*(4), 1500-1507. https://doi.org/10.1182/blood-2004-02-0608

Justiz Vaillant, A. A., & Qurie, A. (2025). Interleukin. In *StatPearls*. https://www.ncbi.nlm.nih.gov/pubmed/29763015

Kaiser, B. K., Yim, D., Chow, I. T., Gonzalez, S., Dai, Z., Mann, H. H., Strong, R. K., Groh, V., & Spies, T. (2007). Disulphide-isomerase-enabled shedding of tumour-associated NKG2D ligands. *Nature*, *447*(7143), 482-486. https://doi.org/10.1038/nature05768

Kang, C., Rostoker, R., Ben-Shumel, S., Rashed, R., Duty, J. A., Demircioglu, D., Antoniou, I. M., Isakov, L., Shen-Orr, Z., Bravo-Cordero, J. J., Kase, N., Cuajungco, M. P., Moran, T. M., LeRoith, D., & Gallagher, E. J. (2021). TMEM176B Regulates AKT/mTOR Signaling and Tumor Growth in Triple-Negative Breast Cancer. *Cells*, *10*(12). https://doi.org/10.3390/cells10123430

Keam, S. J., Lyseng-Williamson, K. A., & Goa, K. L. (2003). Pranlukast: a review of its use in the management of asthma. *Drugs*, *63*(10), 991-1019. https://doi.org/10.2165/00003495-200363100-00005

Khalaf, N. B., Al-Muehatab, D., & Fathallah, D. M. (2021). Vascular endothelial ERp72 is involved in the inflammatory response in a rat model of skeletal muscle injury. *Mol Med Rep*, *23*(3). https://doi.org/10.3892/mmr.2021.11825

Khorana, A. A., Dalal, M., Lin, J., & Connolly, G. C. (2013). Incidence and predictors of venous thromboembolism (VTE) among ambulatory high-risk cancer patients undergoing chemotherapy in the United States. *Cancer*, *119*(3), 648-655. https://doi.org/10.1002/cncr.27772

Khorana, A. A., Francis, C. W., Blumberg, N., Culakova, E., Refaai, M. A., & Lyman, G. H. (2008). Blood transfusions, thrombosis, and mortality in hospitalized patients with cancer. *Arch Intern Med*, *168*(21), 2377-2381. https://doi.org/10.1001/archinte.168.21.2377

Khorana, A. A., Francis, C. W., Culakova, E., Fisher, R. I., Kuderer, N. M., & Lyman, G. H. (2006). Thromboembolism in hospitalized neutropenic cancer patients. *J Clin Oncol*, *24*(3), 484-490. https://doi.org/10.1200/JCO.2005.03.8877

Kikuchi, M., Doi, E., Tsujimoto, I., Horibe, T., & Tsujimoto, Y. (2002). Functional analysis of human P5, a protein disulfide isomerase homologue. *J Biochem*, *132*(3), 451-455. https://doi.org/10.1093/oxfordjournals.jbchem.a003242

Kim, D. S., Irfan, M., Sung, Y. Y., Kim, S. H., Park, S. H., Choi, Y. H., Rhee, M. H., & Kim, H. K. (2017). Schisandra chinensis and Morus alba Synergistically Inhibit In Vivo Thrombus Formation and Platelet Aggregation by Impairing the Glycoprotein VI Pathway. *Evid Based Complement Alternat Med*, *2017*, 7839658. https://doi.org/10.1155/2017/7839658

Kobold, S., Volk, S., Clauditz, T., Kupper, N. J., Minner, S., Tufman, A., Duwell, P., Lindner, M., Koch, I., Heidegger, S., Rothenfuer, S., Schnurr, M., Huber, R. M., Wilczak, W., & Endres, S. (2013). Interleukin-22 is frequently expressed in small- and large-cell lung cancer and promotes growth in chemotherapy-resistant cancer cells. *J Thorac Oncol*, *8*(8), 1032-1042. https://doi.org/10.1097/JTO.0b013e31829923c8

Kofink, M., Papagiannopoulos, M., & Galensa, R. (2007). (-)-Catechin in cocoa and chocolate: occurrence and analysis of an atypical flavan-3-ol enantiomer. *Molecules*, *12*(7), 1274-1288. https://doi.org/10.3390/12071274

Kopustinskiene, D. M., Jakstas, V., Savickas, A., & Bernatoniene, J. (2020). Flavonoids as Anticancer Agents. *Nutrients*, *12*(2). https://doi.org/10.3390/nu12020457

Koupenova, M., Kehrel, B. E., Corkrey, H. A., & Freedman, J. E. (2017). Thrombosis and platelets: an update. *Eur Heart J*, *38*(11), 785-791. https://doi.org/10.1093/eurheartj/ehw550

Kranz, P., Sanger, C., Wolf, A., Baumann, J., Metzen, E., Baumann, M., Gopelt, K., & Brockmeier, U. (2020). Tumor cells rely on the thiol oxidoreductase PDI for PERK signaling in order to survive ER stress. *Sci Rep*, *10*(1), 15299. https://doi.org/10.1038/s41598-020-72259-1

Kumari, N., Dwarakanath, B. S., Das, A., & Bhatt, A. N. (2016). Role of interleukin-6 in cancer progression and therapeutic resistance. *Tumour Biol*, *37*(9), 11553-11572. https://doi.org/10.1007/s13277-016-5098-7

Kuo, T. F., Chen, T. Y., Jiang, S. T., Chen, K. W., Chiang, Y. M., Hsu, Y. J., Liu, Y. J., Chen, H. M., Yokoyama, K. K., Tsai, K. C., Yeh, H. H., Chen, Y. R., Yang, M. T., Yang, C. Y., & Yang, W. C. (2017). Protein disulfide isomerase a4 acts as a novel regulator of cancer growth through the procaspase pathway. *Oncogene*, *36*(39), 5484-5496. https://doi.org/10.1038/onc.2017.156

Lee, A. S. (1981). The accumulation of three specific proteins related to glucose-regulated proteins in a temperature-sensitive hamster mutant cell line K12. *J Cell Physiol*, *106*(1), 119-125. https://doi.org/10.1002/jcp.1041060113

Lee, S. J., Tsang, P. S., Diaz, T. M., Wei, B. Y., & Stetler-Stevenson, W. G. (2010). TIMP-2 modulates VEGFR-2 phosphorylation and enhances phosphodiesterase activity in endothelial cells. *Lab Invest*, *90*(3), 374-382. https://doi.org/10.1038/labinvest.2009.136

Lee, W. J., Hsiao, M., Chang, J. L., Yang, S. F., Tseng, T. H., Cheng, C. W., Chow, J. M., Lin, K. H., Lin, Y. W., Liu, C. C., Lee, L. M., & Chien, M. H. (2015). Quercetin induces mitochondrial-derived apoptosis via reactive oxygen species-mediated ERK activation in HL-60 leukemia cells and xenograft. *Arch Toxicol*, *89*(7), 1103-1117. https://doi.org/10.1007/s00204-014-1300-0

Li, J., Fang, Z., Dal, E., Zhang, H., Yu, K., Ma, M., Wang, M., Sun, R., Lu, M., Wang, H., & Li, Y. (2024). Transmembrane protein 176B regulates amino acid metabolism through the PI3K-Akt-mTOR signaling pathway and promotes gastric cancer progression. *Cancer Cell Int*, *24*(1), 95. https://doi.org/10.1186/s12935-024-03279-4

Li, T., Guo, T., Liu, H., Jiang, H., & Wang, Y. (2021). Platelet-derived growth factor-BB mediates pancreatic cancer malignancy via regulation of the Hippo/Yes-associated protein signaling pathway. *Oncol Rep*, *45*(1), 83-94. https://doi.org/10.3892/or.2020.7859

Li, Y., Yao, J., Han, C., Yang, J., Chaudhry, M. T., Wang, S., Liu, H., & Yin, Y. (2016). Quercetin, Inflammation and Immunity. *Nutrients*, *8*(3), 167. https://doi.org/10.3390/nu8030167

Liang, C., Flaumenhaft, R., Yuan, C., & Huang, M. (2022). Vascular thiol isomerases: Structures, regulatory mechanisms, and inhibitor development. *Drug Discovery Today*, *27*(2), 626-635. https://doi.org/10.1016/j.drudis.2021.10.018

Liao, X., Zhuang, X., Liang, C., Li, J., Flaumenhaft, R., Yuan, C., & Huang, M. (2022). Flavonoids as Protein Disulfide Isomerase Inhibitors: Key Molecular and Structural Features for the Interaction. *J Agric Food Chem*, *70*(14), 4475-4483. https://doi.org/10.1021/acs.jafc.1c07994

Lin, L., Gopal, S., Sharda, A., Passam, F., Bowley, S. R., Stopa, J., Xue, G., Yuan, C., Furie, B. C., Flaumenhaft, R., Huang, M., & Furie, B. (2015). Quercetin-3-rutinoside Inhibits Protein Disulfide Isomerase by Binding to Its b′x Domain. *Journal of Biological Chemistry*, *290*(39), 23543-23552. https://doi.org/10.1074/jbc.m115.666180

Lin, X., Kang, K., Chen, P., Zeng, Z., Li, G., Xiong, W., Yi, M., & Xiang, B. (2024). Regulatory mechanisms of PD-1/PD-L1 in cancers. *Mol Cancer*, *23*(1), 108. https://doi.org/10.1186/s12943-024-02023-w

Linge, A., Kennedy, S., O'Flynn, D., Beatty, S., Moriarty, P., Henry, M., Clynes, M., Larkin, A., & Meleady, P. (2012). Differential expression of fourteen proteins between uveal melanoma from patients who subsequently developed distant metastases versus those who did Not. *Invest Ophthalmol Vis Sci*, *53*(8), 4634-4643. https://doi.org/10.1167/iovs.11-9019

Lovat, P. E., Corazzari, M., Armstrong, J. L., Martin, S., Pagliarini, V., Hill, D., Brown, A. M., Piacentini, M., Birch-Machin, M. A., & Redfern, C. P. (2008). Increasing melanoma cell death using inhibitors of protein disulfide isomerases to abrogate survival responses to endoplasmic reticulum stress. *Cancer Res*, *68*(13), 5363-5369. https://doi.org/10.1158/0008-5472.CAN-08-0035

Lu, D., Ni, Z., Liu, X., Feng, S., Dong, X., Shi, X., Zhai, J., Mai, S., Jiang, J., Wang, Z., Wu, H., & Cai, K. (2019). Beyond T Cells: Understanding the Role of PD-1/PD-L1 in Tumor-

Associated Macrophages. *J Immunol Res*, *2019*, 1919082. https://doi.org/10.1155/2019/1919082

Lu, X., Yang, F., Chen, D., Zhao, Q., Chen, D., Ping, H., & Xing, N. (2020). Quercetin reverses docetaxel resistance in prostate cancer via androgen receptor and PI3K/Akt signaling pathways. *Int J Biol Sci*, *16*(7), 1121-1134. https://doi.org/10.7150/ijbs.41686

Maccio, A., & Madeddu, C. (2013). The role of interleukin-6 in the evolution of ovarian cancer: clinical and prognostic implications--a review. *J Mol Med (Berl)*, *91*(12), 1355-1368. https://doi.org/10.1007/s00109-013-1080-7

Mackman, N. (2012). New insights into the mechanisms of venous thrombosis. *J Clin Invest*, *122*(7), 2331-2336. https://doi.org/10.1172/JCI60229

Mandel, R., Ryser, H. J., Ghani, F., Wu, M., & Peak, D. (1993). Inhibition of a reductive function of the plasma membrane by bacitracin and antibodies against protein disulfide-isomerase. *Proc Natl Acad Sci U S A*, *90*(9), 4112-4116. https://doi.org/10.1073/pnas.90.9.4112

Mazor, R., Alsaigh, T., Shaked, H., Altshuler, A. E., Pocock, E. S., Kistler, E. B., Karin, M., & Schmid-Schonbein, G. W. (2013). Matrix metalloproteinase-1-mediated up-regulation of vascular endothelial growth factor-2 in endothelial cells. *J Biol Chem*, *288*(1), 598-607. https://doi.org/10.1074/jbc.M112.417451

Mazzarella, R. A., Srinivasan, M., Haugejorden, S. M., & Green, M. (1990). ERp72, an abundant luminal endoplasmic reticulum protein, contains three copies of the active site sequences of protein disulfide isomerase. *J Biol Chem*, *265*(2), 1094-1101. https://www.ncbi.nlm.nih.gov/pubmed/2295602

Michie, A. J., Zintel, H. A., & et al. (1949). The nephrotoxicity of bacitracin in man. *Surgery*, *26*(4), 626-632. https://www.ncbi.nlm.nih.gov/pubmed/18141336

Miura, T., Mitsunaga, S., Ikeda, M., Shimizu, S., Ohno, I., Takahashi, H., Furuse, J., Inagaki, M., Higashi, S., Kato, H., Terao, K., & Ochiai, A. (2015). Characterization of patients with advanced pancreatic cancer and high serum interleukin-6 levels. *Pancreas*, *44*(5), 756-763. https://doi.org/10.1097/MPA.0000000000000335

Mortality, G. B. D., & Causes of Death, C. (2016). Global, regional, and national life expectancy, all-cause mortality, and cause-specific mortality for 249 causes of death, 1980-2015: a systematic analysis for the Global Burden of Disease Study 2015. *Lancet*, *388*(10053), 1459-1544. https://doi.org/10.1016/S0140-6736(16)31012-1

Mulder, F. I., Horvath-Puho, E., van Es, N., van Laarhoven, H. W. M., Pedersen, L., Moik, F., Ay, C., Buller, H. R., & Sorensen, H. T. (2021). Venous thromboembolism in cancer patients: a population-based cohort study. *Blood*, *137*(14), 1959-1969. https://doi.org/10.1182/blood.2020007338

Munro, S., & Pelham, H. R. (1987). A C-terminal signal prevents secretion of luminal ER proteins. *Cell*, *48*(5), 899-907. https://doi.org/10.1016/0092-8674(87)90086-9

Murray, G. I., Duncan, M. E., O'Neil, P., McKay, J. A., Melvin, W. T., & Fothergill, J. E. (1998). Matrix metalloproteinase-1 is associated with poor prognosis in oesophageal cancer. *J Pathol*, *185*(3), 256-261. https://doi.org/10.1002/(SICI)1096-9896(199807)185:3<256::AID-PATH115>3.0.CO;2-A

Murray, G. I., Duncan, M. E., O'Neil, P., Melvin, W. T., & Fothergill, J. E. (1996). Matrix metalloproteinase-1 is associated with poor prognosis in colorectal cancer. *Nat Med*, *2*(4), 461-462. https://doi.org/10.1038/nm0496–461

Nagai, H., & Kim, Y. H. (2017). Cancer prevention from the perspective of global cancer burden patterns. *J Thorac Dis*, *9*(3), 448-451. https://doi.org/10.21037/jtd.2017.02.75

Nagarkoti, S., Kim, Y. M., Ash, D., Das, A., Vitriol, E., Read, T. A., Youn, S. W., Sudhahar, V., McMenamin, M., Hou, Y., Boatwright, H., Caldwell, R., Essex, D. W., Cho, J., Fukai, T., & Ushio-Fukai, M. (2023). Protein disulfide isomerase A1 as a novel redox sensor in VEGFR2 signaling and angiogenesis. *Angiogenesis*, *26*(1), 77-96. https://doi.org/10.1007/s10456-022-09852-7

Nakamura, T., Kinjo, C., Nakamura, Y., Kato, Y., Nishikawa, M., Hamada, M., Nakajima, N., Ikushiro, S., & Murota, K. (2018). Lymphatic metabolites of quercetin after intestinal administration of quercetin-3-glucoside and its aglycone in rats. *Arch Biochem Biophys*, *645*, 126-136. https://doi.org/10.1016/j.abb.2018.03.024

Nakamura, T., & Lipton, S. A. (2011). S-nitrosylation of critical protein thiols mediates protein misfolding and mitochondrial dysfunction in neurodegenerative diseases. *Antioxid Redox Signal*, *14*(8), 1479-1492. https://doi.org/10.1089/ars.2010.3570

Nakopoulou, L., Giannopoulou, I., Gakiopoulou, H., Liapis, H., Tzonou, A., & Davaris, P. S. (1999). Matrix metalloproteinase-1 and -3 in breast cancer: correlation with progesterone receptors and other clinicopathologic features. *Hum Pathol*, *30*(4), 436-442. https://doi.org/10.1016/s0046-8177(99)90120-x

Nemere, I., Dormanen, M. C., Hammond, M. W., Okamura, W. H., & Norman, A. W. (1994). Identification of a specific binding protein for 1 alpha,25-dihydroxyvitamin D3 in basal-lateral membranes of chick intestinal epithelium and relationship to transcaltachia. *J Biol Chem*, *269*(38), 23750-23756. https://www.ncbi.nlm.nih.gov/pubmed/8089147

Nemere, I., Safford, S. E., Rohe, B., DeSouza, M. M., & Farach-Carson, M. C. (2004). Identification and characterization of 1,25D3-membrane-associated rapid response, steroid (1,25D3-MARRS) binding protein. *J Steroid Biochem Mol Biol*, *89-90*(1-5), 281-285. https://doi.org/10.1016/j.jsbmb.2004.03.031

Ning, Y., Manegold, P. C., Hong, Y. K., Zhang, W., Pohl, A., Lurje, G., Winder, T., Yang, D., LaBonte, M. J., Wilson, P. M., Ladner, R. D., & Lenz, H. J. (2011). Interleukin-8 is associated with proliferation, migration, angiogenesis and chemosensitivity in vitro and in vivo in colon cancer cell line models. *Int J Cancer*, *128*(9), 2038-2049. https://doi.org/10.1002/ijc.25562

Nishida, N., Yano, H., Nishida, T., Kamura, T., & Kojiro, M. (2006). Angiogenesis in cancer. *Vasc Health Risk Manag*, *2*(3), 213-219. https://doi.org/10.2147/vhrm.2006.2.3.213

Ojha, N., & Dhamoon, A. S. (2025). Myocardial Infarction. In *StatPearls*. https://www.ncbi.nlm.nih.gov/pubmed/30725761

Oliver, J. D., van der Wal, F. J., Bulleid, N. J., & High, S. (1997). Interaction of the thiol-dependent reductase ERp57 with nascent glycoproteins. *Science*, *275*(5296), 86-88. https://doi.org/10.1126/science.275.5296.86

Ozcelik, D., & Pezacki, J. P. (2019). Small Molecule Inhibition of Protein Disulfide Isomerase in Neuroblastoma Cells Induces an Oxidative Stress Response and Apoptosis Pathways. *ACS Chem Neurosci*, *10*(9), 4068-4075. https://doi.org/10.1021/acschemneuro.9b00301

Pahwa, R., Goyal, A., & Jialal, I. (2025). Chronic Inflammation. In *StatPearls*. https://www.ncbi.nlm.nih.gov/pubmed/29630225

Passam, F. H., Lin, L., Gopal, S., Stopa, J. D., Bellido-Martin, L., Huang, M., Furie, B. C., & Furie, B. (2015). Both platelet- and endothelial cell-derived ERp5 support thrombus formation in a laser-induced mouse model of thrombosis. *Blood*, *125*(14), 2276-2285. https://doi.org/10.1182/blood-2013-12-547208

Perez-Baena, M. J., Cordero-Perez, F. J., Perez-Losada, J., & Holgado-Madruga, M. (2023). The Role of GAB1 in Cancer. *Cancers (Basel)*, *15*(16). https://doi.org/10.3390/cancers15164179

Poola, I., DeWitty, R. L., Marshalleck, J. J., Bhatnagar, R., Abraham, J., & Leffall, L. D. (2005). Identification of MMP-1 as a putative breast cancer predictive marker by global gene expression analysis. *Nat Med*, *11*(5), 481-483. https://doi.org/10.1038/nm1243

Popescu, N. I., Lupu, C., & Lupu, F. (2010a). Extracellular protein disulfide isomerase regulates coagulation on endothelial cells through modulation of phosphatidylserine exposure. *Blood*, *116*(6), 993-1001. https://doi.org/10.1182/blood-2009-10-249607

Popescu, N. I., Lupu, C., & Lupu, F. (2010b). Role of PDI in regulating tissue factor: FVIIa activity. *Thromb Res*, *125 Suppl 1*, S38-41. https://doi.org/10.1016/j.thromres.2010.01.034

Popielarski, M., Ponamarczuk, H., Stasiak, M., Watala, C., & Swiatkowska, M. (2019). Modifications of disulfide bonds in breast cancer cell migration and invasiveness. *Am J Cancer Res*, *9*(8), 1554-1582. https://www.ncbi.nlm.nih.gov/pubmed/31497343

Powell, L. E., & Foster, P. A. (2021). Protein disulphide isomerase inhibition as a potential cancer therapeutic strategy. *Cancer Med*, *10*(8), 2812-2825. https://doi.org/10.1002/cam4.3836

Quintero-Fabian, S., Arreola, R., Becerril-Villanueva, E., Torres-Romero, J. C., Arana-Argaez, V., Lara-Riegos, J., Ramirez-Camacho, M. A., & Alvarez-Sanchez, M. E. (2019). Role of Matrix Metalloproteinases in Angiogenesis and Cancer. *Front Oncol*, *9*, 1370. https://doi.org/10.3389/fonc.2019.01370

Ranganathan, S., Halagowder, D., & Sivasithambaram, N. D. (2015). Quercetin Suppresses Twist to Induce Apoptosis in MCF-7 Breast Cancer Cells. *PLoS One*, *10*(10), e0141370. https://doi.org/10.1371/journal.pone.0141370

Read, A., & Schroder, M. (2021). The Unfolded Protein Response: An Overview. *Biology (Basel)*, *10*(5). https://doi.org/10.3390/biology10050384

Reinhardt, C., von Bruhl, M. L., Manukyan, D., Grahl, L., Lorenz, M., Altmann, B., Dlugai, S., Hess, S., Konrad, I., Orschiedt, L., Mackman, N., Ruddock, L., Massberg, S., & Engelmann, B. (2008). Protein disulfide isomerase acts as an injury response signal that enhances fibrin generation via tissue factor activation. *J Clin Invest*, *118*(3), 1110-1122. https://doi.org/10.1172/JCI32376

Salai, K. H. T., Wu, L. Y., Chong, J. R., Chai, Y. L., Gyanwali, B., Robert, C., Hilal, S., Venketasubramanian, N., Dawe, G. S., Chen, C. P., & Lai, M. K. P. (2023). Elevated Soluble TNF-Receptor 1 in the Serum of Predementia Subjects with Cerebral Small Vessel Disease. *Biomolecules*, *13*(3). https://doi.org/10.3390/biom13030525

Samanta, S., Tamura, S., Dubeau, L., Mhawech-Fauceglia, P., Miyagi, Y., Kato, H., Lieberman, R., Buckanovich, R. J., Lin, Y. G., & Neamati, N. (2017). Expression of protein disulfide isomerase family members correlates with tumor progression and patient survival in ovarian cancer. *Oncotarget*, *8*(61), 103543-103556. https://doi.org/10.18632/oncotarget.21569

Segovia, M., Russo, S., Jeldres, M., Mahmoud, Y. D., Perez, V., Duhalde, M., Charnet, P., Rousset, M., Victoria, S., Veigas, F., Louvet, C., Vanhove, B., Floto, R. A., Anegon, I., Cuturi, M. C., Girotti, M. R., Rabinovich, G. A., & Hill, M. (2019). Targeting TMEM176B Enhances Antitumor Immunity and Augments the Efficacy of Immune Checkpoint Blockers by Unleashing Inflammasome Activation. *Cancer Cell*, *35*(5), 767-781 e766. https://doi.org/10.1016/j.ccell.2019.04.003

Seo, H. S., Ku, J. M., Choi, H. S., Choi, Y. K., Woo, J. K., Kim, M., Kim, I., Na, C. H., Hur, H., Jang, B. H., Shin, Y. C., & Ko, S. G. (2016). Quercetin induces caspase-dependent extrinsic apoptosis through inhibition of signal transducer and activator of transcription 3 signaling in HER2-overexpressing BT-474 breast cancer cells. *Oncol Rep*, *36*(1), 31-42. https://doi.org/10.3892/or.2016.4786

Sharda, A., & Furie, B. (2018). Regulatory role of thiol isomerases in thrombus formation. *Expert Review of Hematology*, *11*(5), 437-448. https://doi.org/10.1080/17474086.2018.1452612

Sharda, A. V., Bogue, T., Barr, A., Mendez, L. M., Flaumenhaft, R., & Zwicker, J. I. (2021). Circulating Protein Disulfide Isomerase Is Associated with Increased Risk of Thrombosis in JAK2-Mutated Myeloproliferative Neoplasms. *Clin Cancer Res*, *27*(20), 5708-5717. https://doi.org/10.1158/1078-0432.CCR-21-1140

Shergalis, A., & Neamati, N. (2017). Protein Disulfide Isomerase. In S. Choi (Ed.), *Encyclopedia of Signaling Molecules* (pp. 1-12). Springer New York. https://doi.org/10.1007/978-1-4614-6438-9_101768-1

Shi, S., Ma, B., Sun, F., Qu, C., Li, G., Shi, D., Liu, W., Zhang, H., & An, H. (2022). Zafirlukast inhibits the growth of lung adenocarcinoma via inhibiting TMEM16A channel activity. *J Biol Chem*, *298*(3), 101731. https://doi.org/10.1016/j.jbc.2022.101731

Shiloh, Y. (2003). ATM and related protein kinases: safeguarding genome integrity. *Nat Rev Cancer*, *3*(3), 155-168. https://doi.org/10.1038/nrc1011

Sigismund, S., Avanzato, D., & Lanzetti, L. (2018). Emerging functions of the EGFR in cancer. *Molecular Oncology*, *12*(1), 3-20. https://doi.org/10.1002/1878-0261.12155

Singh, P., Arif, Y., Bajguz, A., & Hayat, S. (2021). The role of quercetin in plants. *Plant Physiol Biochem*, *166*, 10-19. https://doi.org/10.1016/j.plaphy.2021.05.023

Song, B. X., Azhar, L., Koo, G. K. Y., Marzolini, S., Gallagher, D., Swardfager, W., Chen, C., Ba, J., Herrmann, N., & Lanctot, K. L. (2024). The effect of exercise on blood concentrations of angiogenesis markers in older adults: A systematic review and meta-analysis. *Neurobiol Aging*, *135*, 15-25. https://doi.org/10.1016/j.neurobiolaging.2023.12.004

Stalker, T. J., Newman, D. K., Ma, P., Wannemacher, K. M., & Brass, L. F. (2012). Platelet signaling. *Handb Exp Pharmacol*(210), 59-85. https://doi.org/10.1007/978-3-642-29423-5_3

Stetler-Stevenson, W. G., & Seo, D. W. (2005). TIMP-2: an endogenous inhibitor of angiogenesis. *Trends Mol Med*, *11*(3), 97-103. https://doi.org/10.1016/j.molmed.2005.01.007

Stojak, M., Milczarek, M., Kurpinska, A., Suraj-Prazmowska, J., Kaczara, P., Wojnar-Lason, K., Banach, J., Stachowicz-Suhs, M., Rossowska, J., Kalviņš, I., Wietrzyk, J., & Chlopicki, S. (2020). Protein Disulphide Isomerase A1 Is Involved in the Regulation of Breast Cancer Cell Adhesion and Transmigration via Lung Microvascular Endothelial Cells. *Cancers*, *12*(10), 2850. https://doi.org/10.3390/cancers12102850

Stopa, J. D., Neuberg, D., Puligandla, M., Furie, B., Flaumenhaft, R., & Zwicker, J. I. (2017). Protein disulfide isomerase inhibition blocks thrombin generation in humans by interfering with platelet factor V activation. *JCI Insight*, *2*(1), e89373. https://doi.org/10.1172/jci.insight.89373

Stopa, J. D., & Zwicker, J. I. (2018). The intersection of protein disulfide isomerase and cancer associated thrombosis. *Thrombosis Research*, *164*, S130-S135. https://doi.org/10.1016/j.thromres.2018.01.005

Suhail, Y., Cain, M. P., Vanaja, K., Kurywchak, P. A., Levchenko, A., Kalluri, R., & Kshitiz. (2019). Systems Biology of Cancer Metastasis. *Cell Systems*, *9*(2), 109-127. https://doi.org/10.1016/j.cels.2019.07.003

Swiatkowska, M., Szymanski, J., Padula, G., & Cierniewski, C. S. (2008). Interaction and functional association of protein disulfide isomerase with alphaVbeta3 integrin on endothelial cells. *FEBS J*, *275*(8), 1813-1823. https://doi.org/10.1111/j.1742-4658.2008.06339.x

Thamban Chandrika, N., Fosso, M. Y., Alimova, Y., May, A., Gonzalez, O. A., & Garneau-Tsodikova, S. (2019). Novel zafirlukast derivatives exhibit selective antibacterial activity against Porphyromonas gingivalis. *Medchemcomm*, *10*(6), 926-933. https://doi.org/10.1039/c9md00074g

Townsend, D. M., Manevich, Y., He, L., Xiong, Y., Bowers, R. R., Jr., Hutchens, S., & Tew, K. D. (2009). Nitrosative stress-induced s-glutathionylation of protein disulfide isomerase leads to activation of the unfolded protein response. *Cancer Res*, *69*(19), 7626-7634. https://doi.org/10.1158/0008-5472.CAN-09-0493

Tuzovic, M., Herrmann, J., Iliescu, C., Marmagkiolis, K., Ziaeian, B., & Yang, E. H. (2018). Arterial Thrombosis in Patients with Cancer. *Curr Treat Options Cardiovasc Med*, *20*(5), 40. https://doi.org/10.1007/s11936-018-0635-x

Uehara, T., Nakamura, T., Yao, D., Shi, Z. Q., Gu, Z., Ma, Y., Masliah, E., Nomura, Y., & Lipton, S. A. (2006). S-nitrosylated protein-disulphide isomerase links protein misfolding to neurodegeneration. *Nature*, *441*(7092), 513-517. https://doi.org/10.1038/nature04782

Uhrin, P., & Breuss, J. M. (2013). uPAR: a modulator of VEGF-induced angiogenesis. *Cell Adh Migr*, *7*(1), 23-26. https://doi.org/10.4161/cam.22124

Urade, R., Oda, T., Ito, H., Moriyama, T., Utsumi, S., & Kito, M. (1997). Functions of characteristic Cys-Gly-His-Cys (CGHC) and Gln-Glu-Asp-Leu (QEDL) motifs of microsomal ER-60 protease. *J Biochem*, *122*(4), 834-842. https://doi.org/10.1093/oxfordjournals.jbchem.a021830

Valentova, K., Vrba, J., Bancirova, M., Ulrichova, J., & Kren, V. (2014). Isoquercitrin: pharmacology, toxicology, and metabolism. *Food Chem Toxicol*, *68*, 267-282. https://doi.org/10.1016/j.fct.2014.03.018

Vandenbroeck, K., Martens, E., & Alloza, I. (2006). Multi-chaperone complexes regulate the folding of interferon-gamma in the endoplasmic reticulum. *Cytokine*, *33*(5), 264-273. https://doi.org/10.1016/j.cyto.2006.02.004

Vatolin, S., Phillips, J. G., Jha, B. K., Govindgari, S., Hu, J., Grabowski, D., Parker, Y., Lindner, D. J., Zhong, F., Distelhorst, C. W., Smith, M. R., Cotta, C., Xu, Y., Chilakala, S., Kuang, R. R., Tall, S., & Reu, F. J. (2016). Novel Protein Disulfide Isomerase Inhibitor with Anticancer Activity in Multiple Myeloma. *Cancer Res*, *76*(11), 3340-3350. https://doi.org/10.1158/0008-5472.CAN-15-3099

Venetianer, P., & Straub, F. B. (1963). The enzymic reactivation of reduced ribonuclease. *Biochim Biophys Acta*, *67*, 166-168. https://doi.org/10.1016/0006-3002(63)91812-2

Waldner, M. J., Foersch, S., & Neurath, M. F. (2012). Interleukin-6--a key regulator of colorectal cancer development. *Int J Biol Sci*, *8*(9), 1248-1253. https://doi.org/10.7150/ijbs.4614

Wang, C., Li, W., Ren, J., Fang, J., Ke, H., Gong, W., Feng, W., & Wang, C.-c. (2013). Structural Insights into the Redox-Regulated Dynamic Conformations of Human Protein Disulfide

Isomerase. *Antioxidants & Redox Signaling*, *19*(1), 36-45. https://doi.org/10.1089/ars.2012.4630

Wang, X., Lundgren, A. D., Singh, P., Goodlett, D. R., Plymate, S. R., & Wu, J. D. (2009). An six-amino acid motif in the alpha3 domain of MICA is the cancer therapeutic target to inhibit shedding. *Biochem Biophys Res Commun*, *387*(3), 476-481. https://doi.org/10.1016/j.bbrc.2009.07.062

Wang, L., Wu, Y., Zhou, J., Ahmad, S. S., Mutus, B., Garbi, N., Hammerling, G., Liu, J., & Essex, D. W. (2013). Platelet-derived ERp57 mediates platelet incorporation into a growing thrombus by regulation of the alphaIIbbeta3 integrin. *Blood*, *122*(22), 3642-3650. https://doi.org/10.1182/blood-2013-06-506691

Wang, Z., Zhang, H., & Cheng, Q. (2020). PDIA4: The basic characteristics, functions and its potential connection with cancer. *Biomed Pharmacother*, *122*, 109688. https://doi.org/10.1016/j.biopha.2019.109688

Wei, L. H., Kuo, M. L., Chen, C. A., Chou, C. H., Lai, K. B., Lee, C. N., & Hsieh, C. Y. (2003). Interleukin-6 promotes cervical tumor growth by VEGF-dependent angiogenesis via a STAT3 pathway. *Oncogene*, *22*(10), 1517-1527. https://doi.org/10.1038/sj.onc.1206226

Weisbart, R. H. (1992). An antibody that binds a neutrophil membrane protein, ERp72, primes human neutrophils for enhanced oxidative metabolism in response to formyl-methionyl-leucyl-phenylalanine. Implications for ERp72 in the signal transduction pathway for neutrophil priming. *J Immunol*, *148*(12), 3958-3963. https://www.ncbi.nlm.nih.gov/pubmed/1318337

Wendelboe, A. M., & Raskob, G. E. (2016). Global Burden of Thrombosis: Epidemiologic Aspects. *Circ Res*, *118*(9), 1340-1347. https://doi.org/10.1161/CIRCRESAHA.115.306841

Wermuth, H. R., Badri, T., & Takov, V. (2025). Montelukast. In *StatPearls*. https://www.ncbi.nlm.nih.gov/pubmed/29083616

Wu, Y., & Essex, D. W. (2020). Vascular thiol isomerases in thrombosis: The yin and yang. *J Thromb Haemost*, *18*(11), 2790-2800. https://doi.org/10.1111/jth.15019

Xiu-Ying, H., Yue-Xiang, Z., Hui-Si, Y., Hong-Zhou, Y., Qing-Jie, X., & Ting-Hua, W. (2024). PDGFBB facilitates tumorigenesis and malignancy of lung adenocarcinoma associated with PI3K-AKT/MAPK signaling. *Sci Rep*, *14*(1), 4191. https://doi.org/10.1038/s41598-024-54801-7

Xu, S., Butkevich, A. N., Yamada, R., Zhou, Y., Debnath, B., Duncan, R., Zandi, E., Petasis, N. A., & Neamati, N. (2012). Discovery of an orally active small-molecule irreversible inhibitor of protein disulfide isomerase for ovarian cancer treatment. *Proc Natl Acad Sci U S A*, *109*(40), 16348-16353. https://doi.org/10.1073/pnas.1205226109

Xu, S., Sankar, S., & Neamati, N. (2014). Protein disulfide isomerase: a promising target for cancer therapy. *Drug Discovery Today*, *19*(3), 222-240. https://doi.org/10.1016/j.drudis.2013.10.017

Yang, J., Nie, J., Ma, X., Wei, Y., Peng, Y., & Wei, X. (2019). Targeting PI3K in cancer: mechanisms and advances in clinical trials. *Mol Cancer*, *18*(1), 26. https://doi.org/10.1186/s12943-019-0954-x

Yang, S., Jackson, C., Karapetyan, E., Dutta, P., Kermah, D., Wu, Y., Wu, Y., Schloss, J., & Vadgama, J. V. (2022). Roles of Protein Disulfide Isomerase in Breast Cancer. *Cancers (Basel)*, *14*(3). https://doi.org/10.3390/cancers14030745

Yang, Z., Liu, J., Shi, Q., Chao, Y., Di, Y., Sun, J., Zhang, J., Huang, L., Guo, H., & He, C. (2018). Expression of protein disulfide isomerase A3 precursor in colorectal cancer. *OncoTargets and Therapy*, *Volume 11*, 4159-4166. https://doi.org/10.2147/ott.s154452

Yoshimori, T., Semba, T., Takemoto, H., Akagi, S., Yamamoto, A., & Tashiro, Y. (1990). Protein disulfide-isomerase in rat exocrine pancreatic cells is exported from the endoplasmic reticulum despite possessing the retention signal. *J Biol Chem*, *265*(26), 15984-15990. https://www.ncbi.nlm.nih.gov/pubmed/2394756

Zhao, H., Wu, L., Yan, G., Chen, Y., Zhou, M., Wu, Y., & Li, Y. (2021). Inflammation and tumor progression: signaling pathways and targeted intervention. *Signal Transduct Target Ther*, *6*(1), 263. https://doi.org/10.1038/s41392-021-00658-5

Zhou, J., Wu, Y., Chen, F., Wang, L., Rauova, L., Hayes, V. M., Poncz, M., Li, H., Liu, T., Liu, J., & Essex, D. W. (2017). The disulfide isomerase ERp72 supports arterial thrombosis in mice. *Blood*, *130*(6), 817-828. https://doi.org/10.1182/blood-2016-12-755587

Zhou, J., Wu, Y., Rauova, L., Koma, G., Wang, L., Poncz, M., Li, H., Liu, T., Fong, K. P., Bennett, J. S., Kunapuli, S. P., & Essex, D. W. (2022). A novel role for endoplasmic reticulum protein 46 (ERp46) in platelet function and arterial thrombosis in mice. *Blood*, *139*(13), 2050-2065. https://doi.org/10.1182/blood.2021012055

Zhou, J., Wu, Y., Wang, L., Rauova, L., Hayes, V. M., Poncz, M., & Essex, D. W. (2014). The disulfide isomerase ERp57 is required for fibrin deposition in vivo. *J Thromb Haemost*, *12*(11), 1890-1897. https://doi.org/10.1111/jth.12709

Zwicker, J. I., Schlechter, B. L., Stopa, J. D., Liebman, H. A., Aggarwal, A., Puligandla, M., Caughey, T., Bauer, K. A., Kuemmerle, N., Wong, E., Wun, T., McLaughlin, M., Hidalgo, M., Neuberg, D., Furie, B., & Flaumenhaft, R. (2019). Targeting protein disulfide isomerase with the flavonoid isoquercetin to improve hypercoagulability in advanced cancer. *JCI Insight*, *4*(4). https://doi.org/10.1172/jci.insight.125851

Chapter 2

Development of zafirlukast analogues for improved anti-thrombotic activity through thiol isomerase inhibition

In this chapter, analogues of zafirlukast, an FDA approved LTR antagonist, were investigated for enhanced thiol isomerase inhibition. The foundation of this chapter stemmed from our previous observation that zafirlukast acts as a broad-spectrum thiol isomerase inhibitor and performs as an inhibitor of thrombosis and the work of Kaitlind Howard and her development of zafirlukast analogues. I hypothesise that some analogues of zafirlukast will be able to inhibit thrombosis better than the parent compound. Therefore, 35 analogues of this compound were created and tested for thiol isomerase inhibition and effects on platelets. Of the 35 analogues created, one termed compound **21** demonstrated greater potency than zafirlukast for thiol isomerase inhibition and was further investigated and found to exhibit better inhibition of platelet aggregation, P-selectin exposure, levels of surface platelet thiols and *in vivo* thrombus formation than that of the parent compound.

For this work I contributed the cell free assays, reversibility assays, platelet aggregation, P-selectin studies and platelet thiol labelling studies. In addition, I drafted the manuscript, prepared the figures and addressed reviewers' comments. Therefore, I estimate that I have contributed to over 60% of work put into this paper.

The full paper published at *Arteriosclerosis, Thrombosis, and Vascular Biology* can be found at *Arterioscler Thromb Vasc Biol*, *45*(4), e136-e149. https://doi.org/10.1161/ATVBAHA.124.321579.

Development of zafirlukast analogues for improved anti-thrombotic activity through thiol isomerase inhibition

Justine A. Keovilay[1,2], Kaitlind C. Howard[3], Kirk A. Taylor[2], Sabeeya Khan[2], Sienna E. Wurl[1], Melanie K. Szahaj[1], Tanya Sage[2], Nishad Thamban Chandrika[3], Caixia Hou[3], Oleg V. Tsodikov[3], Jonathan M. Gibbins[2], Sylvie Garneau-Tsodikova[3], and Daniel R. Kennedy[1,2,4].

[1] College of Pharmacy and Health Sciences, Western New England University, Springfield, MA, 01119.

[2] Institute for Cardiovascular & Metabolic Research, School of Biological Sciences, University of Reading, UK, RG6 6EX.

[3] Department of Pharmaceutical Sciences, College of Pharmacy, University of Kentucky, 789 S. Limestone St., Lexington, KY, 40536.

[4] Department of Medicine, UMass Chan Medical School-Baystate, Springfield, MA, 01655.

Corresponding Author: Daniel R. Kennedy, Department of Pharmaceutical & Administrative Sciences, College of Pharmacy and Health Sciences, Western New England University, 1215 Wilbraham Road, Springfield, MA, 01119. Tel: 413-796-2413. E-mail: dkennedy@wne.edu

Authors contributions

J.A.K. and K.C.H. drafted the manuscript. K.C.H. and N.T.C. synthesized the zafirlukast analogues. J.A.K., S.K., and K.A.T. performed the platelet experiments. J.A.K., M.K.S., and S.E.W. performed the cell-free enzymatic assays. C.H. performed inhibitor binding assays.

S.K. and K.A.T. performed intravital experiments and T.S. conducted tail bleeding assays. D.K and J.M.G. designed experiments. S.K., J.A.K., O.V.T., and S.G.-T. prepared the figures for the manuscript. D.R.K., J.M.G., S.G.-T., and O.V.T. supervised the project, edited the manuscript and supporting information, and provided funding for the work.

Keywords: Drug repurposing, Zafirlukast, PDI, Structure-activity relationship, Thiol isomerase, Thrombosis.

Acknowledgement: We thank the Bioresource Unit staff at the University of Reading for animal care and husbandry and Parvathy Susikumar for helpful discussions on the intravital work.

Sources of Funding: This work was supported by a National Cancer Institute grant R21CA231000 to D.R.K., a British Heart Foundation project grants (PG/22/10965) to K.A.T., as well as a National Institutes of Health (NIH) F31 fellowship DEO29661 to K.C.H. J.A.K. and S.K. were supported by PhD studentships from Quercis Pharma. The content is solely the responsibility of the authors and does not necessarily represent the official views of the National Institutes of Health.

Disclosures: D.R.K. and J.M.G are inventors on a patent owned by Western New England University repurposing zafirlukast as a potential antithrombotic medication and receive research funding from Quercis Pharma. D.R.K. and S.G.T. are also inventors on a patent owned by Western New England University exploring zafirlukast analogues in thrombosis and cancer.

2.1 Graphical abstract

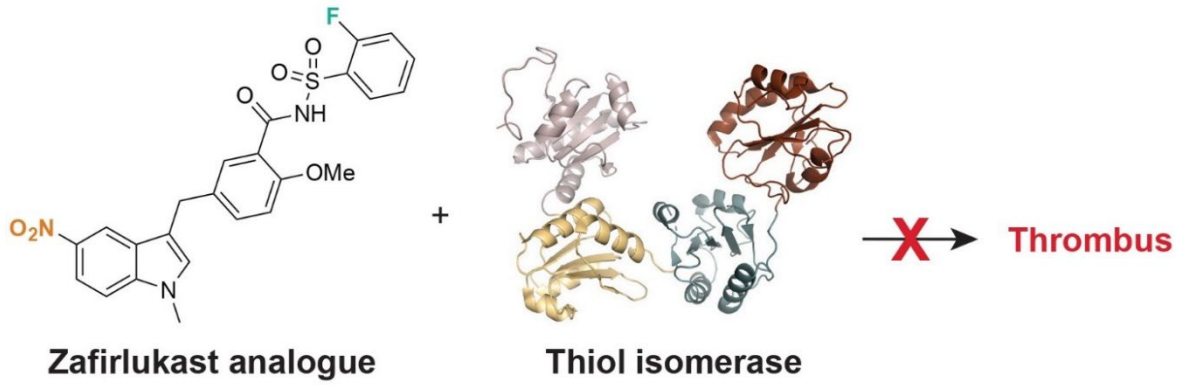

2.2 Abstract

Background: Thiol isomerases play essential and non-redundant roles in platelet activation, aggregation, and thrombus formation. Thiol isomerase inhibitors have the potential to overcome the two major drawbacks of current antithrombotic therapies, as they target both arterial and venous thrombosis without enhancing bleeding risks. Recently, an FDA-approved drug, zafirlukast (ZAF), was shown to be a promising pan-thiol isomerase inhibitor. The objective of this study is to develop analogues of ZAF with optimized thiol isomerase inhibition and antithrombotic activity.

Methods: 35 ZAF analogues were tested in an insulin turbidometric assay for thiol isomerase inhibition. Analogues were tested for platelet activation, aggregation, P-selectin expression, and laser-induced thrombosis in mice and compared with the parent compound.

Results: Of the 35 analogues, 12 retained activity, with one, compound **21** that demonstrated a greater potency than that of ZAF, 5 had a similar potency to that of ZAF, and 6 had a weaker potency. Analogues demonstrated inhibition of platelet aggregation and P-selectin expression as compared to ZAF, consistent with their potencies. ZAF and compound **21** were shown to be reversible inhibitors of thiol isomerases, and not cytotoxic to cultured, lung, liver, and kidney cells. Finally, in an *in vivo* assessment of thrombus formation, compound **21** was able to significantly inhibit thrombus formation without affecting bleeding times.

Conclusions: A ZAF analogue, compound **21**, with properties superior to those of ZAF was synthesized, demonstrating improved inhibition of platelet activation, aggregation, and thrombus formation as compared to the parent ZAF. This approach could yield a promising clinical candidate for treatment and prophylaxis of arterial and venous thrombosis.

Abbreviations

ZAF	zafirlukast
PDI	protein disulfide isomerase
ERp57	endoplasmic reticulum-resident protein 57
ERp72	endoplasmic reticulum-resident protein 72
CysLTR	cysteinyl leukotriene receptor
SAR	structure-activity relationship
PACMA	PACMA-31
PRP	platelet rich plasma
PGI_2	prostacyclin
ACD	acid citrate dextrose
PE	phycoerythrin
CRP	collagen related peptide
MPB	3-(*N*-maleimidopropionyl)-biocytin
SDS-PAGE	sodium dodecyl sulphate polyacrylamide gel electrophoresis
TBS	tris buffered saline
HRP	horseradish peroxidase
TBS-T	tris buffered saline + Tween-20

2.3 Introduction

Thrombosis is the most common underlying pathology related to diseases such as myocardial infarction, stroke, ischemic heart disease, deep vein thrombosis, and pulmonary embolism (Furie & Furie, 2012; Holbrook et al., 2021; Stoll et al., 2008). Yet, despite the prevalence of these diseases, current antithrombotic agents cannot prevent both arterial (Hartwig & Italiano, 2003; Schror, 1997) and venous thrombosis (Heit, 2005; Patel et al., 2022), and they are associated with significant risks of bleeding, limiting their prophylactic use (Sorensen et al., 2000).

Thiol isomerase inhibitors have the potential to overcome these two major limitations to current therapy, as they have the ability to target both arterial and venous thrombosis without an increased risk of bleeding (Holbrook et al., 2021; Jasuja et al., 2012a). Indeed, a clinical study of patients with advanced cancer taking isoquercetin, a selective inhibitor of the thiol isomerase protein disulfide isomerase (PDI), demonstrated decreased platelet-dependent thrombin and circulating soluble P-selectin levels without enhanced bleeding (J. I. Zwicker et al., 2019a). Thiol isomerases have extracellular activities that modulate thrombus formation, fibrin formation, and platelet aggregation (Flaumenhaft & Furie, 2016; Furie & Furie, 2008; Schulman et al., 2016). These enzymes include PDI and closely related endoplasmic reticulum-resident proteins 57 (Holbrook et al., 2012a) and 72 (Holbrook et al., 2018b) (ERp57 and ERp72), which play important roles in both arterial and venous thrombosis through the propagation of platelet activation (Jordan et al., 2005). Inhibition of these enzymes has been shown to decrease platelet activation, aggregation, and adhesion, in addition to inhibiting thrombus formation (Essex & Li, 1999b; Lahav et al., 2002). Interestingly, these enzymes are non-redundant, as a genetic deletion of one thiol isomerase family member, while rescued by the respective recombinant enzyme, is not rescued by other family members (L. Wang et al.,

2013; Zhou et al., 2017; Zhou et al., 2022; Zhou et al., 2014b), suggesting that pan-thiol isomerase inhibitors may have additional effects compared to selective PDI inhibitors.

Previously, we identified zafirlukast (ZAF), an FDA-approved cysteinyl leukotriene receptor (CysLTR1) antagonist used for the treatment of asthma (Spector, 1996), as a pan-inhibitor of thiol isomerase activity (Holbrook et al., 2021). ZAF was shown to modulate platelet function and integrin function *ex vivo,* including inhibiting platelet aggregation and P-selectin expression while also demonstrating *in vivo* inhibition of thrombus formation in live mice (Holbrook et al., 2021). In a previous study, we demonstrated that an analogue of ZAF that lacked the moiety involved in binding the CysLTR1 receptor retained thiol isomerase inhibitory activity (Gelzinis et al., 2023b). Thus, ZAF analogue optimization by medicinal chemistry may yield an analogue with improved potency as a thiol isomerase inhibitor and no activity as a CysLTR1 antagonist. The structure of ZAF offers a rich opportunity for structure-activity relationship (SAR) studies, as its molecular structure contains a cyclopentyl carbamate attached to an *N*-methylindole and an arylsulfonamide scaffold linked *via* a decorated benzoyl ring (Figure 2.1). These chemical moieties suggest various modification possibilities for SAR studies, including varying the identities and positions of the substituents on each of these aromatic and heterocyclic ring systems and altering scaffold organization, with the goal of increasing the inhibition of thiol isomerases and detuning the inhibition of CysLTR1 (Howard & Garneau-Tsodikova, 2022; Howard et al., 2020b). Previously, SAR studies of ZAF were successful in developing potent antibacterial ZAF analogues to combat the periodontal disease (Howard & Garneau-Tsodikova, 2022; Howard et al., 2020b), therefore, there is the potential to develop improved analogues that target thiol isomerases for thrombosis prevention and treatment.

In this study, we investigated 35 ZAF analogues to identify modifications that improve thiol isomerase inhibition potency. Select analogues were explored for their ability to inhibit

platelet aggregation and P-selectin expression. The most promising lead compound **21** was explored for its ability to reversibly inhibit thiol isomerases, block surface thiols, inhibit *in vivo* thrombus formation and effect on bleeding times.

2.4 Materials and Methods

2.4.1 Reagents

Recombinant human ERp57, PDI, and ERp72 were purchased from Abcam (Cambridge, MA, USA). ZAF was purchased from TCI America (Portland, OR, USA). Recombinant insulin (bovine), DTT, buffers, and all other chemicals were purchased from Sigma-Aldrich (St. Louis, MO, USA) and VWR (Radnor, PA, USA). The 96-well and 384-well clear bottom plates were purchased from Corning (Corning, NY, USA).

2.4.2 Chemical synthesis

The ZAF analogues were synthesized as described previously (Howard et al., 2020b; Thamban Chandrika et al., 2019).

2.4.3 The insulin-based turbidometric assay

Initially, the potency of the ZAF analogues in inhibiting thiol isomerase activity was determined by an insulin turbidity assay using ERp57, as previously described (Holbrook et al., 2021). Briefly, the analogues were diluted at specified concentrations for a 5-point dose-response curve in a 384-well plate, and the reactions were run immediately at 37 °C with final concentrations of 20 μg/mL (350 nM) ERp57 and 125 μM insulin in the reaction buffer (100 mM potassium phosphate, pH 7.4 adjusted at room temperature, 2 mM EDTA) in a total volume of 30 μL per well. The reaction was initiated with 0.3 mM DTT, and the turbidity of insulin aggregation was monitored by measuring absorbance at 650 nm every min for 90 min using a SpectraMax M3 plate reader (Molecular Devices, Sunnyvale, CA, USA). The same procedure was used to measure inhibition of PDI and ERp72 by compound **21**, substituting ERp57 for the enzyme of interest. Experiments were performed in quadruplicate.

To determine the reversibility of inhibition, ZAF, compound **21**, the reversible control rutin (Jasuja et al., 2012a), and the irreversible control PACMA-31 (Xu et al., 2012b) (PACMA) were pre-incubated with 180 nM PDI at a final concentration of 30 μM in the same reaction buffer for 0, 0.5, 1, or 4 h. Then, the reactions were initiated by the addition of 125 μM insulin and 0.3 mM DTT, and the turbidity was measured for 90 min. 1% DMSO was used as a control. Experiments for ZAF and compound **21** were performed in triplicate.

2.4.4 The inhibitor binding assay

ERp57 (1 μM) was mixed with compound **21** at specified concentrations in binding buffer (100 mM potassium phosphate, pH 7.4, 2 mM EDTA, 0.3 mM DTT) on ice. The enzyme without inhibitors was mixed with 1% DMSO as a control. The samples were loaded into a 96-well plate at 21 °C, the intrinsic fluorescence of protein tryptophan residues was measured using the excitation wavelength of 290 nm with a cut-off filter at 325 nm, and the emission scanned at the wavelengths of 325-380 nm. At these conditions, the contribution of compound **21** to the measured fluorescence was negligible compared to that of the protein at all concentrations of the inhibitor used in this assay. The titrations were performed in triplicate. Relative fluorescence quenching ($|\Delta\omega|/\omega_0$; the fraction of fluorescence lost) at the fluorescence maximum (339 nm) was plotted as a function of inhibitor concentration and used in a nonlinear regression analysis with SigmaPlot 9.0 (Grafiti) with the following 1:1 binding isotherm, to obtain the values of the equilibrium binding constant K_d:

$$\frac{|\Delta\omega|}{\omega_0} = A\frac{[I]}{K_d + [I]}$$

Here, A is the relative fluorescence quenching at infinite inhibitor concentration, the second fitting parameter.

2.4.5 Cytotoxicity assay

HEK-293, BEAS-2B, and HepG2 cells were plated in 96-well microtiter plates at concentrations of 10,000 cells per well for HEK-293 and 3,000 cells per well for BEAS-2B and HepG2. The plates were incubated with 5% CO_2 at 37 °C for 16 h to allow the cells to adhere to the wells. The medium was removed and fresh medium with ZAF or analogue **21** was added. Negative control contained 0.1% DMSO, and the positive control contained 1% Triton X-100®. The relative cell survival was evaluated after 24 h of incubation by adding resazurin (10 μL of 10 mM solution) for 6 h. A SpectraMax M5 plate reader was used to monitor live cells by fluorescence measurements with 560 nm excitation and 590 nm emission wavelengths and the relative cell survival values were then calculated. Experiments were performed in quadruplicate.

2.4.6 Platelet preparation and stimulation

After receiving approval from the Western New England University IRB, human platelets were collected from consenting, drug-free, donors in tubes containing 3.2% sodium citrate tubes using standard venipuncture techniques. Platelet rich plasma (PRP) was obtained by centrifugation of whole blood at 100×g for 20 min at 20 °C. For washed platelets, 10 μL of 125 μg/mL prostacyclin (PGI_2) was added to PRP and centrifuged at 1410xg for 10 min at 20 °C. Supernatant was removed and platelets were resuspended in 1 mL of Tyrode's buffer (20 mM HEPES, 144 mM NaCl, 3 mM KCl, 12 mM $NaHCO_3$, and 1 mM $MgCl_2$, pH 7.3 adjusted at room temperature) and 150 μL acid citrate dextrose (ACD, 97 mM $Na_3C_6H_5O_7$, 111 mM $C_6H_{12}O_6$ and 78 mM $C_6H_8O_7$) with an additional 21 mL Tyrode's buffer, 3 mL ACD and 10 μL of 125 μg/mL PGI_2 added to the suspension. Platelets were then centrifuged at 1410xg for 10 min at 20 °C, the supernatant removed, and the platelet pellet resuspended at a concentration of $1x10^8$ in Tyrode's buffer. For aggregation assays, PRP was incubated with vehicle (DMSO,

0.1% *v/v* in Tyrode's buffer), ZAF (1.25, 2.5, 5, 10, 20, or 40 μM), compound **21** (1.25, 2.5, 5, 10, or 20 μM), compound **22** or compound **35** (1.25, 2.5, 5, 10, 20, 40 or 80 μM) for 5 min prior to stimulation. Then, collagen **(**1.9 mg/mL diluted in water; 0.19 mg/mL final concentration) was used to stimulate platelets for 180 s in a lumi-aggregometer (PAP-8E, Horsham, PA, USA) with continuous stirring. The experiments were performed in quadruplicate.

2.4.7 P-selectin exposure

To assess P-selectin exposure on platelets, 46 μL of HEPES buffered saline (10 mM HEPES, pH 7.4 adjusted at room temperature, 134 mM NaCl, 5 mM KCl, 2 mM $MgSO_4$), 2 μL of PRP and phycoerythrin (PE) conjugated anti-CD62P (1:50 dilution from the purchased stock; BD Biosciences catalogue #551142) or PE conjugated IgG1 isotype control (1:50 dilution from the purchased stock; BD Biosciences, Franklin Lakes, NJ, USA, catalogue #555750) were incubated with vehicle control (DMSO, 0.1% *v/v* in Tyrode's buffer), ZAF, compound **21**, compound **22** or compound **35** (0, 3, 10, and 30 μM) for 30 min at room temperature. Upon completion of incubation, platelets were stimulated with collagen related peptide (CRP, 5 μg/mL) and allowed to incubate for an additional 30 min at room temperature. The platelets were then fixed with 100 μL of 0.2% formalin. The platelets were analysed on a BD Accuri C6 Plus flow cytometer for P-selectin expression with 10,000 gated events recorded. The experiments were performed in triplicate.

2.4.8 3-(*N*-maleimidylpropionyl biocytin (MPB) thiol labelling and blotting

Washed platelets were treated with vehicle control (DMSO, 0.1% *v/v* in Tyrode's buffer), 20 μM ZAF or 20 μM compound **21** for 5 min then stimulated in the same manner as above. Then 250 μL of drug treated stimulated platelets were incubated with 100 μM MPB

(Cayman Chemical, Ann Arbor, MI, USA) for 20 min at 37°C, and then with excess DTT to quench any unbound MPB. After incubation, 50 μL of SDS-PAGE sample loading buffer containing 125 mM DTT (Cell Signalling Technology, Danvers, MA, USA) was added to each sample, heated for 5 min at 95 °C and then put on ice. 25 μL of each sample was then analysed by SDS-PAGE using a Bio-Rad mini gel system (Bio-Rad, Hercules, CA, USA) in SDS-PAGE running buffer (25 mM Tris, 192 mM glycine, 0.1% SDS, pH 8.3) and transferred to a polyvinylidene difluoride membrane in transfer buffer (25 mM Tris, 192 mM glycine, 20% methanol). After transfer, membranes were blocked for 1 hour at room temperature in blocking buffer (Tris buffered saline [TBS; 15 mM Tris-HCL, 4.6 mM Tris-base, 150 mM NaCl, pH 7.6 adjusted at room temperature] + 5% non-fat dry milk, *w*/*v*) then probed with streptavidin-horseradish peroxidase conjugate (HRP; ThermoFisher Scientific, Waltham, MA, USA) in a 1:5000 dilution in TBS + 0.1% Tween-20 (TBS-T) and chemiluminescence detected with Novex ECL substrate (Invitrogen, Waltham, MA, USA) on a Bio-Rad ChemiDoc imaging system (Bio-Rad, Hercules, CA, USA). Membranes were stripped in buffer (200 mM glycine, 3.5 mM SDS, 1% Tween-20, pH 2.2 adjusted at room temperature) and re-probed with a beta actin primary antibody (1:5000 dilution, Cell Signalling Technology, Danvers, MA, USA) followed by an HRP-coupled secondary antibody (1:10000 dilution, Cell Signalling Technology, Danvers, MA, USA) and chemiluminescence detected as described above. Membranes were analysed using Bio-Rad Image Lab software (Bio-Rad, Hercules, CA, USA). Experiments were performed in quadruplicate.

2.4.9 Assessment of thrombus formation, emboli formation and tail bleeding in mice

To assess the ability of compound **21** to inhibit *in vivo* arterial thrombus formation, intravital microscopy using laser injury was performed. Male C57BL/6J mice aged 4-6 weeks with a weight range of 19-28 g were anaesthetized by intraperitoneal injection of ketamine

(100 mg/kg), medetomidine (1.0 mg/kg), and atropine (0.25 mg/kg) and maintained at 37 °C throughout the duration of the experiment. Platelets were labelled via intravenous infusion of DyLight 649-conjugated anti-GPIb platelet labelling antibody (EmFret Analytics, Wurzburg, Germany; 0.2 μg/g of body weight) as previously reported (Holbrook et al., 2021). After the exposure of the testicular cremaster muscle, the vehicle DMSO in Tyrode's buffer (0.1% *v/v*) or compound **21** was infused intravenously. Then, following a 5-min incubation period, the arterial wall injury was induced by laser ablation (Micropoint, Andor Technology, Belfast, UK). Thrombus formation was observed with an Olympus BX microscope (Olympus, Essex, UK) at 60× magnification and a Hamamatsu (Hamamatsu Photonics, Hertfordshine, UK) CCD camera. The data were analysed using Slidebook 2023 (Intelligent Imaging Innovations, Denver, USA) (Falati et al., 2006; Holbrook et al., 2018b; Holbrook et al., 2012a). Thrombus formation data were smoothed using LOWESS curves within GraphPad Prism to calculate maximum fluorescence intensity for each thrombus. Emboli were recorded using an empty mask that was positioned downstream of the thrombus when the field of view allowed. An embolic event was classified as a transient recording of a platelet mass within this gate and was visually confirmed by the experimenter. The experiments were performed with five separate mice per group, where multiple thrombi were able to be formed per mouse. Only male mice were used in these experiments due to the location of arterial injury at the cremaster muscle, of which only male mice have this anatomical feature. Mice were euthanized using Schedule 1 approved methods (cervical dislocation) at the end of the experiment. For the tail bleeding assay, male C57BL/6J mice (n=10 per group) were anaesthetized by intraperitoneal injection of ketamine and medetomidine, and compound **21** or vehicle was infused into the femoral vein 5 min prior to tail biopsy. Following drug treatment, 0.2 cm of the tail tip was excised, and blood collected into sterile PBS. Time to bleeding cessation was recorded. Mice were euthanized when bleeding had ceased or at 20 min post tail tip excision. All animal experiments

were blinded for both the experimental treatment and the analysis. The animal experiments were approved by the University of Reading Local Ethical Review Panel and authorized by the United Kingdom Home Office.

2.4.10 Statistics

The statistical analyses were performed using GraphPad Prism (Version 9.4.0, San Diego, CA). Data were presented as the mean ± SD. For reversibility, platelet aggregation and P-selectin studies, a two-way ANOVA with a Tukey's *post hoc* test was used as each mean was compared with every other mean. For the MPB thiol labelling study, a one-way ANOVA with a Tukey's *post hoc* test was performed. For *in vivo* thrombus formation and tail bleed assays, a Mann-Whitney test was performed as data was not normally distributed.

2.5 Results

2.5.1 SAR analysis of ZAF analogues for thiol isomerase inhibition

The 35 ZAF analogues evaluated in this study consist of one of two major scaffolds, 1 and 2 (Figure 2.1). In scaffold 1, the organization of the substituents on the benzoyl group (ring B) was kept the same as that found in the parent ZAF (3-methoxy-4-indoyl organization), while in scaffold 2, the organization of the substituents on ring B was different (2-methoxy-5-indoyl organization). The use of two different scaffolds offered an ideal opportunity for initial SAR studies. Of note, none of these ZAF analogues contained the cyclopentyl moiety appended to ring A in ZAF. The removal of the cyclopentyl moiety resulted in a greater than 100-fold reduction in potency of ZAF analogues as CysLTR1 antagonists (Bernstein, 1998b). Moreover, the different organization of scaffold 2 from that of ZAF is expected to lead to further significant reduction or loss of CysLTR1 antagonism for the analogues with this scaffold. For this reason, 30 of the 35 analogues tested in this study belonged to scaffold 2.

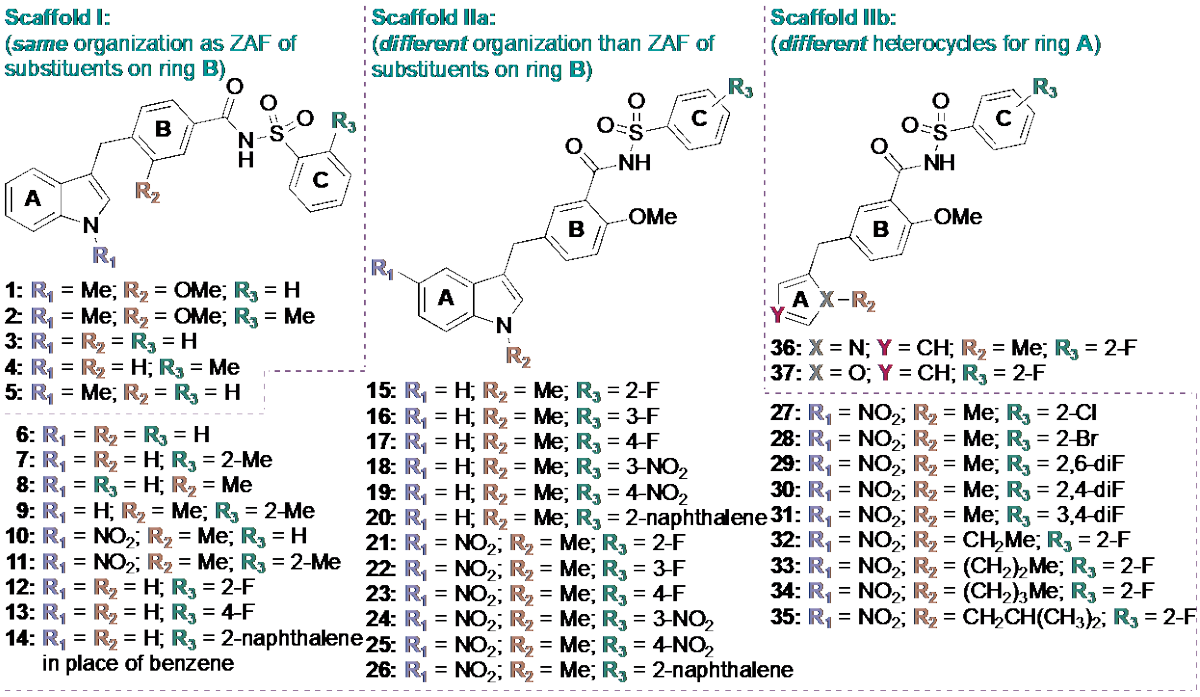

Figure 2.1 The structures of zafirlukast (ZAF) and its 35 analogues tested in this study. (A) The structures of ZAF and the two chemical scaffolds of the synthesized ZAF derivatives. (B) The ZAF analogues with scaffold 1. and (C) The ZAF analogues with scaffold 2. Compounds developed and figure generated by Kaitlind C. Howard and Sylvie Garneau-Tsodikova from the University of Kentucky.

To determine the potency of ZAF and its 35 analogues (**1**-**35**) as thiol isomerase inhibitors, we first tested all compounds for their inhibition of thiol isomerase ERp57 (Table 2.1, Figure 2.2 A,B and Supplemental Figure 2.1). In addition to ZAF, 11 analogues displayed concentration-dependent inhibition of ERp57 (Supplemental Figure 2.1), while the rest of the analogues did not show observable inhibition up to 100 μM. In addition to ZAF, only one of the analogues with scaffold 1 (compound **2**) inhibited ERp57, but this inhibition was weak (IC_{50} = 99 ± 8 μM). Note that IC_{50} in this study is defined as the inhibitor concentration at which the enzyme is inhibited by 50% of its activity in the absence of an inhibitor, regardless of whether the inhibitor can completely inhibit the enzyme or not. In analogue **2**, the identities of R_1, R_2, and R_3 groups all matched those of ZAF, whereas other analogues with scaffold 1, in which these groups were replaced by hydrogens, were inactive as ERp57 inhibitors.

Among the ten active analogues with scaffold 2, one (compound **21**) was 2.5-fold more potent than ZAF (Figure 2.2 A,B), indicating that the inhibition of ERp57 could be uncoupled from CysLTR1 antagonism. The other nine analogues were similarly potent or less potent than ZAF (Supplemental Figure 2.1). Six of these compounds (**22**, **23**, **24**, **27**, **28**, and **34**) had comparable or, at most, ~2-fold weaker inhibition potencies relative to that of ZAF. The other three compounds, **26**, **31**, and **35** were weak inhibitors. These observations indicated that a 2-F was the most preferred substitution at the R_3 position (in the context of R_1 = NO_2 and R_2 = Me), among those tested, whereas the bulkier and nonpolar 2-Cl (compound **27**) and 2-Br (compound **28**) were inferior. A 3-F, 3-NO_2, or a 4-F at the R_3 (compounds **22, 24**, and **23**) were tolerable, but these substituents did not yield potency improvement. With a 2-F at the R_3 and an NO_2 at the R_1 position, increasing the size of an alkyl substituent at the R_2 position (as in compounds **33**, **34**, and **35**) decreased or abolished inhibition potency, although an *n*-butyl group at the R_2 (compound **34**) was tolerable. These compounds contained either 4-F or the polar 3-NO_2 substitutions at the R_3 or a bulky naphthalene ring in place of the benzene ring.

Compounds with other substitutions tested at the R_3 position, including di-F substitutions, were not inhibitory to ERp57. Identities of the groups at the R_1 and R_2 positions were not as varied as the R_3 position in this compound set. Compounds with unsubstituted R_1 and R_2 positions were inactive as ERp57 inhibitors.

Next, we tested the direct binding of the most potent inhibitor (compound **21**) to ERp57. We monitored quenching of intrinsic fluorescence of ERp57, originated mostly from its Trp residues, upon titrating compound **21** (Figure 2.2 C). A significant (25%) saturable quenching signal was observed, consistent with specific binding, yielding the value of the equilibrium binding constant of 4.8 ± 1.7 μM, in agreement with the IC_{50} of this compound. Compound **21** was additionally tested for its inhibition of thiol isomerases PDI and ERp72 (Supplemental Figure 2.2). Compound **21** inhibited both of these enzymes with an IC_{50} ~20 μM, about 2-fold less potently than it did ERp57.

Table 2.1: The potencies of ZAF analogues as ERp57 inhibitors.

Active compounds					
Compound #	**Scaffold**	**R_1**	**R_2**	**R_3**	**IC_{50} (μM)**
ZAF					25 ± 4[a]
2	1	Me	OMe	Me	99 ± 8[b]
21	2	NO_2	Me	2-F	9.9 ± 1.1[a]
22	2	NO_2	Me	3-F	33 ± 9[b]
23	2	NO_2	Me	4-F	44 ± 11[b]
24	2	NO_2	Me	3-NO_2	33 ± 15[b]
26	2	NO_2	Me	2-naphthalene in place of benzene	>100[b]
27	2	NO_2	Me	2-Cl	61 ± 9[b]
28	2	NO_2	Me	2-Br	50 ± 14[b]
31	2	NO_2	Me	3,4-diF	>100[b]
34	2	NO_2	$(CH_2)_3Me$	2-F	40 ± 15[b]
35	2	NO_2	$CH_2CH(CH_3)_2$	2-F	>100[b]
Inactive compounds					
Compound #		**R_1**	**R_2**	**R_3**	**IC_{50} (μM)**
1	1	Me	OMe	H	-[c]
3	1	H	H	H	-
4	1	H	H	Me	-
5	1	Me	H	H	-
6	2	H	H	H	-
7	2	H	H	2-Me	-
8	2	H	Me	H	-
9	2	H	Me	2-Me	-
10	2	NO_2	Me	H	-
11	2	NO_2	Me	2-Me	-
12	2	H	H	2-F	-
13	2	H	H	4-F	-
14	2	H	H	2-naphthalene in place of benzene	-
15	2	H	Me	2-F	-
16	2	H	Me	3-F	-
17	2	H	Me	4-F	-
18	2	H	Me	3-NO_2	-
19	2	H	Me	4-NO_2	-
20	2	H	Me	2-naphthalene in place of benzene	-
25	2	NO_2	Me	4-NO_2	-
29	2	NO_2	Me	2,6-diF	-
30	2	NO_2	Me	2,4-diF	-
32	2	NO_2	CH_2Me	2-F	-
33	2	NO_2	$(CH_2)_2Me$	2-F	-

[a] The corresponding dose-response data for these compounds are presented in Figure 2A,B.

[b] The corresponding dose-response data for these compounds are presented in Figure S1.

[c] The hyphen indicates that no inhibition was detected even at the highest concentration of 100 mM of compound tested.

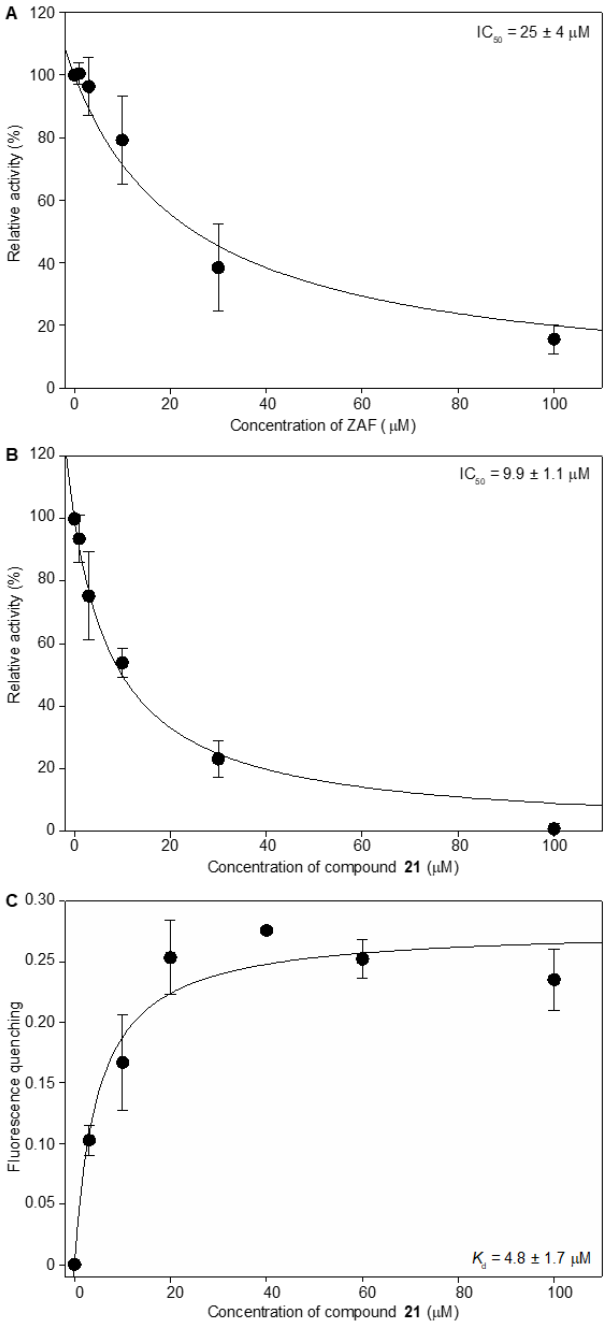

Figure 2.2 Dose-response data for (A) ZAF (n=4) and (B) compound **21** (n=4) in the turbidometric ERp57 activity assay. The corresponding IC_{50} values are shown in the insets and presented in Table 1. (C) The binding isotherm for the formation of compound **21**-ERp57 complex, obtained by monitoring quenching of fluorescence of ERp57 Trp residues (n=3). The K_d value obtained by the nonlinear regression using the 1:1 binding model is given in the inset. Data for Figure 2.2 C. was collected by Caixia Hou from the University of Kentucky, and Figure 2.2 was generated by Oleg V. Tsodikov of the University of Kentucky.

2.5.2 Reversibility of ZAF analogues

The reversibility of potential antithrombotic agents is an important property due to the potential risks from bleeding. Although ZAF did not display enhanced bleeding risk in mice (Holbrook et al., 2021), the reversibility of thiol isomerase inhibition by ZAF and its analogues has not previously been examined. The reversibility of thiol isomerases can be explored using a modified version of the insulin-based turbidometric assay, as previously shown by Jasuja *et al*. (Jasuja et al., 2012a). Since ZAF and compound **21** are pan-thiol isomerase inhibitors, we chose to use PDI to examine the reversibility of these compounds, because reversible (rutin) (Jasuja et al., 2012a) and irreversible (PACMA) (Xu et al., 2012b) inhibitors of this enzyme are known and could be used as controls. An irreversible inhibitor inhibits the enzymatic reaction in a pre-incubation time-dependent manner, as demonstrated by PACMA (Figure 2.3 A). On the contrary, a fast reversible inhibitor binds and dissociates from the protein dynamically, demonstrating similar levels of inhibition independent of pre-incubation time, as evidenced by rutin (Figure 2.3 B). Both ZAF and compound **21** (Figure 2.3 C,D) displayed no pre-incubation time dependence for all four time points, consistent with the effects of reversible thiol isomerase inhibitors.

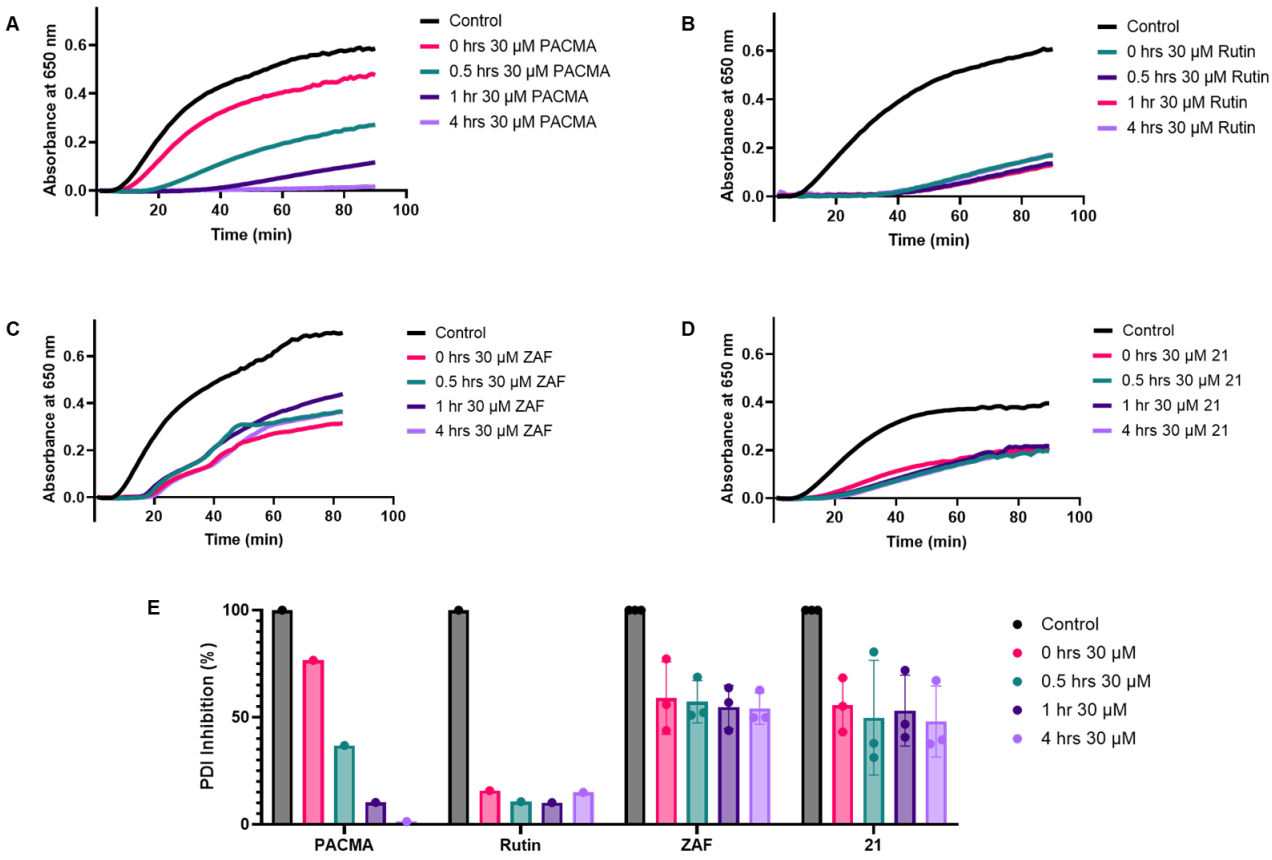

Figure 2.3 The turbidometeric insulin assay to test the pattern of reversibility for PDI inhibitors tested at 30 μM at 4 different time points up to 4 hours. (A) Irreversible PDI inhibitor PACMA (n=1). (B) Reversible PDI inhibitor rutin (n=1). (C) ZAF (n=3). (D) Compound **21** (n=3). (E) A bar graph depicting a summary of the three individual runs for 3 replicates of ZAF and Compound **21** where no time dependent change is seen. Data are presented as mean ± SD. Statistical analysis: two-way ANOVA with Tukey's *post hoc* test.

2.5.3 Platelet aggregation and P-selectin assays of ZAF and compound 21

Platelet aggregation was measured in PRP upon 180 s stimulation with collagen in the presence of 0.1% DMSO, ZAF (1.25-40 μM, Figure 2.4 A), or compound **21** (1.25-20 μM, Figure 2.4 B). ZAF and compound **21** inhibited platelet aggregation in a dose-dependent manner. The endpoint values for ZAF and compound **21** at 180 s from four respective independently replicated runs calculated relative to the DMSO value are displayed in Figure 2.4 C. Compound **21** continued to be more potent than ZAF, demonstrating 31% inhibition at 10 μM, whereas ZAF inhibited platelet aggregation only by 7%. At 20 μM, compound **21** and ZAF inhibited aggregation by 58% and 7%, respectively. A significant difference was seen between the two compounds at both 10 and 20 μM (Figure 2.4 C). When used at 10 μM, compound **21** inhibited platelet aggregation similarly to 40 μM ZAF (Figure 2.4 A,B). The ability of compound **21** to inhibit P-selectin activation was also tested (Figure 2.4 D). Flow cytometry was utilized to assess the P-selectin exposure of platelet-rich plasma treated with ZAF or compound **21**. Compound **21** was also more effective than ZAF at inhibiting P-selectin expression, demonstrating average inhibition of 27% *vs* 5% at 3 μM, 32% *vs* 5% at 10 μM and 50% *vs* 17% at 30 μM, with a significant difference observed between the effects of the two compounds at 30 μM.

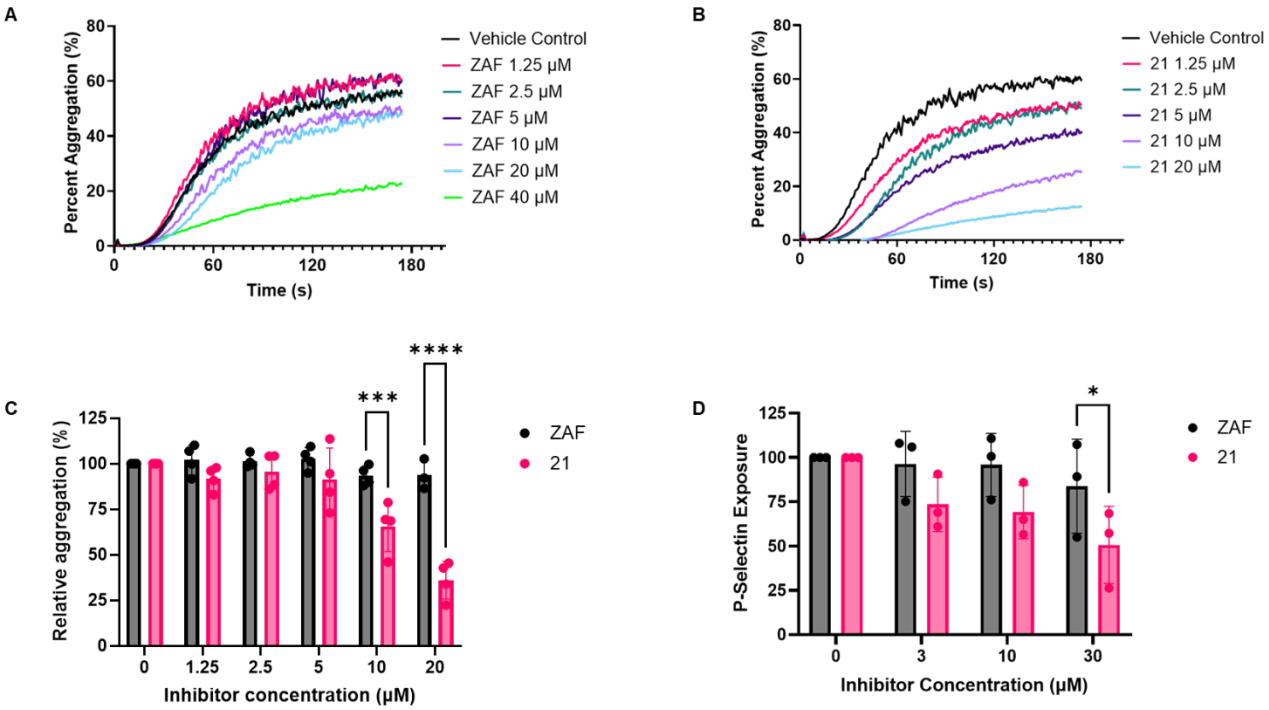

Figure 2.4 Inhibition of platelet aggregation and P-selectin exposure by ZAF and compound **21**. A. through C. PRP was collected from consenting donors and incubated with indicated concentrations of ZAF, compound **21** or vehicle for 5 minutes at 37°C. Platelet aggregation was induced by collagen (1.9 mg/mL) and representative traces of (A) ZAF and (B) compound **21** are presented. (C) The endpoint aggregation values at 180 s for ZAF (n=4) and compound **21** (n=4). Data are presented as mean ± SD. Statistical analysis: two-way ANOVA with Tukey's *post hoc* test. (D) Flow cytometry measurement of P-selectin exposure from PRP treated with ZAF (n=3) or compound **21** (n=3) and stimulated with CRP (5 µg/mL). Data are presented as mean ± SD. Statistical analysis: two-way ANOVA with a Tukey's *post hoc* test.

2.5.4 Correlation of thiol isomerase activity to anti-platelet effects in select analogues

To test if the observed effects of compound **21** on platelet aggregation and P-selectin exposure were through thiol isomerase inhibition, we explored whether additional ZAF analogues inhibited these assays at levels relative to their thiol isomerase inhibitory effect. Thus, the effects of compound **22**, which had a similar inhibitory effect to ZAF in the insulin turbidity assay and compound **35**, which was a weaker inhibitor than ZAF, were examined and compared to ZAF and compound **21** (Figure 2.5 A). As expected, compound **22** had similar activity to ZAF in both platelet aggregation inhibition and P-selectin exposure, while compound **35** inhibited platelet aggregation less effectively (Figure 2.5 B, C). Compound **35** displayed a similar inhibitory effect on P-selectin expression to that of ZAF and compound **22**, but besides that, the overall activity of the compounds in the cell-based assays was correlative with their relative thiol isomerase inhibitory activities (Figure 2.5 D).

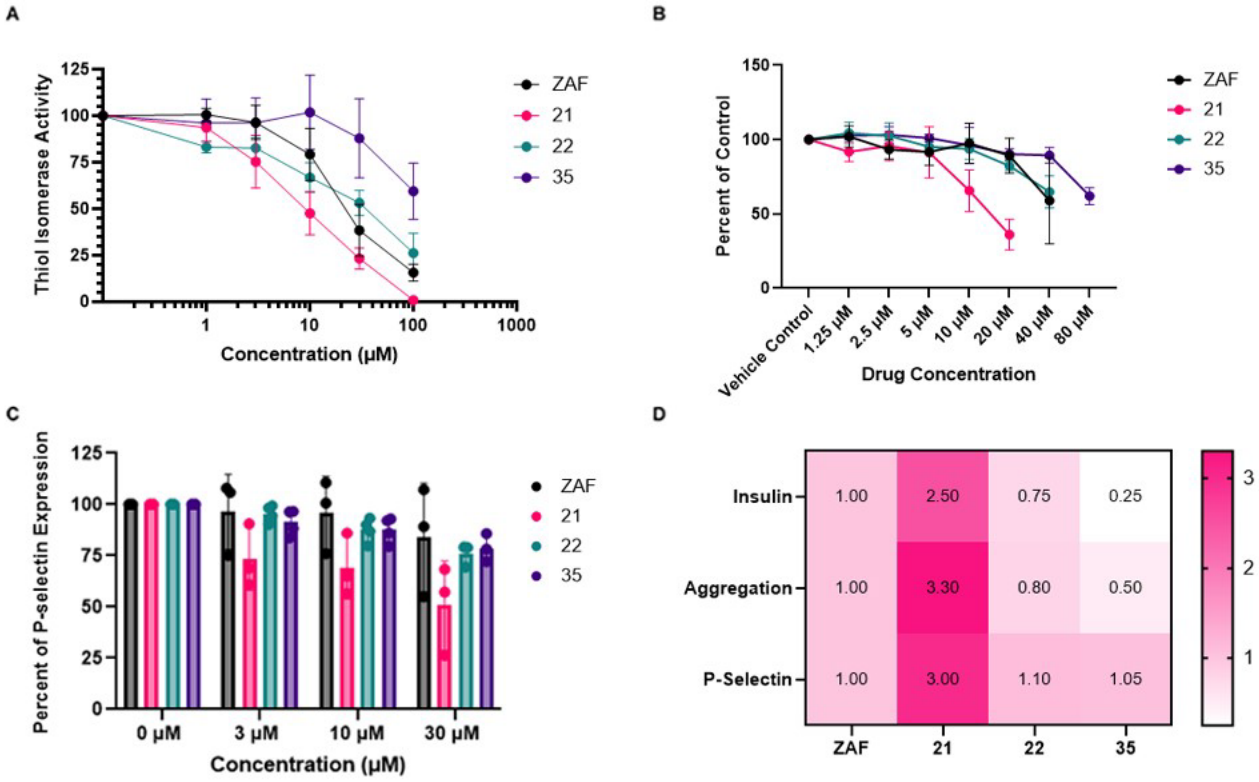

Figure 2.5 The activity of ZAF compared to compounds **21**, **22** and **35.** (A) The insulin turbidity assay comparing the potency for ERp57 inhibition of ZAF, compound **21**, **22** and **35** (n=3). (B) Platelet aggregation with drug concentrations ranging from 0-20 μM for compound **21** (n=3), 0-40 μM for ZAF (n=3) and compound **22** (n=3) and 0-80 μM for compound **35** (n=3). (C) P-selectin expression of platelets treated with ZAF, and compounds **21**, **22** and **35** (n=3). (D) A summary comparison of the relative activities of each compound. Relative activities of the analogues were calculated based on their fold-change compared to ZAF. Data are presented as mean ±SD.

2.5.5 Inhibition of platelet thiols with ZAF and analogue 21

We previously found that the mechanism by which ZAF inhibited MDA-MB-231 cell migration was by mediation of cell-surface thiols (Holbrook et al., 2021). To explore whether our observed inhibition of platelet activity was also associated with modulation of platelet-surface thiols, we explored a similar method for platelets. Platelets were washed, treated with either ZAF or compound **21**, stimulated with collagen and then labelled with MPB and probed with streptavidin-HRP on an immunoblot to visualize platelet thiols. Compound **21** was significantly more effective at reducing detectable platelet thiols than ZAF when compared to the control. At 20 μM compound **21** demonstrated an average inhibition of 41.8%, while ZAF inhibited averaged 17.4% (Figure 2.6).

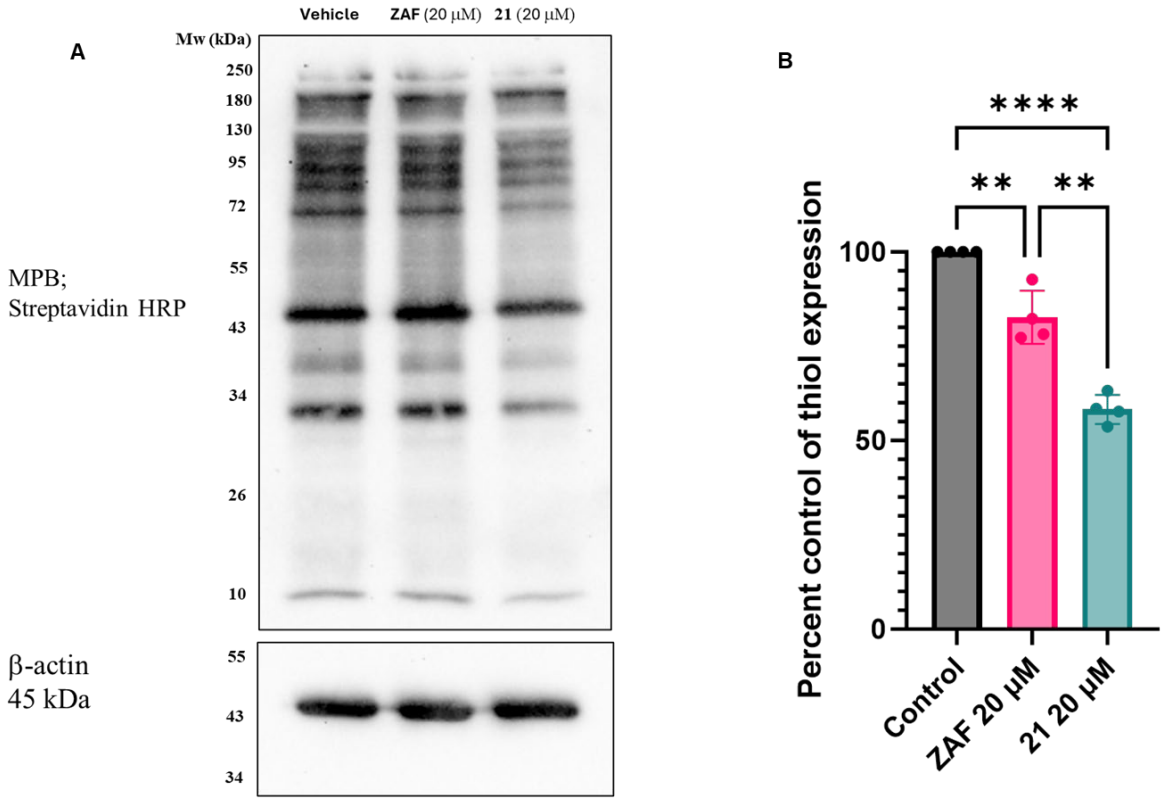

Figure 2.6 **(**A) Surface thiol labelling with MPB (100 μM) from washed platelets treated with ZAF (n=4) or compound **21** (n=4). Thiols were detected on immunoblot with streptavidin-HRP conjugate (1:5000) and chemiluminescence visualized after addition of ECL substrate. (B**)** Quantification of band intensities for surface thiol labelling. Quantification of the total thiols in each lane were calculated using Image Lab software. The average of all bands for each condition was taken and corrected for beta actin levels. Data are presented as mean ± SD. Statistical analysis: one-way ANOVA with a Tukey's *post hoc* test.

2.5.6 Cytotoxicity profile of ZAF analogues

To assess compound safety, we measured the cytotoxicity of ZAF and compound **21** in representative mammalian lung, kidney, and liver cell lines (Figure 2.7). It was determined that neither ZAF nor compound **21** displayed cytotoxicity to HEK-293 kidney cells, BEAS-2B lung cells, and HepG2 liver cells at concentrations up to 128 μM.

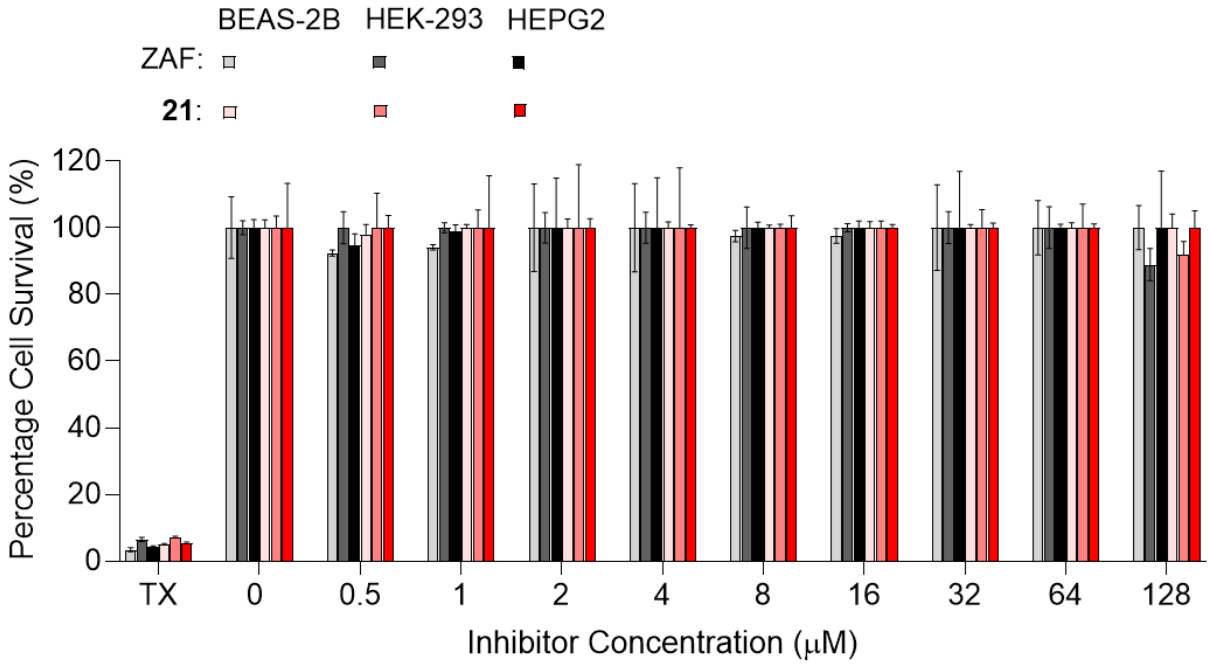

Figure 2.7 The cytotoxicity of ZAF and compound **21** to BEAS-2B, HEK-293, and HepG2 cells determined by a resazurin-based assay (n=4). All cells were treated with either ZAF or compound **21** for 24 hours. The error bars are standard deviations of the quadruplicate measurements. P values for all positive controls were <0.001. For BEAS-2B cells p values for 0.5 μm ZAF and 1 μM ZAF were 0.6082 and 0.8435 respectively. For HEK-293 cells p values for 128 μM ZAF and compound **21** were 0.1935 and 0.5443 respectively. For HEPG2 cells the p value for 0.5 μM ZAF was 0.9093. All other p values were >0.99. Statistical analysis: two-way ANOVA with a Dunnett's *post hoc* test. Data for Figure 2.7 was collected by Kaitlind C. Howard from University of Kentucky.

2.5.7 Inhibition of arterial thrombosis with ZAF analogue 21

We investigated the ability of compound **21** to inhibit arterial thrombosis *in vivo*. Mice were dosed intravenously with either the vehicle control or compound **21**, then subjected to laser injury of the cremaster muscle arterioles. Compared to the vehicle control (Figure 2.8 A), thrombus growth was significantly perturbed after treatment with compound **21** (Figure 2.8 B). Analysis of the maximum fluorescence of individual thrombi averaged almost an 80% decrease in animals treated with compound **21** as compared to those mock-treated with the vehicle control (Figure 2.8 C). In our previous study, ZAF treatment decreased the maximum fluorescence by approximately 15%, so compound **21** had a stronger effect (Holbrook et al., 2021). Interestingly, the thrombi formed in animals treated with compound **21** appeared to be significantly less stable than those formed in control animals, as 3-fold more micro-emboli were identified, signifying thrombi had difficulty forming (Figure 2.8 D). Finally, we assessed the effect that compound **21** had on bleeding times to examine any potential bleeding risk in a murine tail bleed assay. Similar to our previous observations with ZAF, the time to the cessation of tail bleeding was not significantly changed in mice treated with compound **21**, (mean 203 ± 25 s) compared to the mice treated with the vehicle control, (mean 214 ± 23 s) (Figure 2.8 E).

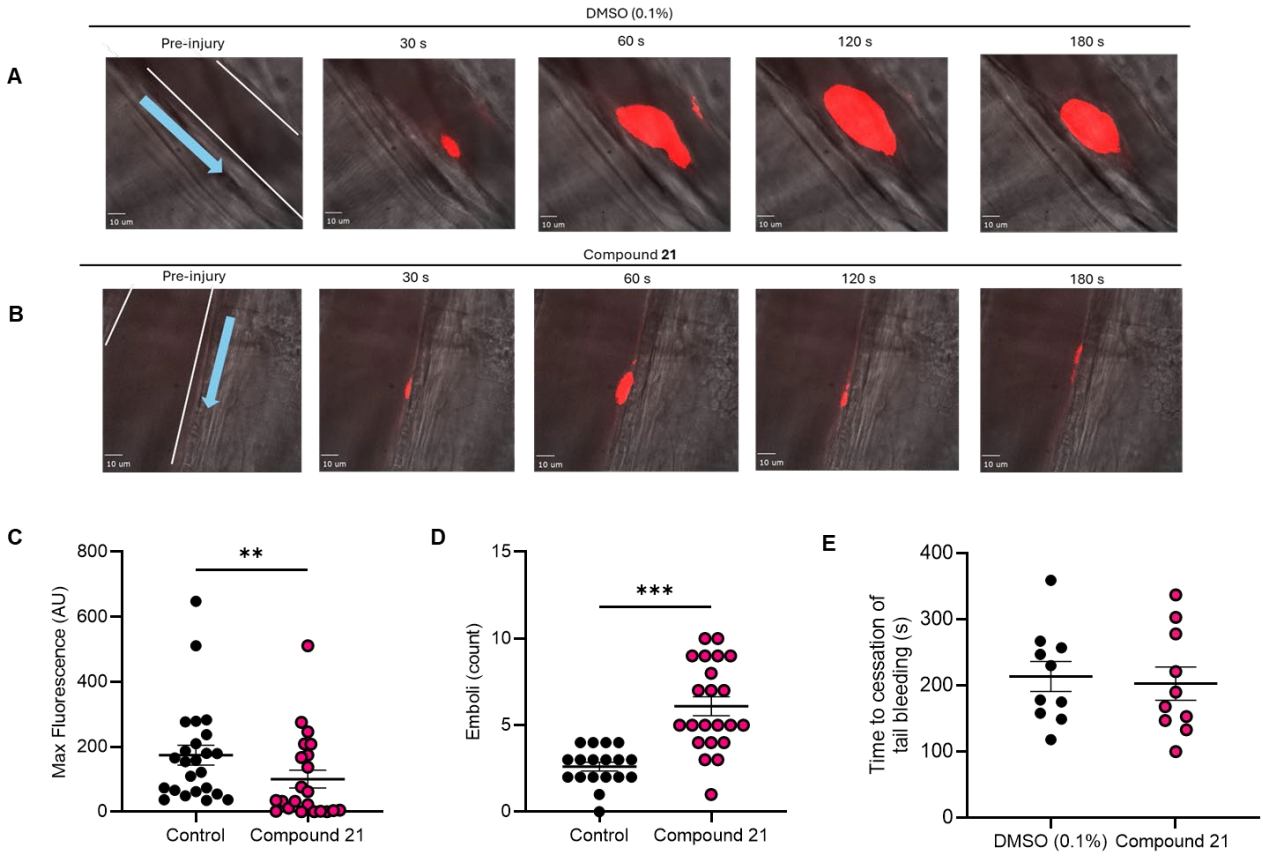

Figure 2.8. Inhibition of thrombus formation by compound **21** *in vivo.* Intravital microscopy using laser injury was performed in male C57BL/6J mice with compound **21** (20 μM; n=5 mice) or vehicle control (0.1% *v/v* DMSO; n=5 mice) infused intravenously, where multiple thrombi were able to be formed per mouse. (A) Representative images of thrombi from mice treated with vehicle control at 30, 60, 120, and 180 seconds. (B) Representative images of thrombi from mice treated with compound **21** at 30, 60, 120, and 180 seconds. The white scale bars are 10 μm. The white lines in the pre-injury images in panels A and B indicate the outline of the vessel and the turquoise arrows indicate the flow of blood. (C) The maximum of integrated fluorescence intensity for 0.1% DMSO (n=24 thrombi) and compound **21** (n=22 thrombi). Data are presented as mean ± SD. Statistical analysis: Mann-Whitney test. AU indicates arbitrary units. (D) Measurement of the formation of emboli released from the individual thrombus released in each mouse. Data are presented as mean ± SD. Statistical analysis: Mann-Whitney test. (E) The effect of compound **21** on bleeding was assessed via tail bleeding assay where time to cessation of bleeding was recorded after DMSO (0.1%) or compound **21** (20 μM) was infused intravenously into C57/BL6 mice for 5 minutes prior to tail biopsy (n=10/group). Data are presented as mean ± SD. Statistical analysis: Mann-Whitney test. Data for Figure 2.8 A-D were collected by Kirk A. Taylor and Sabeeya Khan from the University of Reading. Data for Figure 2.8 E were collected by Tanya Sage and Sabeeya Khan from the University of Reading.

2.6 Discussion

In this study, a library of 35 ZAF analogues yielded one ZAF analogue **21**, which inhibited the thiol isomerase activity of ERp57 more potently than ZAF did, and six that maintained similar activity to the parent compound. Through these studies, we discovered that the presence of the cyclopentyl carbamate group at the C5 position of the indole (ring A) was not needed for the inhibition of ERp57. Future SAR studies with next-generation ZAF analogues will explore ZAF analogues, where the most preferred R_3 substituent on ring C will be kept as 2-F. Compound **21** strongly quenched the Trp fluorescence of ERp57 upon binding. The active domains a and a' of ERp57 contain solvent-exposed Trp residues in their substrate binding sites (Dong et al., 2009), appearing as likely candidates for direct interactions with compound **21**. ZAF and other analogues likely bind to similar sites, but some analogues may permit simultaneous insulin binding at the active site, which could explain why some analogues appear to be unable to completely inhibit the enzyme. Some of the analogues that inhibited ERp57 incompletely had low IC_{50} values, therefore, these analogues may have favourable structural features for further optimization. Future studies will establish the molecular details of thiol isomerase complexes with ZAF analogues and probe the inhibition mechanism in greater detail.

When looking broadly at the data presented in Table 1, compounds belonging to scaffold 1 displayed poor activity, while some of those from scaffold 2 displayed similar or increased activity as inhibitors when compared to the parent ZAF. The higher potency of compound **21** with scaffold 2 indicates that in the context of a substitution pattern distinct from that of ZAF, a cyclopentyl carbamate group at the R_1 of ZAF is not required for thiol isomerase inhibition. In fact, scaffold 2 (Figure 2.1), with its 2-methoxy-5-indoyl substituents on ring B, yielded the most active compound **21**, which was more potent than ZAF (Table 2.1, Figure 2.2).

Previously, we demonstrated that ZAF was able to inhibit platelet aggregation, P-selectin exposure and *in vivo* thrombus formation at physiologically relevant concentrations (Holbrook et al., 2021). Here, we discovered that the effect of ZAF on platelets could be enhanced with analogue optimization. Compared to ZAF, compound **21** was significantly better at inhibiting platelet aggregation at both 10 and 20 μM and demonstrated inhibition at 10 μM similar to that of ZAF at 40 μM (Figure 2.4). Importantly, we also established that ZAF and compound **21** inhibited platelet aggregation in PRP – i.e. in the presence of plasma proteins, compared to our previous study with ZAF which used washed platelets (Holbrook et al., 2021), explaining the observed difference in ZAF's platelet aggregation potency between these two studies. Compound **21** demonstrated greater inhibitory effects than we observed with ZAF in our previous study in the *in vivo* thrombus formation assay (Figure 2.8), approximately 80% inhibition of maximum fluorescence, compared to 15% inhibition by ZAF at the same dose (Holbrook et al., 2021). Taken together, the increased potency of inhibition of platelet function and thrombosis (Figure 2.4), along with effects that correlative with the relative potencies of analogues for thiol isomerase inhibition (Figure 2.5), with enhanced inhibition of platelet surface thiols (Figure 2.6) suggest that ZAF analogues could further improve the antithrombotic properties of the parent compound.

Although we have demonstrated that ZAF inhibits thiol isomerase activity (Gelzinis et al., 2023b; Holbrook et al., 2021), and that the inhibition of thiol isomerase activity is linked to the inhibition of thrombus formation (Holbrook et al., 2012a; Jasuja et al., 2012a; Jordan et al., 2005), it is unknown whether the inhibition of CysLT1 receptor activity contributes to the demonstrated effects of ZAF. Previous studies demonstrated CysLTR1 is expressed intracellularly and on the cell surface of platelets (Hasegawa et al., 2010) and that CysLTR1 and CysLTR2 both serve as substrates for the leukotriene LTC4 (Heise et al., 2000; Lynch et al., 1999), which has been shown to activate mouse platelets (Cummings et al., 2013).

However, the activation of mouse platelets was dependent on CysLTR2 (Cummings et al., 2013), whereas ZAF specifically binds CysLT1 receptor (Dhaliwal & Bajaj, 2024). Additionally, in our previous work, the effects of ZAF on integrin-mediated cell migration were measured by the scratch assay both on the cells that expressed CysLTR1 and CysLTR2 (MDA-MB-231) as well as on the cells that did not express these receptors (HEK-293T) (Holbrook et al., 2021). In that study, ZAF prolonged wound closure time in both types of cells, demonstrating that the drug was not working through CysLT-dependent mechanisms. Additionally, compound **21** has a different scaffold organization from that of ZAF, lacking the cyclopentyl moiety of ZAF that aids its binding to CysLTR. The absence of this moiety reduced ZAF binding to the CysLTR1 receptor by >100-fold (Bernstein, 1998b). This observation and the additional scaffold differences strongly suggest that the analogue has minimal or no effect on the leukotriene receptor. Finally, compounds **21**, **22**, and **35**, all inhibited platelet aggregation to the extent correlative with their relative thiol isomerase inhibitory activity (Figure 2.5). Taken together, these data indicate that the effect of ZAF and compound **21** on platelets is due to its effects on thiol isomerase activity while the inhibition of CysLTR1 receptor has minimal or no effect on these processes.

The potential utility of ZAF analogues extends well beyond the field of anti-thrombotic therapeutics, with applications in cancer and cancer-induced thrombosis, amongst other diseases (Powell & Foster, 2021). We previously demonstrated that ZAF can inhibit tumour growth and tumour metastasis in a xenograft model of ovarian cancer, as well as slowed the rate of rise of a tumour biomarker level in a clinical trial of ovarian cancer (Gelzinis et al., 2023b). As compound **21** proved to be a more potent antithrombotic agent than ZAF, it has a potential to be further developed not only for thrombosis therapy, but as a bifunctional anti-thrombotic and anti-neoplastic agent. Thiol isomerase inhibitors have also been shown to play important regulatory roles in mast cell regulation and food allergy (Krajewski et al., 2020a),

and it would be interesting to see the effect of zafirlukast analogues lacking the CysLTR1 binding moiety in asthma, considering the known inhibitory effects thiol isomerase inhibition has on IgE (Krajewski et al., 2020a). Several PDI inhibitors structurally distinct from ZAF, including antibiotic bacitracin (Essex et al., 2001; Lovat et al., 2008), bepristats/ML359 (Bendapudi, 2014; Khodier et al., 2010), the cytotoxic natural product juniferdin (Khodier et al., 2010), and the abscisic acid derivative origamicin (Ozcelik & Pezacki, 2019) have been identified that are being explored for a multitude of additional disorders and diseases, including neurodegenerative diseases (Ozcelik & Pezacki, 2019; Uehara et al., 2006b) and antiviral agents (Diwaker et al., 2015; Gallina et al., 2002; Walczak & Tsai, 2011). These new ZAF analogues could, therefore, serve as new tools for exploring different disease processes.

2.7 Supplementary figures

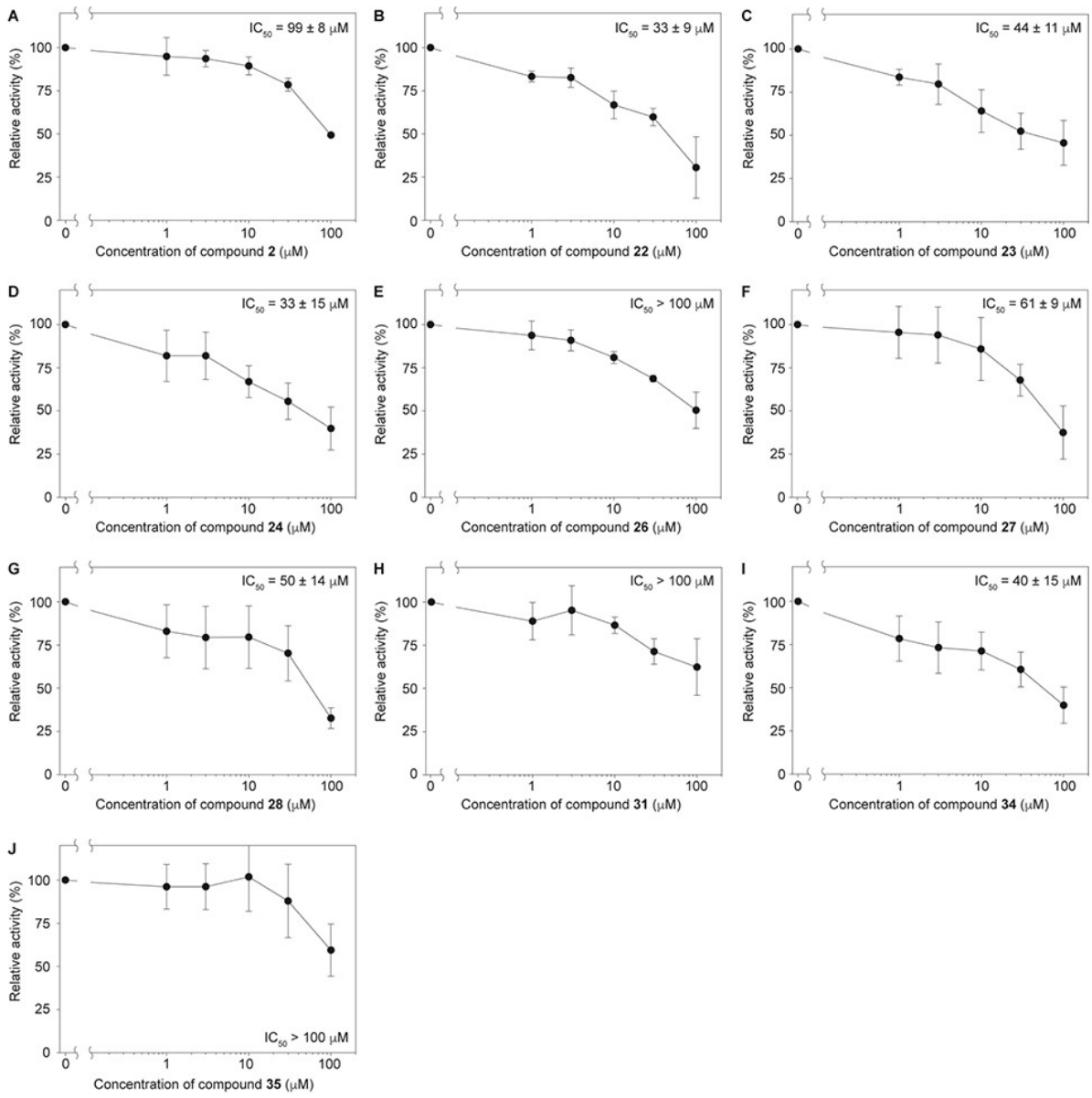

Supplemental Figure 2.1 - Dose-response data for the remaining compounds that demonstrated measurable enzymatic activity in the turbidometric ERp57 activity assay. The corresponding IC50 values are shown in the insets and presented in Table 1. (A) compound 2 (B) compound 22 (C) compound 23 (D) compound 24 (E) compound 26 (F) compound 27 (G) compound 28 (H) compound 31 (I) compound 24 (J) compound 35. Supplemental Figure 2.1 was generated by Oleg V. Tsodikov from the University of Kentucky.

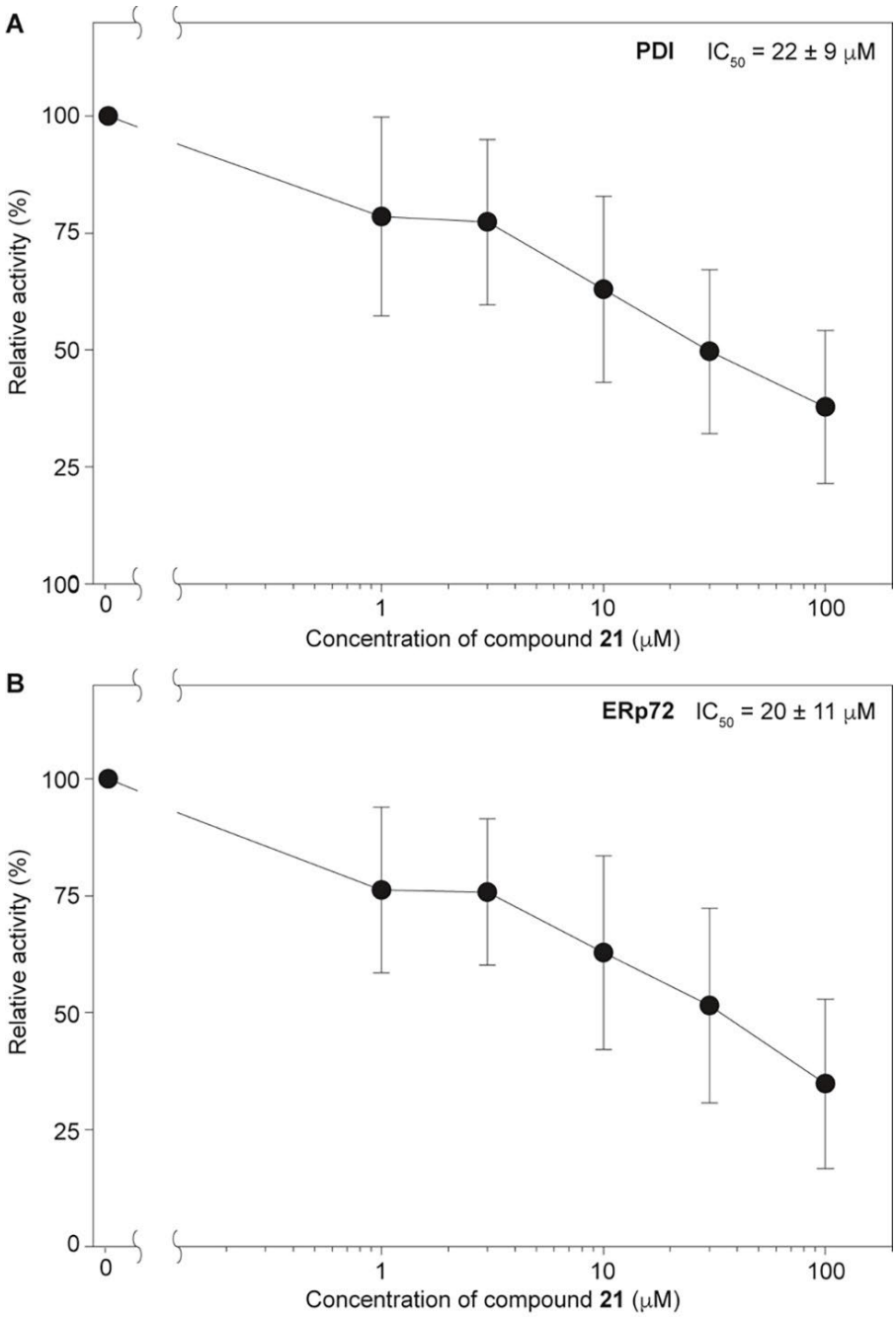

Supplemental Figure 2.2 - Dose-response data for compound **21** inhibition of (A) PDI and (B) ERp72. Supplemental Figure 2.2 was generated by Oleg V. Tsodikov from the University of Kentucky.

2.8 References

Bendapudi, P. K. B., R. H.; Lin, L.; Huang, M.; Furie, B.; Flaumenhaft, R. (2014). ML359, a Small Molecule Inhibitor of Protein Disulfide Isomerase That Prevents Thrombus Formation and Inhibits Oxidoreductase but not Transnitrosylase Activity. *Blood*, *124*(21), 2880.

Bernstein, P. R. (1998). Chemistry and structure-activity relationships of leukotriene receptor antagonists. *Am J Respir Crit Care Med*, *157*(6 Pt 1), S220-226. https://www.ncbi.nlm.nih.gov/pubmed/9620943

Cummings, H. E., Liu, T., Feng, C., Laidlaw, T. M., Conley, P. B., Kanaoka, Y., & Boyce, J. A. (2013). Cutting edge: Leukotriene C4 activates mouse platelets in plasma exclusively through the type 2 cysteinyl leukotriene receptor. *J. Immunol.*, *191*(12), 5807-5810. https://doi.org/10.4049/jimmunol.1302187

Dhaliwal, A., & Bajaj, T. (2024). Zafirlukast. In *StatPearls*. https://www.ncbi.nlm.nih.gov/pubmed/32491776

Diwaker, D., Mishra, K. P., Ganju, L., & Singh, S. B. (2015). Protein disulfide isomerase mediates dengue virus entry in association with lipid rafts. *Viral Immunol.*, *28*(3), 153-160. https://doi.org/10.1089/vim.2014.0095

Dong, G., Wearsch, P. A., Peaper, D. R., Cresswell, P., & Reinisch, K. M. (2009). Insights into MHC class I peptide loading from the structure of the tapasin-ERp57 thiol oxidoreductase heterodimer. *Immunity*, *30*(1), 21-32. https://doi.org/10.1016/j.immuni.2008.10.018

Essex, D. W., & Li, M. (1999). Protein disulphide isomerase mediates platelet aggregation and secretion. *Br. J. Haematol.*, *104*(3), 448-454. https://doi.org/10.1046/j.1365-2141.1999.01197.x

Essex, D. W., Li, M., Miller, A., & Feinman, R. D. (2001). Protein disulfide isomerase and sulfhydryl-dependent pathways in platelet activation. *Biochemistry*, *40*(20), 6070-6075. https://doi.org/10.1021/bi002454e

Falati, S., Patil, S., Gross, P. L., Stapleton, M., Merrill-Skoloff, G., Barrett, N. E., Pixton, K. L., Weiler, H., Cooley, B., Newman, D. K., Newman, P. J., Furie, B. C., Furie, B., & Gibbins, J. M. (2006). Platelet PECAM-1 inhibits thrombus formation *in vivo*. *Blood*, *107*(2), 535-541. https://doi.org/10.1182/blood-2005-04-1512

Flaumenhaft, R., & Furie, B. (2016). Vascular thiol isomerases. *Blood*, *128*(7), 893-901. https://doi.org/10.1182/blood-2016-04-636456

Furie, B., & Furie, B. C. (2008). Mechanisms of thrombus formation. *N. Engl. J. Med.*, *359*(9), 938-949. https://doi.org/10.1056/NEJMra0801082

Furie, B., & Furie, B. C. (2012). Formation of the clot. *Thromb. Res.*, *130 Suppl 1*, S44-S46. https://doi.org/10.1016/j.thromres.2012.08.272

Gallina, A., Hanley, T. M., Mandel, R., Trahey, M., Broder, C. C., Viglianti, G. A., & Ryser, H. J. (2002). Inhibitors of protein-disulfide isomerase prevent cleavage of disulfide bonds in receptor-bound glycoprotein 120 and prevent HIV-1 entry. *J. Biol. Chem.*, *277*(52), 50579-50588. https://doi.org/10.1074/jbc.M204547200

Gelzinis, J. A., Szahaj, M. K., Bekendam, R. H., Wurl, S. E., Pantos, M. M., Verbetsky, C. A., Dufresne, A., Shea, M., Howard, K. C., Tsodikov, O. V., Garneau-Tsodikova, S., Zwicker, J. I., & Kennedy, D. R. (2023). Targeting thiol isomerase activity with zafirlukast to treat ovarian cancer from the bench to clinic. *FASEB J.*, *37*(5), e22914. https://doi.org/10.1096/fj.202201952R

Hartwig, J., & Italiano, J., Jr. (2003). The birth of the platelet. *J. Thromb. Haemost.*, *1*(7), 1580-1586. https://doi.org/10.1046/j.1538-7836.2003.00331.x

Hasegawa, S., Ichiyama, T., Hashimoto, K., Suzuki, Y., Hirano, R., Fukano, R., & Furukawa, S. (2010). Functional expression of cysteinyl leukotriene receptors on human platelets. *Platelets*, *21*(4), 253-259. https://doi.org/10.3109/09537101003615394

Heise, C. E., O'Dowd, B. F., Figueroa, D. J., Sawyer, N., Nguyen, T., Im, D. S., Stocco, R., Bellefeuille, J. N., Abramovitz, M., Cheng, R., Williams, D. L., Jr., Zeng, Z., Liu, Q., Ma, L., Clements, M. K., Coulombe, N., Liu, Y., Austin, C. P., George, S. R., . . . Evans, J. F. (2000).

Characterization of the human cysteinyl leukotriene 2 receptor. *J. Biol. Chem.*, *275*(39), 30531-30536. https://doi.org/10.1074/jbc.M003490200

Heit, J. A. (2005). Venous thromboembolism: Disease burden, outcomes and risk factors. *J. Thromb. Haemost.*, *3*(8), 1611-1617. https://doi.org/10.1111/j.1538-7836.2005.01415.x

Holbrook, L. M., Keeton, S. J., Sasikumar, P., Nock, S., Gelzinis, J., Brunt, E., Ryan, S., Pantos, M. M., Verbetsky, C. A., Gibbins, J. M., & Kennedy, D. R. (2021). Zafirlukast is a broad-spectrum thiol isomerase inhibitor that inhibits thrombosis without altering bleeding times. *Br J Pharmacol*, *178*(3), 550-563. https://doi.org/10.1111/bph.15291

Holbrook, L. M., Sandhar, G. K., Sasikumar, P., Schenk, M. P., Stainer, A. R., Sahli, K. A., Flora, G. D., Bicknell, A. B., & Gibbins, J. M. (2018). A humanized monoclonal antibody that inhibits platelet-surface ERp72 reveals a role for ERp72 in thrombosis. *J. Thromb. Haemost.*, *16*(2), 367-377. https://doi.org/10.1111/jth.13878

Holbrook, L. M., Sasikumar, P., Stanley, R. G., Simmonds, A. D., Bicknell, A. B., & Gibbins, J. M. (2012). The platelet-surface thiol isomerase enzyme ERp57 modulates platelet function. *J. Thromb. Haemost.*, *10*(2), 278-288. https://doi.org/10.1111/j.1538-7836.2011.04593.x

Howard, K. C., & Garneau-Tsodikova, S. (2022). Selective Inhibition of the Periodontal Pathogen Porphyromonas gingivalis by Third-Generation Zafirlukast Derivatives. *J Med Chem*, *65*(21), 14938-14956. https://doi.org/10.1021/acs.jmedchem.2c01471

Howard, K. C., Gonzalez, O. A., & Garneau-Tsodikova, S. (2020). Second generation of zafirlukast derivatives with improved activity against the oral pathogen *Porphyromonas gingivalis*. *ACS Med. Chem. Lett.*, *11*(10), 1905-1912. https://doi.org/10.1021/acsmedchemlett.9b00614

Jasuja, R., Passam, F. H., Kennedy, D. R., Kim, S. H., van Hessem, L., Lin, L., Bowley, S. R., Joshi, S. S., Dilks, J. R., Furie, B., Furie, B. C., & Flaumenhaft, R. (2012). Protein disulfide isomerase inhibitors constitute a new class of antithrombotic agents. *J. Clin. Invest.*, *122*(6), 2104-2113. https://doi.org/10.1172/JCI61228

Jordan, P. A., Stevens, J. M., Hubbard, G. P., Barrett, N. E., Sage, T., Authi, K. S., & Gibbins, J. M. (2005). A role for the thiol isomerase protein ERP5 in platelet function. *Blood*, *105*(4), 1500-1507. https://doi.org/10.1182/blood-2004-02-0608

Khodier, C., VerPlank, L., Nag, P. P., Pu, J., Wurst, J., Pilyugina, T., Dockendorff, C., Galinski, C. N., Scalise, A. A., Passam, F., van Hessem, L., Dilks, J., Kennedy, D. R., Flaumenhaft, R., Palmer, M. A. J., Dandapani, S., Munoz, B., & Schrieber, S. L. (2010). Identification of ML359 as a Small Molecule Inhibitor of Protein Disulfide Isomerase. In *Probe Reports from the NIH Molecular Libraries Program*. https://www.ncbi.nlm.nih.gov/pubmed/24624466

Krajewski, D., Polukort, S. H., Gelzinis, J., Rovatti, J., Kaczenski, E., Galinski, C., Pantos, M., Shah, N. N., Schneider, S. S., Kennedy, D. R., & Mathias, C. B. (2020). Protein disulfide isomerases regulate IgE-mediated mast cell responses and their inhibition confers protective effects during food allergy. *Front. Immunol.*, *11*, 606837. https://doi.org/10.3389/fimmu.2020.606837

Lahav, J., Jurk, K., Hess, O., Barnes, M. J., Farndale, R. W., Luboshitz, J., & Kehrel, B. E. (2002). Sustained integrin ligation involves extracellular free sulfhydryls and enzymatically catalyzed disulfide exchange. *Blood*, *100*(7), 2472-2478. https://doi.org/10.1182/blood-2001-12-0339

Lovat, P. E., Corazzari, M., Armstrong, J. L., Martin, S., Pagliarini, V., Hill, D., Brown, A. M., Piacentini, M., Birch-Machin, M. A., & Redfern, C. P. (2008). Increasing melanoma cell death using inhibitors of protein disulfide isomerases to abrogate survival responses to endoplasmic reticulum stress. *Cancer Res*, *68*(13), 5363-5369. https://doi.org/10.1158/0008-5472.CAN-08-0035

Lynch, K. R., O'Neill, G. P., Liu, Q., Im, D. S., Sawyer, N., Metters, K. M., Coulombe, N., Abramovitz, M., Figueroa, D. J., Zeng, Z., Connolly, B. M., Bai, C., Austin, C. P., Chateauneuf, A., Stocco, R., Greig, G. M., Kargman, S., Hooks, S. B., Hosfield, E., . . . Evans, J. F. (1999). Characterization of the human cysteinyl leukotriene CysLT1 receptor. *Nature*, *399*(6738), 789-793. https://doi.org/10.1038/21658

Ozcelik, D., & Pezacki, J. P. (2019). Small Molecule Inhibition of Protein Disulfide Isomerase in Neuroblastoma Cells Induces an Oxidative Stress Response and Apoptosis Pathways. *ACS Chem Neurosci*, *10*(9), 4068-4075. https://doi.org/10.1021/acschemneuro.9b00301

Patel, S., Singh, R., Preuss, C. V., & Patel, N. (2022). Warfarin. In *StatPearls*.

https://www.ncbi.nlm.nih.gov/pubmed/29261922

Powell, L. E., & Foster, P. A. (2021). Protein disulphide isomerase inhibition as a potential cancer therapeutic strategy. *Cancer Med*, *10*(8), 2812-2825. https://doi.org/10.1002/cam4.3836

Schror, K. (1997). Aspirin and platelets: The antiplatelet action of aspirin and its role in thrombosis treatment and prophylaxis. *Semin. Thromb. Hemost.*, *23*(4), 349-356. https://doi.org/10.1055/s-2007-996108

Schulman, S., Bendapudi, P., Sharda, A., Chen, V., Bellido-Martin, L., Jasuja, R., Furie, B. C., Flaumenhaft, R., & Furie, B. (2016). Extracellular thiol isomerases and their role in thrombus formation. *Antioxid. Redox. Signal*, *24*(1), 1-15. https://doi.org/10.1089/ars.2015.6530

Sorensen, H. T., Mellemkjaer, L., Blot, W. J., Nielsen, G. L., Steffensen, F. H., McLaughlin, J. K., & Olsen, J. H. (2000). Risk of upper gastrointestinal bleeding associated with use of low-dose aspirin. *Am. J. Gastroenterol.*, *95*(9), 2218-2224. https://doi.org/10.1111/j.1572-0241.2000.02248.x

Spector, S. L. (1996). Management of asthma with zafirlukast. Clinical experience and tolerability profile. *Drugs*, *52 Suppl 6*, 36-46. https://doi.org/10.2165/00003495-199600526-00007

Stoll, G., Kleinschnitz, C., & Nieswandt, B. (2008). Molecular mechanisms of thrombus formation in ischemic stroke: Novel insights and targets for treatment. *Blood*, *112*(9), 3555-3562. https://doi.org/10.1182/blood-2008-04-144758

Thamban Chandrika, N., Fosso, M. Y., Alimova, Y., May, A., Gonzalez, O. A., & Garneau-Tsodikova, S. (2019). Novel zafirlukast derivatives exhibit selective antibacterial activity against *Porphyromonas gingivalis*. *Medchemcomm*, *10*(6), 926-933. https://doi.org/10.1039/c9md00074g

Uehara, T., Nakamura, T., Yao, D., Shi, Z. Q., Gu, Z., Ma, Y., Masliah, E., Nomura, Y., & Lipton, S. A. (2006). *S*-nitrosylated protein-disulphide isomerase links protein misfolding to neurodegeneration. *Nature*, *441*(7092), 513-517. https://doi.org/10.1038/nature04782

Walczak, C. P., & Tsai, B. (2011). A PDI family network acts distinctly and coordinately with ERp29 to facilitate polyomavirus infection. *J. Virol.*, *85*(5), 2386-2396. https://doi.org/10.1128/JVI.01855-10

Wang, L., Wu, Y., Zhou, J., Ahmad, S. S., Mutus, B., Garbi, N., Hammerling, G., Liu, J., & Essex, D. W. (2013). Platelet-derived ERp57 mediates platelet incorporation into a growing thrombus by regulation of the alphaIIbbeta3 integrin. *Blood*, *122*(22), 3642-3650. https://doi.org/10.1182/blood-2013-06-506691

Xu, S., Butkevich, A. N., Yamada, R., Zhou, Y., Debnath, B., Duncan, R., Zandi, E., Petasis, N. A., & Neamati, N. (2012). Discovery of an orally active small-molecule irreversible inhibitor of protein disulfide isomerase for ovarian cancer treatment. *Proc. Natl. Acad. Sci., U. S. A.*, *109*(40), 16348-16353. https://doi.org/10.1073/pnas.1205226109

Zhou, J., Wu, Y., Chen, F., Wang, L., Rauova, L., Hayes, V. M., Poncz, M., Li, H., Liu, T., Liu, J., & Essex, D. W. (2017). The disulfide isomerase ERp72 supports arterial thrombosis in mice. *Blood*, *130*(6), 817-828. https://doi.org/10.1182/blood-2016-12-755587

Zhou, J., Wu, Y., Rauova, L., Koma, G., Wang, L., Poncz, M., Li, H., Liu, T., Fong, K. P., Bennett, J. S., Kunapuli, S. P., & Essex, D. W. (2022). A novel role for endoplasmic reticulum protein 46 (ERp46) in platelet function and arterial thrombosis in mice. *Blood*, *139*(13), 2050-2065. https://doi.org/10.1182/blood.2021012055

Zhou, J., Wu, Y., Wang, L., Rauova, L., Hayes, V. M., Poncz, M., & Essex, D. W. (2014). The disulfide isomerase ERp57 is required for fibrin deposition *in vivo*. *J. Thromb. Haemost.*, *12*(11), 1890-1897. https://doi.org/10.1111/jth.12709

Zwicker, J. I., Schlechter, B. L., Stopa, J. D., Liebman, H. A., Aggarwal, A., Puligandla, M., Caughey, T., Bauer, K. A., Kuemmerle, N., Wong, E., Wun, T., McLaughlin, M., Hidalgo, M., Neuberg, D., Furie, B., Flaumenhaft, R., & Investigators, C. (2019). Targeting protein disulfide isomerase with the flavonoid isoquercetin to improve hypercoagulability in advanced cancer. *JCI Insight.*, *4*(4), e125851. https://doi.org/10.1172/jci.insight.125851

Chapter 3

Targeting thiol isomerase activity with zafirlukast to treat ovarian cancer from the bench to clinic

In the previous chapter I investigated analogues of zafirlukast, a broad-spectrum thiol isomerase inhibitor, on haemostatic function. It is clear from this work and other studies published that inhibition of thiol isomerases on platelets is able to reduce thrombosis, however other cells such as cancer cells also express these proteins, many in overabundance and present on the cell surface where they are implicated in cell adhesion, proliferation, metastasis and angiogenesis. Thiol isomerase inhibitors have been primarily explored as either antithrombotic agents or antineoplastic agents. However in lieu of this no other thiol isomerase inhibitor other than nephrotoxic bacitracin has been uncovered, leaving zafirlukast a good candidate with the possibility to inhibit both.

This chapter investigates how zafirlukast effects multiple cancer cell lines and presents a specific focus on an ovarian cancer model. Here I have shown that treating multiple cancer cell lines including ovarian, colon, lung and prostate with zafirlukast resulted in anti-neoplastic activity, without causing measurable damage to non-cancerous cells. Utilizing analogues from the previous chapter that have the cyclopentyl moiety removed I was able to demonstrate zafirlukast indeed targets thiol isomerases and does not act through LTR inhibition. Additionally, I was able to demonstrate multiple effectors through which zafirlukast exerted its action in ovarian cancer cells including inhibition of tissue factor expressed by the cells, and inhibition of EGFR phosphorylation. Moreover, I was able to show that zafirlukast was able to inhibit both cancer growth and metastasis in an ovarian cancer xenograft model. A small clinical pilot study was also conducted demonstrating zafirlukast was able to delay the rate of rise of CA-125 (and ovarian cancer tumour marker) in four patients at risk of tumour marker-only relapse. These findings justify targeting thiol isomerases to not only improve hypercoagulability but also neoplasticity.

For this chapter, I drafted the manuscript in addition to collecting and analysing the majority of the data with the exception of the clinical study. The clinical study was performed by Roelof Bekendam and Jeffrey Zwicker. The analogue was synthesised by Kaitlind Howard. Therefore, I estimate that I have contributed to over 75% of work put into this paper.

The full paper published at *Federation of American Societies for Experimental Biology* can be found at FASEB J. 2023 May;37(5):e22914. doi: 10.1096/fj.202201952R.

Targeting thiol isomerase activity with zafirlukast to treat ovarian cancer from the bench to clinic

Justine A. Gelzinis [1,2], Melanie K. Szahaj[1], Roelof H. Bekendam[3], Sienna E. Wurl[1], Megan M. Pantos[1], Christina A. Verbetsky[1], Alexandre Dufresne[4], Meghan Shea[5], Kaitlind C. Howard[6], Oleg V. Tsodikov[6], Sylvie Garneau-Tsodikova[6], Jeffrey I. Zwicker[3,8], and Daniel R. Kennedy[1,2,7,8].

[1] College of Pharmacy and Health Sciences, Western New England University, Springfield, MA.

[2] Institute for Cardiovascular & Metabolic Research, School of Biological Sciences, University of Reading, UK.

[3] Division of Haemostasis and Thrombosis, Department of Medicine, Beth Israel Deaconess Medical Centre, Harvard Medical School, Boston, MA.

[4] Baystate Research Facility, Baystate Medical Centre and UMass Chan Medical School, Springfield, MA.

[5]Division of Oncology, Department of Medicine, Beth Israel Deaconess Medical Centre, Harvard Medical School, Boston, MA.

[6] Department of Pharmaceutical Sciences, College of Pharmacy, University of Kentucky, 789 S. Limestone St., Lexington, KY 40536.

[7] Department of Medicine, UMass Chan Medical School-Baystate, Springfield, MA.

[8] These authors contributed equally.

Running Title: Zafirlukast use in ovarian cancer

Keywords: PDI, ERp57, ERp5, ERP72, montelukast, CA-125, drug repurposing

Funding: This work was supported by a National Cancer Institute grant R21CA231000 to DRK and JIZ as well as a National Institutes of Health (NIH) F31 fellowship DEO29661 to KCH.

Corresponding Author**:** Daniel R. Kennedy, Department of Pharmaceutical & Administrative Sciences, College of Pharmacy and Health Sciences, Western New England University, 1215 Wilbraham Road, Springfield, MA 01119. Tel: 413-796-2413. E-mail: dkennedy@wne.edu

Conflict of Interest Statement: DRK is an inventor on a patent owned by Western New England University repurposing zafirlukast as a potential anticancer medication and receives research funding from Quercis Pharma. DRK and SGT are also inventors on a patent owned by Western New England University exploring zafirlukast analogues in thrombosis and

cancer. JIZ: Prior research funding from Incyte and Quercegen; Consultancy for Sanofi, CSL Behring, Calyx; Advisory board participation with Pfizer/Bristol Myers Squibb (BMS), Portola, Janssen, and Daiichi.

Data availability statement: The data generated in this study are not publicly available, as release of some information could compromise patient privacy or consent but are available upon reasonable request from the corresponding author.

The authors wish to acknowledge the advice and guidance of Jennifer Ser-Dolansky and Carolanne Lovewell from the Baystate Animal Research Facility.

3.1 Graphical Abstract

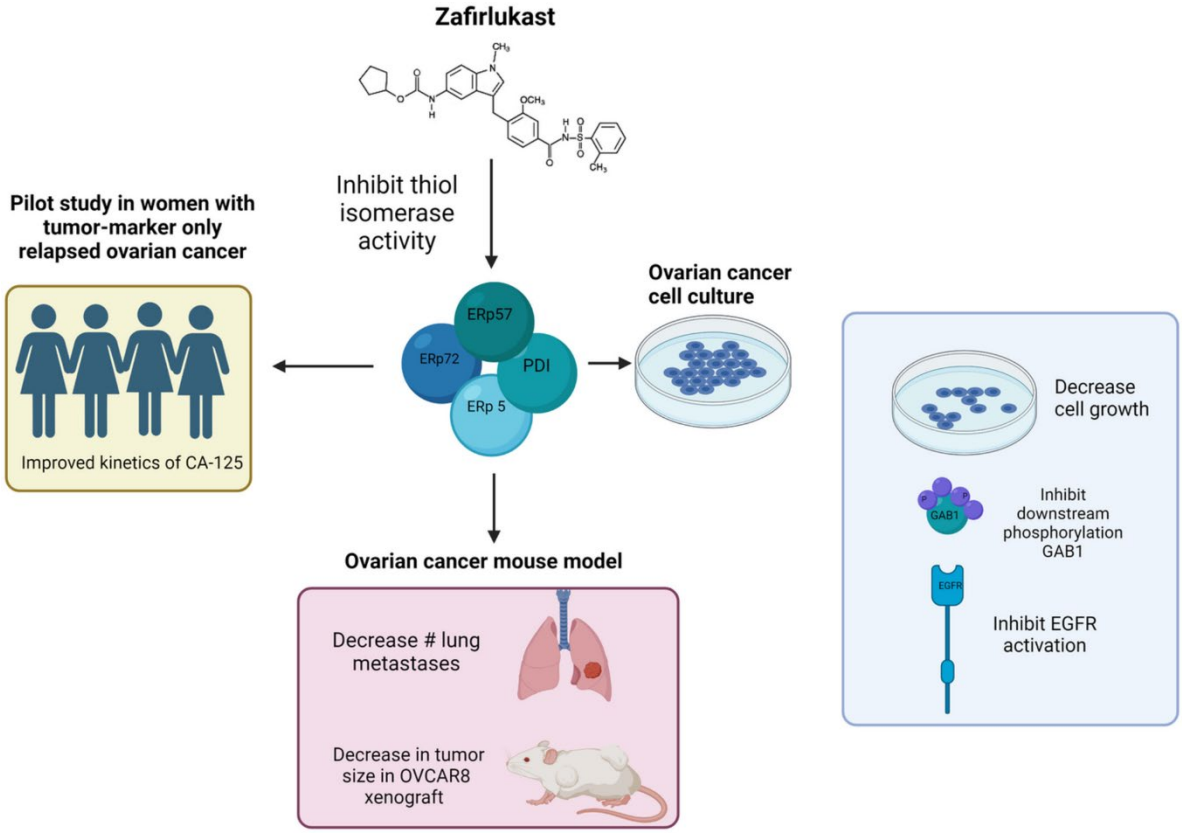

3.2 Abstract

Thiol isomerases, including PDI, ERp57, ERp5, and ERp72 play important and distinct roles in cancer progression, cancer cell signalling, and metastasis. We recently discovered that zafirlukast, an FDA-approved medication for asthma, is a pan-thiol isomerase inhibitor. Zafirlukast inhibited the growth of multiple cancer cell lines with an IC_{50} in the low micromolar range, while also inhibiting cellular thiol isomerase activity, EGFR activation, and downstream phosphorylation of Gab1. Zafirlukast also blocked the procoagulant activity of OVCAR8 cells by inhibiting tissue factor dependent Factor Xa generation. In an ovarian cancer xenograft model, statistically significant differences in tumour size between control vs treated groups were observed by day 18. Zafirlukast also significantly reduced the number and size of metastatic tumours found within the lungs of the mock-treated controls. When added to a chemotherapeutic regimen, zafirlukast significantly reduced growth, by 38% compared to the mice receiving only the chemotherapeutic treatment, and by 83% over untreated controls. Finally, we conducted a pilot clinical trial in women with tumour marker-only (CA-125) relapsed ovarian cancer, where the rate of rise of CA-125 was significantly reduced following treatment with zafirlukast, while no severe adverse events were reported. Thiol isomerase inhibition with zafirlukast represents a novel, well-tolerated therapeutic in the treatment of ovarian cancer.

Abbreviations

PDI	protein disulphide isomerase
ERp	endoplasmic reticulum proteins
LTR	leukotriene receptor
FVII	Factor VII
FX	Factor X
OVCAR8	human ovarian adenocarcinoma
PC3	human prostate adenocarcinoma
A549	human lung carcinoma
HCT116	human colorectal carcinoma
HEK293	human embryonic kidney
SDS-PAGE	Sodium dodecyl sulphate-polyacrylamide gel electrophoresis
PVDF	polyvinylidene fluoride
TBS	tris buffered saline
BSA	bovine serum albumin
HRP	horse radish peroxidase
SC	subcutaneously
i.p.	intraperitoneal
H&E	haematoxylin and eosin
GCIG	Gynaecologic Cancer Intergroup
ULN	upper limit of normal
EGF	epidermal growth factor
EGFR	epidermal growth factor receptor
Gab1	GRB2-associated-binding protein 1
Zafi	zafirlukast

3.3 Introduction

Thiol isomerases, including protein disulfide isomerase (PDI) and the endoplasmic reticulum resident proteins 5, 57, and 72 (ERp5, ERp57, and ERp72) are increasingly recognized for critical activities in regulating protein function external to the endoplasmic reticulum. Thiol isomerases play key roles in maintaining cellular homeostasis by catalysing disulfide bond breakage, formation, and rearrangement (S. Xu et al., 2014). Thiol isomerases are implicated in neurodegenerative diseases (Gonzalez-Perez et al., 2015; Hettinghouse et al., 2018), allergic responses (Krajewski et al., 2020b), thrombosis, and haemostasis (Bekendam et al., 2016; Jasuja et al., 2012b; Liang et al., 2021), as well as cancer (Sharda et al., 2021; Xu et al., 2012a). These thiol isomerases are upregulated in many distinct cancer types including ovarian, prostate, lung, and colon (S. Xu et al., 2014). Considering the ubiquitous roles of thiol isomerases in regulating cellular function, they have been linked to an array of oncologic events including oncogene activation, oncogenic transformation, apoptotic escape, mutation repair, cancer induced thrombosis, and resistance to chemotherapeutic agents (Appenzeller-Herzog & Ellgaard, 2008; Hettinghouse et al., 2018; Shishkin et al., 2013; J. D. Stopa & J. I. Zwicker, 2018; S. Xu et al., 2014). Importantly, these extracellular thiol isomerases are not redundant, each carrying out distinct roles in these processes, and seemingly they vary by cancer type (S. Xu et al., 2014).

Selective inhibitors of PDI, such as PACMA-31 and CCF642 have been shown to inhibit cancer cell growth *in vitro* as well as prolong the life span of mice xenografted with multiple myeloma or ovarian cancer cell lines (Vatolin et al., 2016; Xu et al., 2012a). Additional selective inhibitors of PDI have also been identified and utilized in other disease states, such as thrombosis (Khodier et al., 2010; Liang et al., 2021). PDI, ERp5, ERp57 and ERp72 are all overexpressed in ovarian cancer and associated with shortened survival (Samanta

et al., 2017), making a pan-thiol isomerase inhibitor a potentially attractive antineoplastic agent.

We previously performed a high-throughput screen of FDA-approved or known bioactive compounds for broad-spectrum inhibitors of these four thiol isomerases (Holbrook et al., 2021). The asthma medications zafirlukast, and to a lesser extent, montelukast, which are leukotriene receptor 1 (LTR1) antagonists, were identified as broad-spectrum thiol isomerase inhibitors that inhibited platelet aggregation and thrombus formation in a thiol isomerase-dependent manner (Holbrook et al., 2021). Whether zafirlukast has antitumor activity in ovarian cancer is not known, but this would be anticipated, considering that PACMA-31, another thiol isomerase inhibitor, does (Xu et al., 2012a). This is also supported by the finding that zafirlukast has demonstrated anticancer effects in hepatocellular carcinoma and glioblastoma, among other tumour types (Kumar et al., 2019; Piromkraipak et al., 2018). In this study, we assessed the antineoplastic activity of zafirlukast against ovarian cancer cells in culture, a xenograft model of ovarian cancer, and a pilot clinical study in women with relapsed ovarian cancer, marking the first instance when thiol isomerase inhibitors have been examined in patients for antineoplastic effects.

3.4 Materials and Methods

3.4.1 Reagents

Recombinant PDI, ERp57, ERp72, and ERp5 were purchased from Abcam (Cambridge, MA). Zafirlukast was purchased from TCI America (Portland, OR), cisplatin, gemcitabine, and di-eosin-GSSG were purchased from Cayman Chemicals (Ann Arbor, MI). Factor VII (FVII), Factor X (FX), and the fluorescent Factor Xa cleaving substrate were purchased from Prolytix (Essex Junction, VT). RL90 PDI inhibitory antibody was purchased from ThermoFisher (Waltham, MA), while anti-PDI, anti-ERp57, anti-pEGFR-Y1068, anti-pGAB1-Tyr627, anti-beta-actin, and anti-mouse and anti-rabbit secondary antibodies, as well as EGF were purchased from Cell Signalling (Danvers, MA). Recombinant insulin (bovine), bacitracin, DTT, buffers, and all other chemicals were purchased from Sigma Aldrich (St. Louis, MO); while 96-well and 384-well clear bottom plates were purchased from Corning (Corning, NY).

3.4.2 Chemical Synthesis

The zafirlukast analogue was synthesized as described previously (Howard & Garneau-Tsodikova, 2022).

3.4.3 Cell Culture

Human ovarian adenocarcinoma (OVCAR8) (NCI-DTP Cat# OVCAR-8, RRID:CVCL_1629), human prostate adenocarcinoma (PC3) (ATCC Cat# CRL-1435, RRID:CVCL_0035), and human lung carcinoma cells (A549) (ATCC Cat# CCL-185, RRID:CVCL_0023) were grown in RPMI medium supplemented with 10% fetal bovine serum (FBS), 1% *w*/*v* sodium pyruvate, 10 mM HEPES, 2 mM glutamine, and 100 I.U./mL penicillin/streptomycin. Human colorectal carcinoma cells (HCT116) (NCI-DTP Cat# HCT-

116, RRID:CVCL_0291) were grown in McCoys medium supplemented with 2 mM glutamine, 10% FBS and 100 I.U./mL penicillin/streptomycin. Human embryonic kidney cells (HEK293) (ATCC Cat# CRL-1573, RRID:CVCL_0045) were grown in DMEM high glucose medium supplemented with 4 mM glutamine, 10% FBS and 100 I.U./mL penicillin/streptomycin. For EGF stimulation, OVCAR8 cells were serum starved, treated with zafirlukast for 1 or 4 hours then treated with EGF at a final concentration of 100 ng/mL for 10 minutes.

3.4.4 Insulin-based Turbidimetric Assay

An insulin-based turbidimetric assay was utilized to determine the selectivity of zafirlukast and montelukast for thiol isomerases PDI, ERp57, ERp72, and ERp5. These drugs were diluted in a 6-point dose curve in a 384-well plate, and a final concentration of 10 μg/mL thiol isomerase (30 μg/mL for ERp5 only), 125 μM insulin, 2 mM EDTA, and 100 mM potassium phosphate buffer were added for a total volume of 30 μL per well. The turbidity of insulin aggregation was measured every minute for 75 minutes after initiating the reaction with 0.3 mM DTT using a SpectraMax M3 plate reader (Molecular Devices, Sunnyvale, CA).

3.4.5 PrestoBlue Assay

The indicated cell lines were plated at 5,000 cells per well in a 96-well plate and allowed to grow for 24 hours. The cells were then treated with either a drug or a vehicle control for an additional 2-24 hours prior to the addition of PrestoBlue reagent (Invitrogen, Waltham, MA) for 10-20 minutes at 37°C. Cell viability was determined by measuring the fluorescent signal at an excitation wavelength of 560 nm and emission wavelength of 590 nm. The signal was normalized to a percentage of the control.

3.4.6 Di-eosin-GSSG Disulfide Reductase Assay

OVCAR8 cells were plated at 10,000 cells per well, allowed to grow overnight, then treated with 0-100 μM of zafirlukast, montelukast, or the analogue for 10 minutes. Samples were then subjected to 150 nM of the di-eosin-GSSG probe in the presence of 5 μM of DTT and potassium phosphate buffer (containing 100 mM potassium phosphate (pH 7.4) and 2 mM EDTA). Increase in fluorescence was monitored every 30 seconds for 30 minutes by excitation at 520 nm and emission at 550 nm. Generated data were then normalized to the control for each sample, with raw data representing relative fluorescent units (RFU)/minute.

With blood samples, the assay was performed as previously described (Raturi & Mutus, 2007), with a modification to use plasma at a 1:1 dilution with potassium phosphate buffer (containing 100 mM potassium phosphate (pH 7.4) and 2 mM EDTA). Samples were then subjected to 150 nM of the di-eosin-GSSG probe in the presence of 5 μM DTT. Increase in fluorescence was monitored for 30 minutes by excitation at 520 nm and emission at 550 nm. Generated data from day 28 were then normalized to day 0 control for each sample, with raw data representing relative fluorescent units (RFU)/minute (n=3 for each patient sample).

3.4.7 Western Blotting

Cells were seeded in a 6-well plate, grown to confluence and incubated with zafirlukast for a determined amount of time depending on the experiment. Total cellular extracts were prepared in M-PER extraction buffer (Thermo Scientific, Waltham, MA) and total protein calculated using Pierce Coomassie Plus (Bradford) Assay Reagent (Thermo Scientific, Waltham, MA). Proteins were separated *via* SDS-PAGE and transferred to a PVDF membrane. Membranes were blocked with 5% non-fat milk in Tris Buffered Saline (TBS) and probed with the appropriate primary and HRP-coupled secondary antibodies in 3% bovine serum albumin (BSA) in TBS with 0.1% Tween 20.

Tumour lysates were prepared from 10-20 mg of flash frozen tumour tissue in 1% Triton X-100 buffer, and total protein calculated using the Pierce Detergent Compatible Bradford Assay (Thermo Scientific, Waltham, MA). Samples were electrophoresed and transferred as described above. Membranes were probed with anti-PDI and anti-ERp57 followed by an HRP-coupled antirabbit secondary antibody.

3.4.8 Factor Xa Generation Assay

Cells were plated in 12-well dishes at 100,000 cells per well. After 24 hours of growth, cells were treated with zafirlukast as indicated, washed twice with TBS and read in a SpectraMax M3 plate reader with TBS containing 5 nmol/L FVIIa, 150nmol/L of FX, and 5 mmol/L of $CaCl_2$. The reaction was read every minute for 45 minutes at a fluorescence excitation wavelength of 352 nm and emission wavelength of 450 nm. The signal was normalized to a percentage of the mock-treated control cells.

3.4.9 Animal Studies

Four-week-old female NOG mice (Taconic Biosciences, Germantown NY) were subcutaneously (SC) implanted with OVCAR8 cells grown to confluence and diluted to a concentration of 250,000 cells/100 μL in serum free medium then randomly assigned to a vehicle control (n=13) or test group (n=13). Four mice remained with no injection to serve as a baseline. Twice a week, mice were measured for weight and tumour growth then checked for health concerns. When tumours became apparent, measurements were taken twice a week with a calliper and size was estimated using LXWXW/2. When tumour size reached an average of 30 mm^3 animals were treated based on weight *via* intraperitoneal (i.p.) injections, either with vehicle (1% DMSO, 20% PEG, 2% Tween 80) or 30 mg/kg zafirlukast in vehicle. Injections

were administered daily with freshly prepared drug. Health checks, weigh-ins, and tumour measurements continued twice a week for 32 days.

In a second xenograft study using the same experimental setup as above, all animals received a combined chemotherapy dose of 5 mg/kg cisplatin and 120 mg/kg gemcitabine once weekly in the presence or absence of a daily i.p. injection of zafirlukast (30 mg/kg). Injections, health checks, weigh-ins, and tumour measurements remained the same as the first study.

At the end of each study lungs, kidneys, livers, spleens, and tumours were excised and sent for histology, and tumours were examined by western blotting analysis. Organs and tumours were placed in 10% formalin and switched to 70% ethanol after 24 hours. Organs were sectioned and stained with hematoxylin and eosin (H&E). Slides were viewed at 4× magnification *via* inverted microscopy and graded for metastasis. A 5-point scale of 0-4 was used for grading with a score of 0 equating to no observed metastasis; 1 being small, scattered tumours detected; 2 having scattered but larger tumours; 3 showing a high amount or regions of tumour growth; and 4 having large, dense tumour regions.

3.4.10 Human Studies

We conducted a single arm pilot study in women with tumour-marker only relapsed ovarian cancer. The primary objective of the trial was to determine the potential efficacy of zafirlukast in terms of CA-125 response per Gynaecologic Cancer Intergroup (GCIG) criteria (Rustin et al., 2011). The key secondary objective was to assess changes in CA-125 doubling time in the 3 months prior to enrolment and following the initiation of zafirlukast. Eligible patients were required to have histologically confirmed epithelial ovarian, fallopian tube, or primary peritoneal cancer and have completed at least first-line platinum-based chemotherapy and surgery with a response (Table 3.1). Eligible patients had tumour marker-only relapse, defined as CA-125 more than twice the upper limit of normal (35 U/mL) in the setting of

normal baseline CA-125 levels or a CA-125 greater than twice the nadir count on two consecutive measurements for CA-125 values that remain above baseline without measurable radiographic disease. Participants were required to have adequate organ and marrow function defined as absolute neutrophil count above 1000/μL, platelets ≥90,000/μL, total bilirubin ≤1.3× institutional upper limit of normal (ULN), and creatinine ≤ULN. Participants were excluded if they received cytotoxic chemotherapy including bevacizumab or radiotherapy within 4 weeks prior to study entry or were receiving anticoagulant or antiplatelet therapy.

Zafirlukast was administered at 40 mg twice daily for 28-day cycles. The peak plasma concentration of zafirlukast 40 mg following oral ingestion is ~3 μM (Fischer et al., 2000). The 40 mg dose is double the FDA approved dose for asthma, but is known to be well tolerated (Calhoun, 1998). The treatment continued until progression, study completion or taken off study for other reasons. CA-125 was assessed at baseline and every 28 days. Progression was defined as development of clinical symptoms deemed secondary to ovarian cancer and/or radiographically visible disease and/or doubling in the pre-treatment CA-125 value, confirmed on successive measurements (1-3 weeks after initial measurement) (Rustin et al., 2011).

3.4.11 Statistics

The statistical analysis was performed using GraphPad Prism (Version 9.4.0, San Diego, CA). Data were presented as the mean ± SD. For di-eosin-GSSG assays and the factor Xa assay a one-way ANOVA with a post-hoc Dunnett's test was used for statistical analysis between test groups and the control. For the zafirlukast, RL90, and PACMA-31 time course study a two-way ANOVA with a post-hoc Sidak's test was used for statistical analysis between test groups and the control. For the Western blots, mouse studies, and human studies, a student's t-test was used to evaluate the statistical significance between each test group and the

control group. *P < 0.05, **P < 0.01, ***P < 0.001, or ****P < 0.0001 was considered to be statistically significant.

3.4.12 Study Approval

The animal work in this protocol was approved by the IACUC and IBC of UMass Chan Medical School-Baystate, the protocol for the human studies was approved by the institutional review board at Dana Farber Harvard Cancer Centre and the trial was registered at clinicaltrials.gov (NCT04339140).

3.5 Results

This study demonstrates a novel activity of zafirlukast and montelukast (Figure 3.1 A & B) as thiol isomerase inhibitors. As shown in Figure 3.1 C, zafirlukast inhibited PDI, ERp5, ERp57, and ERp72 in a concentration-dependent manner for all four enzymes at approximately the same IC_{50}, thereby demonstrating pan, non-preferential, inhibition. Montelukast also inhibited all four thiol isomerases albeit with less potency (Figure 3.1 D). It is interesting to note that montelukast is less potent than zafirlukast at inhibiting thiol isomerases, while being 2-3 times more potent than zafirlukast at inhibiting the LTR1 receptor (Aharony, 1998). To further confirm that these drugs are targeting thiol isomerases, we explored the effects of an analogue of zafirlukast that lacks the cyclopentyl moiety (Figure 3.1 E). Removal of the cyclopentyl is predicted to reduce the potency of this analogue against the LTR1 receptor more than 100-fold (Bernstein, 1998b). Interestingly, this zafirlukast analogue maintained a similar potency (~1.5-fold less) to that of zafirlukast at inhibiting thiol isomerases (Figure 3.1 F).

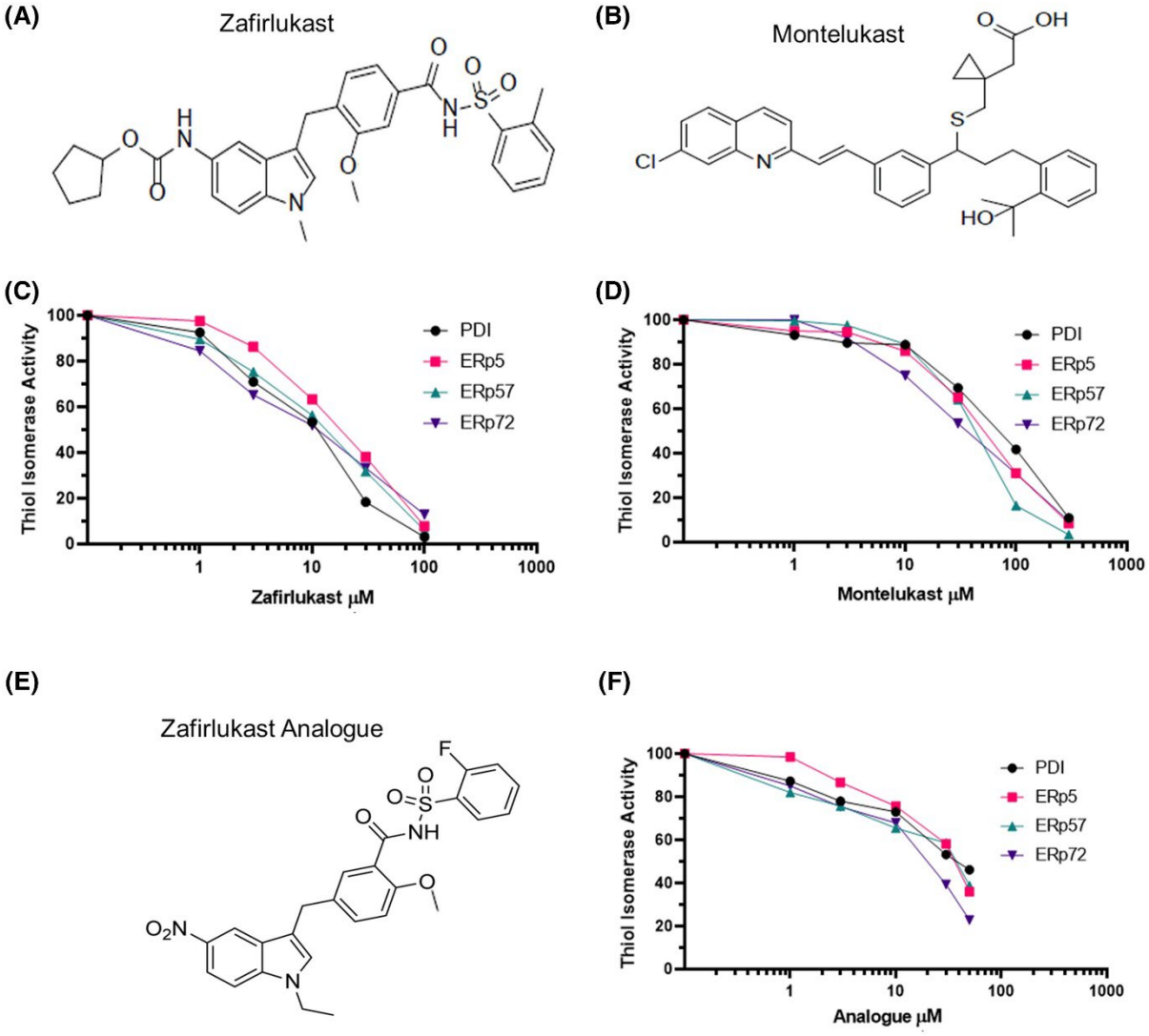

Figure 3.1 Zafirlukast and montelukast are broad-spectrum thiol isomerase inhibitors. The structures of zafirlukast (A) and montelukast (B). Both zafirlukast (n=3) (C) and montelukast (n=3) (D) inhibit the thiol isomerases PDI, ERp5, ERp57, and ERp72 in a concentration-dependent manner when examined *via* the insulin turbidity assay. (E) The structure of a zafirlukast analogue missing the cyclopentyl moiety, decreasing or losing its affinity for the leukotriene receptor. (F) The analogue (n=3) inhibits PDI, ERp5, ERp57, and ERp72 similarly to zafirlukast.

3.5.1 Zafirlukast Inhibits Cellular Thiol Isomerase Activity

The thiol isomerase activity of OVCAR8 cells is also inhibited by zafirlukast treatment. The cleavage of the fluorescent di-eosin-GSSG thiol isomerase substrate was inhibited after treatment with zafirlukast in a concentration-dependent manner. Treatment of OVCAR8 cells with 3, 10, or 30 μM of zafirlukast for 10 minutes significantly inhibited PDI activity, by 18%, 24%, and 45%, respectively (Figure 3.2 A). To confirm that the addition of zafirlukast did not alter thiol isomerase expression within a short treatment time, thiol isomerase levels were measured following 1 hour of treatment with 10 μM and 30 μM zafirlukast in OVCAR8 cells. No significant change in expression was observed (Figure 3.2 B), confirming that the observed change in activity after 10 minutes of treatment was due to enzymatic inhibition and not a decrease in enzyme levels. In order to see a decrease in enzyme levels, it would likely be necessary to treat the cells for an extended period of time. The cellular thiol isomerase activity of OVCAR8 cells also significantly decreased upon treatment with montelukast and the zafirlukast analogue, with montelukast being somewhat less effective (reduction by 20%, 30%, and 40%, at 10, 30, and 100 μM, respectively) than zafirlukast (Figure 3.2 C). In contrast, the zafirlukast analogue was more potent than zafirlukast, significantly inhibiting activity by 25%, 39%, 29%, and 44% at 1, 3, 10, and 30 μM, respectively (Figure 3.2 D).

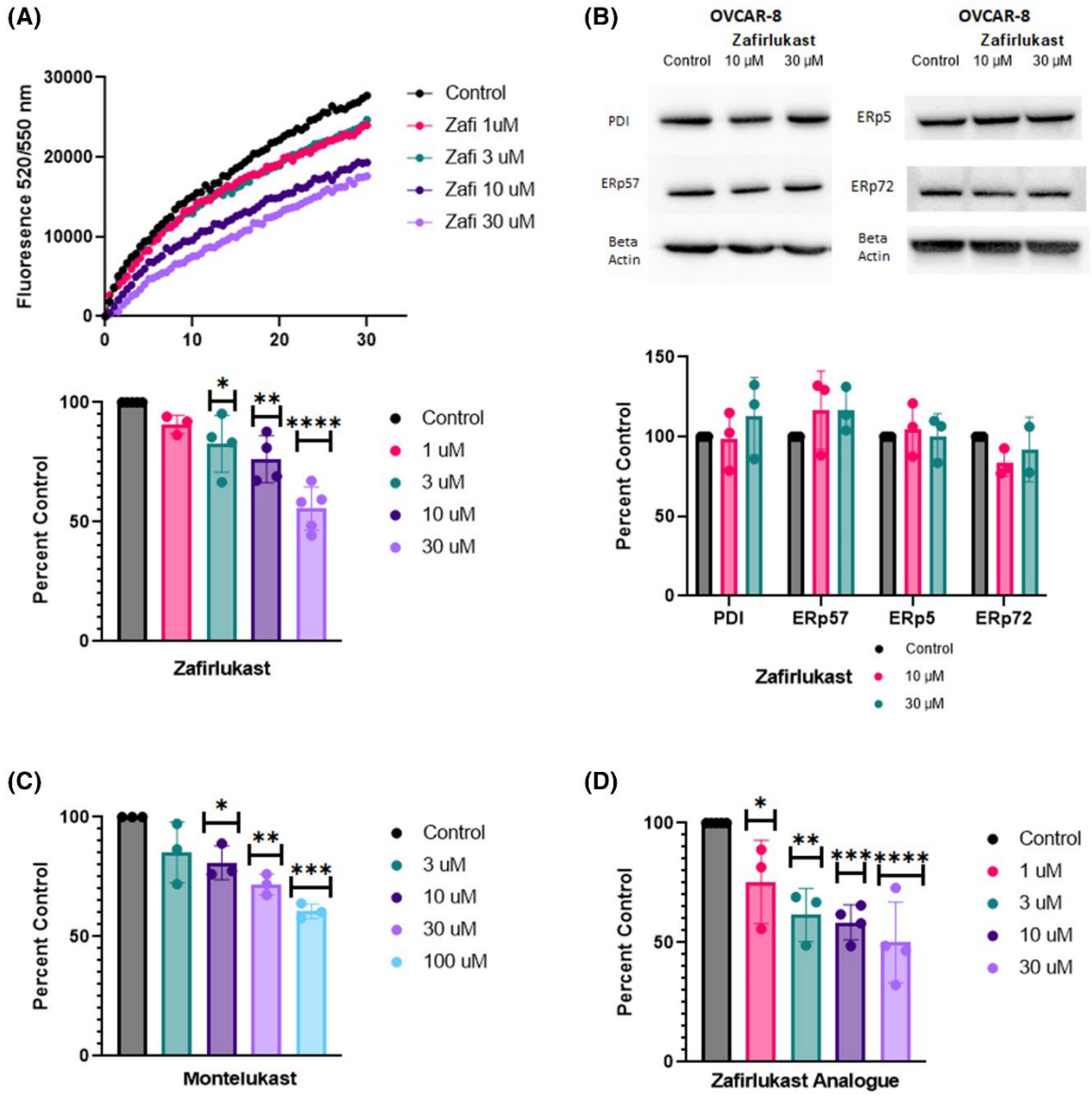

Figure 3.2 Cellular thiol isomerase activity is inhibited by zafirlukast. (A) Cellular thiol isomerase activity is inhibited by zafirlukast treatment in a concentration dependent manner as measured by di-eosin-GSSG fluorescence (n=4) Data is presented as mean ±SD. One-way ANOVA and a post-hoc Dunnett's test where *p=0.0217 for 3 µM zafirlukast, **p=0.0020 for 10 µM zafirlukast and ****p<0.0001 for 30 µM zafirlukast compared to the control. (B) Levels of PDI, ERp5, ERp57, and ERp72 remain similar with increasing concentrations of zafirlukast in OVCAR8 cells (n=3). Data is presented as mean ±SD. A student's t-test was used for comparison to control. No significant changes were present. (C & D) Cellular thiol isomerase activity is also inhibited by (C) montelukast (n=3) and

(D) the zafirlukast analogue (n=4). Data is presented as mean ±SD. One-way ANOVA and a post-hoc Dunnett's test where *p=0.0219 for 10 μM montelukast, **p=0.0018 for 30 μM montelukast and ***p=0.0002 for 100 μM montelukast compared to the control, while *p=0.0383 for 1 μM zafirlukast analogue, **p=0.0017 for 3 μM zafirlukast analogue, ***p= 0.0004 for 10 μM zafirlukast analogue and ****p<0.0001 for 30 μM zafirlukast analogue compared to the control

3.5.2 Zafirlukast has Antineoplastic Activity

As inhibitors of thiol isomerase activity have been shown to have antineoplastic activity (S. Xu et al., 2014), the effect of these drugs on cancer cell viability was evaluated. Zafirlukast inhibited OVCAR8 cancer cell viability with an IC_{50} of 12 μM, while montelukast and the zafirlukast analogue inhibited cell viability about 5- and ~1.5-fold less potently (with IC_{50}'s of 60 and 20 μM, respectively) (Figure 3.3 A). While differences in potency would not be surprising between a cell-free and a cellular activity assay as well as between a cellular activity assay and a viability assay, it is notable that relative potencies of zafirlukast, the zafirlukast analogue and montelukast remained consistent across the assays, with the analogue having a similar potency to that of zafirlukast and montelukast being ~5-fold less potent in each assay (Figure 3.3 B). Due to the potency differences along with the lack of availability of large quantities of the zafirlukast analogue, only zafirlukast was selected for additional studies. Interestingly, zafirlukast inhibited the cell viability, measured through fluorescence after treatment with the PrestoBlue reagent, of three additional cancer cell lines, HCT116 colon cancer cells, A549 lung cancer cells and PC3 prostate cancer cells with an IC_{50} value similar to (slightly more potent) that for OVCAR8 cells, however the IC_{50} for the HEK293 cell line derived from embryonic kidney cells exceeded the concentration tested (>100 μM) (Figure 3.3 C). However, it is important to note that zafirlukast was not tested on kidney cells derived from cancerous tissue, so it is a possibility that zafirlukast does not have a cytotoxic effect towards kidney cells in general, and this should be explored in future studies.

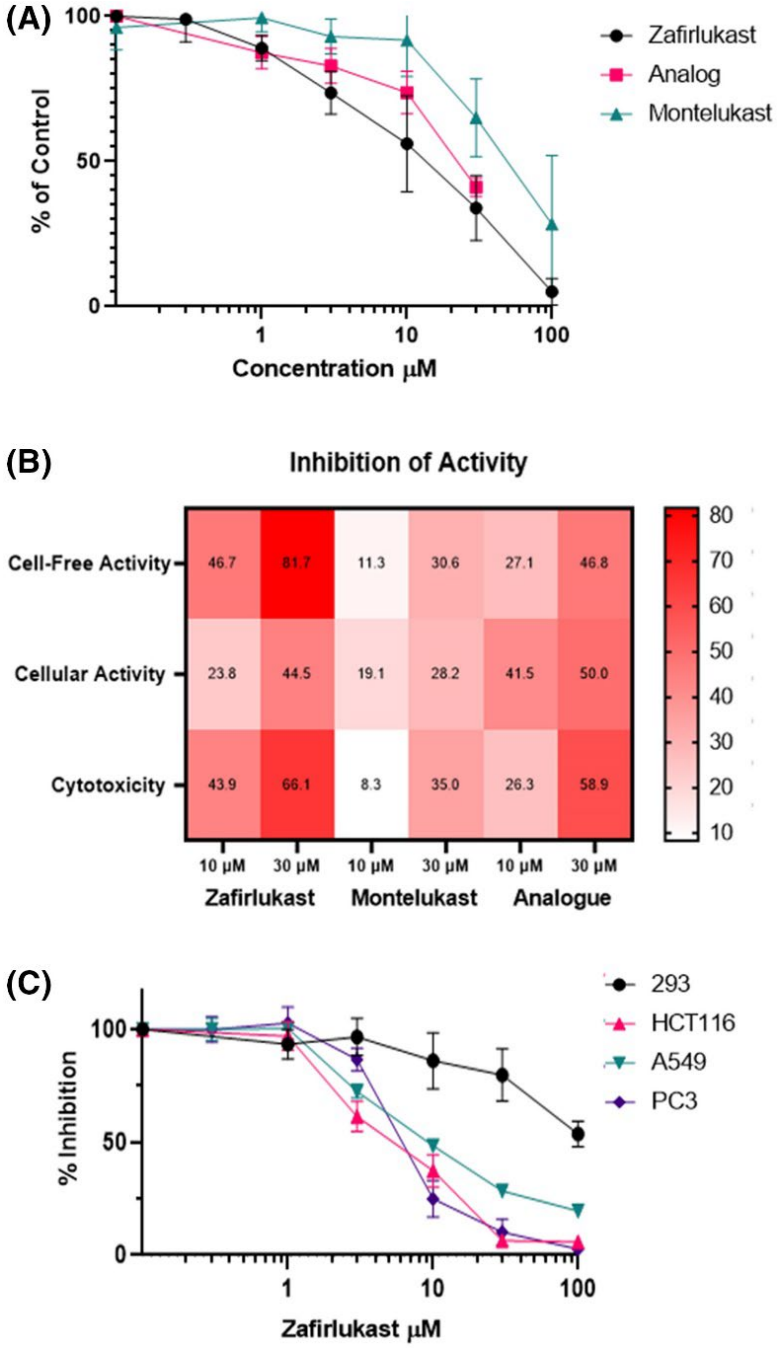

Figure 3.3 Zafirlukast and montelukast selectively cause cancer cell cytotoxicity. (A) Zafirlukast is about 5x more cytotoxic than montelukast and 1.5× more cytotoxic than the analogue (n=3). (B) Comparison of the relative potency of each compound in the experiments from Figure 3.1, Figure 3.2 and Figure 3.3 A. (C) Zafirlukast also induced cytotoxicity to HCT116 colon tumour cells, PC3 prostate cancer cells, and A549 lung cancer cells selectively over the HEK293 non-cancerous cell line (n=3).

3.5.3 Zafirlukast and Downstream Measures of Thiol Isomerase Inhibition in Cancer Cells

Thiol isomerases play important roles in cancer growth and thrombosis. For example, the activation of the EGFR receptor is dependent on ERp57 activity, as gene silencing of ERp57 leads to decreased phosphorylation of EGFR (E. Gaucci et al., 2013). We evaluated whether incubation of cancer cells with zafirlukast altered EGFR activation and phosphorylation of GRB2-associated-binding-protein 1 (Gab1), an immediate downstream target of EGFR signalling, responsible for activation of the Akt cell survival pathway (Mattoon et al., 2004). OVCAR8 cells were treated with zafirlukast for 1 or 4 hours before activation with epidermal growth factor (EGF) for 5 minutes. After four hours of treatment with 10 μM or 30 μM zafirlukast, EGFR phosphorylation significantly decreased, by 39% and 52%, respectively. Phosphorylation also decreased after 1 hour, by 18% and 27% after treatment with 10 μM or 30 μM zafirlukast, respectively (Figure 3.4 A). To further confirm that the decreased activation of EGFR was due to thiol isomerase inhibition, the PDI and ERp57 function blocking antibody RL-90 (Y. Wu et al., 2012) and small molecule thiol isomerase inhibitor PACMA-31 were utilized to examine the effects of thiol isomerase inhibition on EGFR activation and also inhibited EFGR activation in a concentration-dependent manner (Figure 3.4 B). Notably, OVCAR8 cell viability was minimally altered by the concentrations and timepoints of zafirlukast, RL-90 and PACMA-31 used in Figure 3.4 A and B, suggesting decreases in cell viability were not responsible for the observed decreases in EGFR activation (Figure 3.4 C). Furthermore, phosphorylation of Gab1 was significantly decreased under all conditions tested, by 37% following incubation with 10 μM zafirlukast at 1 hour, and further decreased to 5% or less at all other time points and concentrations, demonstrating robust inhibition of the EGFR pathway after zafirlukast treatment (Figure 3.4 D).

Secondly, cancer induced thrombosis is the second leading cause of mortality in cancer patients after metastasis (Abdol Razak et al., 2018), and PDI activity has been demonstrated to enhance the procoagulant activity of cancer cell lines (Z. Lysov et al., 2015). Therefore, we decided to measure the activity of tissue factor released by OVCAR8 cells. In order to do so, the generation of Factor Xa was monitored. Cells treated with 1, 3, 10, and 30 μM zafirlukast for 30 minutes demonstrated a dose dependent decrease in Xa generation (Figure 3.4 E), with significant differences observed at 10 and 30 μM.

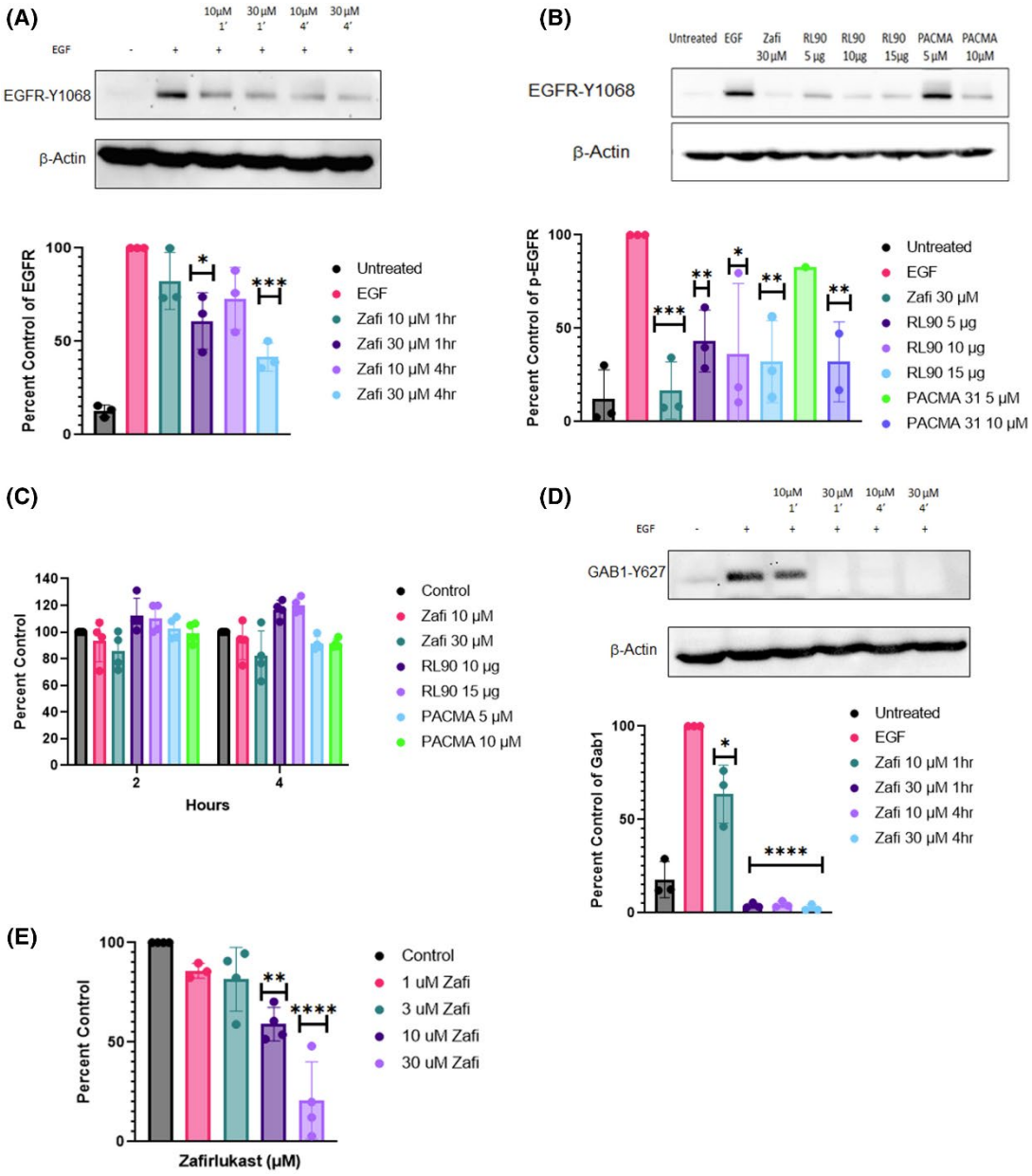

Figure 3.4 Zafirlukast effects downstream measures of thiol isomerase inhibition. (A) Zafirlukast treatment inhibits the activation of the EGFR receptor (n=3). Quantification of phosphorylated EGFR was calculated using Image Lab software and normalized to a beta actin control. Data is presented as mean ±SD. A student's t-test where *p=0.0112 for 1 hour 30 μM treated zafirlukast and ***p= 0.0002 for 4 hour 30 μM treated zafirlukast compared to the EGF control. (B) The known ERp57 inhibitor RL90 and PACMA 31 also inhibit EGFR activation (n=3). Quantification of phosphorylated EGFR was calculated using Image Lab software and normalized to a beta actin control. Data is presented as

mean ±SD. A student's t-test where ***p=0.0007 for 30 μM zafirlukast, **p=0.004 for 5 μg RL90, *p=0.0433 for 10 μg RL90, **p=0.0059 for 15 μg RL90 and **p=0.0092 for 10 μM PACMA 31 compared to the EGF control. (C) A time-course study of zafirlukast RL-90, and PACMA 31's effect on OVCAR8 cell viability (n=4). Data is presented as mean ±SD. A two-way ANOVA and a post-hoc Sidak's test demonstrate no significant changes between the control and any of the test groups. (D) Phosphorylation of Gab1, an immediate downstream target of EGFR phosphorylation (n=3). Quantification of phosphorylated Gab1 was calculated using Image Lab software and normalized to a beta actin control. Data is presented as mean ±SD. A student's t-test where *p=0.0153 for 1 hour 10 μM zafirlukast and ****p<0.0001 for 4 hour 10 μM and 1 and 4 hour 30 μM zafirlukast compared to the EGF control. (E) Zafirlukast inhibits the tissue factor dependent generation of Factor Xa (n=4). Data is presented as mean ±SD. A one-way ANOVA and post-hoc Dunnett's test where **p=0.0041 for 10 μM zafirlukast and ****p<0.0001 for 30 μM zafirlukast.

3.5.4 Zafirlukast Inhibits Tumour Growth in Ovarian Cancer Mouse Xenografts

Following the observed antitumor activity of zafirlukast *in vitro*, we assessed whether zafirlukast inhibited tumour cell growth in a mouse xenograft of OVCAR8 cells. Mice were administered vehicle control or 30 mg/kg zafirlukast consecutively for 32 days *via* intraperitoneal injections. Tumour volumetric measurements were assessed twice weekly (Figure 3.5 A). Zafirlukast treatment significantly decreased tumour size compared to controls with a mean decrease in volume of 42% at day 32 ($p=0.0005$). Examination of PDI and ERp57 levels in tumours by western blot revealed similar levels of both thiol isomerases between the control and zafirlukast treated groups (Figure 3.5 B). Organs (*i.e.*, lung, kidney, liver, and spleen) were examined for metastatic deposits by histology, and representative animals from the control and zafirlukast group were stained with haematoxylin and eosin (H&E). Multiple metastases were detected in the lungs of the control group, while very few metastases were found in the lungs of the zafirlukast treated group (Figure 3.5 C). Using a rating scale of 0-4, where 0 represents no metastases detected and 4 represents large dense metastases, the zafirlukast treated group (score of 0.25) had a significantly smaller amount and size of metastases compared to the control group (score of 2.5) ($p=0.0004$) (Figure 3.5 D). Examination of the livers of animals detected one control mouse that scored a 1, but no other metastases were detected in the livers, kidneys, or spleens of any animal.

Additionally, since multi-drug therapy is commonplace in cancer treatment, zafirlukast was added to a common ovarian cancer regimen of cisplatin and gemcitabine in 5 mg/kg and 120 mg/kg respectively *via* weekly intraperitoneal injection. The addition of zafirlukast significantly reduced the tumour volume relative to cisplatin-gemcitabine alone with a mean decrease of 38% ($p=0.011$) after 4 weeks (Figure 3.5 E), and an 83% decrease in the tumour volume by the end of the study compared to the vehicle control (Figure 3.5 F).

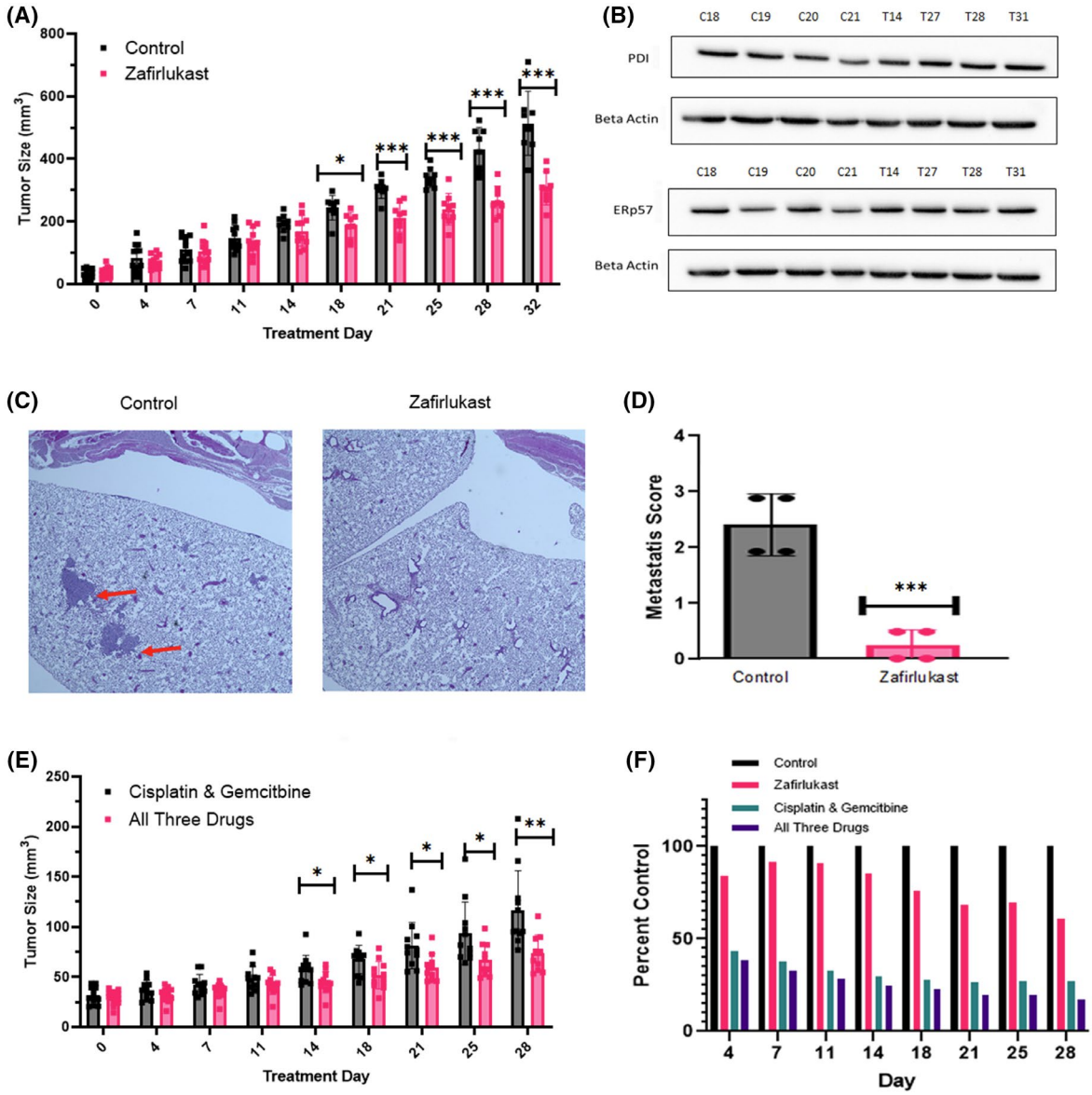

Figure 3.5 Zafirlukast inhibits the growth of OVCAR-8 tumours on xenograft mice. (A) NOG mice were subcutaneously injected with OVCAR8 cells at 4 weeks old (n=13/group). Tumours were allowed to grow to an average size of 30 mm^3 before daily treatment with 30 mg/kg of zafirlukast (red bars) or vehicle control (black bars). Tumour size was measured twice weekly. Data is presented as mean ±SD. A student's t-test where *p=0.0149 at 18 days, ***p=0.0002 at 21 and 25 days, ****p<0.0001 at 28 days and ***p=0.0001 at 28 days. (B) PDI and ERp57 levels in tumours were measured by immunoblotting after day 32 of treatment in control vs zafirlukast treated mice with minimal difference in expression.

(C & D) Lung metastasis (n=4/group) were graded on a scale of 0-4. A significant difference was seen between the control and zafirlukast treated groups. Data is presented as mean ±SD. A student's t-test where ***p=0.0004 for the treated group compared to the control. (E) Similar to A, except mice were treated with 5 mg/kg cisplatin and 120 mg/kg gemcitabine once weekly in the presence (red bars) or absence (black bars) of 30 mg/kg zafirlukast daily (n=12/group). Data is presented as mean ±SD. A student's t-test where *p=0.023, 0.012, 0.018 and 0.027 for days 14, 18, 21 and 25 respectively, and **p=0.004 for day 28. (F) A summary of the three different treatment groups, normalized to the control group by percentage.

3.5.5 A Pilot Clinical Trial of Zafirlukast in Women with Relapsed Ovarian Cancer

In order to assess potential antineoplastic activity of zafirlukast, we conducted a pilot clinical trial in women with tumour marker-only (CA-125) relapsed ovarian cancer. A total of four women were enrolled, and the CA-125 levels were measured at baseline and monthly intervals to assess response after initiation of zafirlukast 40 mg twice daily. None of the women demonstrated a decrease in CA-125 following the initiation of zafirlukast. However, in all 4 women, the rate of rise of CA-125 was reduced following treatment with zafirlukast (Figure 3.6 A-C). Accordingly, the mean change in CA-125 was 0.036 U/mL per day prior to treatment compared with 0.015 U/mL per day following zafirlukast (paired t-test p=0.026). This equated to a mean CA-125 doubling time of 29.8 days in the weeks prior to treatment compared with a mean doubling time of 85.69 days following treatment. Plasma thiol isomerase was evaluated prior (day 0) and after 4 weeks of zafirlukast treatment (day 28). In three out of four patients there was a reduction of plasma thiol isomerase activity (Figure 3.6 D). The degree of thiol isomerase activity reduction correlated (R=0.91) with the CA-125 doubling time (Figure 3.6 E). There were no cases of haemorrhage reported. The only instance of toxicity considered possibly related to zafirlukast was headache (grade 1). Three patients reported abdominal pain (grade 1) and one patient experienced grade 2 hypertension and abdominal bloating. There were no grade 3 or higher adverse events reported on study.

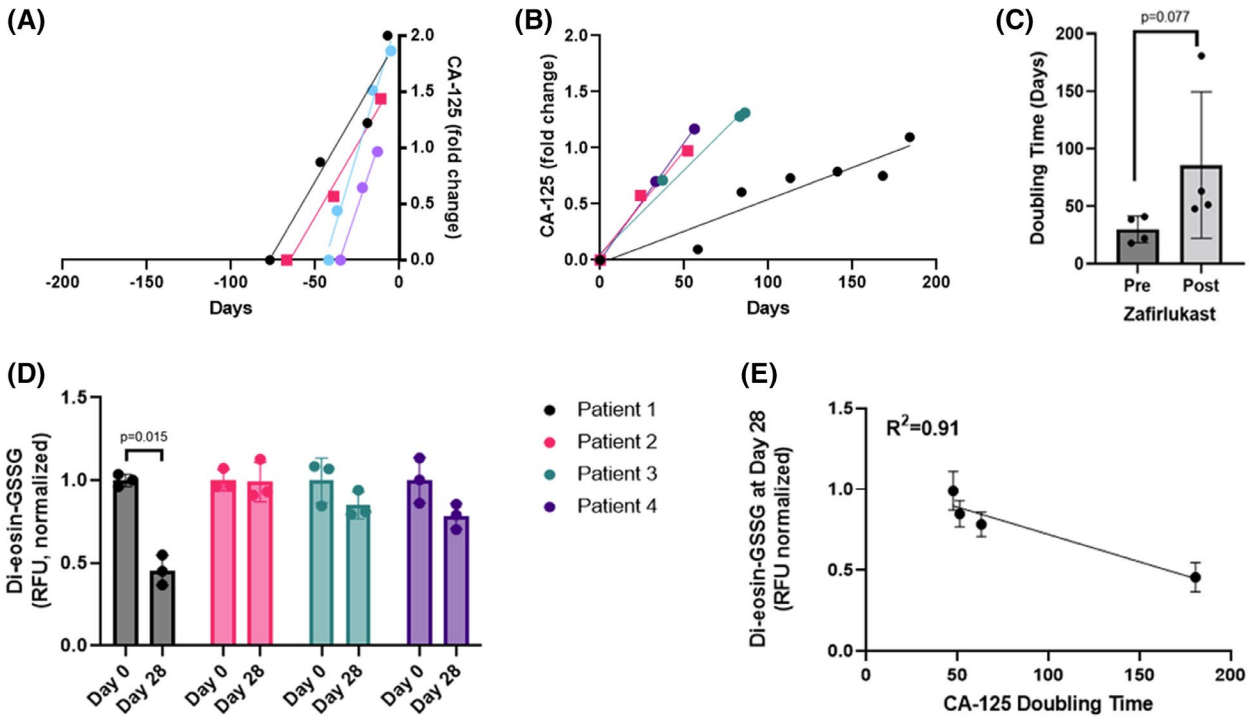

Figure 3.6 Zafirlukast inhibits CA-125 doubling time. The rate of CA-125 doubling time (A) prior to and (B) after zafirlukast treatment. The mean change in CA-125 was 0.036 U/mL per day prior to treatment compared with 0.015 U/mL per day following zafirlukast (paired t-test p=0.026) (C) Comparison of the average pre and post treatment doubling times of CA-125. (D) The relative thiol isomerase activity of each patient 28 days after treatment, the reduction of which was well correlated (E) to the decrease in CA-125 doubling time. Data for figure 3.6 was collected and presented by Roelof H. Bekendam and Jeffrey I. Zwicker of Harvard Medical School.

Patient	**1**	**2**	**3**	**4**
Age	55	66	58	77
Histology	Serous carcinoma	Serous carcinoma	Serous carcinoma	Serous Carcinoma
Initial Stage	IIB	IIIC	IIIB	IA
Grade	High grade	High grade	High grade	High grade
Previous treatment with carboplatin/paclitaxel?	Yes	Yes	Yes	Yes

Table 3.1 Patient characteristics.

3.6 Discussion

Targeting thiol isomerase activity represents a promising mechanism of novel antitumor agents (Bekendam et al., 2016; Stopa et al., 2017; Vatolin et al., 2016; Y. Wu et al., 2012; S. Xu et al., 2014). There are several compounds in therapeutic development including rutin, bepristat, isoquercetin (Bekendam et al., 2016; Jasuja et al., 2012b; J. D. Stopa & J. I. Zwicker, 2018), PACMA-31, and CCF642, but none of these are pan-inhibitors (Vatolin et al., 2016; Xu et al., 2012a). The ability of zafirlukast to inhibit multiple thiol isomerases is potentially advantageous, since each thiol isomerase has distinct roles in cancer, and we observed that zafirlukast broadly inhibited thiol isomerases including PDI, ERp57, ERp5, and ERp72 almost equivalently (Figure 3.1). For example, PDI has a vital role in tumour growth and progression as well as protecting cells from apoptosis (Lovat et al., 2008; Xu et al., 2012a; S. Xu et al., 2014). High levels of ERp5 expression correlate with preventing an efficient antitumor response in Hodgkin lymphomas (Dranoff, 2009; Zocchi et al., 2012) and are associated with prostate (Glen et al., 2010) and breast (Gumireddy et al., 2007) cancer progression. ERp57 is involved in cancer metastasis (Santana-Codina et al., 2013), gene transcription through EFGR signalling (Gaucci et al., 2013), STAT3 (Eufemi et al., 2004), and mTOR pathways (Ramirez-Rangel et al., 2011) while also promoting resistance to treatment with paclitaxel in ovarian cancer (Cicchillitti et al., 2009). While ERp72 is overexpressed in lung adenocarcinoma and plays a role in cisplatin resistance (Tufo et al., 2014). With the exception of bacitracin, which is not used systemically due to nephrotoxicity (Michie et al., 1949), zafirlukast is the first known broad-spectrum thiol isomerase agent systematically evaluated as a therapeutic compound.

Considering the pleiotropic activity of zafirlukast, we cannot definitively conclude that the antitumor activity is exclusively related to thiol isomerase inhibition. Previous studies have determined that agents such as zafirlukast are associated with a decreased cancer risk that was

assumed to be through interaction with the LTR1 receptor (Jang et al., 2022; Tsai et al., 2016) and others have demonstrated the LTR2 receptor can promote invasiveness and metastasis of ovarian cancer cells (Seo et al., 2012). However, we note that, zafirlukast and montelukast demonstrate selectivity for the LTR1 receptor, with minimal effects on the LTR2 receptor (Aharony, 1998). Secondly, montelukast has an increased affinity for the LTR1 receptor in comparison to zafirlukast (Aharony, 1998) yet was 3-5x weaker in our *in vitro* experiments (Figure 3.3 B). Furthermore, using a zafirlukast analogue that was modified to significantly decrease or abolish its affinity for the LTR1 receptor (Bernstein, 1998b) while retaining its potency as a thiol isomerase inhibitor, we observed similar relative effects when compared to zafirlukast and stronger effects than those observed with montelukast (Figure 3.3 B). These observations strongly suggest that zafirlukast does not inhibit cancer cell viability by acting on the LTR1 receptor, but through thiol isomerase inhibition. Finally, our observed delay in CA-125 doubling in our clinical trial correlated with thiol isomerase inhibition (Figure 3.6 D & E). Thus, we believe the available evidence supports that our observed effects are primarily due to thiol isomerase inhibition.

Zafirlukast significantly inhibited tumour growth in a xenograft model of ovarian cancer, which is consistent with previous studies of thiol isomerase inhibitors (Xu et al., 2012a). Interestingly, very few, small metastases were found in the lungs of treated animals in comparison with the control group (Figure 3.5), which, to our knowledge, is a novel finding. We have previously shown that zafirlukast can inhibit cell migration, which would be consistent with slowing metastasis (Holbrook et al., 2021). Future studies should further examine the potential of thiol isomerase inhibitors in effecting metastasis.

Next to metastatic growth, cancer induced thrombosis is the second leading cause of death due to cancer (Khorana et al., 2007; Sørensen et al., 2000). In our previous work, we demonstrated that zafirlukast also inhibits *ex vivo* human platelet aggregation and *in vivo*

mouse thrombus formation induced *via* laser injury (Holbrook et al., 2021). Thus, zafirlukast is the first reported thiol isomerase inhibitor that inhibits cancer cell growth as well as thrombus formation and, as such, should be further explored as a potential preventive agent for cancer-induced thrombosis. Our previous work has demonstrated that circulating PDI is associated with increased risks of cancer-induced thrombosis (Sharda et al., 2021), along with increased levels of tissue factor (Zwicker, 2010). Interestingly, tissue factor is also expressed on the surface of some cancer cells (Beckmann et al., 2021) and in this study we found that both cellular thiol isomerase activity (Figure 3.2 A) and tissue factor dependent Factor Xa generation (Figure 3.4 E) was inhibited by zafirlukast in ovarian cancer cells, which would further support exploration of zafirlukast for cancer-induced thrombosis.

Based on the established safety profile of zafirlukast and its potential benefits as a broad-spectrum thiol isomerase inhibitor that is FDA-approved for the treatment of asthma, we proceeded to assess whether we could detect antineoplastic activity in humans. We elected to use 40 mg twice daily, which is a dose higher than typically used in the treatment of asthma but previously shown to be well tolerated (Calhoun, 1998). The CA-125 did not decline in any of the women treated with zafirlukast but in all instances, there was a slowing in the rate of rise of CA-125 with a greater than two-fold increase in CA-125 doubling time. Additional studies are needed to assess whether higher doses of zafirlukast can effectively stabilize CA-125 levels. The use of zafirlukast or eventually, its analogue, in combination with other chemotherapeutics should be explored, which would be supported by the additive effect of zafirlukast with cisplatin and gemcitabine shown in our xenograft experiments.

An important message from this work is that zafirlukast could be repurposed as a cancer medication as it is already FDA approved, being first used clinically in 1996 for the treatment of asthma via inhibition of the LTR1 receptor and is known to be well tolerated (Schlesinger, 2002). In this study, we found that zafirlukast significantly inhibited tumour growth on its own

and especially in tandem with a standard chemotherapeutic regimen in a xenograft model of ovarian cancer (Figure 3.5). We found that zafirlukast could reduce metastasis (Figure 3.5) and potentially cancer induced thrombosis (Figure 3.4 D), the top two leading causes of death due to cancer (Khorana et al., 2007; Sørensen et al., 2000). Thus, considering the potential thiol isomerase inhibitors have held as potential cancer therapies (Bekendam et al., 2016; Liang et al., 2021; Sharda et al., 2021; Vatolin et al., 2016; Xu et al., 2012a; S. Xu et al., 2014; Zwicker, 2014; J. I. Zwicker et al., 2019b), and our additional findings, it is notable that zafirlukast can be readily studied in the clinic due to its previous FDA approval and established safety profile.

In summary, zafirlukast is the first broad-spectrum thiol isomerase inhibitor that has been shown to inhibit cancer growth in both cells and mice. We demonstrated that cellular thiol isomerase activity was inhibited by zafirlukast and observed a clinical effect on CA-125 that appeared to correlate with thiol isomerase activity. Future clinical studies are needed to further assess the therapeutic benefit of targeting thiol isomerases in ovarian cancer.

3.7 References

Abdol Razak, N. B., Jones, G., Bhandari, M., Berndt, M. C., & Metharom, P. (2018). Cancer-Associated Thrombosis: An Overview of Mechanisms, Risk Factors, and Treatment. *Cancers (Basel)*, *10*(10). https://doi.org/10.3390/cancers10100380

Aharony, D. (1998). Pharmacology of leukotriene receptor antagonists. *Am J Respir Crit Care Med*, *157*(6 Pt 2), S214-218; discussion S218-219, S247-218. https://www.ncbi.nlm.nih.gov/pubmed/9647602

Appenzeller-Herzog, C., & Ellgaard, L. (2008). The human PDI family: versatility packed into a single fold. *Biochim Biophys Acta*, *1783*(4), 535-548. https://doi.org/10.1016/j.bbamcr.2007.11.010

Beckmann, L., Rolling, C. C., Voigtlander, M., Mader, J., Klingler, F., Schulenkorf, A., Lehr, C., Bokemeyer, C., Ruf, W., & Langer, F. (2021). Bacitracin and Rutin Regulate Tissue Factor Production in Inflammatory Monocytes and Acute Myeloid Leukemia Blasts. *Cancers (Basel)*, *13*(16). https://doi.org/10.3390/cancers13163941

Bekendam, R. H., Bendapudi, P. K., Lin, L., Nag, P. P., Pu, J., Kennedy, D. R., Feldenzer, A., Chiu, J., Cook, K. M., Furie, B., Huang, M., Hogg, P. J., & Flaumenhaft, R. (2016). A substrate-driven allosteric switch that enhances PDI catalytic activity. *Nat Commun*, *7*, 12579. https://doi.org/10.1038/ncomms12579

Bernstein, P. R. (1998). Chemistry and structure-activity relationships of leukotriene receptor antagonists. *Am J Respir Crit Care Med*, *157*(6 Pt 1), S220-226. https://www.ncbi.nlm.nih.gov/pubmed/9620943

Calhoun, W. J. (1998). Summary of clinical trials with zafirlukast. *Am J Respir Crit Care Med*, *157*(6 Pt 1), S238-246. https://www.ncbi.nlm.nih.gov/pubmed/9620946

Cicchillitti, L., Di Michele, M., Urbani, A., Ferlini, C., Donat, M. B., Scambia, G., & Rotilio, D. (2009). Comparative proteomic analysis of paclitaxel sensitive A2780 epithelial ovarian cancer cell line and its resistant counterpart A2780TC1 by 2D-DIGE: the role of ERp57. *J Proteome Res*, *8*(4), 1902-1912. http://www.ncbi.nlm.nih.gov/pubmed/19714814

Dranoff, G. (2009). Targets of protective tumor immunity. *Ann N Y Acad Sci*, *1174*, 74-80. https://doi.org/10.1111/j.1749-6632.2009.04938.x

Eufemi, M., Coppari, S., Altieri, F., Grillo, C., Ferraro, A., & Turano, C. (2004). ERp57 is present in STAT3-DNA complexes. *Biochem Biophys Res Commun*, *323*(4), 1306-1312. https://doi.org/10.1016/j.bbrc.2004.09.009

Fischer, J. D., Song, M. H., Suttle, A. B., Heizer, W. D., Burns, C. B., Vargo, D. L., & Brouwer, K. L. (2000). Comparison of zafirlukast (Accolate) absorption after oral and colonic administration in humans. *Pharm Res*, *17*(2), 154-159. https://doi.org/10.1023/a:1007509112383

Gaucci, E., Altieri, F., Turano, C., & Chichiarelli, S. (2013). The protein ERp57 contributes to EGF receptor signaling and internalization in MDA-MB-468 breast cancer cells. *J Cell Biochem*, *114*(11), 2461-2470. https://doi.org/10.1002/jcb.24590

Glen, A., Evans, C. A., Gan, C. S., Cross, S. S., Hamdy, F. C., Gibbins, J., Lippitt, J., Eaton, C. L., Noirel, J., Wright, P. C., & Rehman, I. (2010). Eight-plex iTRAQ analysis of variant metastatic human prostate cancer cells identifies candidate biomarkers of progression: An exploratory study. *Prostate*, *70*(12), 1313-1332. https://doi.org/10.1002/pros.21167

Gonzalez-Perez, P., Woehlbier, U., Chian, R. J., Sapp, P., Rouleau, G. A., Leblond, C. S., Daoud, H., Dion, P. A., Landers, J. E., Hetz, C., & Brown, R. H. (2015). Identification of rare protein disulfide isomerase gene variants in amyotrophic lateral sclerosis patients. *Gene*, *566*(2), 158-165. https://doi.org/10.1016/j.gene.2015.04.035

Gumireddy, K., Sun, F., Klein-Szanto, A. J., Gibbins, J. M., Gimotty, P. A., Saunders, A. J., Schultz, P. G., & Huang, Q. (2007). In vivo selection for metastasis promoting genes in the mouse. *Proc Natl Acad Sci U S A*, *104*(16), 6696-6701. https://doi.org/10.1073/pnas.0701145104

Hettinghouse, A., Liu, R., & Liu, C. J. (2018). Multifunctional molecule ERp57: From cancer to neurodegenerative diseases. *Pharmacol Ther*, *181*, 34-48. https://doi.org/10.1016/j.pharmthera.2017.07.011

Holbrook, L. M., Keeton, S. J., Sasikumar, P., Nock, S., Gelzinis, J., Brunt, E., Ryan, S., Pantos, M. M., Verbetsky, C. A., Gibbins, J. M., & Kennedy, D. R. (2021). Zafirlukast is a broad-spectrum thiol isomerase inhibitor that inhibits thrombosis without altering bleeding times. *Br J Pharmacol*, *178*(3), 550-563. https://doi.org/10.1111/bph.15291

Howard, K. C., & Garneau-Tsodikova, S. (2022). Selective Inhibition of the Periodontal Pathogen Porphyromonas gingivalis by Third-Generation Zafirlukast Derivatives. *J Med Chem*, *65*(21), 14938-14956. https://doi.org/10.1021/acs.jmedchem.2c01471

Jang, H. Y., Kim, I. W., & Oh, J. M. (2022). Cysteinyl Leukotriene Receptor Antagonists Associated With a Decreased Incidence of Cancer: A Retrospective Cohort Study. *Front Oncol*, *12*, 858855. https://doi.org/10.3389/fonc.2022.858855

Jasuja, R., Passam, F. H., Kennedy, D. R., Kim, S. H., van Hessem, L., Lin, L., Bowley, S. R., Joshi, S. S., Dilks, J. R., Furie, B., Furie, B. C., & Flaumenhaft, R. (2012). Protein disulfide isomerase inhibitors constitute a new class of antithrombotic agents. *J Clin Invest*, *122*(6), 2104-2113. https://doi.org/10.1172/JCI61228

Khodier, C., VerPlank, L., Nag, P. P., Pu, J., Wurst, J., Pilyugina, T., Dockendorff, C., Galinski, C. N., Scalise, A. A., Passam, F., van Hessem, L., Dilks, J., Kennedy, D. R., Flaumenhaft, R., Palmer, M. A. J., Dandapani, S., Munoz, B., & Schrieber, S. L. (2010). Identification of ML359 as a Small Molecule Inhibitor of Protein Disulfide Isomerase. In *Probe Reports from the NIH Molecular Libraries Program*. https://www.ncbi.nlm.nih.gov/pubmed/24624466

Khorana, A. A., Francis, C. W., Culakova, E., Kuderer, N. M., & Lyman, G. H. (2007). Thromboembolism is a leading cause of death in cancer patients receiving outpatient chemotherapy. *Journal of Thrombosis and Haemostasis*, *5*(3), 632-634. https://doi.org/10.1111/j.1538-7836.2007.02374.x

Krajewski, D., Polukort, S. H., Gelzinis, J., Rovatti, J., Kaczenski, E., Galinski, C., Pantos, M., Shah, N. N., Schneider, S. S., Kennedy, D. R., & Mathias, C. B. (2020). Protein Disulfide Isomerases Regulate IgE-Mediated Mast Cell Responses and Their Inhibition Confers Protective Effects During Food Allergy. *Front Immunol*, *11*, 606837. https://doi.org/10.3389/fimmu.2020.606837

Kumar, P., Agarwal, A., Singh, A. K., Gautam, A. K., Chakraborti, S., Kumar, U., Kumar, D., Bhattacharya, B., Panda, P., Saha, B., Qidwai, T., Maity, B., & Saha, S. (2019). Antineoplastic properties of zafirlukast against hepatocellular carcinoma via activation of mitochondrial mediated apoptosis. *Regul Toxicol Pharmacol*, *109*, 104489. https://doi.org/10.1016/j.yrtph.2019.104489

Liang, C., Flaumenhaft, R., Yuan, C., & Huang, M. (2021). Vascular thiol isomerases: Structures, regulatory mechanisms, and inhibitor development. *Drug Discov Today*. https://doi.org/10.1016/j.drudis.2021.10.018

Lovat, P. E., Corazzari, M., Armstrong, J. L., Martin, S., Pagliarini, V., Hill, D., Brown, A. M., Piacentini, M., Birch-Machin, M. A., & Redfern, C. P. (2008). Increasing melanoma cell death using inhibitors of protein disulfide isomerases to abrogate survival responses to endoplasmic reticulum stress. *Cancer Res*, *68*(13), 5363-5369. https://doi.org/10.1158/0008-5472.CAN-08-0035

Lysov, Z., Swystun, L. L., Kuruvilla, S., Arnold, A., & Liaw, P. C. (2015). Lung cancer chemotherapy agents increase procoagulant activity via protein disulfide isomerase-dependent tissue factor decryption. *Blood Coagul Fibrinolysis*, *26*(1), 36-45. https://doi.org/10.1097/MBC.0000000000000145

Mattoon, D. R., Lamothe, B., Lax, I., & Schlessinger, J. (2004). The docking protein Gab1 is the primary mediator of EGF-stimulated activation of the PI-3K/Akt cell survival pathway. *BMC Biol*, *2*, 24. https://doi.org/10.1186/1741-7007-2-24

Michie, A. J., Zintel, H. A., & et al. (1949). The nephrotoxicity of bacitracin in man. *Surgery*, *26*(4), 626-632. http://www.ncbi.nlm.nih.gov/pubmed/18141336

Piromkraipak, P., Parakaw, T., Phuagkhaopong, S., Srihirun, S., Chongthammakun, S., Chaithirayanon, K., & Vivithanaporn, P. (2018). Cysteinyl leukotriene receptor antagonists induce apoptosis and inhibit proliferation of human glioblastoma cells by downregulating B-cell lymphoma 2 and inducing cell cycle arrest. *Can J Physiol Pharmacol*, *96*(8), 798-806. https://doi.org/10.1139/cjpp-2017-0757

Ramirez-Rangel, I., Bracho-Valdes, I., Vazquez-Macias, A., Carretero-Ortega, J., Reyes-Cruz, G., & Vazquez-Prado, J. (2011). Regulation of mTORC1 complex assembly and signaling by GRp58/ERp57. *Mol Cell Biol*, *31*(8), 1657-1671. https://doi.org/10.1128/MCB.00824-10

Raturi, A., & Mutus, B. (2007). Characterization of redox state and reductase activity of protein disulfide isomerase under different redox environments using a sensitive fluorescent assay. *Free Radic Biol Med*, *43*(1), 62-70. https://doi.org/10.1016/j.freeradbiomed.2007.03.025

Rustin, G. J., Vergote, I., Eisenhauer, E., Pujade-Lauraine, E., Quinn, M., Thigpen, T., du Bois, A., Kristensen, G., Jakobsen, A., Sagae, S., Greven, K., Parmar, M., Friedlander, M., Cervantes, A., Vermorken, J., & Gynecological Cancer, I. (2011). Definitions for response and progression in ovarian cancer clinical trials incorporating RECIST 1.1 and CA 125 agreed by the Gynecological Cancer Intergroup (GCIG). *Int J Gynecol Cancer*, *21*(2), 419-423. https://doi.org/10.1097/IGC.0b013e3182070f17

Samanta, S., Tamura, S., Dubeau, L., Mhawech-Fauceglia, P., Miyagi, Y., Kato, H., Lieberman, R., Buckanovich, R. J., Lin, Y. G., & Neamati, N. (2017). Expression of protein disulfide isomerase family members correlates with tumor progression and patient survival in ovarian cancer. *Oncotarget*, *8*(61), 103543-103556. https://doi.org/10.18632/oncotarget.21569

Santana-Codina, N., Carretero, R., Sanz-Pamplona, R., Cabrera, T., Guney, E., Oliva, B., Clezardin, P., Olarte, O. E., Loza-Alvarez, P., Mendez-Lucas, A., Perales, J. C., & Sierra, A. (2013). A transcriptome-proteome integrated network identifies endoplasmic reticulum thiol oxidoreductase (ERp57) as a hub that mediates bone metastasis. *Mol Cell Proteomics*, *12*(8), 2111-2125. https://doi.org/10.1074/mcp.M112.022772

Schlesinger, S. (2002). Zafirlukast (Accolate): A new treatment for capsular contracture. *Aesthetic Surgery Journal*, *22*(4), 329-336. https://doi.org/10.1067/maj.2002.126753

Seo, J. M., Park, S., & Kim, J. H. (2012). Leukotriene B4 receptor-2 promotes invasiveness and metastasis of ovarian cancer cells through signal transducer and activator of transcription 3 (STAT3)-dependent up-regulation of matrix metalloproteinase 2. *J Biol Chem*, *287*(17), 13840-13849. https://doi.org/10.1074/jbc.M111.317131

Sharda, A. V., Bogue, T., Barr, A., Mendez, L. M., Flaumenhaft, R., & Zwicker, J. I. (2021). Circulating Protein Disulfide Isomerase Is Associated with Increased Risk of Thrombosis in JAK2-Mutated Myeloproliferative Neoplasms. *Clin Cancer Res*, *27*(20), 5708-5717. https://doi.org/10.1158/1078-0432.CCR-21-1140

Shishkin, S. S., Eremina, L. S., Kovalev, L. I., & Kovaleva, M. A. (2013). AGR2, ERp57/GRP58, and some other human protein disulfide isomerases. *Biochemistry (Mosc)*, *78*(13), 1415-1430. https://doi.org/10.1134/S000629791313004X

Sørensen , H. T., Mellemkjær , L., Olsen , J. H., & Baron , J. A. (2000). Prognosis of Cancers Associated with Venous Thromboembolism. *New England Journal of Medicine*, *343*(25), 1846-1850. https://doi.org/10.1056/nejm200012213432504

Stopa, J. D., Neuberg, D., Puligandla, M., Furie, B., Flaumenhaft, R., & Zwicker, J. I. (2017). Protein disulfide isomerase inhibition blocks thrombin generation in humans by interfering with platelet factor V activation. *JCI Insight*, *2*(1), e89373. https://doi.org/10.1172/jci.insight.89373

Stopa, J. D., & Zwicker, J. I. (2018). The intersection of protein disulfide isomerase and cancer associated thrombosis. *Thromb Res*, *164 Suppl 1*, S130-S135. https://doi.org/10.1016/j.thromres.2018.01.005

Tsai, M. J., Wu, P. H., Sheu, C. C., Hsu, Y. L., Chang, W. A., Hung, J. Y., Yang, C. J., Yang, Y. H., Kuo, P. L., & Huang, M. S. (2016). Cysteinyl Leukotriene Receptor Antagonists Decrease Cancer Risk in Asthma Patients. *Sci Rep*, *6*, 23979. https://doi.org/10.1038/srep23979

Tufo, G., Jones, A. W., Wang, Z., Hamelin, J., Tajeddine, N., Esposti, D. D., Martel, C., Boursier, C., Gallerne, C., Migdal, C., Lemaire, C., Szabadkai, G., Lemoine, A., Kroemer, G., & Brenner, C. (2014). The protein disulfide isomerases PDIA4 and PDIA6 mediate resistance to cisplatin-induced cell death in lung adenocarcinoma. *Cell Death Differ*, *21*(5), 685-695. https://doi.org/10.1038/cdd.2013.193

Vatolin, S., Phillips, J. G., Jha, B. K., Govindgari, S., Hu, J., Grabowski, D., Parker, Y., Lindner, D. J., Zhong, F., Distelhorst, C. W., Smith, M. R., Cotta, C., Xu, Y., Chilakala, S., Kuang, R. R., Tall, S., & Reu, F. J. (2016). Novel Protein Disulfide Isomerase Inhibitor with Anticancer Activity in Multiple Myeloma. *Cancer Res*, *76*(11), 3340-3350. https://doi.org/10.1158/0008-5472.Can-15-3099

Wu, Y., Ahmad, S. S., Zhou, J., Wang, L., Cully, M. P., & Essex, D. W. (2012). The disulfide isomerase ERp57 mediates platelet aggregation, hemostasis, and thrombosis. *Blood*, *119*(7), 1737-1746. https://doi.org/10.1182/blood-2011-06-360685

Xu, S., Butkevich, A. N., Yamada, R., Zhou, Y., Debnath, B., Duncan, R., Zandi, E., Petasis, N. A., & Neamati, N. (2012). Discovery of an orally active small-molecule irreversible inhibitor of protein disulfide isomerase for ovarian cancer treatment. *Proc Natl Acad Sci U S A*, *109*(40), 16348-16353. https://doi.org/10.1073/pnas.1205226109

Xu, S., Sankar, S., & Neamati, N. (2014). Protein disulfide isomerase: a promising target for cancer therapy. *Drug Discov Today*, *19*(3), 222-240. https://doi.org/10.1016/j.drudis.2013.10.017

Zocchi, M. R., Catellani, S., Canevali, P., Tavella, S., Garuti, A., Villaggio, B., Zunino, A., Gobbi, M., Fraternali-Orcioni, G., Kunkl, A., Ravetti, J. L., Boero, S., Musso, A., & Poggi, A. (2012). High ERp5/ADAM10 expression in lymph node microenvironment and impaired NKG2D ligands recognition in Hodgkin lymphomas. *Blood*, *119*(6), 1479-1489. https://doi.org/10.1182/blood-2011-07-370841

Zwicker, J. I. (2010). Predictive value of tissue factor bearing microparticles in cancer associated thrombosis. *Thromb Res*, *125 Suppl 2*, S89-91. https://doi.org/10.1016/S0049-3848(10)70022-0

Zwicker, J. I. (2014). Unconventional approaches to the prevention of cancer associated thrombosis. *Thromb Res*, *133 Suppl 2*, S44-48. https://doi.org/10.1016/S0049-3848(14)50008-4

Zwicker, J. I., Schlechter, B. L., Stopa, J. D., Liebman, H. A., Aggarwal, A., Puligandla, M., Caughey, T., Bauer, K. A., Kuemmerle, N., Wong, E., Wun, T., McLaughlin, M., Hidalgo, M., Neuberg, D., Furie, B., Flaumenhaft, R., & Investigators, C. (2019). Targeting protein disulfide isomerase with the flavonoid isoquercetin to improve hypercoagulability in advanced cancer. *JCI Insight*, *4*(4). https://doi.org/10.1172/jci.insight.125851

Chapter 4

Isoquercetin and zafirlukast cooperatively suppress tumour growth and thromboinflammatory signalling in a xenograft model of ovarian cancer

In chapters 2 and 3 I have focused on the broad-spectrum thiol isomerase inhibitor zafirlukast, for inhibition of thrombosis and cancer. Interestingly, a PDI specific inhibitor, isoquercetin, has been shown clinically to prevent for cancer induced thrombosis, but not for cancer growth itself. As zafirlukast demonstrated cancer growth inhibition this led me to hypothesise that isoquercetin also would also exhibit similar inhibitory effects *in vivo*. Stemming from this idea, is the notion that combining both could potentially lead to additive or synergistic effects, along with allowing for a reduced dose of either drug. Additionally, isoquercetin is a flavonoid and has been shown to exhibit anti-inflammatory antioxidant and anti-viral properties, so it may not only exert inhibition of thiol isomerases but employ other effects as well.

In this chapter, isoquercetin was investigated for its effects on the same ovarian cancer cell line as that of zafirlukast used in the previous chapter. Here I have shown that isoquercetin inhibits tumour cell induced platelet aggregation, along with thiol isomerase and tissue factor expression from ovarian cancer cells. *In vivo*, isoquercetin not only reduced cancer growth on its own but also improved a chemotherapy regimen and worked in combination with zafirlukast at lower concentrations to inhibit tumour growth. Markers for angiogenesis and inflammation were also lowered from isoquercetin on its own and even more so when combined with zafirlukast. This study provides insight that the thiol isomerase inhibitors zafirlukast and isoquercetin have the ability to be used as both antithrombotic agents and anticancer agents, which in turn could also be used prophylactically as a cancer induced thrombosis inhibitor.

For this chapter, I helped design the experiments, drafted the manuscript along with collecting and analysing all of the data, with the exception of the RNA sequencing, which

was performed by Brandon Marzullo and analysed by Jason Hoskins. Therefore, I estimate that I have contributed to over 90% of the work in this paper.

Isoquercetin and zafirlukast cooperatively suppress tumour growth and thromboinflammatory signalling in a xenograft model of ovarian cancer

Justine A. Keovilay[1,2], Jason W. Hoskins[3], Thomas C. Lines[4], and Daniel R. Kennedy[1,2,5].

[1] College of Pharmacy and Health Sciences, Western New England University, Springfield, MA, 01119.

[2] Institute for Cardiovascular & Metabolic Research, School of Biological Sciences, University of Reading, UK, RG6 6EX.

[3] Laboratory of Translational Genomics, National Cancer Institute, National Institute of Health, Bethesda MD, 20892

[4] Quercis Pharma AG, Gubelstrasse 7, 6300 Zug, Switzerland

[5] Department of Medicine, UMass Chan Medical School-Baystate, Springfield, MA, 01655.

Funding: This work was supported by a National Cancer Institute grant R21CA231000 to D.R.K., J.A.K. was supported by a PhD studentship from Quercis Pharma AG. The content is solely the responsibility of the authors and does not necessarily represent the official views of the National Institutes of Health.

Corresponding Author: Daniel R. Kennedy, Department of Pharmaceutical & Administrative Sciences, College of Pharmacy and Health Sciences, Western New England University, 1215 Wilbraham Road, Springfield, MA, 01119. Tel: 413-796-2413. E-mail: dkennedy@wne.edu

Conflict of Interest Statement: J.A.K. and D.R.K. receive research support from Quercis Pharma AG. D.R.K. is an inventor of a patent on zafirlukast owned by Western New England University and licensed to Quercis Pharma AG. T.C.L is CEO of Quercis Pharma AG.

Author contributions: J.A.K. and D.R.K. drafted the manuscript. J.A.K performed all experiments. J.W.H processed and analysed the RNA sequencing data and edited the manuscript. J.A.K. T.C.L and D.R.K. designed experiments. D.R.K., and T.C.L. supervised the project, edited the manuscript, and provided supporting information.

Acknowledgement: We thank Jennifer Ser-Dolansky, Alexandre Dufresne and Carolanne Lovewell from the Baystate Animal Research Facility for their advice and guidance with animal care and histology experiments and Brandon J. Marzullo from the University of Buffalo's Genomics and Bioinformatics Core for performing the RNA sequencing runs. This work utilized the computational resources of the NIH HPC Biowulf cluster (https://hpc.nih.gov).

4.1 Graphical Abstract

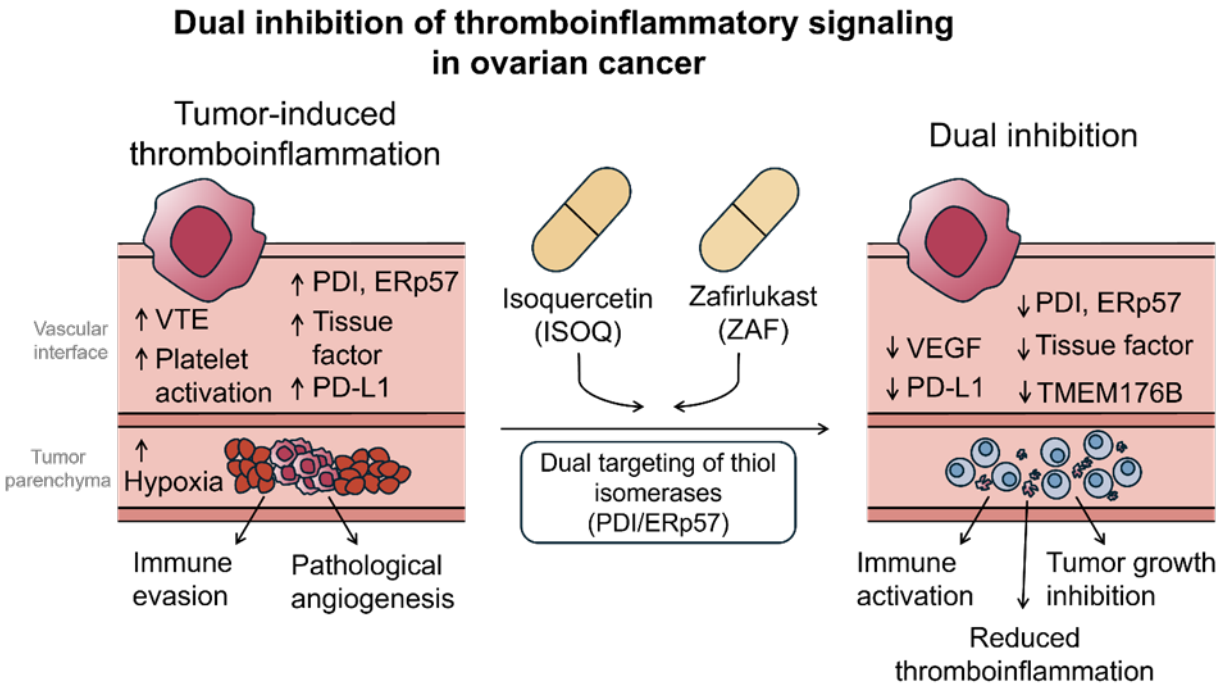

4.2 Abstract

Background: Zafirlukast (ZAF) and isoquercetin are promising antithrombotic and cancer-associated thrombosis agents We hypothesized that a combination of the two agents could be promising for treating both cancer and cancer associated thrombosis while minimizing the side effects associated with cancer therapies such as cisplatin and gemcitabine.

Methods: Mice containing a xenograft of OVCAR8 ovarian cancer cells were drug treated. At the end of the experiment, tumours were collected for immunohistochemistry of VEGF, TMEM176B, tissue factor (TF), ERp57 and PDI, along with immunoblots for PD-L1, and other immunological or angiogenic factors.

Results: ISOQ treatment inhibited both tumour-induced platelet aggregation and tumour-secreted tissue factor, suggesting potential effects on both cancer-induced arterial and cancer-induced venous thrombosis. Tumour growth decreased by over 80% in both treatment groups and levels of P-selectin, PDI, TF, VEGF, TMEM176B and PD-L1 were all significantly reduced. ISOQ displayed synergistic effects with ZAF, improving inhibition of tissue factor, VEGF, TMEM176B and PD-L1 by an average of 30%, with a minimum total inhibition of 80% compared to untreated control.

Conclusions: Both ISOQ and ZAF, individually and especially in combination, demonstrate potential to be incorporated into cancer therapy for cancer-induced thrombosis and in combination with standard chemotherapy for direct cancer treatment.

Abbreviations

PDI	protein disulphide isomerase
ERp	endoplasmic reticulum resident protein
DOACs	direct oral anticoagulants
ZAF	zafirlukast
ISOQ	isoquercetin
VEGF	vascular endothelial growth factor
TMEM176B	transmembrane protein 176B
PD-L1	programmed death ligand 1
DiEGSSG	dieosindiglutathione
FVIIa	Factor VIIa
FX	Factor X
DTT	dithiothreitol
BSA	bovine serum albumin
OVCAR8	human ovarian adenocarcinoma
EDTA	ethylenediaminetetraacetic acid
RFU	relative fluorescent units
TBS	tris buffered saline
PRP	platelet rich plasma
ADP	adenosine diphosphate
TCIPA	tumour cell induced platelet aggregation
HRP	horse radish peroxidase
SDS-PAGE	sodium dodecyl sulphate polyacrylamide gel electrophoresis
PVDF	polyvinylidene difluoride

PCA	principal component analysis
PCs	principal components
DE	differential expression
GSEA	gene set enrichment analysis
HCL	Human Cell Landscape
MMP	matrix metalloproteinase
uPAR	urokinase-type plasminogen activator receptor
TIMP	tissue inhibitor of metalloproteinases
IL	interleukin
s TNF RI	soluble tumour necrosis factor receptor 1
PDGF-BB	platelet derived growth factor – BB
Cis/Gem	cisplatin/gemcitabine
TPM	transcripts per million
ECM	extracellular matrix
EGFR	epidermal growth factor receptor
VTE	venous thromboembolism

4.3 Introduction

Thrombosis is the second leading cause of death for cancer patients, estimated to account for up to 14% of cancer-related mortality. In one recent retrospective study of 100,532 cancer patients, those who experienced a pulmonary embolism had a mortality rate ratio of 5.1 after one year compared to the comparison cohort (Sorensen et al., 2023). Overall annual death rates are almost 3-fold higher for cancer patients with arterial thrombosis, and 50-fold higher for cancer patients with venous thrombosis than in the general population (Khorana et al., 2007). While the relationship between cancer and increased thrombotic activity is complex and multifactorial, increased risk of cancer-induced thrombosis is correlated with increased levels of protein disulphide isomerase (PDI) a key thiol isomerase (Zakhar Lysov et al., 2015). PDI and its related thiol isomerase family members endoplasmic reticulum proteins (ERp) 57, 5 and 72 play important roles in thrombosis formation functioning as an extracellular oxidoreductase (Cho et al., 2008; Cho et al., 2012; Jasuja et al., 2010; Stopa et al., 2017; Swiatkowska et al., 2008). Notably, inhibiting thiol isomerases uniquely blocks both arterial and venous thrombus formation, distinguishing it from many other potential antithrombotic agents (Cho et al., 2008; Holbrook et al., 2021; Jasuja et al., 2012b). Furthermore, unlike current thromboprophylaxis agents, thiol isomerase inhibitors have not demonstrated increased bleeding risk in mice (Holbrook et al., 2021) or human clinical trials (Jeffrey I. Zwicker et al., 2019), as inhibiting the leakage of PDI into the bloodstream from endothelial cells and activated platelets inhibits platelet aggregation and thrombus formation inside the vascular system (Xiong et al., 2020). Yet, PDI inhibition still allows the possibility for blood to clot in the event of an external event such as a cut or traumatic injury causing bleeding outside the vascular system (Holbrook et al., 2021; Kim et al., 2013). These properties allow thiol isomerase inhibitors to mitigate the

bleeding risk that is associated with traditional anti-platelet and anticoagulation agents such as direct oral anticoagulants (DOACs), heparins, aspirin and P2Y12 inhibitors.

Thiol isomerases are also upregulated in many distinct cancer types (Lovat et al., 2008; Samanta et al., 2017; Xu et al., 2019; Shili Xu et al., 2014) and increased levels of thiol isomerases have been positively correlated to increased oncogenic transformation (Hirano et al., 1995), gene transcription (Eufemi et al., 2004), and metastasis (Santana-Codina et al., 2013). Similar to their role in platelets, thiol isomerases can be secreted from tumour cells and perform functions on the cancer cell surface (Zai et al., 1999). Therefore, thiol isomerase inhibitors hold significant promise as dual-acting agents, offering a novel approach to address the challenges of both thrombosis and cancer progression. However, despite this potential, inhibitors of thiol isomerases have been primarily explored for either their antithrombotic (rutin (Jasuja et al., 2012b), galangin (C. Liang et al., 2022) and piericones (Zheng et al., 2023)) or anticancer (PACMA-31 (Xu et al., 2012a), CCF642 (Vatolin et al., 2016) and aziridine-2-carboxlic acid derivatives (Kurpinska et al., 2022)) effects.

The notable exception is zafirlukast (ZAF), an FDA-approved medication which we have demonstrated inhibits platelet aggregation, fibrin formation, P-selectin exposure and intravital thrombus formation (Holbrook et al., 2021). ZAF also inhibits the growth of numerous cancer cell lines, inhibits tumour growth in xenografted mice, provides additive effects in combination with cisplatin/gemcitabine treatment in xenografted mice and inhibits metastasis in mice (Gelzinis et al., 2023a). In a clinical pilot study, ZAF delayed the rate of rise of a key tumour marker (CA-125) in four ovarian cancer patients at risk of tumour marker-only relapse (Gelzinis et al., 2023a). While CA-125 reduction in ovarian cancer patients at risk of tumour marker-only relapse was a promising result, further enhancing ZAF's efficacy was considered to be valuable.

We hypothesized ZAF efficacy could be enhanced by exploring the effect of ZAF in combination with another thiol isomerase inhibitor, the flavonoid isoquercetin (ISOQ) which has previously been identified as a promising agent to prevent cancer-induced thrombosis (Jeffrey I. Zwicker et al., 2019). A Phase 2 study of 64 patients with advanced cancer treated with ISOQ found no primary venous thromboembolisms occurred during the two-month study period (Jeffrey I. Zwicker et al., 2019). In that study, ISOQ also significantly reduced key coagulation markers, including D-dimer levels, platelet-dependent thrombin generation, and circulating soluble P-selectin (Jeffrey I. Zwicker et al., 2019). Less is known about ISOQ 's anti-cancer properties, as they were previously documented only in a single short-term study finding decreased colon cancer growth and vascularization in mice (Da Silva et al., 2022).

The purpose of this study was to explore the potential direct anticancer effects of ISOQ as well as the effect of a ZAF plus ISOQ combination in comparison to either drug alone. We first explored the direct anticancer effects of ISOQ in a xenograft model of ovarian cancer, observing its effects on cancer associated markers such as PDI and P-selectin on thrombosis, as well as vascular endothelial growth factor (VEGF) on angiogenesis and transmembrane protein 176B (TMEM176B) on the inflammasome and programmed death-ligand 1 (PD-L1). We also explored ISOQ's anti-cancer effects in combination with cisplatin/gemcitabine. Finally, we then repeated these experiments to determine the effects of an ISOQ/ZAF combination on these cancer and thrombotic processes in the xenograft model of ovarian cancer.

4.4 Materials and Methods

4.4.1 Reagents

ISOQ was provided by Quercis Pharma (Zug, Switzerland). Recombinant human PDI, angiogenesis array kit, inflammation array kit, and TMEM176B (LR8), PDI and ERp57 antibodies were purchased from Abcam (Waltham, MA, USA). Blue loading buffer and tissue factor, VEGF, PD-L1, β-actin and secondary antibodies were purchased from Cell Signalling Technology (Danvers, MA, USA). ZAF was purchased from TCI America (Portland, OR, USA). Dieosinediglutathione (DiEGSSG), cisplatin and gemcitabine were purchased from Cayman Chemical (Ann Arbor, Michigan, USA). Factor VIIa (FVIIa), Factor X (FX), and the fluorescent Factor Xa cleaving substrate were purchased from Prolytix (Essex Junction, VT, USA). Pierce Bradford plus and detergent compatible protein assay reagents, mPER mammalian protein extraction reagent, Halt protease and phosphatase inhibitor cocktail, RNAlater and P-selectin ELISA kits were purchased from Thermo Fisher Scientific (Waltham, MA, USA). Recombinant insulin (bovine), dithiothreitol (DTT), bovine serum albumin (BSA), buffers, and all other chemicals were purchased from Sigma-Aldrich (St. Louis, MO, USA) and VWR (Radnor, PA, USA). The 96-well and 384-well clear bottom plates were purchased from Corning (Corning, NY, USA).

4.4.2 Cell Culture

Human ovarian adenocarcinoma (OVCAR8) (NCI-DTP Cat#OVCAR-8, RRID: CVCL_1629) were grown in RPMI medium supplemented with 10% fetal bovine serum (FBS), 1% *w*/*v* sodium pyruvate, 10 mM HEPES, 2 mM glutamine, and 100 I.U./mL penicillin/streptomycin.

4.4.3 Thiol Isomerase Activity Assay

OVCAR8 cells were seeded in a black 96 well plate at a concentration of 10,000 cells per 100 µL. The next day, all wells were washed with 100 µL potassium phosphate buffer (100 mM potassium phosphate (pH 7.4) and 2 mM ethylenediaminetetraacetic acid (EDTA)) then supplied with 80 µL of the same buffer and experimental wells treated for 10-minutes with ISOQ (1, 3, 10 or 30 µM). After incubation, a final concentration of 5 µM of DTT and 150 nM of the DiEGSSG fluorescent probe were added to each well immediately prior to reading. For mouse plasma samples, 70 µL of plasma was plated in addition to 10 µL potassium phosphate buffer. A final concentration of 5 µM DTT and 150 nM of the fluorescent probe was added immediately prior to reading at an excitation of 520 nm and an emission of 550 nm for 30 minutes on a BioTek Synergy H1 microplate reader (Agilent, Santa Clara, CA, USA). Generated data were then normalized to the control for each sample, with raw data representing relative fluorescent units (RFU)/minute.

4.4.4 Factor Xa Generation

OVCAR8 cells were seeded at 100,000 cells per well in clear 12-well plates and allowed to grow overnight. Cells were then washed with 1 mL of tris-buffered saline (TBS; 15 mM Tris-HCL, 4.6 mM Tris-base, 150 mM NaCl, pH 7.6 adjusted at room temperature), and incubated with ISOQ (1, 3, 10 or 30 µM) for 30 minutes in 500 µL of TBS. Next, an additional 500 µL of TBS were added along with 1 µL of fluorescent substrate, 5 nmol/l FVIIa, 150 nmol/l of FX, and 5 mmol/l of $CaCl_2$. The plate was then read at an excitation of 352 nm and emission of 470 nm for 45 minutes on a SpectraMax M3 plate reader (Molecular Devices, Sunnyvale, CA, USA).

4.4.5 Platelet Preparation

After receiving approval from the Western New England University IRB, human platelets were collected from consenting, drug-free donors in tubes containing 3.2% sodium citrate using standard venipuncture techniques. Platelet rich plasma (PRP) was obtained by centrifugation of whole blood for 20 min at 100×g. Platelets were then washed via an adenosine diphosphate (ADP) sensitive method, where PRP was centrifuged for 20 minutes at 350×g, the supernatant then carefully aspirated and platelets resuspended to a concentration of 1×10^8 with Tyrodes buffer (20 mM HEPES, 144 mM NaCl, 3 mM KCl, 12 mM $NaHCO_3$, and 1 mM $MgCl_2$, pH 7.3 adjusted at room temperature).

4.4.6 Tumour Cell Induced Platelet Aggregation

Washed platelets were incubated for 5 minutes at 37°C with ISOQ at 10 and 30 μM concentrations, then subjected to light transmission aggregometry. Tumour cell induced platelet aggregation (TCIPA) was induced by allowing platelets to aggregate with 5×10^5 OVCAR8 cells. A negative control, with no agonist, was used to ensure there was no platelet aggregation upon preparation of platelets.

4.4.7 Animal Studies

Immunodeficient NCG mice from Charles River Laboratories or NOG mice from Taconic Biosciences were used to create xenografts from OVCAR8 cells. OVCAR8 cells were injected subcutaneously on the right flank of 4-week-old female NCG or NOG mice, at a concentration of 250,000 cells/100 μL. Tumours were measured twice each week and the size calculated using the formula (LXWXW)/2. Upon tumours reaching an average size of 30 mm^3 NCG mice were treated with 10 mg/kg ISOQ, 30 mg/kg ISOQ, or in combination of 3 mg/kg ISOQ and 10 mg/kg ZAF or 10 mg/kg ISOQ and 10 mg/kg ZAF or a vehicle control

(corn oil) via oral gavage every day for a total of 46 days. NOG mice were treated with a chemotherapy regimen of 5 mg/kg cisplatin and 120 mg/kg gemcitabine, 3 mg/kg ISOQ, 30 mg/kg ISOQ or a combination of ISOQ in the two selected doses together with cisplatin and gemcitabine. Upon the termination of each study, mice were euthanized (CO_2 inhalation followed by cervical dislocation) and blood was retrieved via heart puncture for additional studies. Tumours were excised for histology, placed in 10% formalin and switched to 70% ethanol after 24 hours.

4.4.8 P-selectin ELISA

Blood retrieved from mice in the xenograft study was centrifuged to obtain plasma and then frozen and stored at -20°C. Plasma was then tested for changes in P-selectin *via* ELISA assay according to manufacturer's protocols. Samples were read at 450 nm on a SpectraMax M3 plate reader (Molecular Devices, Sunnyvale, CA, USA).

4.4.9 Immunohistochemistry

Excised tumours were sectioned and stained with tissue-factor, VEGF, TMEM176B, PDI or ERp57 primary antibodies and an Alexa Fluor 488 conjugated secondary antibody. Slides were viewed at 20X magnification on a Nikon Eclipse fluorescence microscope (Nikon, Tokyo, Japan) and images captured in NIS-Elements software (Nikon, Tokyo, Japan). The three brightest areas were captured for each slide, and slides were chosen blindly for analysis. Images were then analysed using Image-J software (NIH, Bethesda, Maryland, USA) where the integrated density was measured for the green channel.

4.4.10 Insulin-based Turbidimetric Assay

An insulin-based turbidimetric assay was utilized to determine the effect of ISOQ and ZAF alone or in combination against PDI. These compounds were diluted to 10 or 30 μM ISOQ or ZAF alone or a combination of 3 μM ISOQ and 10 μM ZAF within a 384-well plate, and a final concentration of 10 μg/mL (175 nM) PDI, 125 μM insulin, 2 mM EDTA, 100 mM potassium phosphate buffer, and 0.3 mM DTT were added for a total volume of 30 μL per well. The turbidity of insulin aggregation was measured kinetically every minute for 90 minutes using a SpectraMax M3 plate reader (Molecular Devices, Sunnyvale, CA, USA).

4.4.11 Angiogenesis and Inflammation Arrays

Tumour lysates were made up in kit provided lysis buffer of pooled tumour samples from mice treated with 10 mg/kg ISOQ, 30 mg/kg ISOQ or vehicle control and the total protein calculated using Pierce Detergent Compatible Bradford Assay Reagent (Thermo Fisher Scientific, Waltham, MA, USA). The pre-determined membranes were blocked at room temperature for 30 minutes with kit provided blocking buffer, where then 1000 μg of protein was incubated with the array membrane overnight at 4°C. Membranes were washed with kit-provided wash buffer followed by incubation with a biotinylated antibody cocktail for 2 hours at room temperature. Membranes were again washed and then incubated with horse radish peroxidase (HRP)-conjugated streptavidin for 2 hours at room temperature and washed for a final time. Membranes were then incubated with kit-provided detection buffer for 2 minutes at room temperature and imaged on a Bio-Rad ChemiDoc (Bio-Rad, Hercules, CA, USA).

4.4.12 Tumour lysate preparation and immunoblotting

Tumours were homogenized and lysed in mPER mammalian protein extraction reagent supplemented with Halt protease and phosphatase inhibitor cocktail. Homogenates were centrifuged for 20 minutes at 16800×g and 4°C, supernatants collected for analysis and total protein concentration was determined via Bradford assay. 1X blue loading buffer with 125 mM DTT was added to each sample and heated for 5 min at 95°C then put on ice. 15 µg of each sample was analysed by sodium dodecyl sulphate polyacrylamide gel electrophoresis (SDS-PAGE) using a Bio-Rad mini gel system (Bio-Rad, Hercules, CA, USA) in SDS-PAGE running buffer (25 mM Tris, 192 mM glycine, 0.1% SDS, pH 8.3) and transferred to a polyvinylidene difluoride membrane in transfer buffer (25 mM Tris, 192 mM glycine and methanol 20%). After transfer, membranes were blocked for 1 hour at room temperature in blocking buffer (TBS + 5% non-fat dry milk, w/v) and then probed with a rabbit monoclonal PD-L1 antibody (1:1000 dilution; TBS + 0.1% Tween-20 [TBS-T] + 3% BSA w/v) followed by an anti-rabbit HRP coupled secondary antibody (1:5000 dilution). Chemiluminescence was detected with Novex ECL substrate (Invitrogen, Waltham, MA, USA) on a Bio-Rad ChemiDoc imaging system (Bio-Rad, Hercules, CA, USA). Membranes were stripped in buffer (200 mM glycine, 3.5 mM SDS, 1% Tween-20, pH 2.2 adjusted at room temperature) and re-probed with a mouse monoclonal beta actin primary antibody (1:5000 dilution) followed by an anti-mouse HRP-coupled secondary antibody (1:10000 dilution) and chemiluminescence detected as described above. Membranes were analysed using Bio-Rad Image Lab software (Bio-Rad, Hercules, CA, USA) and normalized for loading by the beta actin control.

4.4.13 RNA-Sequencing, Differential Expression, and Gene Set Enrichment Analyses.

RNA was extracted from the excised xenograft tumours of mice treated with vehicle (n=4), ISOQ (n=4), or ZAF (n=4) using RNAlater. Sequencing libraries were generated using the Illumina TruSeq Stranded Total RNA Library Prep Kit (Cat. RS-122-2401). Libraries were pooled and sequenced on an Illumina NovaSeq using a 100-cycle NovaSeq SP Reagent Kit (Cat. 20028401). The resulting sequencing reads in fastq file format were processed through the GTEx V10 pipeline (https://github.com/broadinstitute/gtex-pipeline/tree/master/rnaseq) using the GRCh38 human genome reference and GENCODE v39 gene annotations after adapter trimming with CutAdapt. Gene read counts were TPM-normalized and sample similarities were assessed by principal component analysis (PCA). Differential expression (DE) analysis was performed using the edgeR v4.0.16 package (https://bioconductor.org/packages/release/bioc/html/edgeR.html) in R v3.4.1. DE analysis was performed separately on the expressed genes (thresholded at ≥6 reads in ≥20% of samples, and ≥0.1 TPM in ≥20% of samples) for each treatment group comparison (ISOQ vs. controls, and ZAF vs. controls) using a GLM model that included their respective PCs 1-4 as covariables, and significance of DE was determined by quasi-likelihood F-test.
Unfiltered genes ranked by DE magnitude (based on the edgeR GLM models adjusted for PCs 1-4) were assessed for enrichment of pathways/gene sets with up or down-regulation of genes by drug treatment using Gene Set Enrichment Analysis (GSEA) in the WebGestalt webtool (https://www.webgestalt.org/#). Enrichments were tested against the Gene Ontology (GO): Biological Process, GO: Molecular Function, GO: Cellular Compartment, KEGG pathways, Reactome pathways, and Human Cell Landscape (HCL) gene set collections.

4.4.14 Statistics

Statistical analysis was performed using GraphPad Prism (Version 9.4.0, San Diego, CA). Data were presented as the mean ±SD. An unpaired t-test, a one-way ANOVA with a post-hoc Dunnett's test or a two-way ANOVA with a post-hoc Tukey's or Sidak's test was used to evaluate statistical significance. *P < 0.05 **P < 0.01 *** P < 0.001 or **** p < 0.0001 was considered statistically significant.

4.4.15 Study Approval

The animal work in this protocol was approved by the IACUC and IBC of UMass Chan Medical School-Baystate.

4.5 Results

4.5.1 Isoquercetin inhibits cancer-induced platelet aggregation and Factor Xa generation in a dose-dependent manner

One of the unique aspects of thiol isomerase inhibitors is their ability to inhibit both arterial (platelet-derived) and venous (coagulation-derived) thrombosis. For tumour-induced arterial thrombosis, we investigated the ability of ISOQ to inhibit TCIPA. OVCAR8 cells were incubated with platelets in the presence or absence of ISOQ to induce aggregation, where 30 μM ISOQ inhibited aggregation by 55.5% ($p = 0.0123$; Figure 4.1 A).

For venous thrombosis, we explored the generation of tumour cell derived tissue factor by examining activation of the coagulation cascade. Tissue factor activity can be measured through Factor Xa production, and previously we have shown the thiol isomerase inhibitor, ZAF, was able to inhibit Factor Xa generation from these ovarian cancer cells (Gelzinis et al., 2023a). Here, the treatment of OVCAR8 cells with 10 or 30 μM ISOQ significantly decreased Factor Xa generation in OVCAR8 cells by 29.3% ($p = 0.0136$) and 42.8% ($p = 0.0006$), respectively (Figure 4.1 B).

4.5.2 Isoquercetin inhibits cellular thiol isomerase activity.

Previously, we have shown OVCAR8 cells exert thiol isomerase activity (Gelzinis et al., 2023a). Therefore, given the role of PDI in association with platelet aggregation (Essex & Li, 1999a) and tissue factor de-encryption (Manukyan et al., 2008), we investigated the ability of ISOQ to inhibit PDI activity from cancer cells. Treatment of OVCAR8 cells with 1, 3, 10 or 30 μM ISOQ for 10 minutes significantly inhibited cell surface thiol isomerase activity by 18.2% ($p = 0.0327$), 30.4% ($p = 0.0014$), 34.2% ($p = 0.0002$) and 36% ($p = 0.0001$) respectively (Figure 4.1 C). The maximum level of inhibition was less than 50% suggesting that some PDI activity is insensitive to ISOQ.

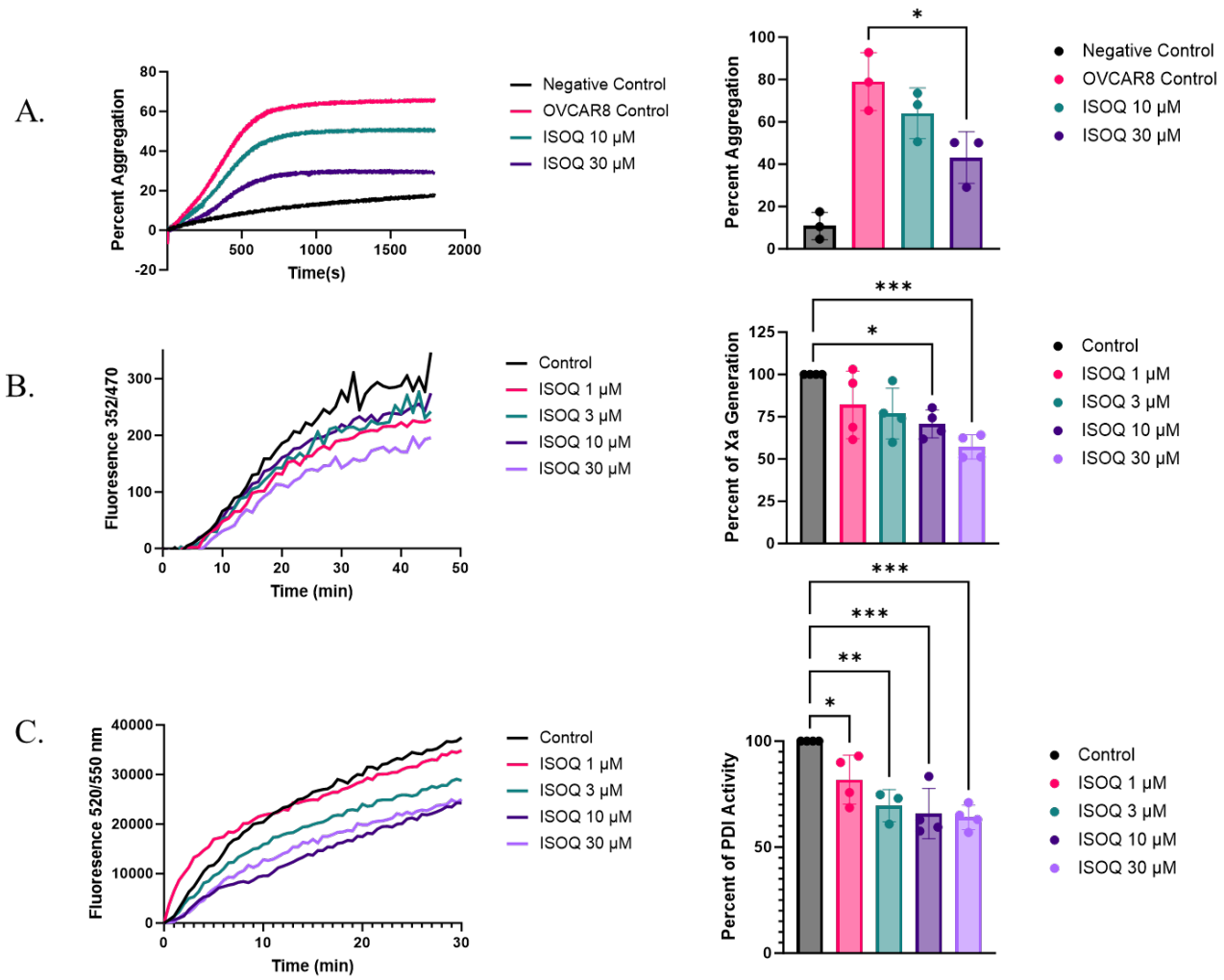

Figure 4.1 ISOQ inhibits multiple factors related to cancer induced thrombosis *in vitro*. (A) ISOQ inhibits ovarian cancer (OVCAR8) tumour cell induced platelet aggregation (n=3), (B) tumour cell (OVCAR8) generated Factor Xa generation (n=4) and (C) tumour cell (OVCAR8) PDI activity (n=4). Data are presented as mean ± SD. Data (A, B and C) were analysed *via* one-way ANOVA with Dunnet's multiple comparisons test where *P < 0.05, **P < 0.01 and ***P < 0.001.

4.5.3 Isoquercetin inhibits tumour growth, lowers P-selectin, and inhibits thiol isomerases in an ovarian cancer xenograft model

To examine the effect of ISOQ treatment on tumour growth, we treated mice xenografted with OVCAR8 cancer cells for 46 days via oral gavage with ISOQ or with a vehicle control. Tumour volumetric measurements were taken twice weekly. After 21 days, tumour growth was reduced by 52.5% ($p = 0.0283$) and 56.2% ($p = 0.0203$) in the 10 mg/kg and 30 mg/kg groups compared to the control, respectively (Figure 4.2 A). By the end of the study, tumours in the ISOQ treated mice were reduced by 81.6% ($p < 0.0001$) for 10 mg/kg ISOQ and 82.5% ($p < 0.0001$) for 30 mg/kg ISOQ compared to the control group (Figure 4.2 A).

To assess the *in-vivo* efficacy of ISOQ on cancer induced thrombosis, we measured the drug's effects on both soluble P-selectin levels expression and thiol isomerase activity in the blood of these mice. P-selectin levels were reduced by 25% ($p = 0.0465$) and 47.1% ($p = 0.0027$) in the 10 mg/kg and 30 mg/kg ISOQ dosage groups, respectively, indicating a dose-dependent effect (Figure 4.2 B). Plasma thiol isomerase activity was also reduced significantly by both concentrations of ISOQ. As shown in Figure 4.2 C, at 10 mg/kg ISOQ thiol isomerase activity was reduced by 23.9% ($p = 0.0001$), and at 30 mg/kg, by 43.1% ($p < 0.0001$).

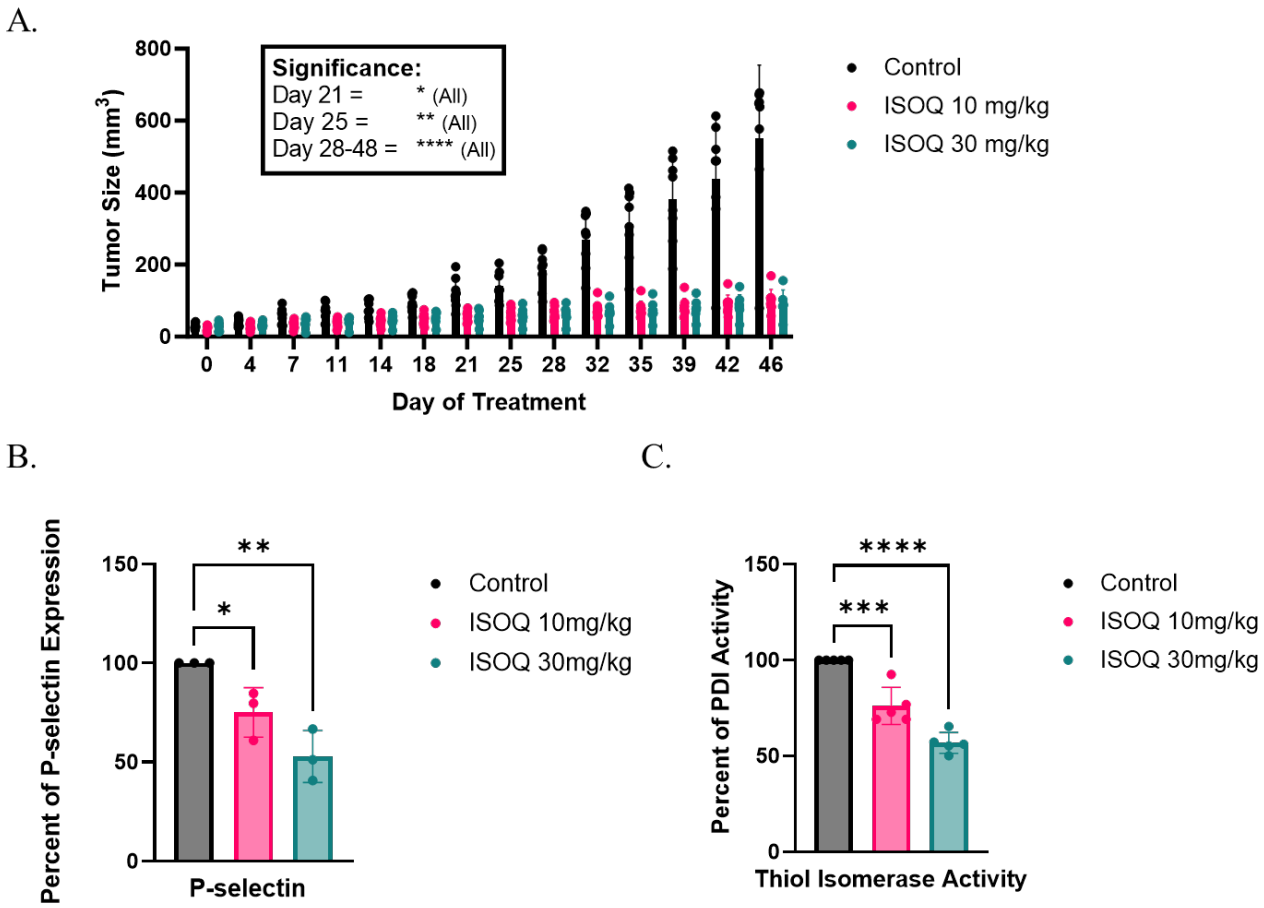

Figure 4.2 ISOQ inhibits tumour growth in a xenograft model of ovarian cancer. (A) ISOQ was administered orally *via* oral gavage daily and the measurements of tumours taken twice weekly. 10 mg/kg (n=8) and 30 mg/kg (n=8) doses demonstrated significant inhibition compared to the control (n=8) by treatment day 21. (B) P-selectin expression from pooled mouse plasma collected upon termination of the experiment (n=3). (C) Thiol isomerase activity from pooled mouse plasma collected upon termination of the experiment (n=4). Data are presented as mean ± SD. Data were analysed *via* two-way ANOVA with Tukey's multiple comparisons test (A), or one-way ANOVA with Dunnet's multiple comparisons test (B and C) where *P < 0.05, **P < 0.01 ***P < 0.001 and ****P < 0.0001.

4.5.4 Isoquercetin alters tissue factor, VEGF and TMEM176B expression in tumours

The data from the Factor Xa generation experiments led us to investigate tissue factor levels in the excised tumours. Immunofluorescence staining with a tissue factor antibody demonstrated a significant decrease in expression in tumours following treatment with ISOQ. Mice treated with 10 mg/kg ($p = 0.0112$) or 30 mg/kg ($p = 0.0324$) ISOQ demonstrated a significant and similar decrease in expression of tissue factor of approximately 55% compared to the control mice (Figure 4.3 A).

As angiogenesis plays a critical role in tumour growth (Liu et al., 2023), and chronic inflammation is associated with many cancer types and promotes tumour progression (Zhao et al., 2021), we further explored the effects of ISOQ treatment in these areas. First, we examined VEGF levels in the tumours via immunohistochemistry. Both 10 mg/kg ($p = 0.0001$) and 30 mg/kg ($p = 0.0007$) ISOQ similarly and significantly reduced the expression of VEGF in the ovarian cancer tumours by approximately 70% (Figure 4.3 B). Finally, we investigated whether ISOQ influenced the inflammation marker and inflammasome activation trigger TMEM176B (Kang et al., 2021). Immunofluorescent staining of excised tumours with an anti-TMEM176B antibody demonstrated a decrease in expression from mice treated with ISOQ, where 10 mg/kg inhibited expression of TMEM176B by 30% ($p = 0.1624$) and 30 mg/kg inhibited expression of TMEM176B by 45% ($p = 0.0461$; Figure 4.3 C).

We confirmed effects on angiogenesis by exploring the levels of angiogenesis related proteins in the tumours using a pre-designed angiogenesis array on which pooled samples of lysates from tumours of each treatment group were plated. Significant reductions in Matrix metalloproteinase-1 (MMP-1) and matrix metalloproteinase-9 (MMP-9) were observed in both treatment groups (Figure 4.4 A). MMP-1 was reduced by 50% ($p = < 0.0001$) after treatment with 10 mg/kg ISOQ and 70% ($p < 0.0001$) after treatment with 30 mg/kg ISOQ,

while MMP-9 was reduced by 42% ($p = 0.0144$) after treatment with 10 mg/kg ISOQ and 58% ($p = 0.001$) after treatment with 30 mg/kg ISOQ. There was also a significant reduction in urokinase-type plasminogen activator receptor (uPAR) after treatment with 30 mg/kg ISOQ, as it decreased by 70% ($p < 0.0001$). Finally, there was significant upregulation of the MMP tissue inhibitor of metalloproteinases -2 (TIMP-2), which increased by 63% after treatment with 10 mg/kg ($p = 0.0002$) and by 99% after treatment with 30 mg/kg ISOQ ($p < 0.0001$). Taken together, these findings are consistent with an overall reduction in tumour growth and angiogenesis (Figure 4.4 A).

We explored additional inflammatory markers through a pre-determined inflammation array and found multiple proteins from pooled tumour lysates were significantly altered, including interleukin-6 (IL-6), interleukin-8 (IL-8), soluble tumour necrosis factor receptor 1 (s TNF RI), and the platelet derived growth factor -BB (PDGF-BB). After treatment with 10 mg/kg ISOQ significant reductions were observed in IL-8 levels (35%; $p = 0.0005$), s TNF RI levels (40%; $p = 0.0014$), and PDGF-BB levels (39%; $p < 0.0001$). After treatment with 30 mg/kg ISOQ, a significant reduction was observed in IL-8 levels (36%; $p = 0.0006$), s TNF RI levels (48%; $p = 0.0003$), PDGF-BB levels (61%; $p < 0.0001$) and IL-6 levels (26%; $p = 0.0207$; Figure 4.4 B).

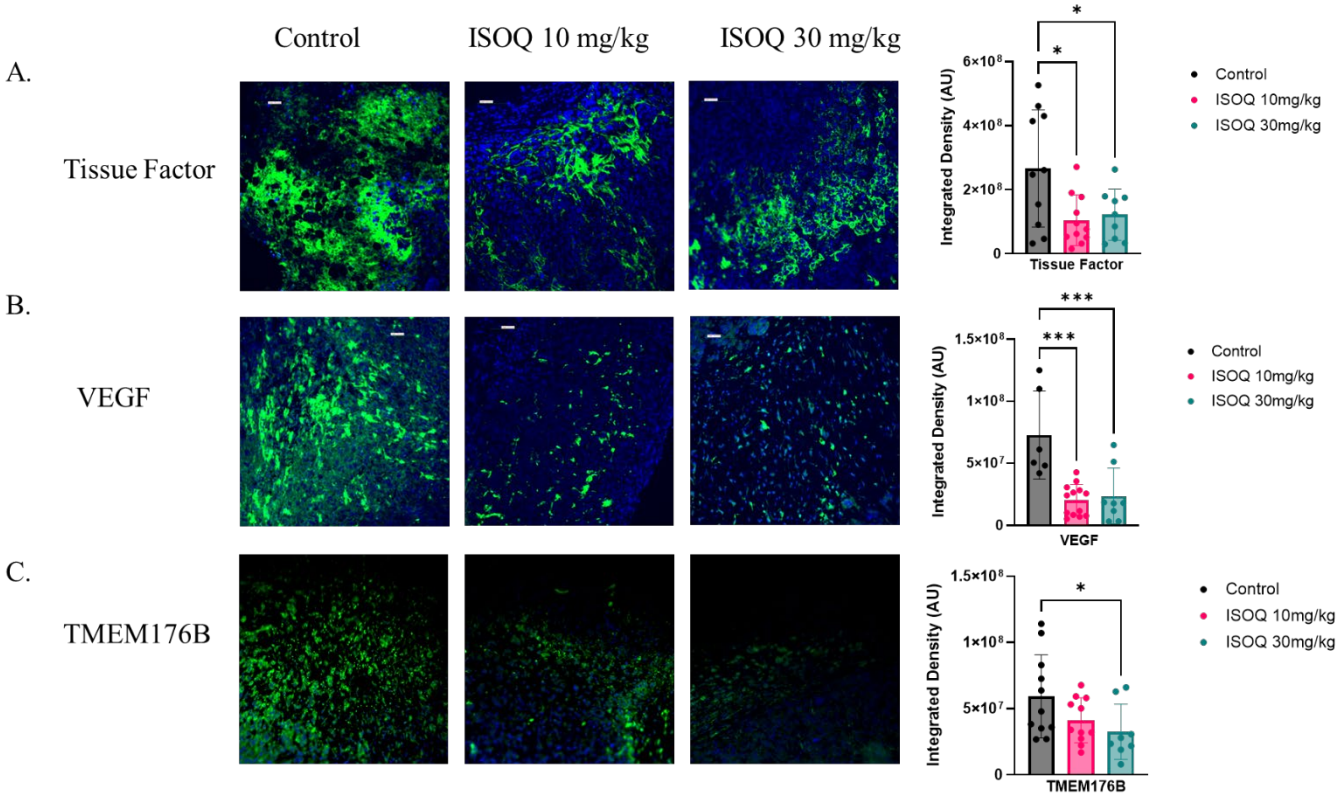

Figure 4.3 ISOQ reduces the expression of factors related to thrombosis, angiogenesis and inflammation. Immunohistochemistry was performed on the excised mouse tumours to examine (A) tissue factor, (B) VEGF, and (C) TMEM176B levels of expression. Images are representative of 4-5 mice per group, with 3 images taken per mouse of the areas of highest expression. Scale bars are 100 μm. Data are presented as mean ± SD. Data (A, B and C) were analysed *via* one-way ANOVA with Dunnet's multiple comparisons test where *P < 0.05 and ***P < 0.001.

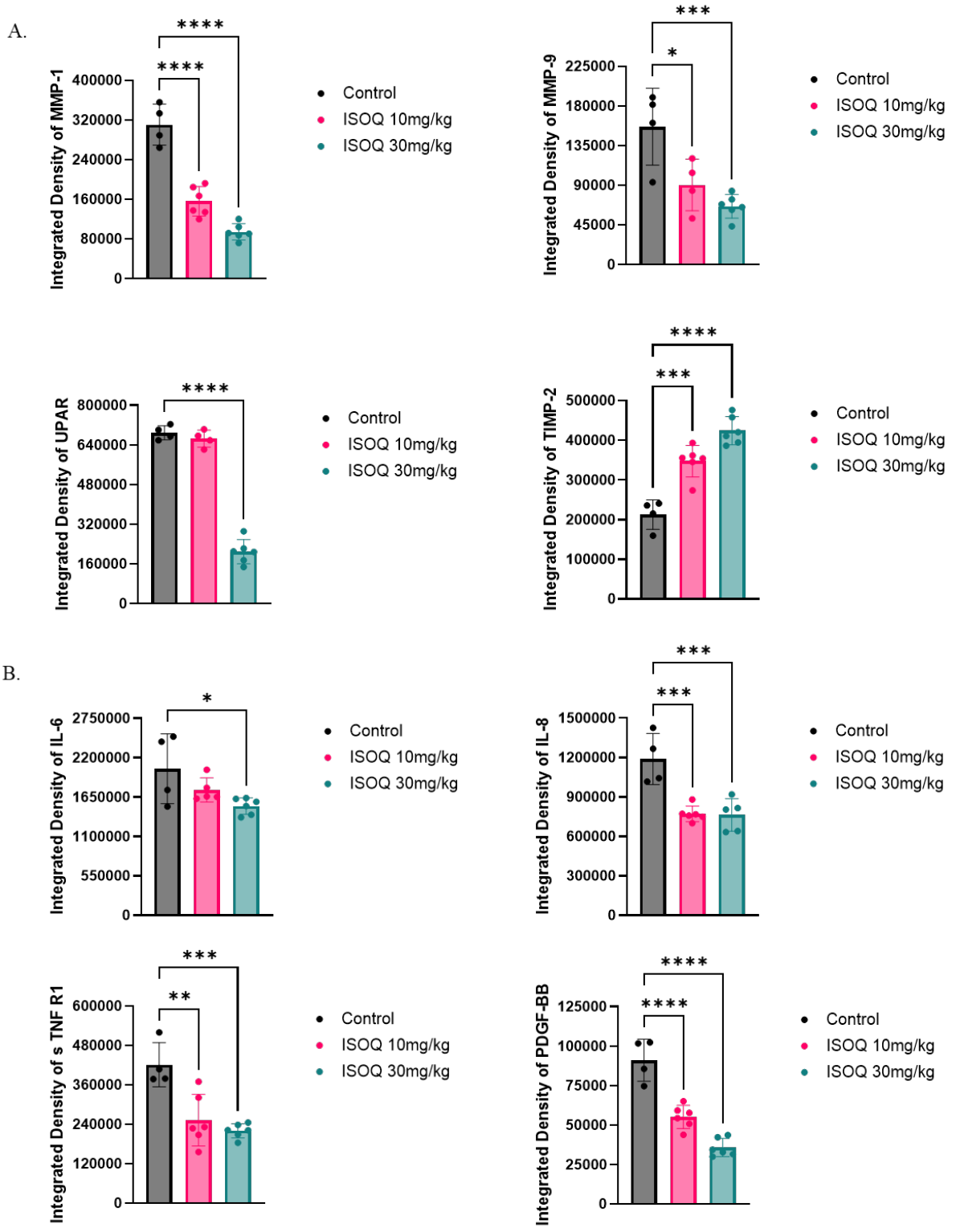

Figure 4.4 ISOQ alters proteins related to angiogenesis and inflammation. (A) Angiogenesis and (B) inflammation arrays were performed on pooled mouse tumour lysates to examine 43 different proteins involved in these processes. Of the 43, 8 proteins demonstrated significant changes in

expression including matrix metalloproteinase (MMP) 1 and 9, urokinase-type plasminogen activator receptor (uPAR), tissue inhibitor of metalloproteinases 2 (TIMP-2), Interleukin (IL) 6 and 8, soluble tumour necrosis factor receptor 1 (s TNF R1) and platelet derived growth factor BB (PDGF-BB). Data are presented as mean ± SD. Data were analysed *via* one-way ANOVA with Dunnet's multiple comparisons test where *P < 0.05, **P < 0.01, ***P < 0.001 and ****P < 0.0001.

4.5.5 Isoquercetin inhibits levels of Programmed Cell Death Ligand 1 (PD-L1)

Considering that the knockdown of ERO1-α, an oxidase that works in collaboration with PDI, results in a decrease in PD-L1 expression, a protein expressed by tumour cells that helps them evade immune system detection (Tanaka et al., 2017), we explored potential effects of ISOQ treatment on PD-L1 expression levels. Reduced PD-L1 levels are associated with better prognosis and enhanced tumour responsiveness to immunotherapies (Chen et al., 2016). Treatment with 10 mg/kg ISOQ reduced PD-L1 in homogenates of excised tumours by 19% ($p = 0.0937$), while 30 mg/kg ISOQ significantly reduced PD-L1 levels in these homogenates by 49% ($p < 0.0001$) (Figure 4.5).

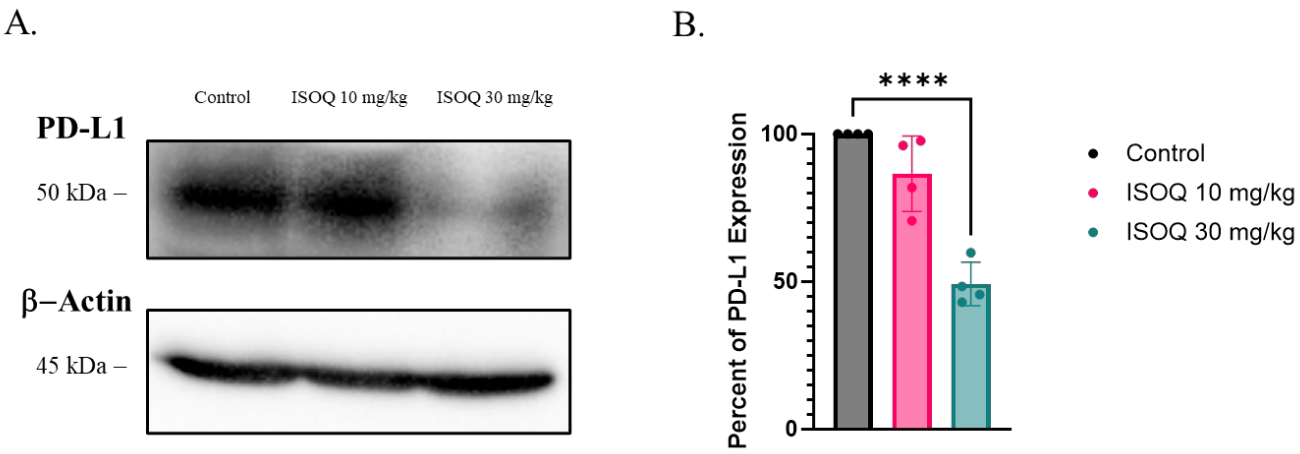

Figure 4.5 ISOQ lowers PD-L1 expression. A representative immunoblot and subsequent quantitation of PD-L1 levels (n=4) from pooled tumours of mice after treatment with 10 or 30 mg/kg of ISOQ compared to the control. Beta actin was used as a loading control. Data are presented as mean ± SD. Data were analysed *via* one-way ANOVA with Dunnet's multiple comparisons test where ****$p < 0.001$.

4.5.6 Isoquercetin enhances the effects of Cisplatin and Gemcitabine in an ovarian cancer xenograft model

Based on ISOQ's significant anti-tumour activity, we investigated its potential to enhance standard chemotherapy in OVCAR8 xenograft tumours. We tested five treatment groups: (1) 5 mg/kg cisplatin plus 120 mg/kg gemcitabine alone, (2) ISOQ at 3 mg/kg, (3) ISOQ at 30 mg/kg, (4) 5 mg/kg cisplatin/120 mg/kg gemcitabine plus ISOQ at 3 mg/kg, and (5) 5 mg/kg cisplatin/120 mg/kg gemcitabine plus ISOQ at 30 mg/kg. Chemotherapy drugs were administered weekly via IP injection, while ISOQ was given daily by oral gavage. These experiments utilized NCG mice to demonstrate the effectiveness of ISOQ in two distinct mouse strains, since NOG mice were used in Figure 4.2.

All treatment groups showed significant tumour growth inhibition by day 10 (Figure 4.6 A). By study completion, the results showed the cisplatin/gemcitabine combination inhibited tumour growth by 71.3% ($p < 0.0001$). ISOQ alone inhibited tumour growth by 49.5% ($p < 0.0001$) at 3 mg/kg and 58.2% ($p < 0.0001$) at 30 mg/kg. Finally, when ISOQ was used in combination with cisplatin/gemcitabine, tumour growth was inhibited by 77.3% (3 mg/kg ISOQ; $p < 0.0001$) and 84% (30 mg/kg ISOQ; $p < 0.0001$) at the end of the study (Figure 4.6 B). Notably, high-dose ISOQ (30 mg/kg) combined with chemotherapy produced significantly better anti-tumour effects than chemotherapy alone, with combination-treated tumours being 44.3% ($p = 0.0376$) smaller than those treated with chemotherapy alone at the end of study (Figure 4.6 C).

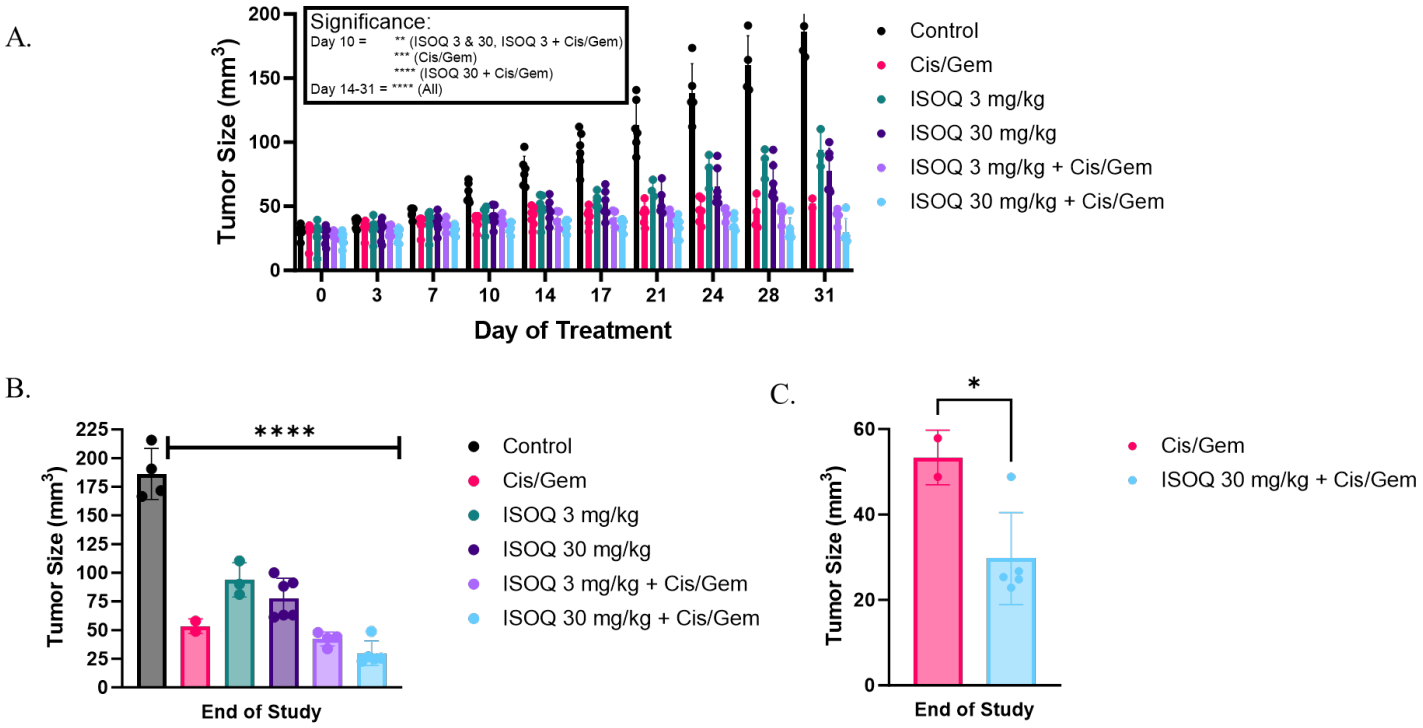

Figure 4.6 ISOQ works in combination with a chemotherapy regimen to inhibit tumour growth. (A) High and low doses of ISOQ alone and in combination with a chemotherapy regimen were examined *in vivo* for their effectiveness on tumour growth (n=8 per group). (B) At the end of the study all treated groups significantly inhibited tumour growth compared to the control. (C) A combination of 30 mg/kg of ISOQ and chemotherapy (cisplatin and gemcitabine) inhibit tumour growth significantly better than chemotherapy alone. Data are presented as mean ± SD. Data were analysed *via* two-way ANOVA with Tukey's multiple comparisons test (A), one-way ANOVA with Dunnet's multiple comparisons test (B) or an unpaired t-test (C) where *P < 0.05, **P < 0.01 ***P < 0.001 and ****P < 0.0001.

4.5.7 Isoquercetin in combination with zafirlukast enhances the efficacy of thiol isomerase, ovarian cancer, VEGF, TMEM176B, tissue factor and PD-L1 inhibition

Considering the promising effects of ISOQ treatment in this ovarian cancer xenograft model, we explored the potential effects of an ISOQ/ZAF combination, as we hypothesized that combining the drugs could enhance efficacy while avoiding the side effects of more cytotoxic agents such as cisplatin/gemcitabine.

Initial cell-free insulin assays of the combination demonstrated promising thiol isomerase/PDI inhibition. The combination of ISOQ at 3 μM and ZAF at 10 μM (ISOQ3/ZAF10) inhibited PDI activity by 58.5% ($p < 0.0001$), comparable to 30 μM ISOQ alone (54.5%; $p < 0.0001$) and superior to 30 μM ZAF alone (29.8%; $p = 0.0073$). All three treatment conditions inhibited thiol isomerase activity significantly compared to the control. (Supplemental Figure 4.1).

Based on these results, we tested two combination treatments in the OVCAR8 xenograft model using lower levels of each drug: ISOQ 3mg/kg, ZAF 10 mg/kg, (ISOQ3/ZAF10) or ISOQ 10mg/kg, ZAF 10 mg/kg, (ISOQ10/ZAF10). The size of the tumours was measured bi-weekly as shown in Figure 4.7 A, with the ISOQ3/ZAF10 combination inhibiting growth by 73% ($p < 0.0001$) and the ISOQ10/ZAF10 inhibiting tumour growth by 75% ($p < 0.0001$) compared to the control group. Excised tumours were isolated and then stained for tissue-factor, VEGF or TMEM176B via immunohistochemistry. Both combinations showed remarkable efficacy, as tissue factor was reduced by 90% in both ISOQ3/ZAF10 ($p = 0.003$) and ISOQ10/ZAF10 ($p = 0.0048$) treatment groups (Figure 4.7 B). VEGF was reduced by 90% ($p = 0.0008$) in the ISOQ3/ZAF10 and 95% ($p = 0.0008$) in the ISOQ10/ZAF10 treated group compared to the control (Figure 4.7 C). Similarly, TMEM176B was reduced by 66% ($p = 0.025$) in the ISOQ3/ZAF10 and 80.5% ($p = 0.0117$) in the ISOQ10/ZAF10 treated (Figure 4.7 D).

Notably, both combination groups showed superior protein inhibition compared to high-dose (30 mg/kg) monotherapy of either agent, shown in Table 4.1, which summarizes the ISOQ alone data from Figure 4.3, ZAF alone data from Supplemental Figure 4.2 and combination data from Figures 4.7 and 4.8. Although not significant, the combination demonstrated a trend in inhibition of VEGF, TMEM176B and tissue factor compared to the monotherapy of ISOQ. Compared to ISOQ alone, VEGF levels were decreased an additional 22% with the ISOQ3/ZAF10 combination and additional 27% with the ISOQ10/ZAF10 combination (Figure 4.8 A). The TMEM176B levels decreased an additional 21% with the ISOQ3/ZAF10 combination and additional 36% with the ISOQ10/ZAF10 combination (Figure 4.8 B). Tissue Factor levels decreased an additional 36% in both combination groups (Figure 4.8 C). PD-L1 levels decreased significantly for the ISOQ10/ZAF10 combination compared to the control ($p < 0.0001$) and by an additional 33% compared to ISOQ alone ($p = 0.0016$; Figure 4.8 D).

Compared to ZAF alone, VEGF levels decreased by an additional 25% with the ISOQ3/ZAF10 combination and an additional 30% with the ISOQ10/ZAF10 combination (Figure 4.8 A). The TMEM176B levels were decreased by an additional 12% with the ISOQ3/ZAF10 combination and an additional 27% with the ISOQ10/ZAF10 combination (Figure 4.8 B). Tissue Factor levels decreased by an additional 16% in both combination groups (Figure 4.8 C). Finally, PD-L1 levels decreased significantly by an additional 38% in the ISOQ10/ZAF10 combination (Figure 4.8 D; $p = 0.0011$). Overall, each of these 4 markers was decreased by a minimum of 80% in the ISOQ/ZAF drug combination, while 3x higher monotherapy of either agent averaged 57%, 30% worse than the average of the combination therapy, despite the difference in drug levels.

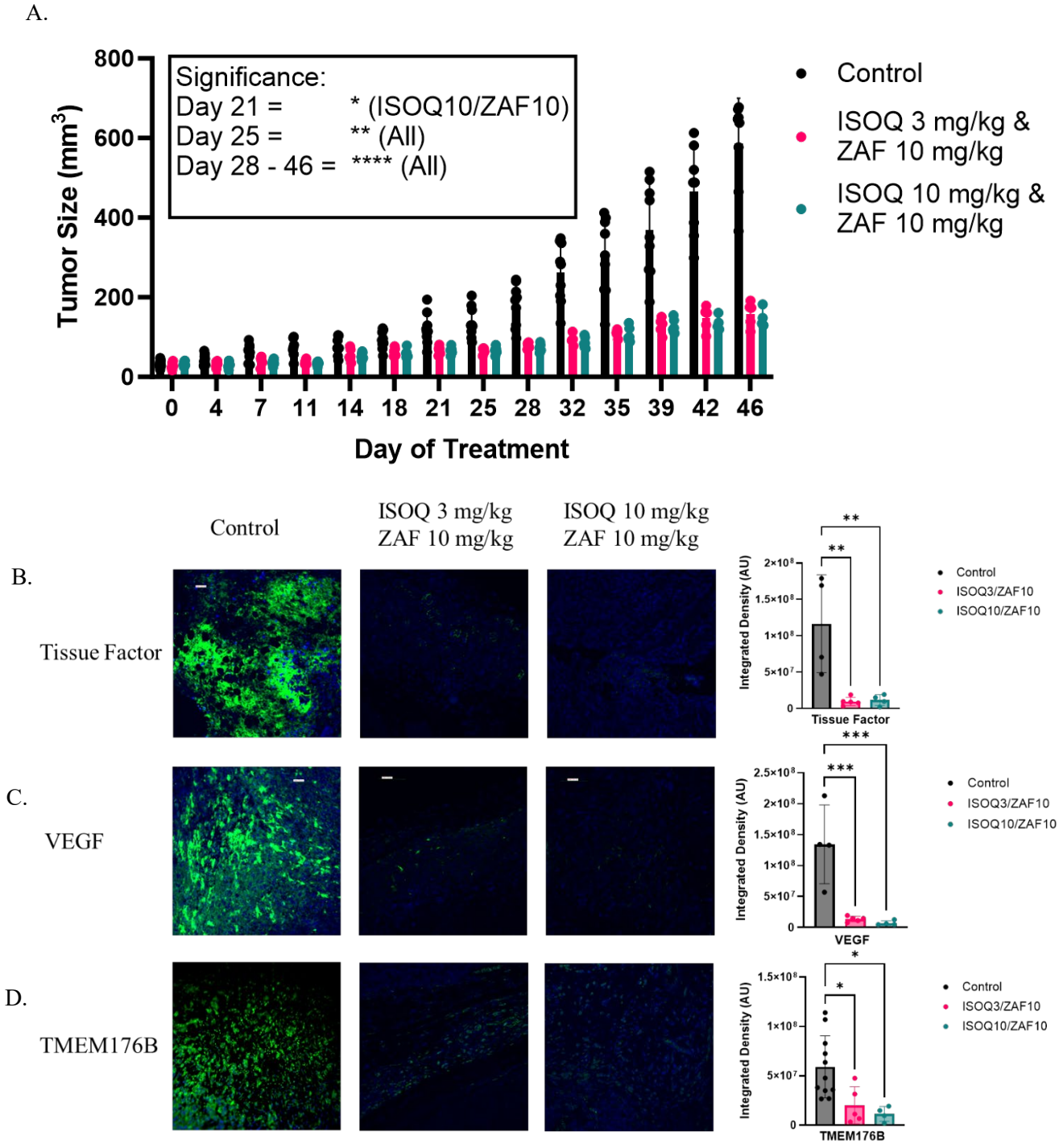

Figure 4.7 ISOQ and ZAF work together to inhibit tumour growth and related processes. (A) A combination of 3 mg/kg and 10 mg/kg ZAF (n=8) or 10 mg/kg ISOQ and 10 mg/kg ZAF (n=8) were examined on their effectiveness to inhibit tumour growth in an ovarian cancer xenograft model. Both combinations significantly inhibited tumour growth compared to the control group (n=8). Excised tumours were examined for (B) tissue factor, (C) VEGF, and (D) TMEM176B levels of expression.

Images are representative of 3-5 mice per group, with 3 images taken per mouse of the areas of highest expression. Scale bars are 100 μm. Data are presented as mean ± SD. Data (B, C and D) were analysed *via* one-way ANOVA with Dunnet's multiple comparisons test where *P < 0.05, **P < 0.01 and ***P < 0.001.

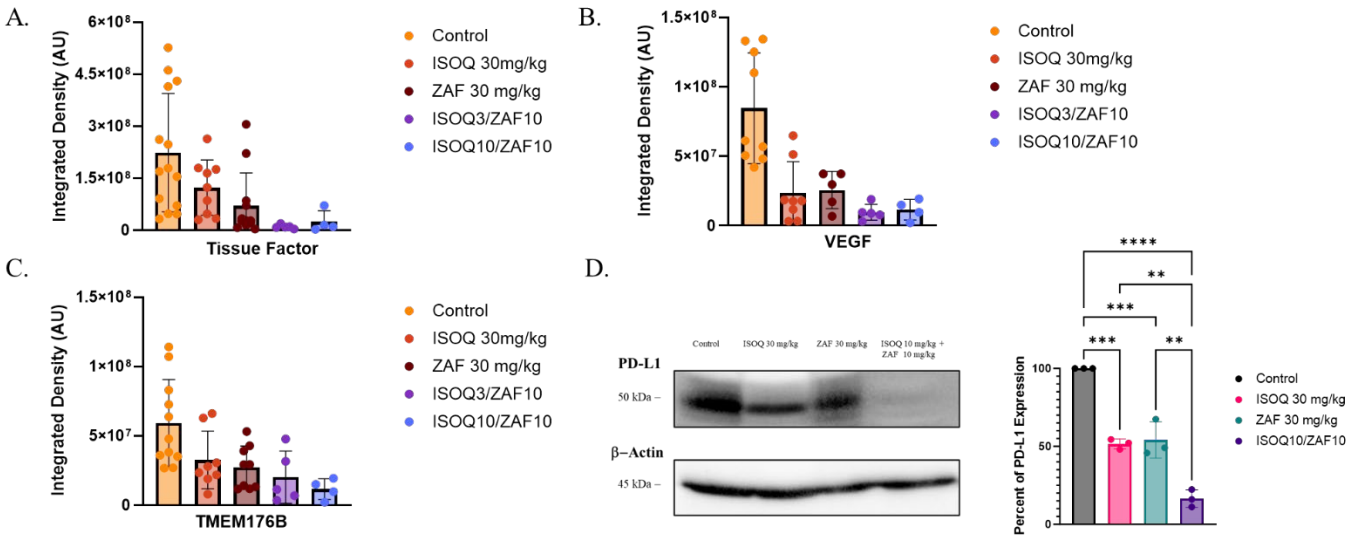

Figure 4.8 ISOQ and ZAF combination is more efficacious than either drug alone. (A) Comparison of the combination therapy results in Figure 7 compared to ISOQ alone and ZAF alone from Figure 4.3 and Supplemental Figure 4.2 respectively for (A) tissue factor, (B) VEGF, and (C) TMEM176B levels of expression. (D) A representative immunoblot and subsequent quantitation of PD-L1 levels (n=4) from pooled tumours of mice after treatment with 30 mg/kg of ISOQ, ZAF or 10 mg/kg of both ISOQ and ZAF compared to the control. Beta-actin was used as a loading control. Data are presented as mean ± SD. Data were analysed *via* one-way ANOVA with Dunnet's multiple comparisons test where ***P < 0.001.

	ISOQ 30 mg/kg	**ZAF 30 mg/kg**	**ISOQ 3 mg/kg + ZAF 10 mg/kg**	**ISOQ 10 mg/kg + ZAF 10 mg/kg**
VEGF	68	65	90	95
TMEM176B	45	54	66	81
Tissue Factor	54	74	90	90
PD-L1	51	46	-	84

Table 4.1 Percentage of inhibition for VEGF, TMEM176B, tissue factor and PD-L1 for the combination therapies of ISOQ/ZAF compared to either drug alone. ISOQ data is from Figure 4.3. ZAF alone from Supplemental 2 and the combinations are from Figure 4.7. PD-L1 data is from Figure 4.5 and 4.8 D.

4.5.8 Common and distinct effects of isoquercetin and zafirlukast treatments observed on tumour transcriptome

To further investigate the mechanisms of inhibitory effects between ISOQ and ZAF on the xenografted mice, we performed total RNA-seq on the excised OVCAR8 xenograft tumours from control mice, 30 mg/kg ISOQ treated, and 30 mg/kg ZAF treated mice (n=4 for each treatment group). After QC, one control sample was omitted from further analyses due to low RNA integrity (RIN=2.3). Principal component analyses (PCA) of transcripts per million (TPM)-normalized expression values for all expressed genes demonstrated poor clustering of samples by treatment group, which indicated unknown factors drove the majority of expression variance across samples (Supplemental Figure 4.3 A). When the PCA was split into the ISOQ vs. control and ZAF vs. control comparisons, clustering by treatment group was observed in the PC5 vs. PC6 dimensions (Supplemental Figure 4.3 B and C). Therefore, to focus the differential expression (DE) analysis on gene expression differences relevant to treatment type, we used the first four principal components (PCs) from the ISOQ vs. control and ZAF vs. control PCAs as covariables in their respective generalized linear models for DE analysis with edgeR to adjust for the unknown confounding factors.

While the unknown sources of noise in this experiment precluded high confidence in the treatment-induced differential expression of more than a handful of specific genes (only 16 and 3 genes with DE at FDR<0.1 in ISOQ vs. control and ZAF vs. control, respectively), we nonetheless identified significant up or down-regulation of biologically meaningful gene sets/pathways using gene set enrichment analysis (GSEA) based on DE magnitude (Supplemental Figure 4.4). One strong contrast observed between the two drugs was the more common upregulation of significantly enriched gene sets by ISOQ treatment, while ZAF treatment resulted almost exclusively in downregulation of significant gene sets. Common themes noted among the upregulated gene sets due to ISOQ treatment included cytoskeletal

remodelling, cell cycle, rRNA processing, and other nucleic acid metabolic pathways (Supplemental Figure 4.4 A, C, E, G, I and K). Interesting themes among the downregulated gene sets due to ZAF treatment included immune-related pathways, cell adhesion, extracellular matrix (ECM), axonogenesis, neuron migration, and astrocytes (Supplemental Figure 4.4 B, D, F, H, J and L). It is notable that genes and gene sets involved in such neural processes and cell types have been previously associated with cancer-related processes such as metastasis, tumour microenvironment regulation, and tumour angiogenesis.(Shalabi et al., 2024; Tan et al., 2023) Downregulation of ECM and neural-related gene sets was also observed with ISOQ treatment, though the trend was far less striking, and the enrichments tended to be less significant (Supplemental Figure 4.4 C and G). Regardless, the transcriptomic effects on ECM-related gene sets by both drug treatments were largely consistent with the angiogenesis protein array results and included several downregulated genes encoding coagulation related factors, as might be expected for anti-thrombotic drugs.

4.5.9 Isoquercetin and Zafirlukast have distinct effects toward thiol isomerase inhibition

Despite observing some expected effect on ECM and coagulation-related factors, it was somewhat surprising to find such distinct effects between ISOQ and ZAF in the tumour transcriptome experiments. ISOQ is known to be a selective PDI inhibitor, while ZAF has been shown to inhibit thiol isomerases more broadly, but these findings are based on enzymatic assay with recombinant proteins (Bekendam et al., 2016; Holbrook et al., 2021; Jasuja et al., 2012b). To examine the *in vivo* effects of ISOQ and ZAF on thiol isomerase expression, we explored the levels of PDI (PDIA1) and another thiol isomerase, ERp57 (PDIA3), by immunohistochemistry from the tumours collected in Figure 4.2 (ISOQ) and Supplemental Figure 4.2 (ZAF). As expected, ISOQ treatment had significant inhibitory effects on PDI levels, as they were reduced by 61% with 30 mg/kg ISOQ ($p = 0.0002$) (Figure 4.9 A), with a minimal (9%) reduction in ERp57 levels ($p = 0.8041$) (Figure 4.9 B). Interestingly, while 30 mg/kg ZAF inhibited PDI levels by 41% ($p = 0.0097$) (Figure 4.9 C) it had a much stronger effect inhibiting ERp57, 86% ($p = 0.0034$), Figure 4.9 D) suggesting the effectiveness of the ISOQ/ZAF combination may be due to strong inhibition of both PDI and ERp57.

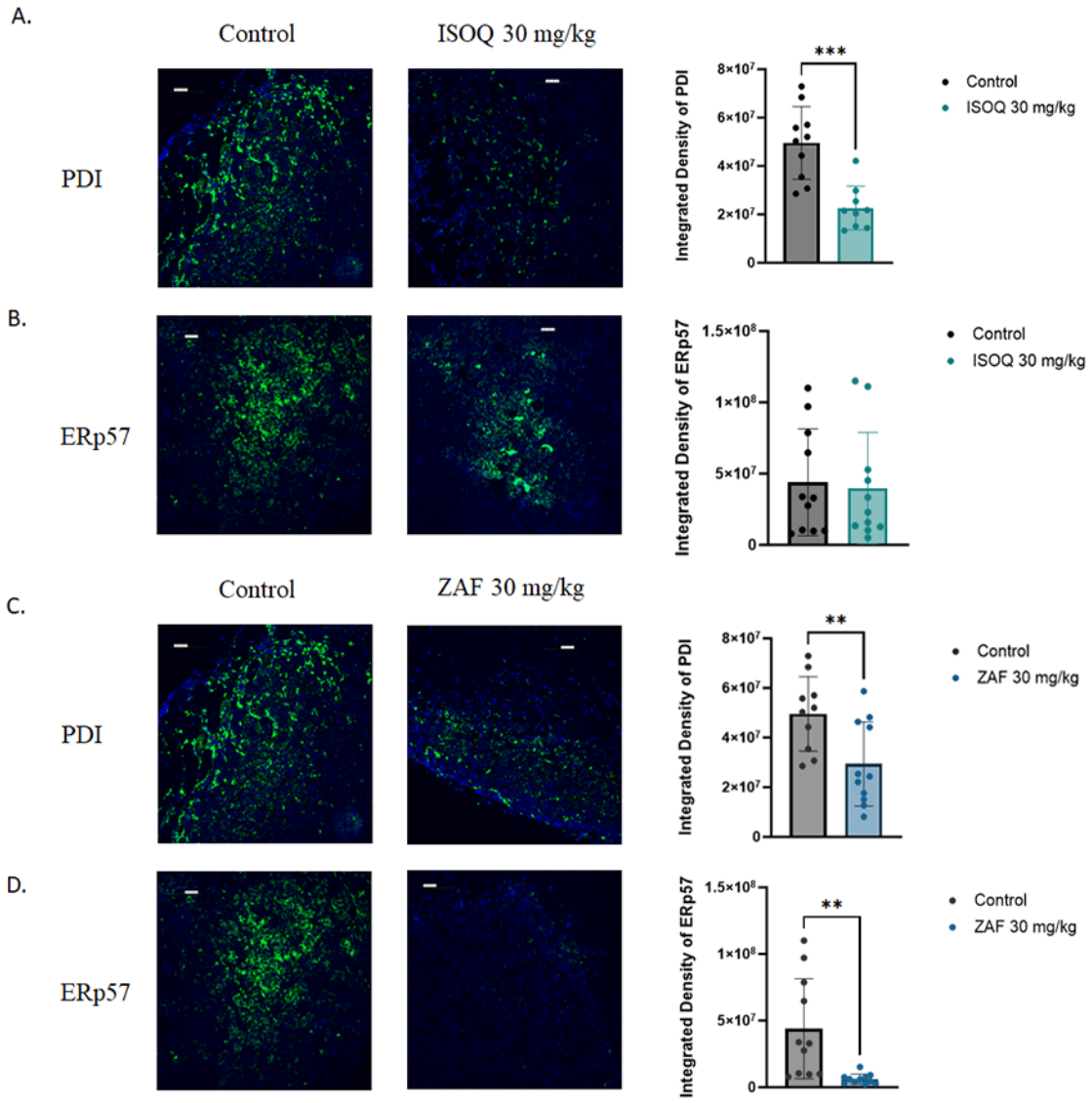

Figure 4.9 ISOQ has stronger inhibition of PDI, while ZAF more strongly targets ERp57.

ISOQ's effect on (A) PDI and (B) ERp57 compared to the mock treated control xenografts and ZAF's effect on (C) PDI and (D) ERp57 compared to the same xenograft controls. Images are representative of 3-5 mice per group, with 3 images taken per mouse of the areas of highest expression. Scale bars are 100 µm. Data are presented as mean ± SD. Data were analysed *via* an unpaired t-test where **P < 0.01 and ***P < 0.001.

4.6 Discussion

While the effect of ISOQ on thrombotic processes in procoagulant cancers such as ovarian cancer is well established (Jeffrey I. Zwicker et al., 2019), ISOQ 's direct anti-cancer properties in ovarian cancer were unknown. Our current study demonstrated sustained tumour growth inhibition of ovarian cancer cells in two different strains of mice (Figure 4.2 & 4.6). In this study, ISOQ was determined to lower both cellular and plasma PDI activity as well as inhibit tumour growth in a manner consistent with direct, chemotherapeutic effects which were significantly enhanced when given in combination with a standard ovarian cancer treatment of cisplatin/gemcitabine (Figure 4.6).

ISOQ was determined through functional studies to be modulating both angiogenic and inflammatory signalling pathways, including tissue factor, VEGF, TMEM176B, and PD-L1 (Figures 4.3, 4.4 & 4.5). Immunohistochemical analysis revealed that ISOQ treatment reduced VEGF expression by more than 50% (Figure 4.3). The anti-angiogenic effects were further substantiated by the decreased expression MMP1, MMP9 and uPAR, with concurrent upregulation of the angiogenesis inhibitor TIMP-2 in Figure 4.4 and the RNA sequencing data was consistent with gene sets previously identified to be involved in angiogenic processes. Another significant finding was ISOQ 's ability to reduce chronic inflammation, as evidenced by decreased TMEM176B expression. Chronic inflammation is a known driver of tumour progression across multiple cancer types (Zhao et al., 2021). TMEM176B is an immunoregulatory cation channel that has been shown to modulate anti-tumour immunity. Specifically, its inhibition enhances CD8+ T-cell-mediated tumour control and potentiates the therapeutic efficacy of anti-PD-L1 and anti-CTLA-4 antibodies (Segovia et al., 2019). Mechanistically, pharmacologic targeting of TMEM176B is hypothesized to activate the inflammasome, potentially contributing to the observed synergy with immune checkpoint blocker (Segovia et al., 2019), consistent with our PD-L1 data in Figures 4.5 and 4.8 D.

TMEM176B inhibition has been demonstrated to suppress cell proliferation via modulation of the AKT/mTOR pathway, as well as decreased tumour growth in both syngeneic and xenografted tumour studies (Kang et al., 2021).

Our previous data had determined that ZAF inhibited ovarian cell growth both in cell culture and in a xenograft mouse model, also displaying additive effects when given in combination with cisplatin/gemcitabine (Gelzinis et al., 2023a). We would have expected the combination of ISOQ and ZAF to have some additive effects compared to either drug alone, but were surprised to find that using a combination of the two drugs at levels 3-10-fold lower had such enhanced effects on the suppression of multiple markers, including VEGF, TMEM176B, tissue factor and PD-L1, compared to either agent alone, suggesting that each compound may work through their own differential modes of action other than thiol isomerase inhibition. In fact, the combination of ISOQ and ZAF was almost as effective at lowering tumour size in the xenograft as the combination of cisplatin/gemcitabine was with ISOQ (85% from Figure 4.6) or ZAF (83%) (Gelzinis et al., 2023a). As ISOQ and ZAF are both known to have very few side effects, especially compared to chemotherapeutic agents like cisplatin and gemcitabine, these findings indicate a strong potential for the use of an ISOQ/ZAF combination as part of a cancer treatment regimen to potentially increase therapeutic efficacy.

To determine why ISOQ and ZAF had such strong effects in combination, we explored mechanistic differences between the two drugs. Previously we have shown that ZAF did not alter thiol isomerase protein levels in OVCAR8 cells after 1 hour (Gelzinis et al., 2023b), however in this study we observed a reduction in both PDI and ERp57 expression levels in tumours removed from the mice. This reduction in expression is likely due to a longer duration of treatment. A potential mechanism for the regulation of amount of protein seen in these tumours could be that PDI and ERp57 are overexpressed on the tumour cell

surface and ZAF is inhibiting these proteins from being bound to the cell surface therefore reducing the expression of PDI and ERp57, where the same mechanism could be proposed for ISOQ's effect on the expression of PDI. It is notable that ZAF's effect on ERp57 seemed stronger than its effect on PDI (Figure 4.9), which would suggest that the combination is primarily affecting different thiol isomerases. PDI and ERp57 have some overlapping roles in their anti-cancer effects, as we found both inhibit the expression of VEGF, tissue factor, TMEM176B and PD-L1, while others have found another member of the TMEM family, TMEM16A, to be inhibited in lung cancer cells by both ISOQ (Zhang et al., 2017) and by ZAF (Shi et al., 2022). However, there are known distinctions between the roles of PDI and ERp57 in oncogenesis as PDI has been associated with vital roles in tumour growth and progression as well as protecting cells from apoptosis (Lovat et al., 2008; Xu et al., 2012a; S. Xu et al., 2014), while ERp57 is involved in cancer metastasis (Santana-Codina et al., 2013), gene transcription through epidermal growth factor receptor (EGFR) signalling (E. Gaucci et al., 2013) and promoting resistance to treatment in ovarian cancer (Cicchillitti et al., 2009). It is also possible that the strong combination effects are due to other mechanistic actions of ISOQ, such as its ability to inhibit the phosphorylation of ERK and JNK, proteins that are part of the MAPK pathway (Kim et al., 2017). Both ERK and JNK are involved in angiogenesis (Naruishi et al., 2003; Song et al., 2023) and inflammation (Hammouda et al., 2020; Lucas et al., 2022). Interestingly, inhibition of JNK inhibits IL-6 induced production of VEGF in fibroblasts (Naruishi et al., 2003), where in Figure 4.3 and Figure 4.3 we see a reduction in both VEGF and IL-6 from treatment with ISOQ. The RNA-sequencing results demonstrated numerous differences between the effects of ISOQ treatment and ZAF treatment of the tumours again suggesting differential modes of action for each compound. It was perhaps surprising that ISOQ treatment more commonly resulted in upregulation of significantly enriched gene sets, while ZAF treatment resulted almost exclusively in

downregulation of significant gene sets. At the level of individual genes, the known genes most significantly affected by ISOQ were SECTM1 and TSPAN1, genes involved in cancer cell progression through mesenchymal (Wang et al., 2018; Yao et al., 2024) transitions and TGFBI, which along with SECTM1, is involved in the immune system (Yao et al., 2024; Zhou et al., 2023). Meanwhile, xenografted mice treated with zafirlukast had the most reduced levels of ANXA8, a gene known to be higher in ovarian cancer and associated with poor prognosis (Gou et al., 2019). It is also associated with blood vessel development and the inflammatory response (Gou et al., 2019). We also cannot rule out that ZAF and ISOQ have effects on other targets beyond thiol isomerases. Such as the fact that when ISOQ is ingested it can be metabolised into quercetin (Mbikay & Chretien, 2022), which can activate caspase-3, inhibit the phosphorylation of kinases such as Akt, mTOR and ERK, and reduce MMP and VEGF secretion (Lotfi et al., 2023).

A second major benefit of adding an ISOQ/ZAF combination to therapeutic cancer regimens would be to reduce cancer and chemotherapy induced thrombosis, as patients receiving traditional chemotherapies have an even greater risk of developing a thrombotic event than a general cancer patient. For example, one retrospective study found an 11% annual incidence of venous thromboembolism (VTE) in these patients (Otten et al., 2004), including almost 18% for those on a regimen of cyclophosphamide, methotrexate, 5-fluorouracil, vincristine and prednisone for metastatic breast cancer, compared to 2% that did not receive therapy (Otten et al., 2004). Increased risk of thrombotic events is not limited to traditional chemotherapies, as antibodies targeting PD-L1 and VEGF have both demonstrated to induce an increased thrombotic risk (Sato et al., 2019; Watson & Al-Samkari, 2021). Previously reported clinical data demonstrates that ISOQ improves markers of coagulation in advanced cancer patients, half of which were enrolled at the start of chemotherapy treatment, with no reported VTEs or major haemorrhages reported in that study (Jeffrey I. Zwicker et

al., 2019), nor in our study with zafirlukast (Gelzinis et al., 2023a). Therefore, it would be of interest to try adding a combination of ISOQ/ZAF to a chemotherapeutic regimen, especially one currently using anti-VEGF or PD-L1 antibodies, since ISOQ and ZAF both inhibit these proteins (Figure 4.8). However, it is important to note that even though ISOQ and ZAF demonstrated no major haemorrhages in their respective clinical studies (Gelzinis et al., 2023b; Jeffrey I. Zwicker et al., 2019) and ZAF demonstrated no significant risk of bleeding in a tail bleed assay (Holbrook et al., 2021), the possibility of a combination of both inhibitors still may pose a risk of bleeding, especially long term. As it has been demonstrated in this chapter, both ISOQ and ZAF target more proteins than just thiol isomerases, such as tissue factor a protein essential within the extrinsic coagulation cascade, with the combination of the two inhibitors nearly depleting the protein in tumour tissue. Going forward a long-term study of the combination of ISOQ and ZAF on bleeding risk would be essential to demonstrate the inhibitor combination does not deplete the body of essential factors related to clotting, such as tissue factor, and increase the potential of excess bleeding.

Overall, this study shows that the therapeutic efficacy of ZAF is enhanced if given in combination with ISOQ. Further, the combination effects on tissue factor, PD-L1 and VEGF suggests that the combined use could be even more effective or allow for clinical dose lowering of a chemotherapy regiment such as cisplatin and gemcitabine. These data provide strong evidence that the ISOQ/ZAF combination has significant potential for prophylactic antithrombotic treatment in cancer and additive direct anticancer effects, providing strong rationale for a future clinical trial adding this combination to the standard of care chemotherapy in ovarian cancer patients.

4.7 Supplementary Figures

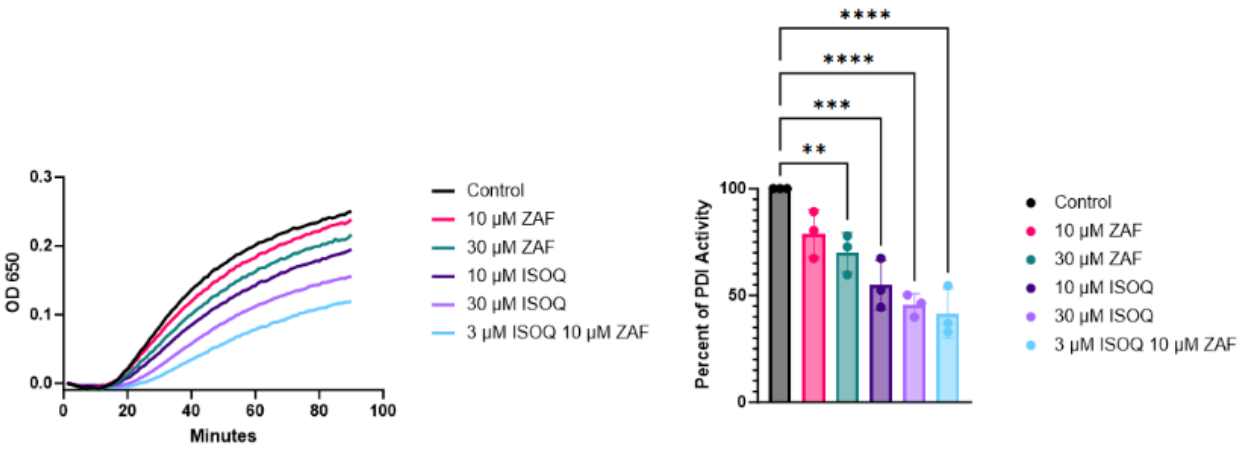

Supplemental Figure 4.1 A combination of ISOQ and ZAF inhibits thiol isomerase activity more effectively than individually. A cell free insulin based turbidimetric assay was used to compare the effectiveness of a combination of ISOQ and ZAF versus each compound alone on PDI inhibition. Data are presented as mean ± SD. Data were analysed *via* one-way ANOVA with Dunnet's multiple comparisons test where **P < 0.01, ***P < 0.001 and ****P < 0.0001.

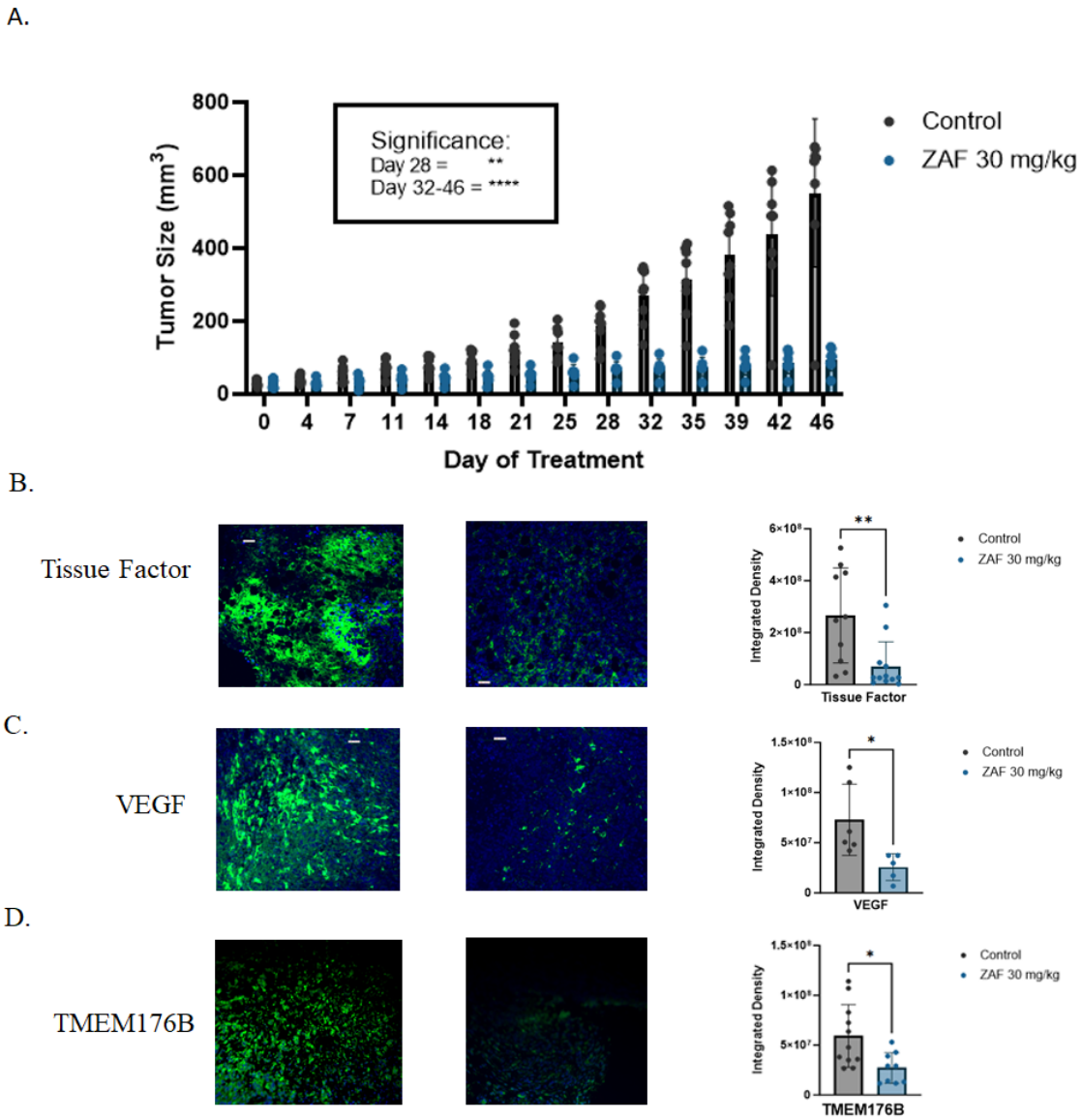

Supplemental Figure 4.2 ZAF inhibits tumour growth in a xenograft model of ovarian cancer. (A) Drug was administered orally *via* oral gavage daily and measurements of tumours taken twice weekly. Both 10 mg/kg (n=8) and 30 mg/kg (n=8) doses showed significant inhibition by treatment day 25. Data are presented as mean ± SD. Excised tumours were examined for (B) VEGF, (C) TMEM176B and (D) tissue factor levels of expression. Images are representative of 3-5 mice per group, with 3 images taken per mouse of the areas of highest expression. Scale bars are 100 µm. Data are presented as mean ± SD. Data (B, C and D) were analysed *via* an unpaired t-test where *P < 0.05 and **P < 0.01. Data (A) were analysed *via* two-way ANOVA with Sidak's multiple comparisons test where **P < 0.01, and ****P < 0.0001.

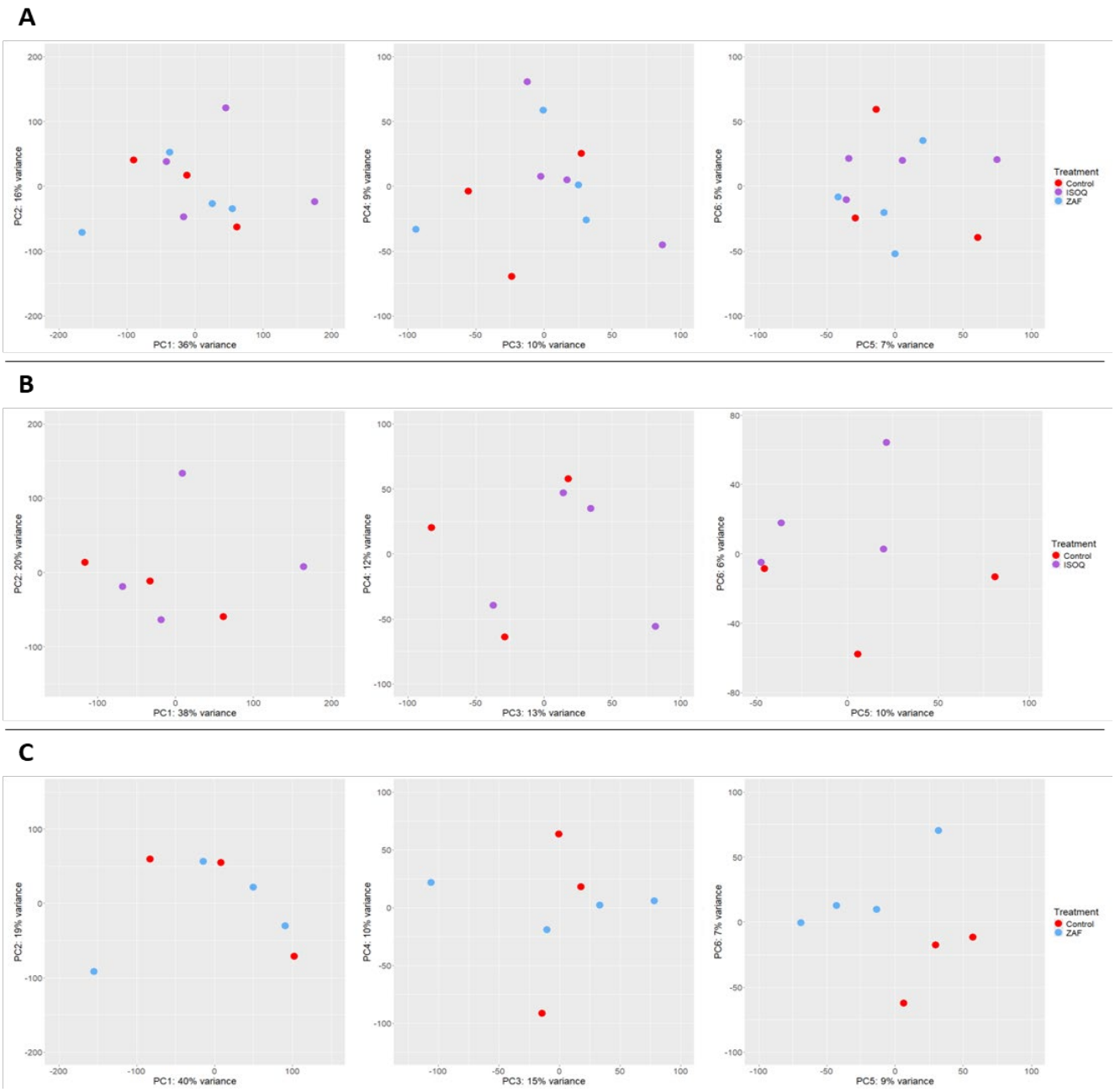

Supplemental Figure 4.3 RNA-seq principal component analysis of tumour samples.

Scatter plots for the top 6 principal components (PCs) from principal component analyses (PCA) based on the TPM values of all expressed genes in (A) the tumours from all three treatment groups, (B) only the tumours from the control and ISOQ treatment groups, or (C) only the tumours from the control and ZAF treatment groups. Data for Supplemental Figure 4.3 was obtained and analysed by Jason W. Hoskins from the NIH.

A

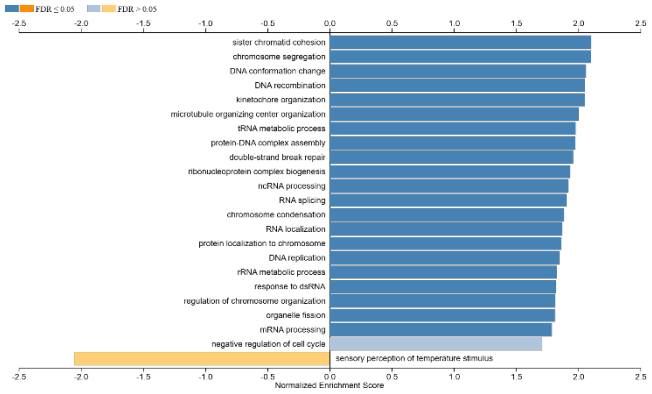
FDR ≤ 0.05
FDR > 0.05
sister chromatid cohesion
chromosome segregation
DNA conformation change
DNA recombination
kinetochore organization
microtubule organizing center organization
tRNA metabolic process
protein-DNA complex assembly
double-strand break repair
ribonucleoprotein complex biogenesis
ncRNA processing
RNA splicing
chromosome condensation
RNA localization
protein localization to chromosome
DNA replication
rRNA metabolic process
response to dsRNA
regulation of chromosome organization
organelle fission
mRNA processing
negative regulation of cell cycle
sensory perception of temperature stimulus
Normalized Enrichment Score

B

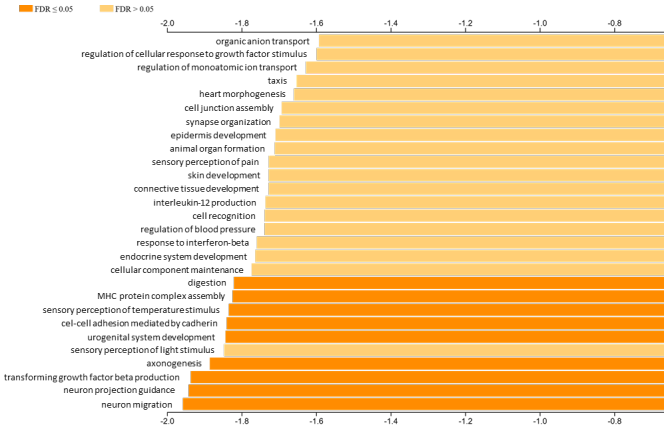
FDR ≤ 0.05
FDR > 0.05
organic anion transport
regulation of cellular response to growth factor stimulus
regulation of monoatomic ion transport
taxis
heart morphogenesis
cell junction assembly
synapse organization
epidermis development
animal organ formation
sensory perception of pain
skin development
connective tissue development
interleukin-12 production
cell recognition
regulation of blood pressure
response to interferon-beta
endocrine system development
cellular component maintenance
digestion
MHC protein complex assembly
sensory perception of temperature stimulus
cel-cell adhesion mediated by cadherin
urogenital system development
sensory perception of light stimulus
axonogenesis
transforming growth factor beta production
neuron projection guidance
neuron migration

C

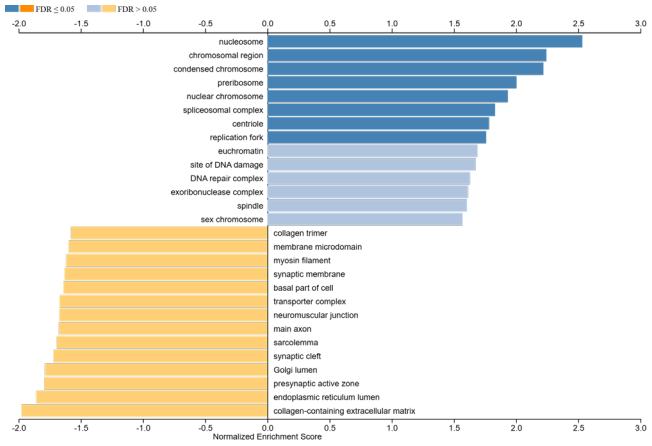
FDR ≤ 0.05
FDR > 0.05
nucleosome
chromosomal region
condensed chromosome
preribosome
nuclear chromosome
spliceosomal complex
centriole
replication fork
euchromatin
site of DNA damage
DNA repair complex
exoribonuclease complex
spindle
sex chromosome
collagen trimer
membrane microdomain
myosin filament
synaptic membrane
basal part of cell
transporter complex
neuromuscular junction
main axon
sarcolemma
synaptic cleft
Golgi lumen
presynaptic active zone
endoplasmic reticulum lumen
collagen-containing extracellular matrix
Normalized Enrichment Score

D

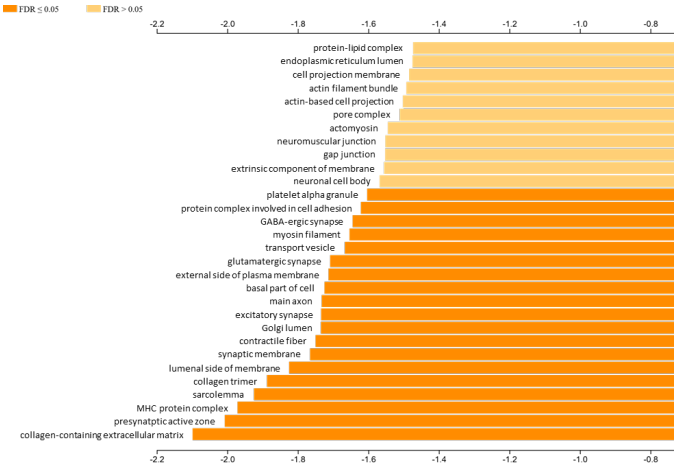
FDR ≤ 0.05
FDR > 0.05
protein-lipid complex
endoplasmic reticulum lumen
cell projection membrane
actin filament bundle
actin-based cell projection
pore complex
actomyosin
neuromuscular junction
gap junction
extrinsic component of membrane
neuronal cell body
platelet alpha granule
protein complex involved in cell adhesion
GABA-ergic synapse
myosin filament
transport vesicle
glutamatergic synapse
external side of plasma membrane
basal part of cell
main axon
excitatory synapse
Golgi lumen
contractile fiber
synaptic membrane
lumenal side of membrane
collagen trimer
sarcolemma
MHC protein complex
presynaptic active zone
collagen-containing extracellular matrix

E

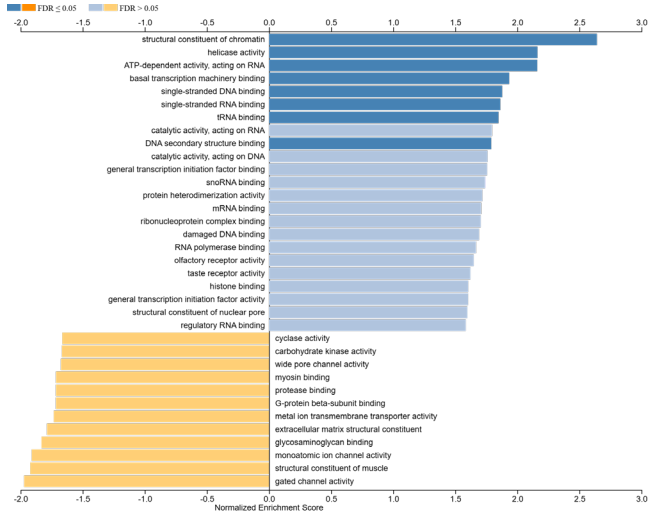
FDR ≤ 0.05
FDR > 0.05
structural constituent of chromatin
helicase activity
ATP-dependent activity, acting on RNA
basal transcription machinery binding
single-stranded DNA binding
single-stranded RNA binding
tRNA binding
catalytic activity, acting on RNA
DNA secondary structure binding
catalytic activity, acting on DNA
general transcription initiation factor binding
snoRNA binding
protein heterodimerization activity
mRNA binding
ribonucleoprotein complex binding
damaged DNA binding
RNA polymerase binding
olfactory receptor activity
taste receptor activity
histone binding
general transcription initiation factor activity
structural constituent of nuclear pore
regulatory RNA binding
cyclase activity
carbohydrate kinase activity
wide pore channel activity
myosin binding
protease binding
G-protein beta-subunit binding
metal ion transmembrane transporter activity
extracellular matrix structural constituent
glycosaminoglycan binding
monoatomic ion channel activity
structural constituent of muscle
gated channel activity
Normalized Enrichment Score

F

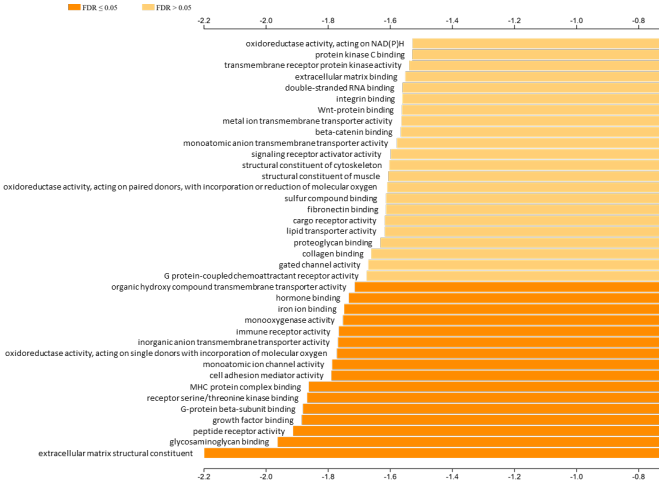
FDR ≤ 0.05
FDR > 0.05
oxidoreductase activity, acting on NAD(P)H
protein kinase C binding
transmembrane receptor protein kinase activity
extracellular matrix binding
double-stranded RNA binding
integrin binding
Wnt-protein binding
metal ion transmembrane transporter activity
beta-catenin binding
monoatomic anion transmembrane transporter activity
signaling receptor activator activity
structural constituent of cytoskeleton
structural constituent of muscle
oxidoreductase activity, acting on paired donors, with incorporation or reduction of molecular oxygen
sulfur compound binding
fibronectin binding
cargo receptor activity
lipid transporter activity
proteoglycan binding
collagen binding
gated channel activity
G protein-coupled chemoattractant receptor activity
organic hydroxy compound transmembrane transporter activity
hormone binding
iron ion binding
monooxygenase activity
immune receptor activity
inorganic anion transmembrane transporter activity
oxidoreductase activity, acting on single donors with incorporation of molecular oxygen
monoatomic ion channel activity
cell adhesion mediator activity
MHC protein complex binding
receptor serine/threonine kinase binding
G-protein beta-subunit binding
growth factor binding
peptide receptor activity
glycosaminoglycan binding
extracellular matrix structural constituent

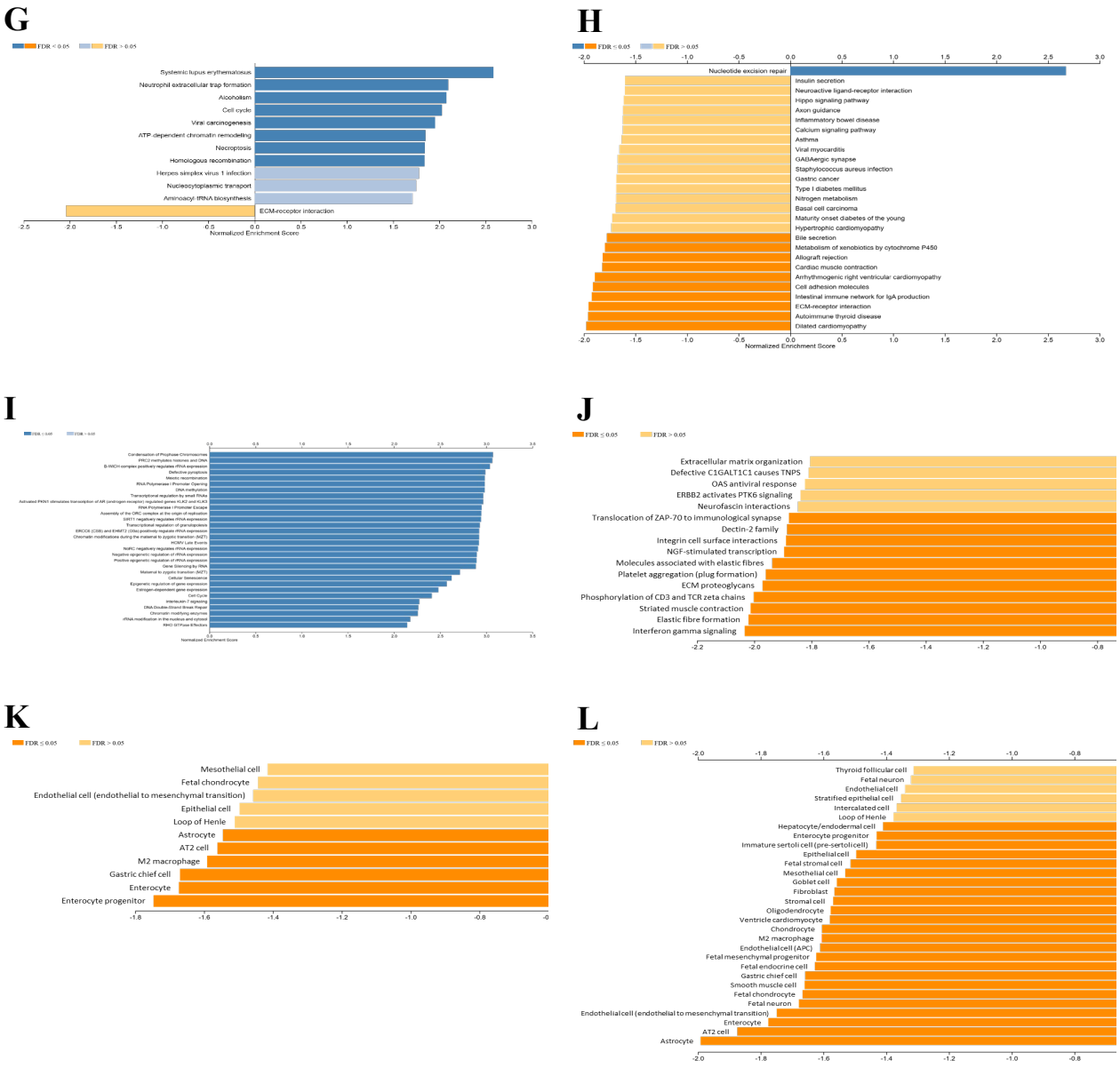

Supplemental Figure 4.4 Top GSEA enriched gene sets based on DE analysis.

Bar plots summarizing up to 30 nominally significantly (P<0.05) enriched gene sets based on gene DE magnitudes from the (A, C, E, G, I, K) ISOQ vs. control, and (B, D, F, H, J, L) ZAF vs. control comparisons. The gene set collections against which enrichments were tested were (A, B) Gene Ontology (GO): Biological Process, (C, D) GO: Cellular Component, (E, F) GO: Molecular Function, (G, H) KEGG Pathways, (I, J) Reactome Pathways, and (K, L) Human Cell Landscape. Darker shaded bars indicate gene sets significantly enriched at FDR<0.05. Data for Supplemental Figure 4.4 was obtained and analysed by Jason W. Hoskins from the NIH.

4.8 References

Bekendam, R. H., Bendapudi, P. K., Lin, L., Nag, P. P., Pu, J., Kennedy, D. R., Feldenzer, A., Chiu, J., Cook, K. M., Furie, B., Huang, M., Hogg, P. J., & Flaumenhaft, R. (2016). A substrate-driven allosteric switch that enhances PDI catalytic activity. *Nat Commun*, *7*, 12579. https://doi.org/10.1038/ncomms12579

Chen, J., Jiang, C. C., Jin, L., & Zhang, X. D. (2016). Regulation of PD-L1: a novel role of pro-survival signalling in cancer. *Ann Oncol*, *27*(3), 409-416. https://doi.org/10.1093/annonc/mdv615

Cho, J., Furie, B. C., Coughlin, S. R., & Furie, B. (2008). A critical role for extracellular protein disulfide isomerase during thrombus formation in mice. *J Clin Invest*, *118*(3), 1123-1131. https://doi.org/10.1172/JCI34134

Cho, J., Kennedy, D. R., Lin, L., Huang, M., Merrill-Skoloff, G., Furie, B. C., & Furie, B. (2012). Protein disulfide isomerase capture during thrombus formation in vivo depends on the presence of β3 integrins. *Blood*, *120*(3), 647-655. https://doi.org/10.1182/blood-2011-08-372532

Cicchillitti, L., Di Michele, M., Urbani, A., Ferlini, C., Donat, M. B., Scambia, G., & Rotilio, D. (2009). Comparative proteomic analysis of paclitaxel sensitive A2780 epithelial ovarian cancer cell line and its resistant counterpart A2780TC1 by 2D-DIGE: the role of ERp57. *J Proteome Res*, *8*(4), 1902-1912. https://doi.org/10.1021/pr800856b

Da Silva, D. D. C., Orfali, G. D. C., Santana, M. G., Palma, J. K. Y., Assunção, I. R. D. O., Marchesi, I. M., Grizotto, A. Y. K., Martinez, N. P., Felliti, S., Pereira, J. A., & Priolli, D. G. (2022). Antitumor effect of isoquercetin on tissue vasohibin expression and colon cancer vasculature. *Oncotarget*, *13*(1), 307-318. https://doi.org/10.18632/oncotarget.28181

Essex, D. W., & Li, M. (1999). Protein disulphide isomerase mediates platelet aggregation and secretion. *Br J Haematol*, *104*(3), 448-454. https://doi.org/10.1046/j.1365-2141.1999.01197.x

Eufemi, M., Coppari, S., Altieri, F., Grillo, C., Ferraro, A., & Turano, C. (2004). ERp57 is present in STAT3-DNA complexes. *Biochem Biophys Res Commun*, *323*(4), 1306-1312. https://doi.org/10.1016/j.bbrc.2004.09.009

Gaucci, E., Altieri, F., Turano, C., & Chichiarelli, S. (2013). The protein ERp57 contributes to EGF receptor signaling and internalization in MDA-MB-468 breast cancer cells. *J Cell Biochem*, *114*(11), 2461-2470. https://doi.org/10.1002/jcb.24590

Gelzinis, J. A., Szahaj, M. K., Bekendam, R. H., Wurl, S. E., Pantos, M. M., Verbetsky, C. A., Dufresne, A., Shea, M., Howard, K. C., Tsodikov, O. V., Garneau-Tsodikova, S., Zwicker, J. I., & Kennedy, D. R. (2023). Targeting thiol isomerase activity with zafirlukast to treat ovarian cancer from the bench to clinic. *FASEB J*, *37*(5), e22914. https://doi.org/10.1096/fj.202201952R

Gou, R., Zhu, L., Zheng, M., Guo, Q., Hu, Y., Li, X., Liu, J., & Lin, B. (2019). Annexin A8 can serve as potential prognostic biomarker and therapeutic target for ovarian cancer: based on the comprehensive analysis of Annexins. *J Transl Med*, *17*(1), 275. https://doi.org/10.1186/s12967-019-2023-z

Hammouda, M. B., Ford, A. E., Liu, Y., & Zhang, J. Y. (2020). The JNK Signaling Pathway in Inflammatory Skin Disorders and Cancer. *Cells*, *9*(4). https://doi.org/10.3390/cells9040857

Hirano, N., Shibasaki, F., Sakai, R., Tanaka, T., Nishida, J., Yazaki, Y., Takenawa, T., & Hirai, H. (1995). Molecular cloning of the human glucose-regulated protein ERp57/GRP58, a thiol-dependent reductase. Identification of its secretory form and inducible expression by the oncogenic transformation. *Eur J Biochem*, *234*(1), 336-342. http://www.ncbi.nlm.nih.gov/pubmed/8529662

Holbrook, L. M., Keeton, S. J., Sasikumar, P., Nock, S., Gelzinis, J., Brunt, E., Ryan, S., Pantos, M. M., Verbetsky, C. A., Gibbins, J. M., & Kennedy, D. R. (2021). Zafirlukast is a broad-spectrum thiol isomerase inhibitor that inhibits thrombosis without altering bleeding times. *Br J Pharmacol*, *178*(3), 550-563. https://doi.org/10.1111/bph.15291

Jasuja, R., Furie, B., & Furie, B. C. (2010). Endothelium-derived but not platelet-derived protein disulfide isomerase is required for thrombus formation in vivo. *Blood*, *116*(22), 4665-4674. https://doi.org/10.1182/blood-2010-04-278184

Jasuja, R., Passam, F. H., Kennedy, D. R., Kim, S. H., van Hessem, L., Lin, L., Bowley, S. R., Joshi, S. S., Dilks, J. R., Furie, B., Furie, B. C., & Flaumenhaft, R. (2012). Protein disulfide isomerase inhibitors constitute a new class of antithrombotic agents. *J Clin Invest*, *122*(6), 2104-2113. https://doi.org/10.1172/JCI61228

Kang, C., Rostoker, R., Ben-Shumel, S., Rashed, R., Duty, J. A., Demircioglu, D., Antoniou, I. M., Isakov, L., Shen-Orr, Z., Bravo-Cordero, J. J., Kase, N., Cuajungco, M. P., Moran, T. M., LeRoith, D., & Gallagher, E. J. (2021). TMEM176B Regulates AKT/mTOR Signaling and Tumor Growth in Triple-Negative Breast Cancer. *Cells*, *10*(12). https://doi.org/10.3390/cells10123430

Khorana, A. A., Francis, C. W., Culakova, E., Kuderer, N. M., & Lyman, G. H. (2007). Thromboembolism is a leading cause of death in cancer patients receiving outpatient chemotherapy. *Journal of Thrombosis and Haemostasis*, *5*(3), 632-634. https://doi.org/10.1111/j.1538-7836.2007.02374.x

Kim, D. S., Irfan, M., Sung, Y. Y., Kim, S. H., Park, S. H., Choi, Y. H., Rhee, M. H., & Kim, H. K. (2017). Schisandra chinensis and Morus alba Synergistically Inhibit In Vivo Thrombus Formation and Platelet Aggregation by Impairing the Glycoprotein VI Pathway. *Evid Based Complement Alternat Med*, *2017*, 7839658. https://doi.org/10.1155/2017/7839658

Kim, K., Hahm, E., Li, J., Holbrook, L. M., Sasikumar, P., Stanley, R. G., Ushio-Fukai, M., Gibbins, J. M., & Cho, J. (2013). Platelet protein disulfide isomerase is required for thrombus formation but not for hemostasis in mice. *Blood*, *122*(6), 1052-1061. https://doi.org/10.1182/blood-2013-03-492504

Kurpinska, A., Suraj-Prazmowska, J., Stojak, M., Jarosz, J., Mateuszuk, L., Niedzielska-Andres, E., Smolik, M., Wietrzyk, J., Kalvins, I., Walczak, M., & Chlopicki, S. (2022). Comparison of anti-cancer effects of novel protein disulphide isomerase (PDI) inhibitors in breast cancer cells characterized by high and low PDIA17 expression. *Cancer Cell Int*, *22*(1), 218. https://doi.org/10.1186/s12935-022-02631-w

Liang, C., Cai, M., Xu, Y., Fu, W., Wu, J., Liu, Y., Liao, X., Ning, J., Li, J., Huang, M., & Yuan, C. (2022). Identification of Antithrombotic Natural Products Targeting the Major Substrate Binding Pocket of Protein Disulfide Isomerase. *J Nat Prod*, *85*(5), 1332-1339. https://doi.org/10.1021/acs.jnatprod.2c00080

Liu, Z. L., Chen, H. H., Zheng, L. L., Sun, L. P., & Shi, L. (2023). Angiogenic signaling pathways and anti-angiogenic therapy for cancer. *Signal Transduct Target Ther*, *8*(1), 198. https://doi.org/10.1038/s41392-023-01460-1

Lotfi, N., Yousefi, Z., Golabi, M., Khalilian, P., Ghezelbash, B., Montazeri, M., Shams, M. H., Baghbadorani, P. Z., & Eskandari, N. (2023). The potential anti-cancer effects of quercetin on blood, prostate and lung cancers: An update. *Front Immunol*, *14*, 1077531. https://doi.org/10.3389/fimmu.2023.1077531

Lovat, P. E., Corazzari, M., Armstrong, J. L., Martin, S., Pagliarini, V., Hill, D., Brown, A. M., Piacentini, M., Birch-Machin, M. A., & Redfern, C. P. (2008). Increasing melanoma cell death using inhibitors of protein disulfide isomerases to abrogate survival responses to endoplasmic reticulum stress. *Cancer Res*, *68*(13), 5363-5369. https://doi.org/10.1158/0008-5472.CAN-08-0035

Lucas, R. M., Luo, L., & Stow, J. L. (2022). ERK1/2 in immune signalling. *Biochem Soc Trans*, *50*(5), 1341-1352. https://doi.org/10.1042/BST20220271

Lysov, Z., Swystun, L. L., Kuruvilla, S., Arnold, A., & Liaw, P. C. (2015). Lung cancer chemotherapy agents increase procoagulant activity via protein disulfide isomerase-dependent tissue factor decryption. *Blood Coagulation & Fibrinolysis*, *26*(1), 36-45. https://doi.org/10.1097/mbc.0000000000000145

Manukyan, D., von Bruehl, M. L., Massberg, S., & Engelmann, B. (2008). Protein disulfide isomerase as a trigger for tissue factor-dependent fibrin generation. *Thromb Res*, *122 Suppl 1*, S19-22. https://doi.org/10.1016/S0049-3848(08)70013-6

Mbikay, M., & Chretien, M. (2022). Isoquercetin as an Anti-Covid-19 Medication: A Potential to Realize. *Front Pharmacol*, *13*, 830205. https://doi.org/10.3389/fphar.2022.830205

Naruishi, K., Nishimura, F., Yamada-Naruishi, H., Omori, K., Yamaguchi, M., & Takashiba, S. (2003). C-jun N-terminal kinase (JNK) inhibitor, SP600125, blocks interleukin (IL)-6-induced vascular endothelial growth factor (VEGF) production: cyclosporine A partially mimics this inhibitory effect. *Transplantation*, *76*(9), 1380-1382. https://doi.org/10.1097/01.TP.0000085661.52980.95

Otten, H. B., Mathijssen, J., ten Cate, H., & et al. (2004). Symptomatic venous thromboembolism in cancer patients treated with chemotherapy: An underestimated phenomenon. *Archives of Internal Medicine*, *164*(2), 190-194. https://doi.org/10.1001/archinte.164.2.190

Samanta, S., Tamura, S., Dubeau, L., Mhawech-Fauceglia, P., Miyagi, Y., Kato, H., Lieberman, R., Buckanovich, R. J., Lin, Y. G., & Neamati, N. (2017). Expression of protein disulfide isomerase family members correlates with tumor progression and patient survival in ovarian cancer. *Oncotarget*, *8*(61), 103543-103556. https://doi.org/10.18632/oncotarget.21569

Santana-Codina, N., Carretero, R., Sanz-Pamplona, R., Cabrera, T., Guney, E., Oliva, B., Clezardin, P., Olarte, O. E., Loza-Alvarez, P., Mendez-Lucas, A., Perales, J. C., & Sierra, A. (2013). A transcriptome-proteome integrated network identifies endoplasmic reticulum thiol oxidoreductase (ERp57) as a hub that mediates bone metastasis. *Mol Cell Proteomics*, *12*(8), 2111-2125. https://doi.org/10.1074/mcp.M112.022772

Sato, R., Imamura, K., Sakata, S., Ikeda, T., Horio, Y., Iyama, S., Akaike, K., Hamada, S., Jodai, T., Nakashima, K., Ishizuka, S., Sato, N., Saruwatari, K., Saeki, S., Tomita, Y., & Sakagami, T. (2019). Disorder of Coagulation-Fibrinolysis System: An Emerging Toxicity of Anti-PD-1/PD-L1 Monoclonal Antibodies. *J Clin Med*, *8*(6). https://doi.org/10.3390/jcm8060762

Segovia, M., Russo, S., Jeldres, M., Mahmoud, Y. D., Perez, V., Duhalde, M., Charnet, P., Rousset, M., Victoria, S., Veigas, F., Louvet, C., Vanhove, B., Floto, R. A., Anegon, I., Cuturi, M. C., Girotti, M. R., Rabinovich, G. A., & Hill, M. (2019). Targeting TMEM176B Enhances Antitumor Immunity and Augments the Efficacy of Immune Checkpoint Blockers by Unleashing Inflammasome Activation. *Cancer Cell*, *35*(5), 767-781 e766. https://doi.org/10.1016/j.ccell.2019.04.003

Shalabi, S., Belayachi, A., & Larrivee, B. (2024). Involvement of neuronal factors in tumor angiogenesis and the shaping of the cancer microenvironment. *Front Immunol*, *15*, 1284629. https://doi.org/10.3389/fimmu.2024.1284629

Shi, S., Ma, B., Sun, F., Qu, C., Li, G., Shi, D., Liu, W., Zhang, H., & An, H. (2022). Zafirlukast inhibits the growth of lung adenocarcinoma via inhibiting TMEM16A channel activity. *J Biol Chem*, *298*(3), 101731. https://doi.org/10.1016/j.jbc.2022.101731

Song, Y. Y., Liang, D., Liu, D. K., Lin, L., Zhang, L., & Yang, W. Q. (2023). The role of the ERK signaling pathway in promoting angiogenesis for treating ischemic diseases. *Front Cell Dev Biol*, *11*, 1164166. https://doi.org/10.3389/fcell.2023.1164166

Sorensen, H. T., Pedersen, L., van Es, N., Buller, H. R., & Horvath-Puho, E. (2023). Impact of venous thromboembolism on the mortality in patients with cancer: a population-based cohort study. *Lancet Reg Health Eur*, *34*, 100739. https://doi.org/10.1016/j.lanepe.2023.100739

Stopa, J. D., Neuberg, D., Puligandla, M., Furie, B., Flaumenhaft, R., & Zwicker, J. I. (2017). Protein disulfide isomerase inhibition blocks thrombin generation in humans by interfering with platelet factor V activation. *JCI Insight*, *2*(1), e89373. https://doi.org/10.1172/jci.insight.89373

Swiatkowska, M., Szymanski, J., Padula, G., & Cierniewski, C. S. (2008). Interaction and functional association of protein disulfide isomerase with alphaVbeta3 integrin on endothelial cells. *FEBS J*, *275*(8), 1813-1823. https://doi.org/10.1111/j.1742-4658.2008.06339.x

Tan, R., Wang, F., Zhou, Y., Huang, Z., An, Z., & Xu, Y. (2023). Neural functions in cancer: Data analyses and database construction. *Front Genet*, *14*, 1062052. https://doi.org/10.3389/fgene.2023.1062052

Tanaka, T., Kutomi, G., Kajiwara, T., Kukita, K., Kochin, V., Kanaseki, T., Tsukahara, T., Hirohashi, Y., Torigoe, T., Okamoto, Y., Hirata, K., Sato, N., & Tamura, Y. (2017). Cancer-associated oxidoreductase ERO1-alpha promotes immune escape through up-regulation of PD-L1 in

human breast cancer. *Oncotarget*, *8*(15), 24706-24718. https://doi.org/10.18632/oncotarget.14960

Vatolin, S., Phillips, J. G., Jha, B. K., Govindgari, S., Hu, J., Grabowski, D., Parker, Y., Lindner, D. J., Zhong, F., Distelhorst, C. W., Smith, M. R., Cotta, C., Xu, Y., Chilakala, S., Kuang, R. R., Tall, S., & Reu, F. J. (2016). Novel Protein Disulfide Isomerase Inhibitor with Anticancer Activity in Multiple Myeloma. *Cancer Res*, *76*(11), 3340-3350. https://doi.org/10.1158/0008-5472.CAN-15-3099

Wang, Y., Liang, Y., Yang, G., Lan, Y., Han, J., Wang, J., Yin, D., Song, R., Zheng, T., Zhang, S., Pan, S., Liu, X., Zhu, M., Liu, Y., Cui, Y., Meng, F., Zhang, B., Liang, S., Guo, H., . . . Liu, L. (2018). Tetraspanin 1 promotes epithelial-to-mesenchymal transition and metastasis of cholangiocarcinoma via PI3K/AKT signaling. *J Exp Clin Cancer Res*, *37*(1), 300. https://doi.org/10.1186/s13046-018-0969-y

Watson, N., & Al-Samkari, H. (2021). Thrombotic and bleeding risk of angiogenesis inhibitors in patients with and without malignancy. *J Thromb Haemost*, *19*(8), 1852-1863. https://doi.org/10.1111/jth.15354

Xiong, B., Jha, V., Min, J. K., & Cho, J. (2020). Protein disulfide isomerase in cardiovascular disease. *Exp Mol Med*, *52*(3), 390-399. https://doi.org/10.1038/s12276-020-0401-5

Xu, S., Butkevich, A. N., Yamada, R., Zhou, Y., Debnath, B., Duncan, R., Zandi, E., Petasis, N. A., & Neamati, N. (2012). Discovery of an orally active small-molecule irreversible inhibitor of protein disulfide isomerase for ovarian cancer treatment. *Proc Natl Acad Sci U S A*, *109*(40), 16348-16353. https://doi.org/10.1073/pnas.1205226109

Xu, S., Liu, Y., Yang, K., Wang, H., Shergalis, A., Kyani, A., Bankhead, A., 3rd, Tamura, S., Yang, S., Wang, X., Wang, C. C., Rehemtulla, A., Ljungman, M., & Neamati, N. (2019). Inhibition of protein disulfide isomerase in glioblastoma causes marked downregulation of DNA repair and DNA damage response genes. *Theranostics*, *9*(8), 2282-2298. https://doi.org/10.7150/thno.30621

Xu, S., Sankar, S., & Neamati, N. (2014). Protein disulfide isomerase: a promising target for cancer therapy. *Drug Discovery Today*, *19*(3), 222-240. https://doi.org/10.1016/j.drudis.2013.10.017

Yao, Z., Zhang, F., Qi, C., Wang, C., Mao, M., Zhao, C., Qi, M., Wang, Z., Zhou, G., Jiang, X., & Xia, H. (2024). SECTM1 promotes the development of glioblastoma and mesenchymal transition by regulating the TGFbeta1/Smad signaling pathway. *Int J Biol Sci*, *20*(1), 78-93. https://doi.org/10.7150/ijbs.84591

Zai, A., Rudd, M. A., Scribner, A. W., & Loscalzo, J. (1999). Cell-surface protein disulfide isomerase catalyzes transnitrosation and regulates intracellular transfer of nitric oxide. *J Clin Invest*, *103*(3), 393-399. https://doi.org/10.1172/JCI4890

Zhang, X., Li, H., Zhang, H., Liu, Y., Huo, L., Jia, Z., Xue, Y., Sun, X., & Zhang, W. (2017). Inhibition of transmembrane member 16A calcium-activated chloride channels by natural flavonoids contributes to flavonoid anticancer effects. *Br J Pharmacol*, *174*(14), 2334-2345. https://doi.org/10.1111/bph.13841

Zhao, H., Wu, L., Yan, G., Chen, Y., Zhou, M., Wu, Y., & Li, Y. (2021). Inflammation and tumor progression: signaling pathways and targeted intervention. *Signal Transduct Target Ther*, *6*(1), 263. https://doi.org/10.1038/s41392-021-00658-5

Zheng, G., Lv, K., Wang, H., Huang, L., Feng, Y., Gao, B., Sun, Y., Li, Y., Huang, J., Jin, P., Xu, X., Horgen, F. D., Fang, C., & Yao, G. (2023). Piericones A and B as Potent Antithrombotics: Nanomolar Noncompetitive Protein Disulfide Isomerase Inhibitors with an Unexpected Chemical Architecture. *J Am Chem Soc*, *145*(5), 3196-3203. https://doi.org/10.1021/jacs.2c12963

Zhou, J., Lyu, N., Wang, Q., Yang, M., Kimchi, E. T., Cheng, K., Joshi, T., Tukuli, A. R., Staveley-O'Carroll, K. F., & Li, G. (2023). A novel role of TGFBI in macrophage polarization and macrophage-induced pancreatic cancer growth and therapeutic resistance. *Cancer Lett*, *578*, 216457. https://doi.org/10.1016/j.canlet.2023.216457

Zwicker, J. I., Schlechter, B. L., Stopa, J. D., Liebman, H. A., Aggarwal, A., Puligandla, M., Caughey, T., Bauer, K. A., Kuemmerle, N., Wong, E., Wun, T., McLaughlin, M., Hidalgo, M., Neuberg, D., Furie, B., & Flaumenhaft, R. (2019). Targeting protein disulfide isomerase

with the flavonoid isoquercetin to improve hypercoagulability in advanced cancer. *JCI Insight*, *4*(4). https://doi.org/10.1172/jci.insight.125851

Chapter 5

General Discussion

When I began this project, zafirlukast was identified as an antithrombotic thiol isomerase inhibitor, able to inhibit platelet aggregation and thrombus formation (Holbrook et al., 2021). Thus, since zafirlukast was an FDA approved medication, it was the first known FDA approved drug that affected thiol isomerase activity, however numerous other studies had identified thiol isomerase inhibitors as antithrombotic or anticancer agents. Based on this information, and some preliminary data, our lab began a pilot clinical trial of zafirlukast's anticancer effect in ovarian cancer patients in collaboration with Dr. Jeffery Zwicker at Harvard Medical School. The pilot study included 4 patients and clinical data indicated that zafirlukast had potential in these patients, as the clinical effect strongly correlated with reduction of PDI activity, but the actual efficacy in most patients could have been better.

Thus, this project explored various methods to increase the potential efficacy of zafirlukast, either alone or in therapeutic combination. The major questions we addressed were designed to explore the mechanistic effects of thiol isomerase inhibition and then once knowing the important pathways inhibited by treatment, to further explore methods to enhance efficacy through chemical SAR or use of combinatorial agents.

5.1 Mechanisms of thiol isomerase inhibition

In this work, we explored the mechanisms by which thiol isomerase inhibition affected cancer, demonstrating impacts on cancer signalling, cancer metastasis, angiogenesis, cancer inflammation and cancer induced thrombosis. Zafirlukast was first looked at in this thesis as a broad-spectrum thiol isomerase inhibitor and thiol isomerases play a role mechanistically in cancer progression. For example, PDI has a role in PERK signalling and tumour cell resistance to endoplasmic reticulum stress (Kranz et al., 2020). PDI is required for the signalling of the transmembrane protein kinase PERK (Kranz et al., 2020), which is a protein responsible for facilitating tumour growth (Bobrovnikova-Marjon et al., 2010). In **Appendix III,** I demonstrated zafirlukast is able to inhibit PERK expression in ovarian cancer cells, confirming zafirlukast maintains this known effect of thiol isomerase inhibitors in cancer inhibition. Zafirlukast has a strong affinity toward the inhibition of ERp57 (Figure 4.9) so we expected it would inhibit the EGFR pathway, as previous data has demonstrated ERp57 RNA-silencing limits EGFR receptor activation, preventing downstream kinase activation (Elisa Gaucci et al., 2013). Zafirlukast was able to inhibit the phosphorylation of EGFR and the phosphorylation of downstream target Gab1, therefore strengthening the argument zafirlukast has a stronger affinity towards ERp57 and demonstrating another mechanism in which the drug can be used for cancer therapy.

After confirming that zafirlukast inhibited some previously demonstrated cell signalling pathways, we decided to explore its effects in areas of importance to cancer where thiol isomerase effects were unknown. In **Chapter 3**, ovarian tumour xenografted mice treated with zafirlukast demonstrated less lung metastasis from the primary site of the tumour than control mice. Metastasis is the leading cause of cancer death (Seyfried & Huysentruyt, 2013). Thus, the decrease in metastasis is of great importance. There are many different ways to explore metastasis, but in order for tumour cells to exit the primary tumour site and

enter circulation for metastasis to occur they require new blood vessels (Zetter, 1998). Therefore, we decided to explore this process of angiogenesis.

In **Chapter 4** zafirlukast was explored for its inhibition of the expression of angiogenic factor VEGF in the ovarian xenograft tumours, where it significantly inhibited VEGF expression. This could be related to the fact that PDI is associated with VEGF-induced H_2O_2 signalling, acting as a redox sensor leading to angiogenesis (Nagarkoti et al., 2023). Additionally, RNAseq data for tumours from zafirlukast treated mice supports a downregulation of a collagen-containing ECM gene set including MMPs and other ECM related genes necessary for ECM remodelling, cancer cell migration and the initiation of angiogenesis, demonstrating its potential as an angiogenesis inhibitor as well. However, analysis of the pathways that lead to angiogenesis were not explored in this thesis. Future research should investigate modulation of PLC-γ, PI3K/AKT and MAPK, which are downstream targets of the VEGF-A/VEGFR2 complex, to determine if these proteins can also be downregulated by zafirlukast, such has been shown for VEGF. Inhibition of these targets would further support the notion that zafirlukast could also act as an angiogenesis inhibitor.

In addition to angiogenesis, thiol isomerases have been linked to another process of metastasis, cell migration (Goplen et al., 2006; S. Li et al., 2016; Ye et al., 2018), making it unsurprising that zafirlukast, a broad-spectrum thiol isomerase inhibitor, is able to inhibit this mechanism (Holbrook et al., 2021). Interestingly, cell migration is mediated by integrins which bring forth the expression of ECM degrading proteases including MMPs (Koistinen, 2000-2013), where in **Chapter 4,** zafirlukast was able to downregulate an ECM gene set including MMPs. Additionally, thiol isomerases regulate integrin activation on platelets and cancer cells (Holbrook et al., 2021) therefore possibly linking the downregulation in the ECM gene set to thiol isomerase inhibition.

Once tumour cells have left the primary tumour and entered circulation, they must evade immune system detection to make it to their destination and avoid cell death. When PD-L1 expressed on cancer cells interacts with PD-1 on T-cells, it inhibits the ability of the T-cells to target cancer cells allowing for cancer cell survival (Han et al., 2020). PD-1/PD-L1 inhibitors including nivolumab, pembrolizumab, JQ1, atezolizumab, avelumab and cemiplimab comprise a group of drugs reported to play a crucial role in improving cancer treatment (Han et al., 2020). Therefore, due to the inhibition of metastasis from zafirlukast in **Chapter 3,** in **Chapter 4** I explored if zafirlukast and isoquercetin had any effect on immune system evasion through inhibition of PD-L1 expression in the ovarian tumours. Western blots of PD-L1 support the notion that both zafirlukast and isoquercetin act as inhibitors of expression of PD-L1 further strengthening the application both drugs have toward cancer treatment.

Linked to various steps in angiogenesis and metastasis is chronic inflammation (Singh et al., 2019), and it is clear that zafirlukast would have an effect on inflammation due to its original use to prevent leukotriene-induced inflammation (Dhaliwal & Bajaj, 2024). Therefore, based on the results of zafirlukast to inhibit metastasis and angiogenic factors and its past usage as a leukotriene receptor antagonist, in **Chapter 4** we decided to investigate the inflammation factor TMEM176B. In the ovarian xenograft tumours zafirlukast was able to inhibit the expression of TMEM176B. It is possible that there is a relationship between thiol isomerases and TMEM proteins as one study demonstrates zafirlukast inhibited lung adenocarcinoma growth through TMEM16A inhibition (Shi et al., 2022). Future studies could test this possible relationship by using other thiol isomerase inhibitors to see if the TMEM16A pathway is affected. An additional possibility is that zafirlukast not only acts as a broad-spectrum thiol isomerase inhibitor but also as a broad-spectrum TMEM inhibitor. In

this aspect, it would be interesting to explore through immunoblotting of OVCAR8 cells treated with zafirlukast if other TMEM proteins can be inhibited.

It is unsurprising that isoquercetin influenced inflammation as well as this compound has been previously demonstrated to act as an anti-inflammatory agent (Ma et al., 2018; Shi et al., 2021). One factor effected by isoquercetin in the ovarian tumours was interleukin-6 (IL-6). Interestingly, a previous study from our lab demonstrated that multiple PDI inhibitors including PACMA-31, rutin, curcumin and bacitracin, were able to lower IL-6 in IgE activated bone marrow mononuclear cells, where zafirlukast was excluded due to its previously known activity against allergy as a leukotriene inhibitor. This study observed PDI inhibited Ig-E mediated mast cell activation in food allergy where the PDI specific inhibitor PACMA-31 decreased allergic diarrhoea, mast cell activation and the number of intestinal mast cells in mice (Krajewski et al., 2020b). Thus, our finding that isoquercetin inhibited inflammation would further support these data and indicate a potential for thiol isomerase inhibition as a preventative treatment for allergies,

Following metastasis, cancer induced thrombosis is the second leading cause of death for cancer patients (Harry et al., 2025). Previously, isoquercetin demonstrated the clinical potential of thiol isomerase inhibition against cancer-induced thrombosis (Jeffrey I. Zwicker et al., 2019). While the effects of isoquercetin on cancer were unknown (until chapter 4), based on **Chapter 3** and our previous work (Holbrook et al., 2021), zafirlukast has both anti-thrombotic and anti-cancer activities. Therefore, I began to explore zafirlukast's effects as a possible inhibitor of cancer induced thrombosis. It is thought that PDI is responsible for the de-encryption of non-active tissue factor (Chen et al., 2006), and it is known that tissue factor is expressed on multiple tumour types (Li et al., 2022). Therefore, zafirlukast could potentially inhibit PDI on tumour cells preventing the activation of tissue factor thus preventing cancer induced thrombosis. This idea was supported by the inhibition of tissue

factor induced Factor Xa generation from OVCAR8 cells (Figure 3.4). Furthermore, in **Chapter 4** zafirlukast was also able to lower the level of expression of tissue factor in the ovarian tumours. Thiol isomerases such as ERp57 also play a role in P-selectin expression, where blocking ERp57 inhibits P-selectin expression (Yi Wu et al., 2012), and zafirlukast demonstrated the ability to inhibit soluble P-selectin in blood retrieved from xenografted mice **(Appendix V**). Additionally, we demonstrated that zafirlukast binds reversibly to the thiol isomerases, an important finding as reversible anti-thrombotic agents only bind to platelet receptors temporarily leading to a shorter duration of action, which reduces bleeding risk (Bultas, 2013). This decreased risk of bleeding can be important in the occurrence of an injury or required surgery. As multiple thiol isomerases are involved in cancer induced thrombosis a broad-spectrum thiol isomerase inhibitor such as zafirlukast is an ideal candidate to help combat this complication of cancer.

5.2 Methods to enhance the efficacy of zafirlukast

In **Chapter 2** I began to address the questions of improving the efficacy of zafirlukast by exploring its structure activity relationship to thiol isomerase inhibitory activity. To do so, I explored 35 analogues created during 2 rounds of optimization of zafirlukast for ERp57 activity. Each analogue lacked the moiety that binds to the leukotriene receptor so that some analogues were still active is consistent with our hypothesis that zafirlukast's anti-thrombotic activity and anti-cancer activity is due to thiol isomerase inhibition. This finding was further supported by a notable decrease in free thiols on the surface of the platelet after zafirlukast treatment (Figure 2.6). Finally, of our original 25 compounds, only one displayed enhanced thiol isomerase inhibition activity, demonstrating it was possible to alter zafirlukast to perform better as an inhibitor; however, the 2.5-fold increase in potency was somewhat disappointing and further optimization with 10 additional compounds did not result in further enhancement of efficacy, with each of these analogues being less effective than the original. We further explored the potential of other "lukast" drugs, montelukast and pranlukast but determined both of these agents were less effective than zafirlukast at thiol isomerase inhibition.

Since it did not appear the efficacy of zafirlukast was going to be easily improved through chemical optimization, we next explored potential enhancements in efficacy through delivery methods. Delivered via i.p. injection, zafirlukast significantly inhibited tumour growth in a xenograft model of ovarian cancer where 30 mg/kg of zafirlukast inhibited tumour growth by a mean decrease in tumour volume of 42% compared to the control (Figure 3.5). Generally, i.p. delivery is considered to have a higher bioavailability (Al Shoyaib et al., 2019), so it was a little surprising to find that oral gavage of zafirlukast displayed enhanced effects compared to i.p. injection, as mice receiving 30 mg/kg zafirlukast via oral gavage had reduced tumour growth by 82.7% (Supplemental Figure 4.2), a significant difference

compared to the i.p. treated mice. The observation that oral delivery was enhanced compared to i.p. was especially interesting as zafirlukast was resuspended in corn oil for gavage delivery and previous studies found that giving zafirlukast with food can decrease absorption by 40% or more (Dekhuijzen & Koopmans, 2002). Thus, future directions could further explore the pharmaceutical properties of zafirlukast pills and tablets for potential increases in efficacy.

Our most successful method to increase efficacy was through the use of zafirlukast in combination with other agents. It was not surprising that adding zafirlukast to a standard chemotherapeutic regimen for ovarian cancer (cisplatin/gemcitabine) resulted in additive and significant increases in tumour growth inhibition (Figure 3.5). It was a little more surprising that we saw significant increases in the inhibition of cancer markers when combining two thiol isomerase inhibitors, zafirlukast and isoquercetin, together. Isoquercetin, although not FDA approved is generally regarded as safe and can be used clinically, therefore making it the most obvious thiol isomerase inhibitor to add in combination with zafirlukast for eventual clinical effects. Isoquercetin has been shown clinically to inhibit markers of hypercoagulability in cancer patients (Jeffrey I. Zwicker et al., 2019), and anti-tumour activity in a colon cancer xenograft (Da Silva et al., 2022). The hypothesis that a combination of zafirlukast and isoquercetin could have added effects was first confirmed in the cell free assay, where low concentrations of zafirlukast and isoquercetin combined demonstrated better inhibition of PDI than higher concentrations of each on their own (Supplemental Figure 4.1). This was further supported in a xenograft model where the low dose combination allowed for similar efficacy to the high dose of zafirlukast and approaching the efficacy of a standard chemotherapeutic regiment, cisplatin/gemcitabine (Figure 4.7). It is possible these enhanced effects are due to alternative modes of action of isoquercetin through metabolism, as isoquercetin is generally considered a “pro-drug” and when ingested

is metabolised into quercetin (Mbikay & Chretien, 2022). Where quercetin has been shown to decrease the activity of kinases such as JAK3 MET, PAK3 and others in multiple cancer cell lines (Boly et al., 2011). It has also been shown that ingestion of compounds containing isoquercetin are able to block collagen-induced phosphorylation of ERK, JNK and Akt in platelets (Kim et al., 2017), kinases which also play critical roles in cancer progression (Dhillon et al., 2007; Yang et al., 2019). These results lead to the conclusion that combining zafirlukast and isoquercetin have the potential to increase the overall efficacy of both thiol isomerase inhibitors for cancer inhibition and should continue to be explored in this aspect.

5.3 Implications of the thesis

The major implication of this work is that the efficacy of thiol isomerase inhibition is enhanced by using zafirlukast and isoquercetin together. Future clinical studies could explore this combination alone, or in concert with a common clinical regimen to hopefully improve therapeutic outcomes. Additionally, the significance of this work extends beyond potential anti-cancer and anti-thrombotic implications. A combination of zafirlukast and isoquercetin may also be beneficial in the treatment of bacterial and viral infections. Zafirlukast has demonstrated anti-bacterial activity against the oral pathogens *Porphyromonas gingivalis* and *Streptococcus mutans* (Gerits et al., 2017) along with *Mycobacterium abscessus* seen in cystic fibrosis patients (Niet et al., 2024). Additionally, zafirlukast derivatives, such as those developed in **Chapter 2**, demonstrated improved anti-bacterial activity against *Porphyromonas gingivalis* (Howard & Garneau-Tsodikova, 2022; Howard et al., 2020a; Thamban Chandrika et al., 2019). Zafirlukast has also been shown to have anti-viral properties, such as that against Zika virus along with Dengue and yellow fever (Chen et al., 2024). The compound also exhibits antiviral properties against Covid-19, where it inhibits the viral helicase (Mehyar et al., 2021). If zafirlukast alone is unable to treat these infections, the combination of zafirlukast and isoquercetin could be a better option, especially considering the preference to use multiple agents to treat microorganisms to help prevent the development of resistance.

Recently, pinocembrin 7-O-(3”-galloyl-4”,6”-(S)-hexahydroxydiphenoyl)-beta-D-glucose (PGHG) has been identified as another broad-spectrum thiol isomerase inhibitor. It was able to inhibit SARS-CoV-2 viral replication, demonstrating the relationship between thiol isomerases and the Covid-19 virus lies within the active-site cystines of PDI and Covid-19’s main protease (Yang et al., 2025). A clinical trial tested the efficacy of zafirlukast in patients with moderate Covid-19, however there was no difference in symptom recovery,

oxygen requirement or length of hospital stay compared to the placebo group. However, the dose used was a standard asthma dose of 10 mg to avoid potential hepatotoxicity (Ghobain et al., 2022). It is possible that a higher dose is required to see desired effects, and as demonstrated in **Chapter 3**, can be taken safely at 40 mg twice daily. Additionally, as both zafirlukast and isoquercetin have anti-viral effects on Covid-19 (Mbikay & Chretien, 2022; Mehyar et al., 2021) it would be interesting to try clinically in combination. With a combination therapy, it could be possible to lower the doses of each to remove the risk of hepatotoxicity, as demonstrated in the cancer model in **Chapter 4**. Seeing as compound 21 had better thiol isomerase inhibition, it may also be possible to develop the analogues from **Chapter 2** as better anti-viral agents, especially for the use and possibly as a preventative against Covid-19.

5.4 Future prospects and limitations

Considering the numerous mechanisms affected by both zafirlukast and isoquercetin, the potential effects of thiol isomerase inhibition could be extremely beneficial if further explored clinically. One limitation of this study was the low number of participants in the pilot clinical study in **Chapter 3**. Therefore, the future next steps would be to expand on the use of zafirlukast clinically in relation to cancer. With the demonstrated improved efficacy in **Chapter 4** of zafirlukast in combination with isoquercetin, a potential clinical trial may examine these agents in combination for the greatest chance of success, likely in combination with a standard chemotherapy regimen such as cisplatin/gemcitabine, since both zafirlukast and isoquercetin were able to reduce tumour size significantly in mice compared to chemotherapy alone in **Chapters 3 and 4** respectively.

One noteworthy observation of this work was that the combination of zafirlukast and isoquercetin seemingly targeted the expression of different thiol isomerases based upon the immunohistochemistry in **Chapter 4.** Even though it is a pan-thiol inhibitor, zafirlukast was able to better inhibit the expression of ERp57 in xenografted tumours, where unsurprisingly, isoquercetin was only able to inhibit PDI. The immunohistochemistry data is supported by the EGFR inhibition discovered in **Chapter 3**, since EGFR inhibition has previously been linked to ERp57 inhibition (Elisa Gaucci et al., 2013). Future work can further explore the thiol isomerase specific effects of zafirlukast for PDI, ERp5, ERp57 and ERp72 or other thiol isomerases such as ERp46. Additionally, it would be beneficial to continue to explore mechanisms such as angiogenesis, PD-1/PD-L1 and cell migration in more detail, and other possible pathways and mechanisms effected by zafirlukast. The RNAseq data from **Chapter 4**, could provide potential leads for possible pathways to explore. However, there are limitations to the RNAseq data as it was only performed on 4 mice per group and contained

fairly large variations between the samples. Nonetheless, zafirlukast should continue to be investigated as a thiol isomerase inhibitor with the intent to target thrombosis and cancer.

Considering the effect zafirlukast had on our xenograft model, it would also be of interest to expand these studies to other cancer models beyond ovarian cancer. In **Chapter 3**, we found zafirlukast had similar effects on prostate, colon, and lung cancer cells as it did to the ovarian cancer line. However, as demonstrated in **Appendix II**, using a colon cancer (HCT116) xenograft model, zafirlukast was able to slow tumour growth but was less effective than it was in the ovarian cancer model. This could be due to the fact HCT116 cells express more ERp57 and PDI than OVCAR8 cells (**Appendix II**) and the concentration of zafirlukast was not enough to overcome the amount of thiol isomerases expressed by the HCT116 cells to inhibit growth in the same manner as it did for the OVCAR8 model. Further research would benefit from follow up xenograft models using prostate, lung or other cancer models to determine if zafirlukast would be a plausible addition to a treatment regimen for more than just ovarian cancer.

5.5 Conclusion

The results from this thesis support the hypothesis that zafirlukast and isoquercetin can constitute a novel approach to target thrombosis, cancer and cancer induced thrombosis through thiol isomerase inhibition both individually and in combination. This was first shown in **Chapter 2** by developing zafirlukast analogues for better thrombotic inhibition. Altering zafirlukast to a more potent compound (21) was able to better inhibit platelet aggregation, P-selectin exposure and arterial thrombus formation all while maintaining a safe profile to non-cancerous cells and haemostasis. This study was also able to demonstrate zafirlukast and compound 21 targeted surface platelet thiols indicating they were working through thiol isomerase inhibition. As it was established zafirlukast and analogues are effective against thrombosis, **Chapter 3** transitioned to the effects zafirlukast has on cancer. Here zafirlukast had an effect at inhibiting thiol isomerase activity from the surface of ovarian cancer cells, all the while not altering the expression of PDI or ERp57. Demonstrating this cell surface inhibition of activity and not overall expression is important for healthy cells that need PDI and ERp57 for normal function in the endoplasmic reticulum. Zafirlukast exhibited cytotoxicity only to cancer cells and did not significantly affect a non-cancerous cell line, suggesting thiol isomerases have greater activity in cancer cells or zafirlukast targets cancer cells in an underlying mechanism, which has yet to be uncovered. Regardless, this finding is important for future clinical use. When used *in vivo*, there were significant effects on cancer growth demonstrating considerate inhibition on its own and when combined with chemotherapy. This effect was also supported in **Chapter 4** with an additional thiol isomerase inhibitor, isoquercetin. The combination of both drugs demonstrated either additive or synergistic effects *in vivo*, demonstrating tumour growth inhibition comparable to that of the high doses of zafirlukast and isoquercetin on their own, where it also had a greater effect at inhibiting angiogenesis and inflammation markers,

demonstrating these thiol isomerase inhibitors as multi-purpose drugs. Thrombosis, cancer growth, metastasis, angiogenesis, inflammation and cancer induced thrombosis can all be targeted with these inhibitors and with the information provided in this thesis, further insight into more detailed mechanisms should be explored in addition to a comprehensive study of these compounds *in vivo* and clinically.

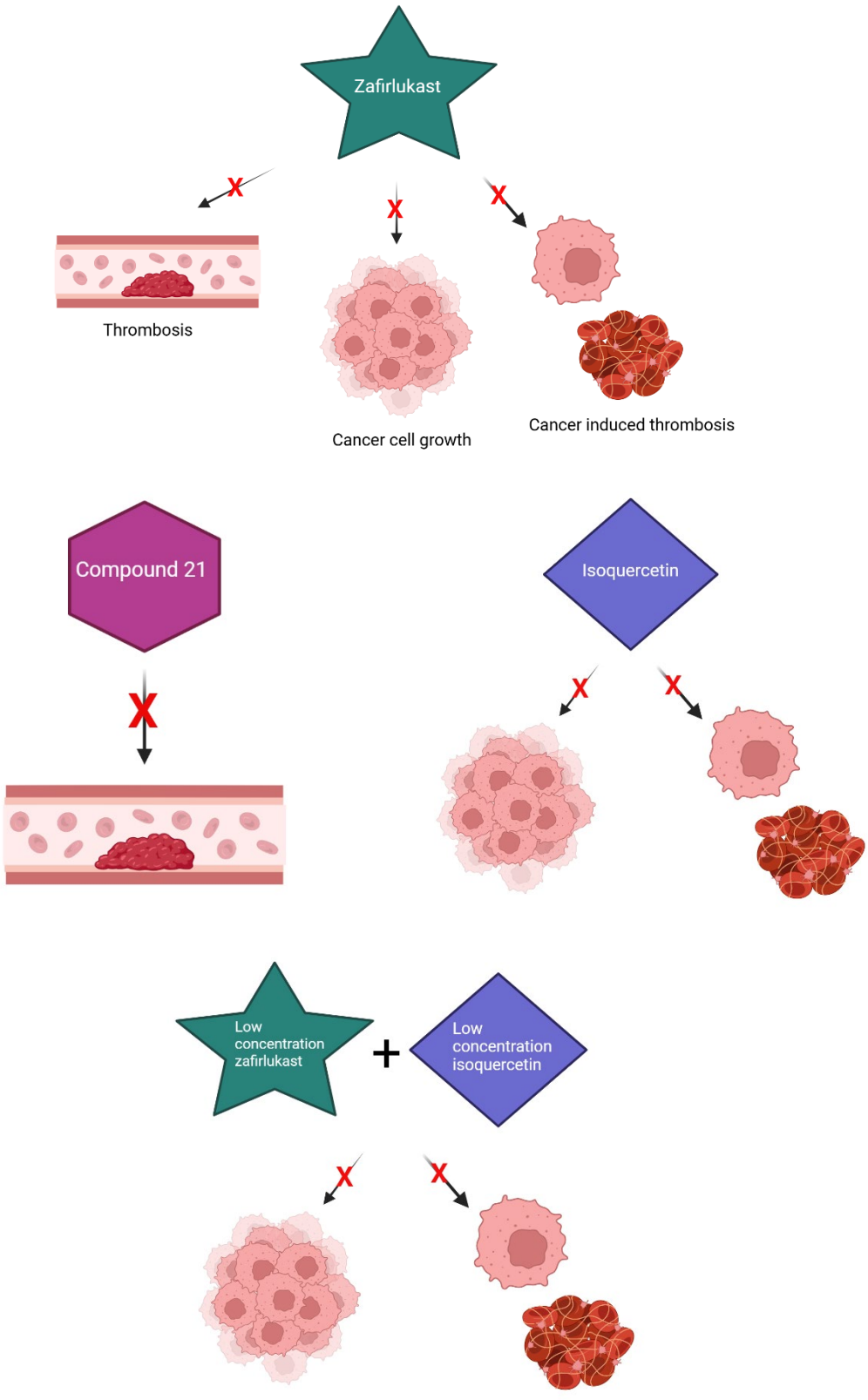

Figure 5.1 Zafirlukast and isoquercetin constitute a novel approach to target thrombosis, cancer growth and cancer induced thrombosis. Zafirlukast, a broad-spectrum thiol isomerase inhibitor can target thrombosis, tumour cell growth and cancer induced thrombosis, however when tested in a pilot

clinical trial could have had better efficacy. Therefore, we developed compound 21, a more potent thiol isomerase inhibitor and inhibitor of thrombosis, but only by about 2-fold. Therefore, we turn to another thiol isomerase inhibitor, isoquercetin, which additionally inhibits tumour growth, and when put in combination with zafirlukast gave us similar results to the monotherapy at lower concentrations and enhanced inhibition of tissue factor and VEGF expression. Although these studies focused specifically on ovarian cancer, metastasis, angiogenesis and cancer induced thrombosis are hallmarks of many advanced cancers and these therapeutics could potentially be used on a wide range of malignancies.

5.6 References

Al Shoyaib, A., Archie, S. R., & Karamyan, V. T. (2019). Intraperitoneal Route of Drug Administration: Should it Be Used in Experimental Animal Studies? *Pharm Res*, *37*(1), 12. https://doi.org/10.1007/s11095-019-2745-x

Bobrovnikova-Marjon, E., Grigoriadou, C., Pytel, D., Zhang, F., Ye, J., Koumenis, C., Cavener, D., & Diehl, J. A. (2010). PERK promotes cancer cell proliferation and tumor growth by limiting oxidative DNA damage. *Oncogene*, *29*(27), 3881-3895. https://doi.org/10.1038/onc.2010.153

Boly, R., Gras, T., Lamkami, T., Guissou, P., Serteyn, D., Kiss, R., & Dubois, J. (2011). Quercetin inhibits a large panel of kinases implicated in cancer cell biology. *Int J Oncol*, *38*(3), 833-842. https://doi.org/10.3892/ijo.2010.890

Bultas, J. (2013). Antiplatelet therapy—A pharmacologist's perspective. *Cor et Vasa*, *55*(2), e86-e94. https://doi.org/https://doi.org/10.1016/j.crvasa.2013.03.003

Chen, V. M., Ahamed, J., Versteeg, H. H., Berndt, M. C., Ruf, W., & Hogg, P. J. (2006). Evidence for activation of tissue factor by an allosteric disulfide bond. *Biochemistry*, *45*(39), 12020-12028. https://doi.org/10.1021/bi061271a

Chen, Y., Li, Y., Lu, L., & Zou, P. (2024). Zafirlukast, as a viral inactivator, potently inhibits infection of several flaviviruses, including Zika virus, dengue virus, and yellow fever virus. *Antimicrob Agents Chemother*, *68*(7), e0016824. https://doi.org/10.1128/aac.00168-24

Da Silva, D. D. C., Orfali, G. D. C., Santana, M. G., Palma, J. K. Y., Assunção, I. R. D. O., Marchesi, I. M., Grizotto, A. Y. K., Martinez, N. P., Felliti, S., Pereira, J. A., & Priolli, D. G. (2022). Antitumor effect of isoquercetin on tissue vasohibin expression and colon cancer vasculature. *Oncotarget*, *13*(1), 307-318. https://doi.org/10.18632/oncotarget.28181

Dekhuijzen, P. N., & Koopmans, P. P. (2002). Pharmacokinetic profile of zafirlukast. *Clin Pharmacokinet*, *41*(2), 105-114. https://doi.org/10.2165/00003088-200241020-00003

Dhaliwal, A., & Bajaj, T. (2024). Zafirlukast. In *StatPearls*. https://www.ncbi.nlm.nih.gov/pubmed/32491776

Dhillon, A. S., Hagan, S., Rath, O., & Kolch, W. (2007). MAP kinase signalling pathways in cancer. *Oncogene*, *26*(22), 3279-3290. https://doi.org/10.1038/sj.onc.1210421

Gaucci, E., Altieri, F., Turano, C., & Chichiarelli, S. (2013). The protein ERp57 contributes to EGF receptor signaling and internalization in MDA-MB-468 breast cancer cells. *Journal of Cellular Biochemistry*, *114*(11), 2461-2470. https://doi.org/10.1002/jcb.24590

Gelzinis, J. A., Szahaj, M. K., Bekendam, R. H., Wurl, S. E., Pantos, M. M., Verbetsky, C. A., Dufresne, A., Shea, M., Howard, K. C., Tsodikov, O. V., Garneau-Tsodikova, S., Zwicker, J. I., & Kennedy, D. R. (2023a). Targeting thiol isomerase activity with zafirlukast to treat ovarian cancer from the bench to clinic. *FASEB J*, *37*(5), e22914. https://doi.org/10.1096/fj.202201952R

Gerits, E., Van der Massen, I., Vandamme, K., De Cremer, K., De Brucker, K., Thevissen, K., Cammue, B. P. A., Beullens, S., Fauvart, M., Verstraeten, N., & Michiels, J. (2017). In vitro activity of the antiasthmatic drug zafirlukast against the oral pathogens Porphyromonas gingivalis and Streptococcus mutans. *FEMS Microbiol Lett*, *364*(2). https://doi.org/10.1093/femsle/fnx005

Ghobain, M. A., Rebh, F., Saad, A., Khan, A. H., Mehyar, N., Mashhour, A., Islam, I., Alobaida, Y., Alaskar, A. S., Boudjelal, M., & Jeraisy, M. A. (2022). The efficacy of Zafirlukast as a SARS-CoV-2 helicase inhibitor in adult patients with moderate COVID-19 Pneumonia (pilot randomized clinical trial). *J Infect Public Health*, *15*(12), 1546-1550. https://doi.org/10.1016/j.jiph.2022.11.016

Goplen, D., Wang, J., Enger, P. Ø., Tysnes, B. B., Terzis, A. J. A., Laerum, O. D., & Bjerkvig, R. (2006). Protein Disulfide Isomerase Expression Is Related to the Invasive Properties of Malignant Glioma. *Cancer Research*, *66*(20), 9895-9902. https://doi.org/10.1158/0008-5472.can-05-4589

Han, Y., Liu, D., & Li, L. (2020). PD-1/PD-L1 pathway: current researches in cancer. *Am J Cancer Res*, *10*(3), 727-742. https://www.ncbi.nlm.nih.gov/pubmed/32266087

Holbrook, L. M., Keeton, S. J., Sasikumar, P., Nock, S., Gelzinis, J., Brunt, E., Ryan, S., Pantos, M. M., Verbetsky, C. A., Gibbins, J. M., & Kennedy, D. R. (2021). Zafirlukast is a broad-spectrum thiol isomerase inhibitor that inhibits thrombosis without altering bleeding times. *Br J Pharmacol*, *178*(3), 550-563. https://doi.org/10.1111/bph.15291

Howard, K. C., & Garneau-Tsodikova, S. (2022). Selective Inhibition of the Periodontal Pathogen Porphyromonas gingivalis by Third-Generation Zafirlukast Derivatives. *J Med Chem*, *65*(21), 14938-14956. https://doi.org/10.1021/acs.jmedchem.2c01471

Howard, K. C., Gonzalez, O. A., & Garneau-Tsodikova, S. (2020a). Second Generation of Zafirlukast Derivatives with Improved Activity against the Oral Pathogen Porphyromonas gingivalis. *ACS Med Chem Lett*, *11*(10), 1905-1912. https://doi.org/10.1021/acsmedchemlett.9b00614

Kim, D. S., Irfan, M., Sung, Y. Y., Kim, S. H., Park, S. H., Choi, Y. H., Rhee, M. H., & Kim, H. K. (2017). Schisandra chinensis and Morus alba Synergistically Inhibit In Vivo Thrombus Formation and Platelet Aggregation by Impairing the Glycoprotein VI Pathway. *Evid Based Complement Alternat Med*, *2017*, 7839658. https://doi.org/10.1155/2017/7839658

Koistinen, P. H., J. (2000-2013). *Integrins in Cancer Cell Invasion*. Landes Bioscience. https://www.ncbi.nlm.nih.gov/books/NBK6070/

Krajewski, D., Polukort, S. H., Gelzinis, J., Rovatti, J., Kaczenski, E., Galinski, C., Pantos, M., Shah, N. N., Schneider, S. S., Kennedy, D. R., & Mathias, C. B. (2020a). Protein disulfide isomerases regulate IgE-mediated mast cell responses and their inhibition confers protective effects during food allergy. *Front. Immunol.*, *11*, 606837. https://doi.org/10.3389/fimmu.2020.606837

Kranz, P., Sanger, C., Wolf, A., Baumann, J., Metzen, E., Baumann, M., Gopelt, K., & Brockmeier, U. (2020). Tumor cells rely on the thiol oxidoreductase PDI for PERK signaling in order to survive ER stress. *Sci Rep*, *10*(1), 15299. https://doi.org/10.1038/s41598-020-72259-1

Li, S., Li, C., Ryu, H. H., Lim, S. H., Jang, W. Y., & Jung, S. (2016). Bacitracin Inhibits the Migration of U87-MG Glioma Cells via Interferences of the Integrin Outside-in Signaling Pathway. *J Korean Neurosurg Soc*, *59*(2), 106-116. https://doi.org/10.3340/jkns.2016.59.2.106

Li, X., Cao, D., Zheng, X., Wang, G., & Liu, M. (2022). Tissue factor as a new target for tumor therapy-killing two birds with one stone: a narrative review. *Ann Transl Med*, *10*(22), 1250. https://doi.org/10.21037/atm-22-5067

Ma, C., Jiang, Y., Zhang, X., Chen, X., Liu, Z., & Tian, X. (2018). Isoquercetin ameliorates myocardial infarction through anti-inflammation and anti-apoptosis factor and regulating TLR4-NF-kappaB signal pathway. *Mol Med Rep*, *17*(5), 6675-6680. https://doi.org/10.3892/mmr.2018.8709

Mbikay, M., & Chretien, M. (2022). Isoquercetin as an Anti-Covid-19 Medication: A Potential to Realize. *Front Pharmacol*, *13*, 830205. https://doi.org/10.3389/fphar.2022.830205

Mehyar, N., Mashhour, A., Islam, I., Alhadrami, H. A., Tolah, A. M., Alghanem, B., Alkhaldi, S., Somaie, B. A., Al Ghobain, M., Alobaida, Y., Alaskar, A. S., & Boudjelal, M. (2021). Discovery of Zafirlukast as a novel SARS-CoV-2 helicase inhibitor using in silico modelling and a FRET-based assay. *SAR QSAR Environ Res*, *32*(12), 963-983. https://doi.org/10.1080/1062936X.2021.1993995

Nagarkoti, S., Kim, Y. M., Ash, D., Das, A., Vitriol, E., Read, T. A., Youn, S. W., Sudhahar, V., McMenamin, M., Hou, Y., Boatwright, H., Caldwell, R., Essex, D. W., Cho, J., Fukai, T., & Ushio-Fukai, M. (2023). Protein disulfide isomerase A1 as a novel redox sensor in VEGFR2 signaling and angiogenesis. *Angiogenesis*, *26*(1), 77-96. https://doi.org/10.1007/s10456-022-09852-7

Niet, S., Green, K. D., Schimmel, I. M., Bakker, J., Lodder, B., Reits, E. A., Garneau-Tsodikova, S., & van der Wel, N. N. (2024). Zafirlukast induces DNA condensation and has bactericidal effect on replicating Mycobacterium abscessus. *Antimicrob Agents Chemother*, *68*(8), e0002924. https://doi.org/10.1128/aac.00029-24

Seyfried, T. N., & Huysentruyt, L. C. (2013). On the origin of cancer metastasis. *Crit Rev Oncog*, *18*(1-2), 43-73. https://doi.org/10.1615/critrevoncog.v18.i1-2.40

Shi, S., Ma, B., Sun, F., Qu, C., Li, G., Shi, D., Liu, W., Zhang, H., & An, H. (2022). Zafirlukast inhibits the growth of lung adenocarcinoma via inhibiting TMEM16A channel activity. *J Biol Chem*, *298*(3), 101731. https://doi.org/10.1016/j.jbc.2022.101731

Shi, Y., Chen, X., Liu, J., Fan, X., Jin, Y., Gu, J., Liang, J., Liang, X., & Wang, C. (2021). Isoquercetin Improves Inflammatory Response in Rats Following Ischemic Stroke. *Front Neurosci*, *15*, 555543. https://doi.org/10.3389/fnins.2021.555543

Singh, N., Baby, D., Rajguru, J. P., Patil, P. B., Thakkannavar, S. S., & Pujari, V. B. (2019). Inflammation and cancer. *Ann Afr Med*, *18*(3), 121-126. https://doi.org/10.4103/aam.aam_56_18

Thamban Chandrika, N., Fosso, M. Y., Alimova, Y., May, A., Gonzalez, O. A., & Garneau-Tsodikova, S. (2019). Novel zafirlukast derivatives exhibit selective antibacterial activity against Porphyromonas gingivalis. *Medchemcomm*, *10*(6), 926-933. https://doi.org/10.1039/c9md00074g

Wu, Y., Ahmad, S. S., Zhou, J., Wang, L., Cully, M. P., & Essex, D. W. (2012). The disulfide isomerase ERp57 mediates platelet aggregation, hemostasis, and thrombosis. *Blood*, *119*(7), 1737-1746. https://doi.org/10.1182/blood-2011-06-360685

Yang, J., Nie, J., Ma, X., Wei, Y., Peng, Y., & Wei, X. (2019). Targeting PI3K in cancer: mechanisms and advances in clinical trials. *Mol Cancer*, *18*(1), 26. https://doi.org/10.1186/s12943-019-0954-x

Yang, M., Zirena, I. H., Kennedy, Q. P., Patel, A., Merrill-Skoloff, G., Sack, K. D., Fulcidor, E., Scartelli, C., Guo, S., Bekendam, R. H., Owegie, O. C., Xie, H., Ghiran, I. C., Levy, O., Lin, L., & Flaumenhaft, R. (2025). Galloylated polyphenols represent a new class of antithrombotic agents with broad activity against thiol isomerases. *J Thromb Haemost*. https://doi.org/10.1016/j.jtha.2025.01.021

Ye, Q., Fu, P., Dou, J., & Wang, N. (2018). Downregulation of PDIA3 inhibits proliferation and invasion of human acute myeloid leukemia cells. *Onco Targets Ther*, *11*, 2925-2935. https://doi.org/10.2147/OTT.S162407

Zetter, B. R. (1998). Angiogenesis and tumor metastasis. *Annu Rev Med*, *49*, 407-424. https://doi.org/10.1146/annurev.med.49.1.407

Zwicker, J. I., Schlechter, B. L., Stopa, J. D., Liebman, H. A., Aggarwal, A., Puligandla, M., Caughey, T., Bauer, K. A., Kuemmerle, N., Wong, E., Wun, T., McLaughlin, M., Hidalgo, M., Neuberg, D., Furie, B., & Flaumenhaft, R. (2019). Targeting protein disulfide isomerase with the flavonoid isoquercetin to improve hypercoagulability in advanced cancer. *JCI Insight*, *4*(4). https://doi.org/10.1172/jci.insight.125851

Chapter 6

Appendices

6.1 Appendix I – Pranlukast as a thiol isomerase inhibitor

Pranlukast is part of a family of leukotriene receptor antagonists also including montelukast and zafirlukast. As montelukast and zafirlukast are known thiol isomerase inhibitors (Holbrook et al., 2021) I wanted to determine if pranlukast would also act as a thiol isomerase inhibitor and possess *in vitro* inhibitory qualities of zafirlukast. In this section I helped guide an undergraduate student in laboratory work, and the experiments executed in this appendix were performed by myself and the help of the undergraduate student.

First, it was determined that pranlukast could inhibit ERp57 in a cell free assay (**Chapter 3**) with an IC_{50} of approximately 25 μM. In comparison to zafirlukast, it was 2-fold less effective at inhibiting ERp57 and compared to montelukast it had 2.5-fold better inhibition of ERp57 (Figure App. I-1). Using the same assay to test for reversibility as used in **Chapter 2**, it was determined pranlukast is also a reversible inhibitor of PDI (Figure App. I-2). Cytotoxicity was also investigated using the Presto Blue assay that was used in **Chapter 3**, and pranlukast demonstrated no cytotoxicity to OVCAR8 cells except at a high concentration of 100 μM (Figure App. I-3). The discrepancy between the cell free assay and cytotoxicity assay indicate pranlukast may be less capable of entering cells compared to zafirlukast, although this notion would need to be further explored. Additionally, pranlukast was investigated for its ability to inhibit factor Xa generation from OVCAR8 cells as zafirlukast was in **Chapter 3.** Interestingly, pranlukast only demonstrated a minimal inhibition of 25% for all concentrations (Figure App. I-4). Finally, pranlukast was investigated for its ability to inhibit P-selectin exposure as was done in **Chapter 2** with zafirlukast. Pranlukast did inhibit P-selectin exposure by 20% for 3 and 10 μM concentrations and 25% for 30 μM demonstrating similar effects to zafirlukast (Figure App.

I-5). These results suggest pranlukast may be better at targeting platelets rather than cancer cells, consistent with the hypothesis that pranlukast is poorly cell membrane permeable.

The results from this appendix demonstrate that although pranlukast can inhibit the thiol isomerase ERp57 in a cell free assay, it is not as effective as zafirlukast when used in a cellular assay, indicating zafirlukast is the more promising leukotriene receptor antagonist to repurpose towards the treatment of cancer and cancer induced thrombosis.

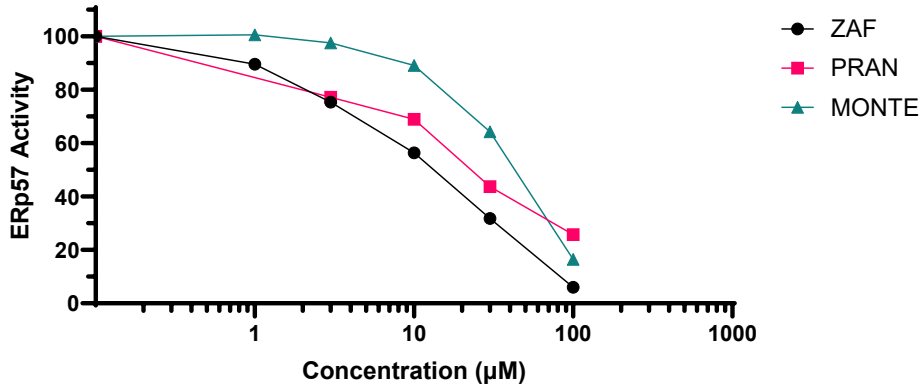

Figure App. I-1. Pranlukast (PRAN) is an inhibitor of ERp57. Pranlukast was able to inhibit ERp57 in the turbidometeric cell free insulin assay 2-fold worse than zafirlukast (ZAF), but 2.5-fold better than montelukast (MONTE).

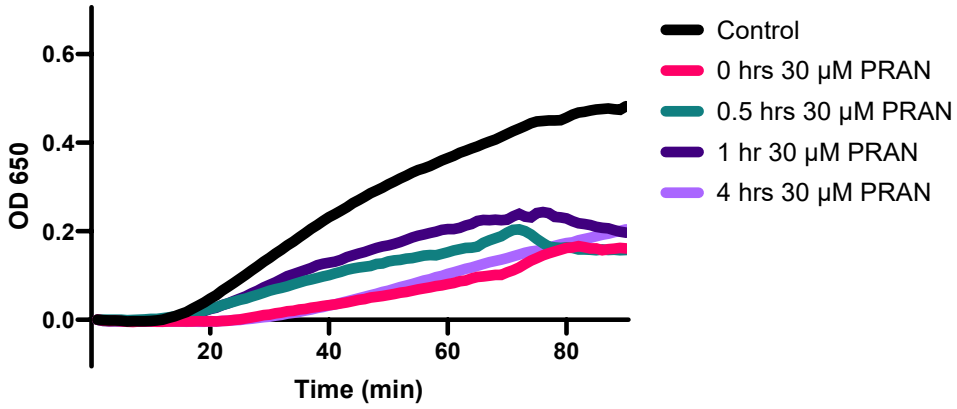

Figure App. I -2. Pranlukast (PRAN) is a reversible thiol isomerase inhibitor. A modified version of the turbidometeric insulin assay to test the reversibility of pranlukast against PDI at 30 μM at 4 different time points up to 4 hours.

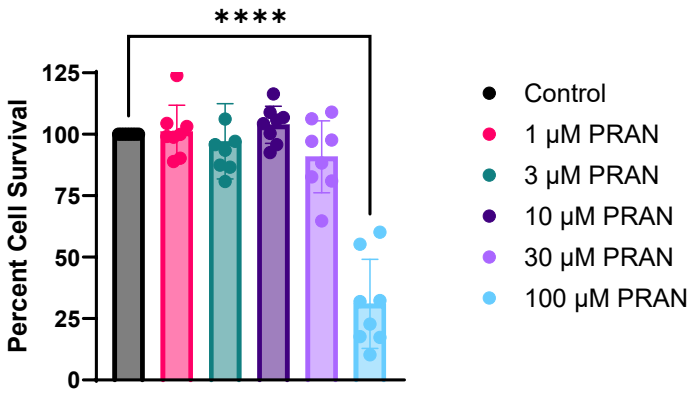

Figure App. I-3. Pranlukast (PRAN) does not demonstrate cytotoxicity in OVCAR8 cells. Pranlukast was only able to demonstrate significant cytotoxicity at a concentration of 100 μM. Data are presented as mean ±SD. Data were analyzed *via* a one-way ANOVA and *post hoc* Dunnett's test where ****p<0.0001.

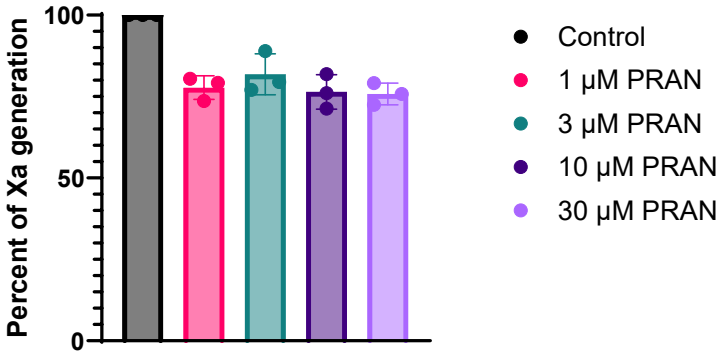

Figure App. I-4. Pranlukast (PRAN) minimally inhibits tissue factor-dependent Factor Xa generation. Four different concentrations (1-30 μM) non-significantly inhibited Xa generation at approximately 20-25%. Data are presented as mean ±SD. Data were analyzed *via* a one-way ANOVA and *post hoc* Dunnett's test.

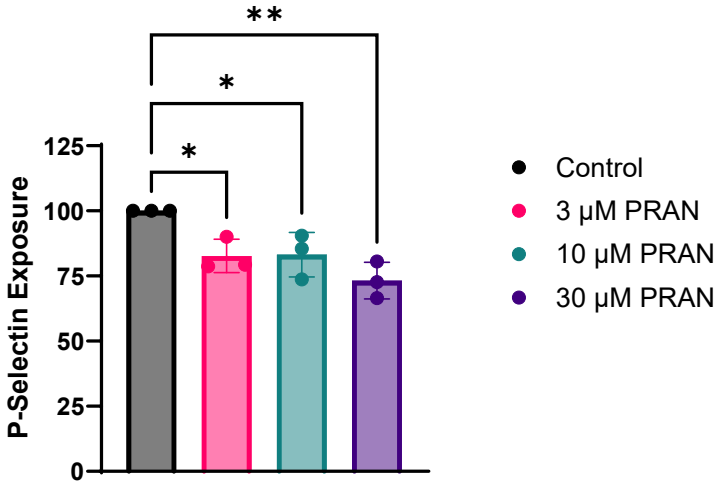

Figure App. I-5. Pranlukast (PRAN) inhibits P-selectin exposure on platelets. All three concentrations (3-30 µM) demonstrated significant inhibition. Data are presented as mean ±SD. Data were analyzed *via* a one-way ANOVA and *post hoc* Dunnett's test where *p<0.05 and **p<0.01.

References

Holbrook, L. M., Keeton, S. J., Sasikumar, P., Nock, S., Gelzinis, J., Brunt, E., Ryan, S., Pantos, M. M., Verbetsky, C. A., Gibbins, J. M., & Kennedy, D. R. (2021). Zafirlukast is a broad-spectrum thiol isomerase inhibitor that inhibits thrombosis without altering bleeding times. *Br J Pharmacol*, *178*(3), 550-563. https://doi.org/10.1111/bph.15291

6.2 Appendix II – The effect of thiol isomerase inhibitors on an HCT116 xenograft

Thiol isomerases are expressed on certain types of cancer cells, therefore at the very beginning of this thesis the expression of ERp57 and PDI were explored on four different cancer and one non-cancerous cell lines. Western blots (as performed in **Chapter 3**) of ovarian, colon, lung and prostate cancer cells and embryonic kidney cells demonstrate ERp57 and PDI are expressed in all five types of cells (Figure App. II-1). In **Chapter 3** I demonstrated that zafirlukast was cytotoxic to the four cancer cell lines including OVCAR8 (ovarian) and HCT116 (colon) (Figure App. II-2). With this data in **Chapter 3** I explored the inhibition of xenografted ovarian tumor growth with zafirlukast *via* i.p. injection then again in **Chapter 4** *via* oral gavage and in combination with isoquercetin. In this model, tumors were allowed to grow to 30 mm^3, which generally took about 30 days, before treatment with zafirlukast began. In **Appendix II**, I explored whether zafirlukast could inhibit the formation and growth of a xenograft, if treatment started at day 0. I also decided to explore a different cancer model, to extend our findings beyond ovarian cancer. Therefore, a xenograft model was developed with HCT116 colon cancer cells, and treatment of the mice via oral gavage with zafirlukast, isoquercetin or the combination was initiated immediately after tumors were xenografted.

No tumors were seen through day 7. On day 11 tumors began growing in 3 mice of the control group, 1 mouse in the isoquercetin group, and 2 mice in the combo group. By day 14 tumors were observed in all 4 groups, where the inhibition was 71% for the isoquercetin group, 64% for the zafirlukast group and 81% for the combination group (Figure App.II-3). The size of the control tumors remained larger in size than those tumors of the treatment groups for the duration of the study, and by day 32 the isoquercetin group and zafirlukast group had significantly smaller tumors than the control group, where they inhibited growth by 76 and 56% respectively (Figure App. II-3). Then on day 35 and through the end of the

study all three groups had significantly smaller tumors compared to the control group. By the end of the study isoquercetin, zafirlukast and the combination groups significantly inhibited tumor growth by 68, 65 and 58% respectively (Figure App. II-3). The study was concluded on day 41 due to the aggressive nature of this particular cell line, and tumors in the control group reaching a volume of greater than 1000 mm^3.

The results from this study overall remain inconclusive. Unfortunately, the facility we use for our mouse studies was closing, and there was only time for one last mouse study. Ideally, this study should have been broken up into multiple studies to test variables one at a time. Treatment immediately after xenografting for the ovarian cancer cells was not performed, where this should have been the first variable tested. Then, after this experiment, move on to treating an HCT116 xenograft after tumors reached 30 mm^3 by oral gavage using a dose-response. Once this was completed and dependent on results, I would then want to perform the experiment that was addressed in this appendix.

It is possible, inhibition is cancer type dependent, as in the ovarian model tumors treated with zafirlukast seemed to level off with a mean tumor size of around 90 mm^3, where in the HCT116 tumors treated with zafirlukast continued to grow with a mean size of 370 mm^3 (Table App. II -1) Additionally, the HCT116 tumors grew much more quickly, while ovarian tumors leveled off and grew more slowly (Figure App. II-4). This observation could be due to the fact HCT116 cells have a faster doubling time compared to the OVCAR8 cells or the fact that HCT116 cells express a greater amount of PDI and ERp57 than the OVCAR8 cells (Figure App. II-1). With there being less thiol isomerase expression in the OVCAR8 cells compared to HCT116 cells, it is plausible it would require less inhibitor, so a treatment of 30 mg/kg would be enough to inhibit growth, where a higher level of thiol isomerases in the HCT116 cells may need a higher dose of zafirlukast to see the same results. In this aspect it would be interesting to explore the effect zafirlukast has on an *in vivo* model xenografted

with other types of cancer such as lung or prostate to determine if other cell lines with less or more thiol isomerase expression are able to inhibit xenograft growth similar to OVCAR8 or HCT116 xenografts. Seeing as expression levels of PDI and ERp57 are lower in lung (A549) and higher in prostate (PC3) (Figure App. II-1) and were additionally shown in **Chapter 3** to be inhibited with zafirlukast *in vitro*.

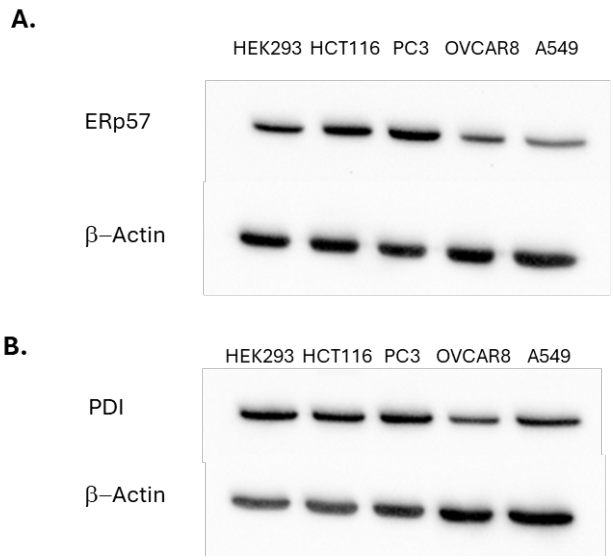

Figure App. II-1. Representative western blots of 4 different cancerous cell lines HCT116 (colon), PC3 (prostate), OVCAR8 (ovarian), A549 (lung), and one non-cancerous cell line HEK293 (embryonic kidney). (A) Relative expression of ERp57 in the 5 different cells lines. (B) Relative expression of PDI in the 5 different cell lines. Beta actin was used as the loading control.

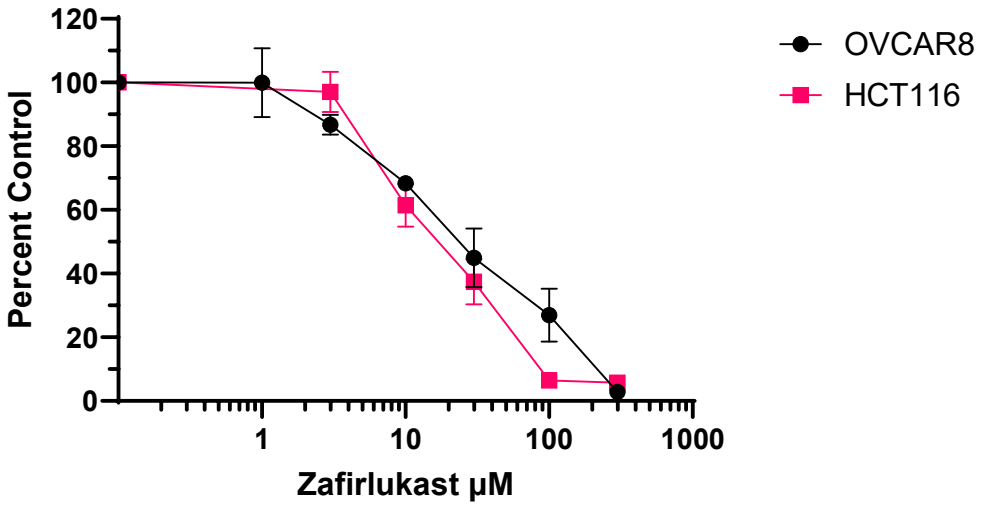

Figure App. II-2. Zafirlukast demonstrates cytotoxicity to OVCAR8 and HCT116 cells *in vitro*.

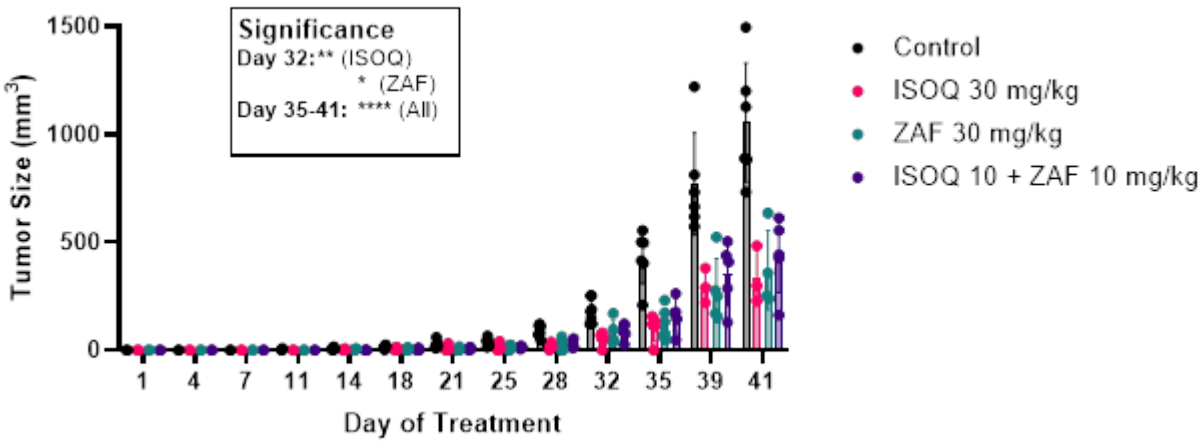

Figure App. II-3. Zafirlukast, isoquercetin and a combination of both compounds were examined *in vivo* for their effectiveness on colon cancer tumor growth immediately after xenografting (n=8 per group). Data are presented as mean ±SD. Data were analyzed *via* two-way ANOVA with a *post hoc* Tukey's test where *P<0.05, **P<0.01 and ****P<0.0001.

A.

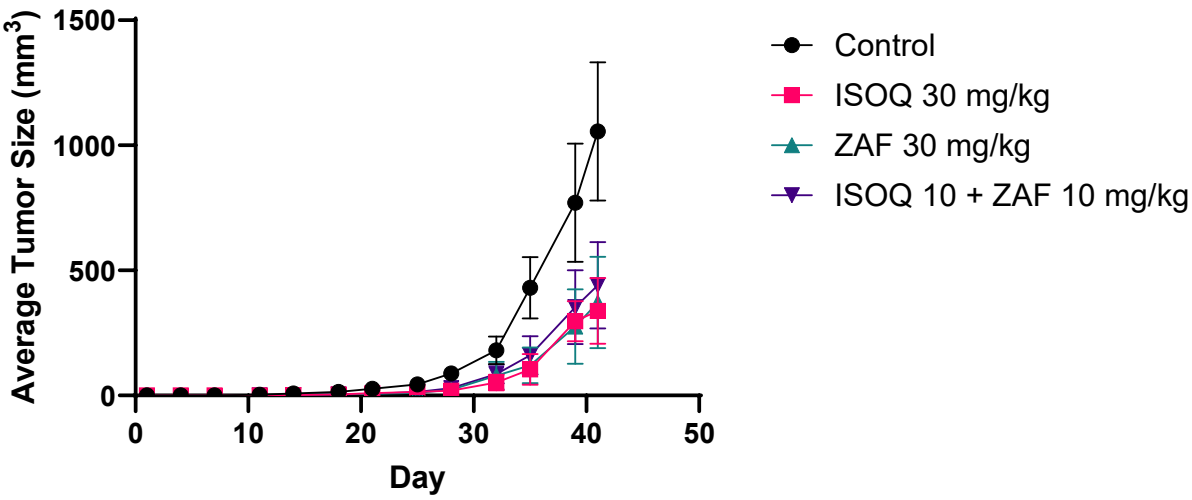

B.

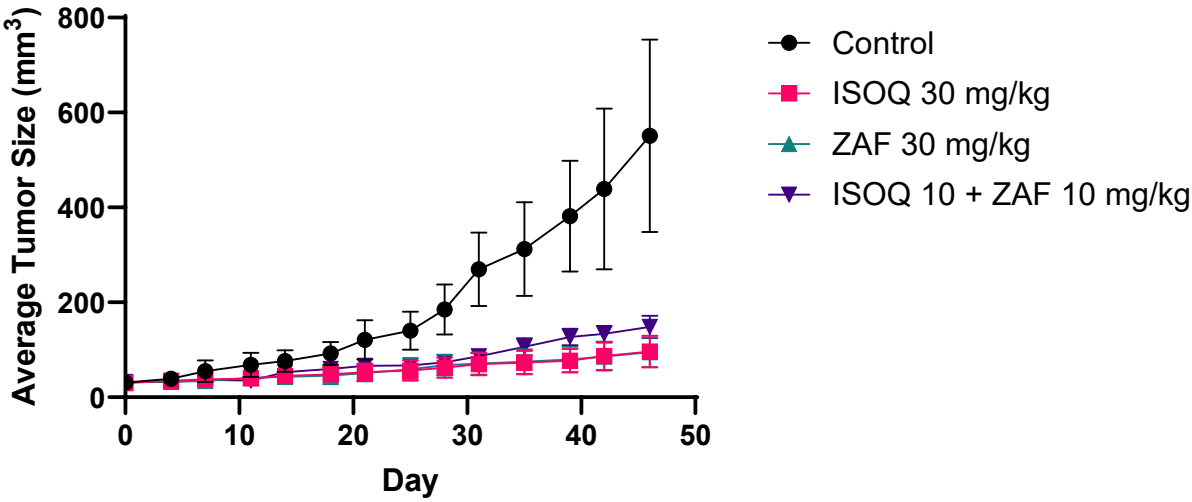

Figure App. II-4. Growth comparison of (A) HCT116 xenografts and (B) OVCAR8 xenografts. Day 0 for HCT116 represents the start of treatment immediately after xenografting was performed. Day 0 for OVCAR8 represents the start of treatment where the average tumor size for all groups was 30 mm^3.

	HCT116				OVCAR8			
	Control	ISOQ 30 mg/kg	ZAF 30 mg/kg	Combo	Control	ISOQ 30 mg/kg	ZAF 30 mg/kg	Combo
Day 1	0	0	0	0	30.77	29.44	32.57	32.47
Day 4	0	0	0	0	38.91	35.10	32.25	32.12
Day 7	0	0	0	0	55.06	37.95	34.38	37.11
Day 11	2.61	0.34	0	0.68	68.11	39.67	40.78	34.96
Day 14	8.15	2.33	2.93	1.57	76.97	44.78	42.82	52.8
Day 18	14.22	4.92	5.26	4.51	92.05	48.65	45.98	59.56
Day 21	26.81	9.76	6.44	6.60	121.3	53.07	51.23	66.35
Day 25	44.21	14.73	11.14	13.80	140.63	56.27	58.92	66.69
Day 28	88.34	19.09	23.40	28.78	185.3	62.41	67.74	73.89
Day 32	180.94	52.22	79.82	85.20	269.38	69.89	71.18	86.56
Day 35	430.81	104.89	120.83	160.94	312.45	72.67	75.03	106.21
Day 39	771.10	296.93	275.52	353.56	381.41	77.13	79.57	127.27
Day 41	1055.73	337.97	371.4	440.28	439.21	86.86	85.82	133.68

Table App. II-1. A comparison of the tumor growth of HCT116 xenografts vs. OVCAR8 xenografts. Tumor sizes are in mm^3.

6.3 Appendix III – Miscellaneous data of Chapter 2

The purpose of **Appendix III** is to include miscellaneous data from **Chapter 2** that did not make it into publication. One mechanism I investigated in this appendix is whether zafirlukast and three of its analogues (21, 22 and 35) would have an effect on thromboxane A_2 (TxA_2) generation. This was performed by first treating platelet rich plasma with zafirlukast or analogues and then stimulating them with collagen. Samples were then subjected to an ELISA to dectect thromboxane B_2 (TxB_2), a stable metabolite of TxA_2, via manufacturers protocol. The results showed no significant change in TxB_2 production compared to the control for zafirlukast, compound 21, 22 and 35 (Figure App. III-1). These results were surprising as it was recently shown that PDI is linked to the TxA_2 generation pathway via inhibition with the PDI specific inhibitor, bepristat (Przyborowski et al., 2022). Zafirlukasts inability to inhibit TxB_2 production could be due to the fact it better inhibits ERp57 compared to PDI as demonstrated in **Chapter 4**. Additionally, in the experiments I ran, I did not use a known TxA_2 control inhibitor, such as aspirin, which would demonstrate that the experiment worked and confirm the effects of zafirlukast or compound 21. Therefore, in the future it may be beneficial to run the same experiment with zafirlukast in addition to aspirin to see if the results remain the same.

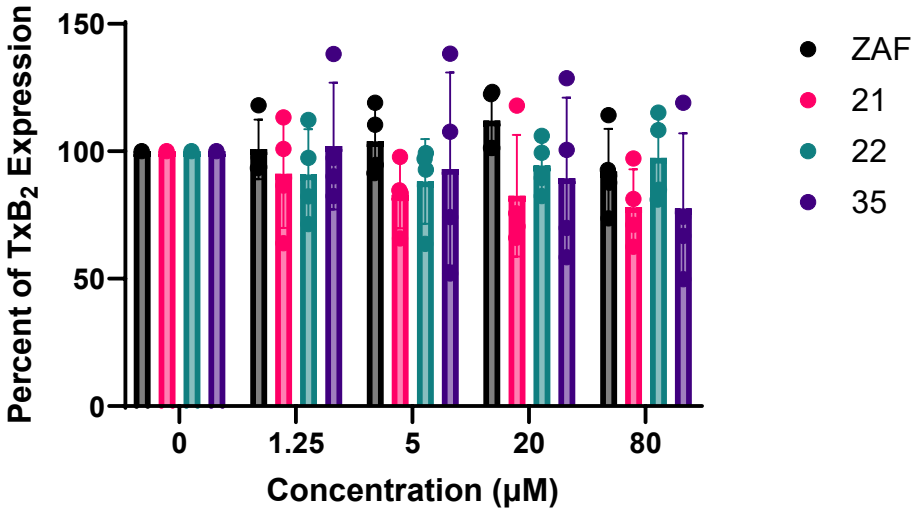

Figure App III-1. Zafirlukast and 3 of its analogues (21, 22 and 35) do not inhibit thromboxane production. Data are presented as mean ±SD. Data were analyzed *via* two-way ANOVA with a *post hoc* Tukey's test, where no significance was observed.

References

Przyborowski, K., Kurpinska, A., Wojkowska, D., Kaczara, P., Suraj-Prazmowska, J., Karolczak, K., Malinowska, A., Pelesz, A., Kij, A., Kalvins, I., Watala, C., & Chlopicki, S. (2022). Protein disulfide isomerase-A1 regulates intraplatelet reactive oxygen species-thromboxane A(2) -dependent pathway in human platelets. *J Thromb Haemost*, *20*(1), 157-169. https://doi.org/10.1111/jth.15539

6.4 Appendix IV – Miscellaneous data of Chapter 3

The purpose of **Appendix IV** is to include miscellaneous data from **Chapter 3** that did not make it into publication. Recently it has been shown that PDI is necessary for PERK signaling and tumor cell resistance to endoplasmic reticulum stress (Kranz et al., 2020). Therefore, in **Appendix IV** I wanted to explore whether the broad-spectrum thiol isomerase inhibitor zafirlukast could inhibit PERK expression in OVCAR8 cells. OVCAR8 cells were treated with 10 or 30 μM zafirlukast or 10 μM known PDI inhibitors PACMA 31 and CCF 642 then harvested and subjected to western blotting (as performed in **Chapter 3**; Figure App. IV-1). Densitometry of four separate western blots demonstrated a significant decrease in the expression of PERK for 30 μM zafirlukast and 10 μM PACMA 31 or CCF 642 relative to the housekeeping protein beta actin (Figure App. IV-2). These results demonstrate through the selective PDI inhibitors PACMA 31 and CCF 642 that PERK is PDI dependent, while zafirlukast had some activity, but not as robust consistent with the data in **Chapter 4**.

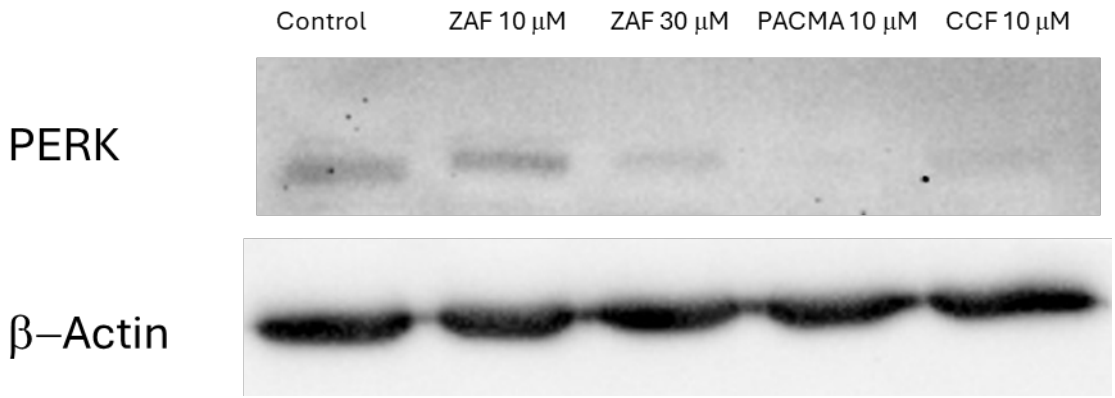

Figure App IV-1. Zafirlukast inhibits PERK expression. A representative western blot demonstrating PERK expression in OVCAR8 cells when treated with vehicle, zafirlukast, PACMA 31 or CCF 642. Beta actin was used as the loading control.

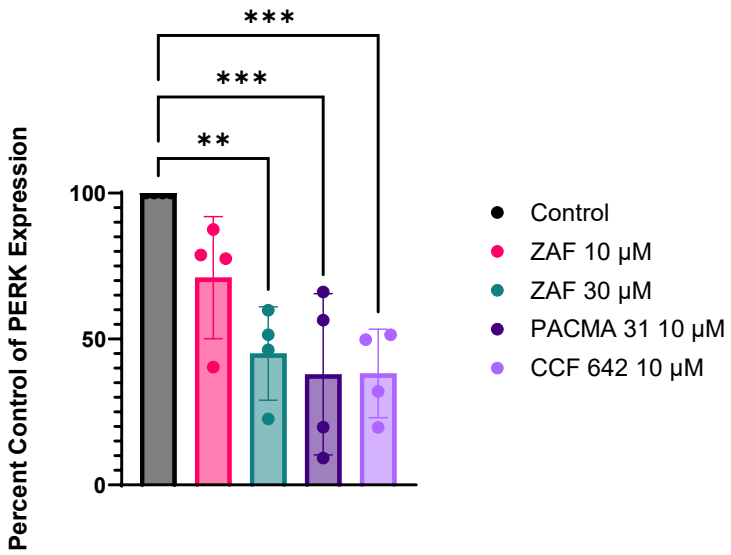

Figure App IV-2. Zafirlukast significantly reduces PERK expression. Known PDI specific inhibitors PACMA 31 and CCF 642 also show a significant decrease in PERK expression. Data are presented as mean ±SD. Data were analyzed *via* a one-way ANOVA and *post hoc* Dunnett's test where **p<0.01 and ***p<0.001.

References

Kranz, P., Sanger, C., Wolf, A., Baumann, J., Metzen, E., Baumann, M., Gopelt, K., & Brockmeier, U. (2020). Tumor cells rely on the thiol oxidoreductase PDI for PERK signaling in order to survive ER stress. *Sci Rep*, *10*(1), 15299. https://doi.org/10.1038/s41598-020-72259-1

6.5 Appendix V – Miscellaneous data of Chapter 4

The purpose of **Appendix V** is to include miscellaneous data from **Chapter 4** that did not make it into publication. In **Chapter 4**, isoquercetin was explored for its effect on soluble P-selectin and thiol isomerase activity in the blood of mice xenografted with ovarian tumors. Zafirlukast was explored for the same in the same method as in **Chapter 4**. 30 mg/kg treatement with zafirluakst signficantly inhibited soluble P-selectin by 42% and thiol isomerase activity by 30.5% (Figure App. V-1). Another factor of coagulation that was explored was D-Dimer, which is released when a blood clot breaks down (Bounds & Kok, 2025). Blood obtained from mice xenografted with ovarian tumors was subjected to an ELISA assay to measure levels of D-Dimer via manufacturers protocols. Results demonstrated no significant difference in D-Dimer levels in any of the test groups (10 mg/kg isoquercetin, 30 mg/kg isoquercetin, 30 mg/kg zafirlukast) compared to the control group (Figure App. V-2).

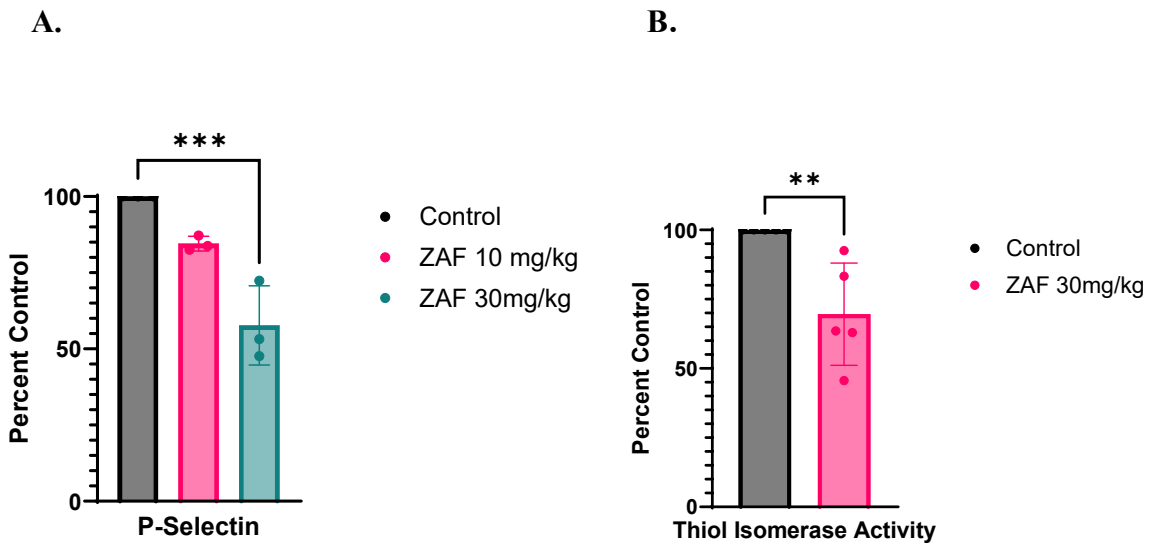

Figure App V-1. Zaffirlukast significantly effects (A) P-selectin and (B) thiol isomerase activity in mouse blood. Data are presented as mean ±SD. For A data were analyzed *via* a one-way ANOVA and *post hoc* Dunnett's test where ***p<0.001. For B data were analyzed *via* a student's t-test where **p<0.01.

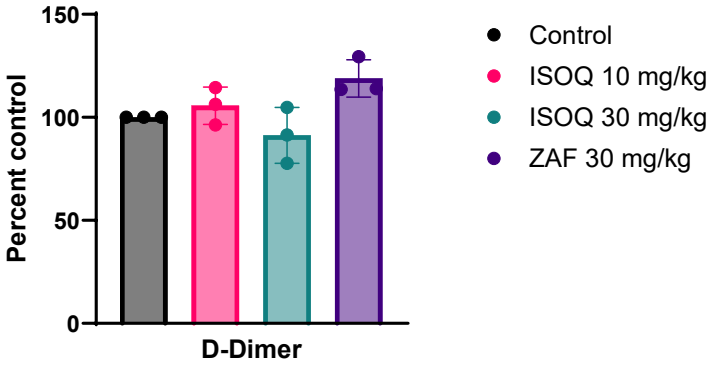

Figure App V-2. Isoquercetin and zafirlukast have no effect on D-Dimer levels in ovarian xenografted mice. Data are presented as mean ±SD. Data were analyzed *via* a one-way ANOVA and *post hoc* Dunnett's test.

References

Bounds, E. J., & Kok, S. J. (2025). D Dimer. In *StatPearls*. https://www.ncbi.nlm.nih.gov/pubmed/28613718